Nanoparticles based on different generation adamantane dendrons : design, synthesis and self-assembly studies

Adriano Aloisi

UNIVERSITÉ DE STRASBOURG

EDSC
École Doctorale des
Sciences Chimiques

Université de Strasbourg

ECOLE DOCTORALE DES SCIENCES CHIMIQUES

Nanoparticles based on different generation adamantane dendrons: design, synthesis and self-assembly studies

by

Adriano Aloisi

Thesis submitted for the degree of Doctor of Philosophy in Chemistry

15th December 2017

Supervisor:	**Dr. Alberto Bianco**
Members of the jury:	**Dr. Eric Doris**
	Prof. Stefano Cicchi
	Dr. Jean-François Nierengarten

UNIVERSITÉ DE STRASBOURG

ÉCOLE DOCTORALE DES SCIENCES CHIMIQUES

THÈSE présentée par :

Adriano ALOISI

soutenue le : **15 Décembre 2017**

pour obtenir le grade de : **Docteur de l'université de Strasbourg**

Discipline/ Spécialité : Chimie

Nanoparticules dendritiques à base d'adamantane: Conception, synthèse et étude de leur auto-assemblage

THÈSE dirigée par :

Mr. Alberto BIANCO Directeur de recherche, CNRS, Université de Strasbourg

RAPPORTEURS :

Mr. Eric DORIS Directeur de recherche, CEA

Mr. Stefano CICCHI Professeur, Université de Florence

AUTRES MEMBRES DU JURY :

Mr. Jean-François NIERENGARTEN Directeur de recherche, CNRS, Université de Strasbourg

Acknowledgments

Three years ago, I started my thesis and I would never have thought that time would pass so quickly. My thesis was an incredible adventure. Among all the people who made it possible to complete my thesis, I would like to express my gratitude to my supervisor, Dr. Alberto Bianco for giving me the opportunity to do my PhD in his research group, for his help and his attention. It was a pleasure for me to work for him. I also would like to thank him for giving me the opportunity to do the internship at the laboratory of Prof. Jensen, in Copenhagen.

I would like to thank the jury members Dr. Eric Doris, Prof. Stefano Cicchi and Dr. Jean-François Nierengarten for accepting to read and judge my work.

I thank Prof. Sylviane Muller for accepting me within the UPR 3572, an interdisciplinary environment.

I also would like to thank the Prof. Knud. J. Jensen from the University of Copenhagen for the great collaboration and for giving me the opportunity to develop new skills. Thank you for this three amazing months that I spent in Copenhagen and thanks to all the team for their support and good mood, especially Kaspar, Niels, Patricia and Shunliang.

I would like to thanks Dr. D. Ferrandon for the collaboration on labelled fipronil and thanks to Dr Adrien Franchet my direct interlocutor in this project.

I want to acknowledge all the people in the analytical platform of the University of Strasbourg, Maurice Coppe, Bruno Vincent and Lionel Allouche from the NMR, Cathy Royer for the TEM, Noemie Bourgeois for the CD and Stéphanie Kouaho for the mass spectrometry.

Thanks to all the members of the ICT team for making me feel welcome and especially to Isabelle Clauss, the secretary of our laboratory, for all the work that she did for me.

I would like to thank my colleagues and ex-colleagues for their advices and all the time that we shared in the Lab (Cécilia, Olivier, Jean-Baptiste, Quyen, Matteo, Raji, Dinesh, Cristina, Illaria, Isabella, Julie and especially Maxime for teaching me the secrets of adamantane).

A special thanks to all my colleagues who have become my friends: Maud (for your football skills), Sophia and Janina (the twins), Giacomo (the lardon's fan), Farouk (the future president) Aude, Chloé, Marie, Amandine, Simone, Flora, Pauline, Laurie, Matthieu and Benjamin (for the fifa nights), Diane for the dancing sessions (and for the corrections). We spent crazy times together, our relationship considerably helped me to complete this thesis.

I also would like to thank my childhood friends (Simon, Claudio, Benjamin, Fabio, Yann), with whom I spent all my time since we were 3 years old. Thank you for your support.

Thanks to you Margot, my girlfriend, for supporting me (especially when I spend my time watching football or formula one).

Of course, I would like also to give many thanks to my family, especially my parents and my sister for their support and all their sacrifices. I will return it to you.

I would like to finish with a citation from Pythagore:
« Les amis sont des compagnons de voyage, qui nous aident à avancer sur le chemin d'une vie plus heureuse »

Thanks to all of you.

Abstract

Adamantane is a hydrocarbon composed of four connected cyclohexane rings, and it is the most stable form of $C_{10}H_{16}$ isomers. Highly reactive compared to other hydrocarbons it could be easily functionalized. Following the previous work done in your Lab, I designed and synthesized novel 1st and 2nd generation adamantane-based dendrons without linker between the adamantane moieties. The obtained dendrons are highly dense and less flexible. I also synthesized different adamantane-based dendrons differing on their functional groups to study their self-assembly properties by transmission electron microscopy. This study confirmed the tendency to form spherical particles which was strongly dependent on the concentration, the type of solvent and support where the molecules were deposited. Additionally, I designed two dendrons, which display three mannose motifs at the periphery and a different focal point. The aim was to obtain a molecule able to interfere with TLR4 (Toll like receptor) signalling. TLR4 is a receptor involved in inflammatory reactions in human monocytes and dendritic cells in response to bacterial infection. The first dendrons possesses a lipid chain at the focal point and is aimed as reference compound. Indeed, it has been established than glycolipid conjugates interfere with TLR4. The molecule has been designed as a potential cell imaging agent. The lipid chain can be substituted with a hydrophobic fluorophore (NBD), so to use the derivative in cell imaging and explore the interaction with the cell receptors. The synthesis of the derivatives is still in progress. I also worked on the incorporation of adamantane into a peptide backbone to form foldamers. In this context, I developed the synthesis of a γ-amino acid based on adamantane protected with two methyl esters. In collaboration with the team of Prof. K. J. Jensen at the University of Copenhagen, I developed a robust strategy to incorporate adamantane into a peptide backbone. We designed a series of peptide sequences aimed to adopt a specific conformation in solution. We observed that using L- or D-tyrosine as C-terminal amino acid residue, the peptide turn right and left, respectively. These results confirmed the possibility of designing novel types of foldamers with potential biological applications.

Finally, in collaboration with Dr. Ferrandon (CNRS) and his team, I synthesized a fipronil derivative labelled with fluorescein *via* click chemistry. The conjugate allowed to do cell imaging and confirmed a novel host defense mechanism in *Drosophila melanogaster*.

Table of contents

Acronyms and Abbreviations

ACN	Acetonitrile
AcOEt	Ethyl acetate
AMP	Anti-Microbial Peptide
Ar	Argon
Boc	*tert*-butyloxycarbonyl
Boc_2O	Di-*tert*-butyl dicarbonate
Cbz	Carbobenzyloxy
Cbz-OSu	N-(Benzyloxycarbonyloxy)succinimide
CD	Circular Dichroism or Cluster differentiation
COMU	1-[1-(cyano-2-ethoxy-2oxoethyliddeneaminooxy)-dimethylamino-morpholino]-uronium hexafluorophosphate
CuAAC	Copper(I)-catalyzed alkyne-azide cycloaddition
Da	Dalton
DC	Dendritic Cell
DCM	Dichloromethane
DIC	*N,N*'-diisopropylcarbodiimide
DIEA	*N,N*-diisopropylethylamine
DLS	Dynamic light scattering
DMAP	4-dimethylaminopyridine
DMF	*N,N*-dimethylformamide
DMSO	Dymethylsulfoxide
DNA	Deoxyribonucleic acid
DNase	Deoxyribonuclease
ECOD	7-ethoxycoumarine-O-deethylase
EDC	1-ethyl-3-(3-dimethylaminopropyl) carbodiimide
EPR	Enhanced permeability and retention
ESI	Electrospray ionization mass spectrometer
Et_2O	Diethyl ether
EtOH	Ethanol
FITC	Fluorescein Isothiocyanate
Fmoc	Fluoren-9-ylmethyloxycarbonyl

FT-IR	Fourier transform infrared
GSH	Glutathione
GST	Glutathione-S-transferase
HATU	hexafluorophosphate de (diméthylamino)-N,N-diméthyl(3H-[1,2,3]triazolo[4,5-b]pyridin-3-yloxy)méthaniminium
HBTU	2-(1*H*-benzotriazol-1-yl)-1,1,3,3-tetramethyluroniumhexafluorophosphate
HCl	Hydrochloric acid
HF	Hydrofluoric acid
HMBA	Hydroxymethylbenzoic acid
HOAt	1-hydroxy-7-azabenzotriazole
HOBt	1-hydroxy-benzotriazole
RP-HPLC	Reversed Phase High Performance Liquid Chromatography
LPS	Lipopolysaccharide
IL	Interleukin
MGC	Mannoside Glycolipid Conjugate
MD	Myeloid Differentiation
MeCN	Acetonitrile
MeOH	Methanol
MW	Microwave or Molecular Weight
NBD	Nitrobenzoxidazole
ND	Not detected
NEt_3	Triethylamine
NHS	*N*-hydroxy succinimide
NIR	Near-infrared
NMR	Nuclear magnetic resonance
N/P	Cationic charge per negative charge
Oxyma	Ethyl 2-cyano-2-(hydroxyimino) acetate
PAMAM	Polyamidoamine
PBS	Phosphate buffered saline
Pd/C	Palladium on carbon
PDI	Polydispersity
pDNA	Plasmid DNA
PEG	Polyethylene glycol

PEI	Polyethylenimine
pH	Potential of Hydrogen
PPI	Poly(propylene imine)
PTC	Phase-transfer catalysis
RNA	Ribonucleic acid
RES	Reticuloendothelial system
SEM	Scanning Electron Microscopy
SPPS	Solid Phase Peptide Synthesis
rt	room temperature
tBu	*tert*-butyl
TBTU	O-(Benzotriazol-1-yl)-N,N,N',N'-tetramethyluronium tetrafluoroborate
TEG	Triethylene glycol
TEM	Transmission electron microscopy
TFA	Trifluoroacetic acid
THF	Tetrahydrofuran
TLC	Thin Layer Chromatography
TLR	Toll Like Receptor
TNF	Tumor necrosis factor
TSTU	*N*,*N*,*N*′,*N*′-tetramethyl-*O*-(*N*-succinimidyl)uronium tetrafluoroborate
UV-Vis	Ultraviolet-Visible

Résumé de Thèse

I. Introduction

Depuis près de deux siècles, les médicaments apportent des progrès thérapeutiques continus. A travers des innovations majeures, on a pu soigner et guérir des maladies jusqu'alors incurables. En optimisant des principes actifs déjà connues, en n'en découvrant d'autres, mais également en améliorant leurs propriétés (absorption, distribution, métabolisme, élimination et toxicité), les médicaments de nouvelle génération apportent des bénéfices parfois majeurs pour les patients. Ces dix dernières années, une nouvelle classe de médicament a vu le jour : les nanomédicaments. Ces molécules thérapeutiques, dont la taille est de l'ordre du nanomètre (< 100 nm), sont de plus en plus présentes, notamment dans la vectorisation de principes actifs. Le principe de vectorisation, plus particulièrement de nano-vectorisation, est de transporter un médicament dans l'organisme et de l'amener, à l'aide de nanoparticules, jusqu'à une cible prédéfinie. Parmi les différentes classes de nanoparticules développées, les dendrons et les dendrimères sont très prometteurs. Ces nanoparticules hyper-ramifiées ont déjà démontré leur efficacité dans des applications biologiques.[1] Je me suis intéressé plus en détails au dendron qui n'est autre qu'un morceau de dendrimère. De ce fait, un dendron est composé de trois parties distinctes: d'un point focal, de sa structure ramifiée et de sa périphérie. La présence d'un point focal qui habituellement possède une fonction chimique différente de la périphérie, permet de le fonctionnaliser de manière sélective. Cette sélectivité point focal/périphérie permet de multi-fonctionnaliser les dendrons très facilement, permettant, par exemple, de combiner des molécules pour la thérapie (des anticancéreux) avec d'autres pour l'imagerie (des fluorochromes). Ainsi ces molécules sont dit théranostiques (thérapie + diagnostique) étant donné leur capacité à traiter tout en restant traçables. Depuis quelques années le Laboratoire, dans lequel j'ai effectué ma thèse, s'intéresse au développement de dendrons à base d'adamanante.[2] L'utilisation de l'adamantane pour construire des dendrons et/ou dendrimères est pertinente du fait de ses caractéristiques physicochimiques. En effet, ce tricycle rigide issu du pétrole est uniquement composé de liaison CH et CH_2. Or, les liaisons CH appelées « bridgehead » sont beaucoup plus réactives. Cela permet de fonctionnaliser sélectivement l'adamantane pour former des dérivés mono-, bi-, tri- ou tétra-substitués. De plus, de part sa structure, les répulsions stériques des différents groupements sont minimisées (Figure 1).[3]

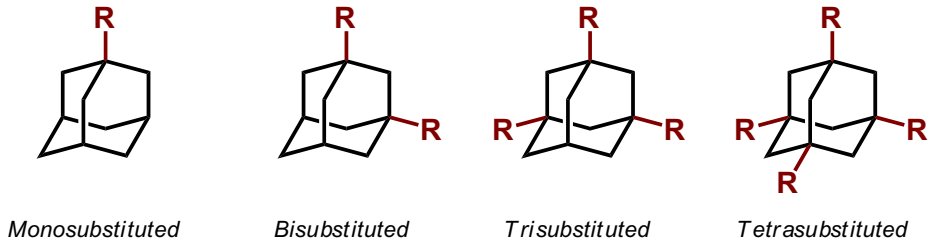

Figure 1: *Fonctionnalisations sélectives de l'adamantane.*

Objectifs de la thèse

Le premier objectif de ma thèse était la synthèse de dendrons à base d'adamantane sans espaceurs, afin d'obtenir un dendron compact et plus rigide. En effet, les dendrons sont habituellement synthétisés à l'aide d'espaceurs entre différentes générations. Cela permet de diminuer les contraintes stériques, mais modifie également les caractéristiques intrinsèques du dendron comme sa solubilité et sa fléxibilité. Dans mon cas, les dendrons synthétisés sans espaceurs sont beaucoup plus compact, rigide et également hautement encombrés (exponentiellement avec le nombre de génération). Différents dendrons ont été synthétisés et fonctionnalisés (point focal et périphérie). Ces derniers ont été caractérisés et étudiés par microscopie électronique en transmission dans le but d'observer leur capacité d'auto-assemblage. Mon second objectif a consisté à fonctionnaliser un dendron afin de bénéficier de l'effet multivalent (la répétition d'un motif – ligand – qui permet d'augmenter l'interaction entre ce dernier et son récepteur),[4] j'ai essayé de trimériser le motif mannose en périphérie d'un dendron de première génération. Ce dernier doit également être fonctionnalisé avec un groupement lipidique afin d'obtenir une molécule possédant des propriétés anti-inflammatoire. En parallèle, mon troisième objectif a été de concevoir un acide aminé à base d'adamantane afin de l'introduire dans des séquences peptidiques et étudier l'influence de l'adamantane sur la structure secondaire des peptides. En effet, certains peptides non naturels, de par leurs structures secondaires (repliement), acquirent des propriétés jouent un rôle primordial en biologie et sont appelés foldamères. Ainsi de nombreuses applications des foldamères ont été explorées, dans la reconnaissance moléculaire[5] ou comme antibiotiques.[6] Enfin mon dernier objectif a été la synthèse d'un insecticide couplé à une sonde fluorescente dans le but de faire de l'imagerie cellulaire et d'élucider le mécanisme d'élimination de ce dernier.

II. Résultats et Discussion

II.1 Conception et synthèse de différentes générations de dendrons à base d'adamantane

Tout d'abord, la synthèse de dendrons passe par la fonctionnalisation de l'adamantane afin de pouvoir les assembler entre eux par la suite et obtenir ainsi les molécules désirées. Pour obtenir ces blocs de construction, nous commençons avec un produit commercial bon marché, le 1-bromoadamantane qui après cinq étapes permet d'obtenir l'acide aminoadamantane-1,3,5-tricarboxylique (Schéma 1). Ce dernier constitue le cœur pour construire les dendrons de différentes générations. Cette synthèse a été développée par notre Laboratoire et optimisée au fil des années pour aboutir à une synthèse multi-étapes ne nécessitant pas d'étapes de purification par colonne de gel de silice.[7]

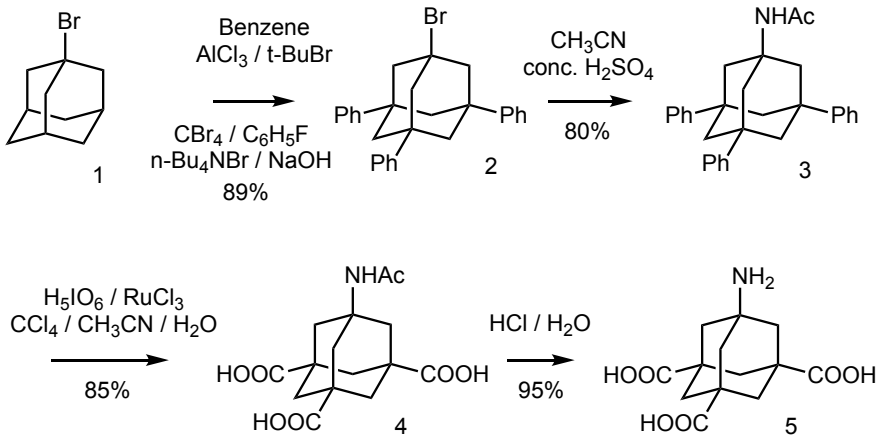

Schéma 1 : *Synthèse de l'acide aminoadamantane-1,3,5-tricarboxyliques.*

Le « building block » (**5**) obtenu représente également la 1ère génération de dendrons. Ensuite la stratégie de synthèse se décompose en deux étapes. Tout d'abord une fraction du building block est protégé au niveau de l'amine primaire par un groupement *tert*-butoxycarbonyle (Boc). D'autre part, une seconde partie du « building block » (**5**) est protégée au niveau des acides par des groupements esters. Cela permet de contrôler la réaction d'amidation entre deux

adamantanes et d'obtenir la seconde génération de dendrons (Figure 2, gauche). Le produit obtenu a été caractérisé par RMN ^{1}H et ^{13}C, IR, et par spectrométrie de masse.

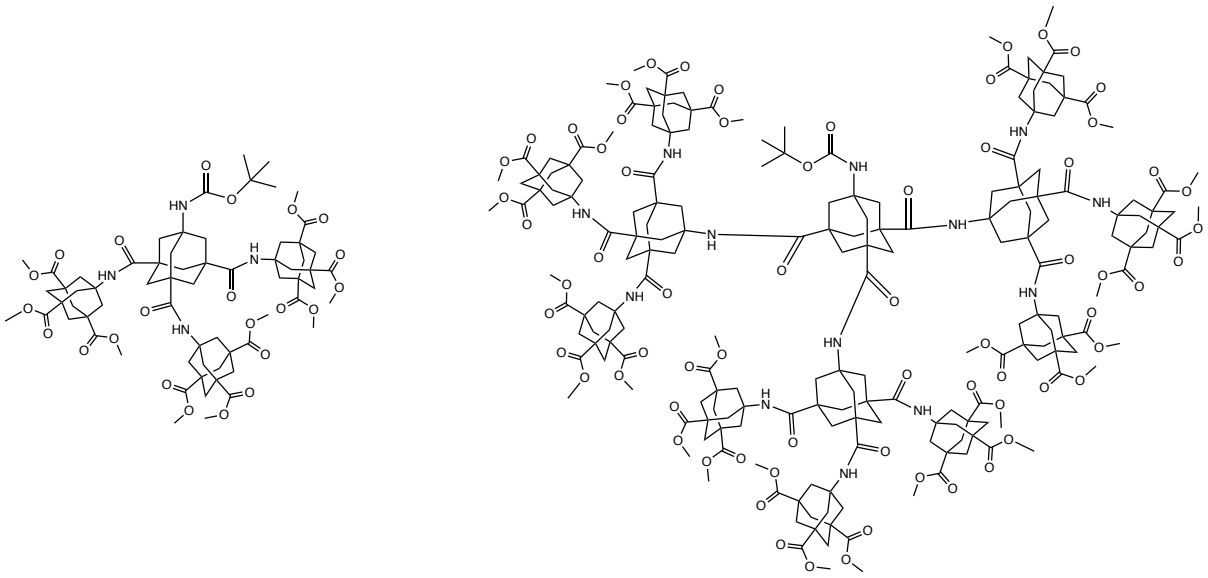

***Figure 2** : Représentation de la 2ème et 3ème génération de dendrons à base d'adamantane.*

Après déprotection du groupement Boc en milieu acide, on récupère l'amine libre correspondante, qui peut à nouveau réagir avec un « building block » (**5**) protégé au niveau de l'amine pour former la troisième génération de dendrons (Figure 2, droite). Ce dernier, beaucoup plus encombré n'a pas encore été isolé et caractérisé. Cependant des simulations par ordinateur laisse penser que sa synthèse est possible. De plus, le facteur limitant étant clairement la faible réactivité de l'amine libre au point focal, il est possible d'augmenter considérablement cette réactivité par l'utilisation des micro-ondes. Des tests ont été menés mais n'ont pas permis d'isoler le dendron désiré. Cependant les paramètres étant nombreux (agents de couplage, solvant, température, puissance, et utilisation d'une base) d'autres tests doivent être effectués. La 1ère et la 2ème génération de dendrons obtenues ont été également étudiées par microscopie électronique à transmission afin d'évaluer leurs auto-assemblages. De plus, cela permet d'étudier l'impact des groupements en périphérie et/ou au point focal sur l'auto-assemblage des dendrons ainsi que les effets de la concentration, du solvant et également du support sur ce processus.

II.2 Trimérisation du mannose avec un dendron à base d'adamantane

L'utilisation de plusieurs motifs mannoses, reliés par liaison éthylène glycol et conjugués à une chaine lipidique a démontré une forte activité anti-inflammatoire en inhibant le TLR4 (TLR pour « Toll-like receptor »), un des récepteurs qui contrôle l'activation cellulaire.[8] Nous proposons d'utiliser l'adamantane pour obtenir des dendrons fonctionnalisés en périphérie avec le motif mannose. Afin de garder une bonne flexibilité, d'améliorer la biocompatibilité et augmenter la solubilité des molécules, les mannoses sont reliés à l'adamantane à l'aide de liaisons tetraéthylène glycol. De plus, pour que la molécule garde son caractère hydrophobe, le point focal du dendron est fonctionnalisé avec un groupement lipidique (acide hexacosanoique) ou bien avec un alcyne. L'utilisation d'un alcyne nous permet par la suite d'effectuer une réaction dite de chimie « click » et d'y attacher un fluorochrome afin de faire de l'imagerie cellulaire et donc d'obtenir une molécule théranostique. Cette synthèse multi-étapes se décompose comme suit: tout commence par la synthèse de l'adamantane fonctionnalisé. Pour ce faire nous utilisons l'aminoadamantane-1,3,5-tricarboxylique (obtenue précédemment en partant du 1-bromo-adamanatane) qui est dans un premier temps estérifié en périphérie (Schéma 2). En effet, il se trouve que l'amine primaire est plus réactive quand les groupements acides sont estérifiés.

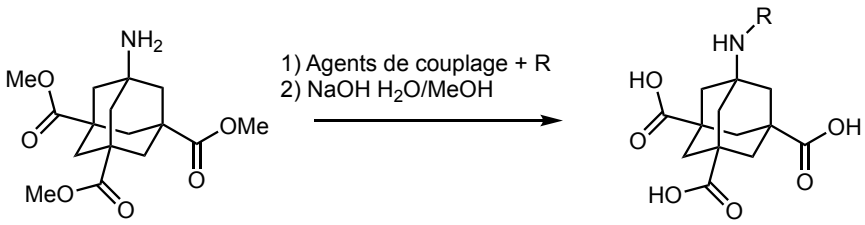

***Schéma 2** : Synthèse de l'adamantane tri-acide fonctionnalisé.*

Ensuite, à l'aide d'agents de couplage, les groupements lipophiles (R= acide hexacosanoique) ou alcyne (R= acide 5-hexynoique) sont introduits via une liaison amide. Enfin, les esters sont déprotégés par saponification pour récupérer les acides libres correspondants. Malheureusement, il se trouve que le dérivé avec l'acide hexacosanoique est difficile à hydrolyser. En effet, outre le fait que sa réactivité est limitée par la formation potentielle de micelles, sa solubilité dans un milieu polaire (permettant l'hydrolyse) est fortement diminuée. En parallèle, le 2,3,4,6-tetra-*O*-acetyl-α-D-mannopyranosyl trichloroacetimidate réagit avec le α-azido-ω-hydroxy tetra(ethylene glycol) qui est ensuite réduit pour obtenir l'amine libre correspondante (Schéma 3).

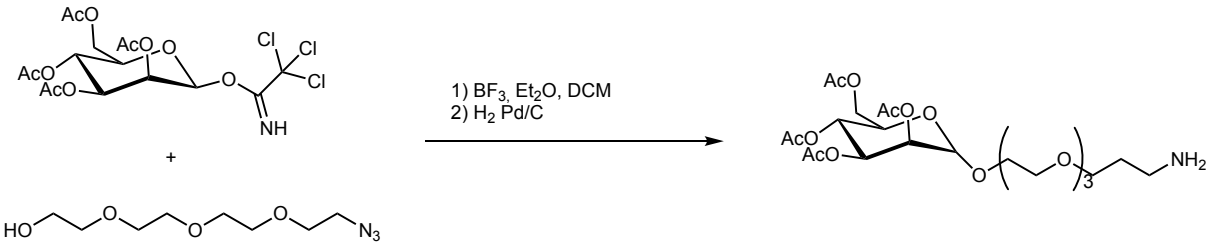

***Schéma 3** : Synthèse du motif, mannose-triethylèneglycol déprotégé.*

Ce dernier peut alors réagir avec l'adamantane fonctionnalisé, synthétisé précédemment. Cependant les premiers tests de couplage utilisant HBTU et HOBt comme activateurs des fonctions acides en présence de DIEA n'ont pas permis d'isoler le produit désiré. Une fois la réaction de couplage mis au point, il s'en suivra une hydrolyse des groupements protecteurs du mannose (acétates), effectuée par une solution de methoxide de sodium dans le méthanol afin d'obtenir les produits finaux (Schéma 4).

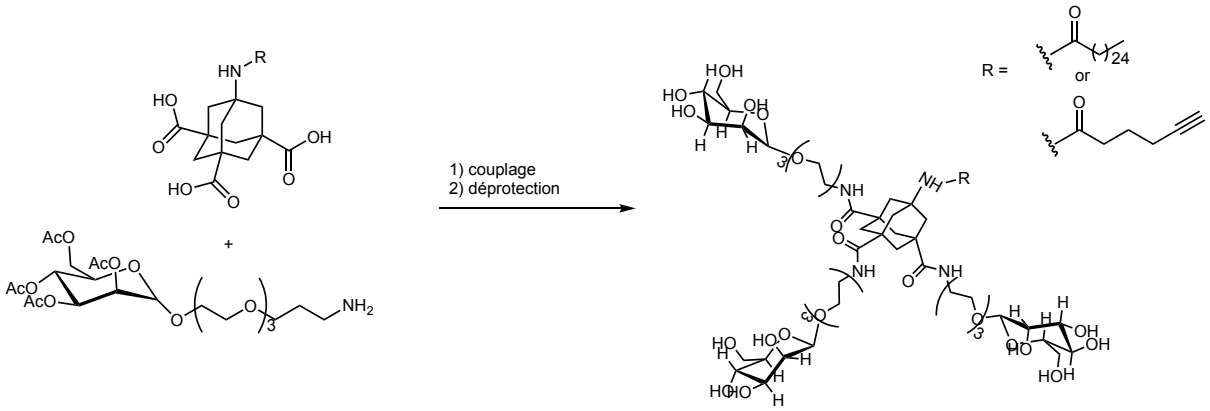

***Schéma 4 :** Couplage final et dé-protection totale pour obtenir les molécules désirées.*

Pour finir, dans le cas du dérivé alcyne, le nitrobenzoxiadazole préalablement fonctionnalisé avec un groupement azide, sera attaché au point focal via une réaction de type « click.

Les principales difficultés rencontrées ont été les étapes de purification. En effet, les chaines tetraethylène-glycol rendent les produits très polaires. De ce fait, les extractions sont impossibles et les colonnes sur silice extrêmement compliquées. De plus, à cause du caractère amphiphile des molécules (notamment pour le dérivé comportant la chaine lipidique C_{24}) elles ont tendance à former des micelles, ce qui limite considérablement les rendements obtenus.

II.3 Utilisation de l'adamantane dans la synthèse de foldamères

Les foldamères sont des oligomères non naturels possédant une structure secondaire (hélice α, feuillet β, etc.) conçues pour mimer l'effet de protéines ou d'autres biopolymères. En effet, la structure secondaire est à la base de nombreux systèmes de reconnaissance dans le vivant, ainsi la conformation adoptée par un peptide peut jouer un rôle primordial et ouvre la porte à de nombreuses applications (antimicrobiens, vectorisation, agonistes ou antagonistes d'un récepteur).[9] Les foldamères possèdent généralement une bonne biocompatibilité du fait de leur ressemblance avec les molécules naturelles. De nombreuses familles de foldamères existent selon leurs origines (abiotic ou biotic), leurs types de repliements (simple brin, double brin, etc.) et également leurs structures (peptidomimétiques, nucleotidomimetiques, etc.). Nous avons décidé d'utiliser de l'adamantane fonctionnalisé pour fabriquer des peptides non naturels et observer son impact sur la structure secondaire de ces oligomères. Dans un premier temps, j'ai synthétisé un acide γ-aminé basé sur l'adamantane. Une fois encore, le produit de départ n'était autre que le 1-bromoadamantane. Facilement fonctionnalisé comme expliqué précédemment, l'étape clé a été l'hydrolyse sélective d'un seul ester. De ce fait, ce dernier possède également deux groupements acides carboxyliques protégés en méthyle ester (Figure 3). L'acide aminé a ensuite été protégé pour être utilisé en synthèse peptidique en phase solide (SPPS). Cependant, le dérivé Fmoc protégé n'a jamais été isolé avec de bon rendement. Or la synthèse en phase solide dite Fmoc est beaucoup plus répandue de par sa facilité d'utilisation. Face à ce problème de réactivité nous avons décidé de protéger l'amine libre avec un groupement Boc. La réaction entre l'amine libre de l'adamantane et le dicarbonate de di-*tert*-butyl a été beaucoup plus concluante.

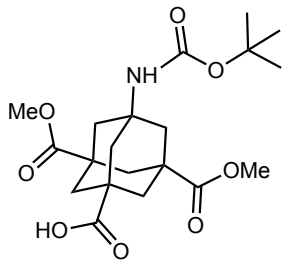

Figure 3 : *Acide aminé basé sur l'adamantane, protégé par un groupement Boc et deux fonctions méthyle esters.*

En collaboration avec l'Université de Copenhague et l'équipe du Pr. K. J. Jensen, nous avons tout d'abord élaboré un protocole de synthèse en phase solide assisté aux microondes, qui permet l'incorporation du motif adamantane dans la séquence peptidique ainsi que l'addition d'acide aminé en aval du motif adamantane. De plus, dans le but d'économiser du produit, nous avons considérablement diminué la quantité d'acide aminé ajoutée par couplage. Etant donné la difficulté d'utiliser une synthèse solide de type Boc, nous avons développé une synthèse qui combine le dérivé Boc protégé avec des acides aminés naturels protégés avec le Fmoc. Nous avons mis au point des dé-protections sélectives des groupements Boc (acid) et des groupements Fmoc (basic) sans affecter la résine, le lien avec la résine ou les groupements protecteurs des chaines latérales.

De plus, l'optimisation lors de la séquence de clivage de la résine nous permet de contrôler la présence ou non des groupements esters. Enfin, par simulation sur ordinateur, nous avons observés que l'introduction d'une tyrosine en position N-terminale d'un peptide composé d'adamantane protégé et de glycine, peut induire une conformation spécifique du peptide ("folding"). De plus, selon que la tyrosine soit L ou D, les foldamères obtenus seraient énantiomères.

Afin de valider cette hypothèse, nous avons synthétisé les peptides suivants:

1 - H-L-Tyr-Gly-Ada(Me)$_2$-Gly-Ada(Me)$_2$-Gly-Ada(Me)$_2$-Gly-OH
2 - H-L-Tyr-Gly-Ada-Gly-Ada-Gly-Ada-Gly-OH
3 - H-D-Tyr-Gly-Ada(Me)$_2$-Gly-Ada(Me)$_2$-Gly-Ada(Me)$_2$-Gly-OH
4 - H-D-Tyr-Gly-Ada-Gly-Ada-Gly-Ada-Gly-OH

De plus, nous avons également synthétisé un peptide comprenant successivement cinq résidus adamantane. Ce dernier homopeptide a pour but d'étudier si une autre conformation préférentielle peut être observée. Cependant, par manque d'acide aminé à base d'adamantane, uniquement le dérivé avec la L-tyrosine a été synthétisé.

5 - H-Tyr-Gly-Ada(Me)$_2$-Ada(Me)$_2$-Ada(Me)$_2$-Ada(Me)$_2$-Ada(Me)$_2$-Gly-OH

Les peptides synthétisés ont été caractérisés par spectrométrie de masse, puis étudié par dichroïsme circulaire (CD) afin d'observer si une conformation préférentielle était adoptée. Le dichroïsme circulaire permet de déterminer l'ellipticité d'une solution, c'est à dire sa capacité à absorber la lumière polarisé (gauche et droite). Pour nous affranchir des concentrations des

solutions et comparer plus rigoureusement nos échantillons, nous avons déterminé l'ellipticité spécifique de chaque échantillon. Pour ce faire, les échantillons sont préalablement titrés par UV en se basant sur l'absorbance de la tyrosine selon la loi de Beer-Lambert. Enfin, la capacité d'un peptide à adopter une conformation préférentielle est due aux interactions faibles au sein de la structure mais également aux interactions avec le solvant. C'est pourquoi nous avons étudiés le repliement de nos peptides dans le méthanol ainsi que dans le trifluoroéthanol.

On observe bien un signal spécifique en CD dans le méthanol, notamment pour les peptides alternés et estérifiés (numéro 1 et 3). De plus, l'addition d'une tyrosine L ou D dans la partie N-terminale du peptide semble induire une chiralité pendant le repliement de la molécule (Figure 4) et donc d'image spéculaires au CD.

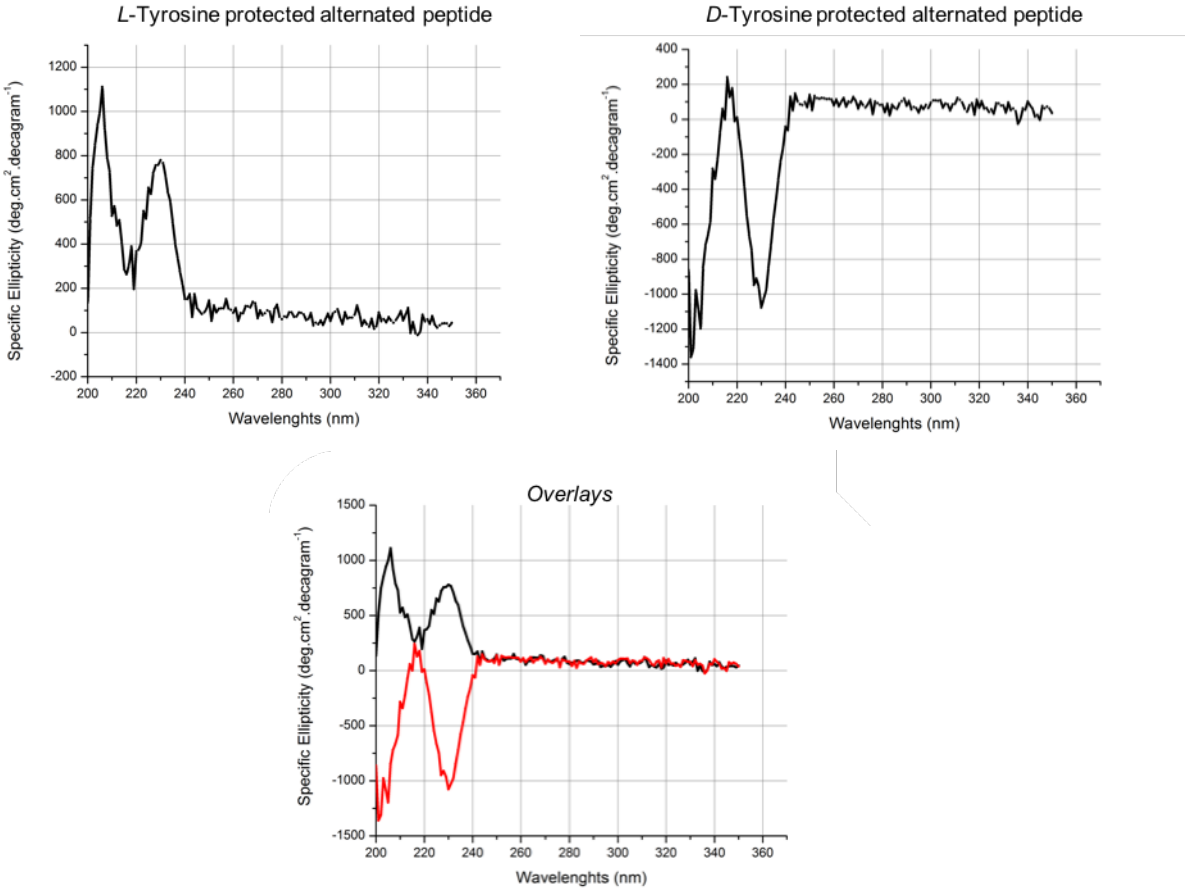

Figure 4 : *Ellipticité spécifique des peptides 1 et 3 dans le méthanol.*

Dans les cas des peptides alternés déprotégés (2 et 4), le composé 4 a également été étudié en CD dans le méthanol mais aucune conformation préférentielle n'a été observée. Le composé 2

n'a pas été analysé par CD ; en effet ce dernier n'a pas pu être convenablement purifié de sels après l'hydrolyse des groupements esters. De ce fait, la force ionique en solution du peptide 2 serait totalement différente et pourrait perturber ou induire le repliement. Cependant, il serait intéressant de tester les peptides 2 et 4 en présence de cations comme le calcium afin de voir si ce dernier en interagissant avec les groupements acides carboxyliques peut induire un repliement. L'homopeptide protégé 5 a également été étudié par CD. Alors que aucune conformation préférentielle ne soit observée dans le méthanol, l'analyse dans le trifluoroethanol (TFE) a permis d'observer un signal confirmant que la molécule adopte une structure secondaire. Ces résultats ont permis de démontrer qu'incorporer de l'adamantane dans une séquence peptidique permet d'induire un repliement particulier pouvant potentiellement être utilisé dans des futures applications biologiques. Enfin, il serait intéressant d'étudier plus en détail les repliements de ces peptides, par exemple, dans un tampon physiologique (PBS) mais également d'obtenir des cristaux pour faire de la diffraction des rayons X.

II.4 Synthèse de fipronil couplé à une sonde fluorescente

Le fipronil est un produit phytosanitaire qui présente un effet insecticide et acaricide. Abondamment utilisé depuis 1990 pour protéger les cultures et plantation contre les insectes, il est fortement utilisé pour sa sélectivité envers les insectes par rapport au mammifère.[10] Controversé depuis une vingtaine d'année, il semblerait que son écotoxicité soit plus importante qu'annoncée par ses fabricants, notamment sur les abeilles domestiques et d'autres apidés sauvages. Plus récemment, il a été mis en avant suite au scandale sanitaire concernant la contamination d'œufs destinés à l'homme par le fipronil. En effet, des millions d'œufs ont été contaminés, bien que ce dernier soit banni part l'Union Européen dans l'utilisation sur des animaux destinés à l'hommes.

Le Dr. Ferrandon du CNRS étudie la réponse immunitaire et le développement chez les insectes. Son équipe est à la base d'une nouvelle théorie qui expliquerait un mécanisme d'élimination du fipronil chez la Drosophile: la purge lipidique. En effet, en exposant des Drosophiles (*Drosophilia melanogaster*) à de fortes doses de fipronil, ils ont observé l'agglomération des lipides pour former des gouttes qui sont ensuite expulsées dans le lumen de l'intestin et donc éliminées. Le fipronil affectionnant particulièrement les cellules adipeuses, la question était de savoir si ce mécanisme était induit par le fipronil mais également si le

fipronil était bien éliminé. Pour ce faire nous avons décidé de coupler le fipronil à une sonde fluorescente qui peut être suivie par microscopie confocale.

Nous avons sélectionné la fluorescéine comme sonde fluorescente ($\lambda_{emission}$ = 512 nm), puis nous l'avons couplée au fipronil. Après différents tests peu concluant (liaison thio-urée, liaison peptidique), nous avons finalement décidé d'utiliser la cycloaddition de Huisgen (ou chimie « click »). D'une part le fipronil a été fonctionnalisé avec une fonction alcyne, d'autre part la fluorescéine a été purifié avec une fonction azide. Les deux précurseurs ont été purifiés par HPLC préparative et reliés par chimie « click » pour donner le conjugué fipronil-fluorescéine désiré (Figure 5).

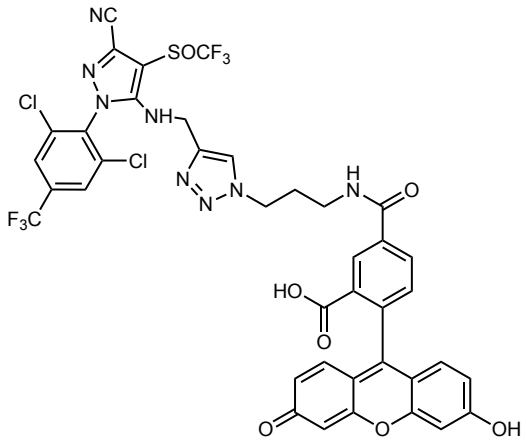

Figure 5 : *Fipronil-fluorescéine via chimie « click » utilisé pour l'imagerie cellulaire.*

Le conjugué ainsi obtenu, beaucoup plus stable, a été administré aux *Drosophila melanogaster* et a permis de confirmer la co-localisation du fipronil dans les gouttes lipidiques des enterocytes, confirmant ainsi la théorie de la purge lipidique.

Conclusion

La synthèse de dendrons sans espaceurs a été rendue possible par l'optimisation de la réaction de couplage entre deux molécules d'adamantane. Ainsi la 1ère et la 2ème génération de dendrons ont pu être synthétisées et caractérisées, mais la 3ème génération n'a pas encore été isolée. Cependant l'utilisation de micro-onde pour augmenter la nucléophilicité de l'amine libre sur l'adamantane est une voie très prometteuse. Plusieurs 1ère et 2ème générations de dendrons ont été analysées par microscopie électronique à transmission, afin d'étudier leurs auto-

assemblages et l'importance des groupements fonctionnels (au point focal ainsi qu'en périphérie).

La synthèse des précurseurs pour obtenir un dendron de première génération fonctionnalisée avec des mannoses en périphérie a été effectuée. Le point focal a, quant à lui, été fonctionnalisé avec une chaine lipophile ou avec un dérivé alcyne (pour l'introduction futur d'un fluorochrome). Ainsi la molécule peut être suivie en direct par imagerie dans des tests avec des cellules.

La synthèse d'un acide γ-aminé base sur l'adamantane a permis d'introduire le motif adamantane au sein d'une séquence peptidique. L'analyse par dichroïsme circulaire a confirmé qu'une conformation préférentielle (apparition d'une structure secondaire) était adoptée par certains des peptides préparés. De plus, la tyrosine en position N-terminale joue un rôle primordial dans le repliement du peptide puisqu'elle permet d'obtenir des molécules chirales selon qu'elle soit L ou D.

Enfin, la synthèse d'un insecticide (fipronil) couplé à un fluorochrome (la fluorescéine) a été effectué dans le but d'étudier le mécanisme d'élimination de ce dernier chez la D*rosophilia melagonaster*. Le composé développé à remplis les critères demandés, à savoir : stabilité, pas de perte d'activité et visibilité au microscope confocale, ce qui a permis de confirmer le mécanisme d'élimination du firponil sur ce modèle.

Bibliographie

(1) Kesharwani, P.; Iyer, A. K. Recent Advances in Dendrimer-Based Nanovectors for Tumor-Targeted Drug and Gene Delivery. *Drug Discov. Today* **2015**, *20* (5), 536–547.

(2) Grillaud, M.; Bianco, A. Multifunctional Adamantane Derivatives as New Scaffolds for the Multipresentation of Bioactive Peptides. *J. Pept. Sci.* **2015**, *21* (5), 330–345.

(3) Fattahi, A.; Lis, L.; Tehrani, Z. A.; Marimanikkuppam, S. S.; Kass, S. R. Experimental and Computational Bridgehead C–H Bond Dissociation Enthalpies. *J. Org. Chem.* **2012**, *77* (

(4) Lamanna, G.; Russier, J.; Dumortier, H.; Bianco, A. Enhancement of Anti-Inflammatory Drug Activity by Multivalent Adamantane-Based Dendrons. *Biomaterials* **2012**, *33* (22), 5610–5617.

(5) Prince, R. B.; Barnes, S. A.; Moore, J. S. Foldamer-Based Molecular Recognition. *J. Am. Chem. Soc.* **2000**, *122* (12), 2758–2762.

(6) Tew, G. N.; Scott, R. W.; Klein, M. L.; DeGrado, W. F. De Novo Design of Antimicrobial Polymers, Foldamers, and Small Molecules: From Discovery to Practical Applications. *Acc. Chem. Res.* **2010**, *43* (1), 30–39.

(7) Lamanna, G.; Russier, J.; Ménard-Moyon, C.; Bianco, A. HYDRAmers: Design, Synthesis and Characterization of Different Generation Novel Hydra-like Dendrons Based on Multifunctionalized Adamantane. *Chem. Commun. Camb. Engl.* **2011**, *47* (31), 8955–8957.

(8) Flacher, V.; Neuberg, P.; Point, F.; Daubeuf, F.; Muller, Q.; Sigwalt, D.; Fauny, J.-D.; Remy, J.-S.; Frossard, N.; Wagner, A.; Mueller, C. G.; Schaeffer, E. Mannoside Glycolipid Conjugates Display Anti-Inflammatory Activity by Inhibition of Toll-like Receptor-4 Mediated Cell Activation. *ACS Chem. Biol.* **2015**, *10* (12), 2697–2705.

(9) Mojsoska, B.; Jenssen, H. Peptides and Peptidomimetics for Antimicrobial Drug Design. *Pharm. Basel Switz.* **2015**, *8* (3), 366–415.

(10) Hainzl, D.; Casida, J. E. Fipronil Insecticide: Novel Photochemical Desulfinylation with Retention of Neurotoxicity. *Proc. Natl. Acad. Sci. U. S. A.* **1996**, *93* (23), 12764–12767.

Chapter I: Introduction

I. 1 Introduction to adamantane

Adamantane or tricycle[3.3.1.1^{3,7}]decane (figure 1) is a colorless crystalline chemical compound with the following chemical formula $C_{10}H_{16}$. It is a cycloalkane composed of four connected cyclohexane rings arranged in an armchair configuration. Among all the isomers with $C_{10}H_{16}$ formula, it is the most stable form.[1] The spatial arrangement of adamantane carbon atoms is similar to that of the diamond crystal,[2] which explains the name "Adamantane" that takes its origin from the Greek "adamantinos" (relating to steel or diamond).

***Figure 1**: Adamantane structures (source Pubchem).*

Adamantane was first isolated from petroleum by the Czech chemists S. Landa, V. Machacek and M. Mzourek in 1933.[3] They used fractional distillation to separate organic molecules of petroleum based on their boiling points. Due to the low natural source of adamantane (0,0001 to 0,03%) they only produced few milligrams of this molecule but they noticed its high boiling and melting points compared to other hydrocarbons. This discovery launched a new chemistry field studying the synthesis and properties of polyhedral organic compounds. The origin of diamondoids is still unclear. The absence of diamondoids in sediments and immature peats suggested that they are not product of a biosynthesis.[4] Thus, the formation of diamondoids most likely begins during early diagenesis, as supported by their detection in immature source rocks and coals. Additionally, artificial maturation of organic matter shows that diamondois can be produced during oil formation.[5] Currently, the formation mechanisms of lower diamondoids are mainly attributed to Lewis acid catalyzed rearrangements of polycyclic hydrocarbons[6] and high temperature cracking of high molecular mass fractions.[7]

The biodegradability of diamondoids has been investigated,[8] and has led to the conclusion that diamondoids are subject to biodegradation, especially adamantane, by following a possible microbial degradation pathway.

In 1941, Vladimir Prelog was the first chemist to successfully synthesize adamantane, but the process was too complicated for regular use. In 1956, the process was refined and simplified but it was still too complex for translation to an industrial scale. Finally, in 1957 Paul von Ragué Schleyer accidentally discovered a simple and efficient process of synthesis in two steps (figure 2).[9] Firstly, dicyclopentadiene was hydrogenated in the presence of a catalyst (Pt), then the resultant product was transformed into adamantane using a Lewis acid like $AlCl_3$. The driving force for the acid catalyzed rearrangement is provided by the high thermodynamic stability of the ring system obtained with a high degree of branched ring system.[10] Nowadays, adamantane costs less than 1$ per gram.

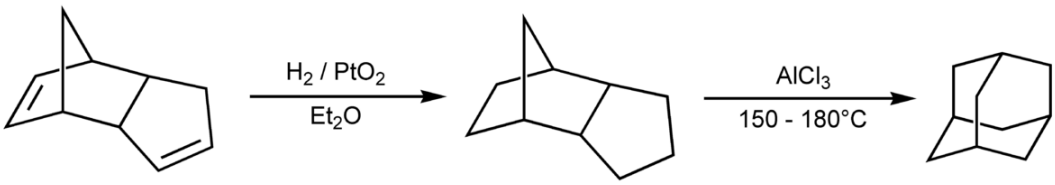

***Figure 2**: Synthesis of adamantane from dicyclopentadiene.*

The mechanism of adamantane rearrangements has been investigated[11] but still not fully elucidated. The difficulties involved are due to the rearrangement of the tricyclodecanes into adamantane, which is possible through several pathways. The crystal structure of adamantane has been investigated using electron diffraction by Nowacki.[12] He demonstrated that adamantane is characterized by a C-C bond distance of 1,54 ± 0,02 Å and a C-H bond of 1,11± 0,02 Å, and he confirmed the tetrahedral bond angles ($C_3C_2C_3$ angle = 109,8 ± 1,5°) (figure 3). The adamantane is highly symmetrical and at ambient conditions it crystallizes in a face centered cubic structure (F*m*3*m*, Z=4).[13]

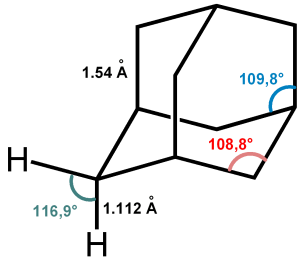

***Figure 3**: Adamantane structure.*

Moreover, the thermodynamic properties of adamantane have been revisited recently,[14] concluding that it has the physical state of a colorless solid and a melting point at 267 °C (higher than all other hydrocarbons with the same molecular weight). This high melting point is caused by the very rigid system, which needs for melting a considerable quantity of heat[15] and suggests a low entropy of fusion associated with a rotational transition in the solid state.[16] Adamantane smells like camphor, is insoluble in water but has a high solubility in many organic solvents. Nevertheless, water vapor distillation process can be applied and the compound has good thermal stability. Exclusively composed of CH and CH_2 bonds (called bridgehead and bridge positions) (figure 4), adamantane is highly reactive compare to other hydrocarbons.

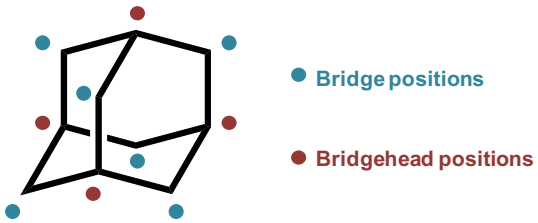

***Figure 4**: Adamantane is composed of two equivalent site, corresponding to the bridge and bridgehead position.*

Adamantane itself does not offer lots of applications. It is mainly used in some etching masks[17] and polymer formulations. In solid state NMR spectroscopy, adamantane is a common standard for chemical shift referencing.[18] Alkyl derivatives of adamantane showed potential technological applications, such as working fluid in hydraulic systems or, in the case of adamantane-based polymers, might find application for coatings of touchscreens.[19] In the biomedical field, the well-defined 3D conformation, the hydrophobicity and the lipophilicity provide to adamantane-based compounds favorable properties for their transport through biological membranes. The first adamantane derivative used as a drug was amantadine in 1967 as an antiviral drug against influenza virus[20] and since it can be used for both prevention and therapy of influenza A.[21] Soon after, it was found that adamantine is useful against Parkinson's disease[22] due to its capacity to inhibit *N*-methyl-D-aspartate (NMDA) receptors.[23] This was the begin of a novel and important research field leading to several drugs based on adamantane, like bromantane, dopamantine, memantine and rimantadine (figure 5).

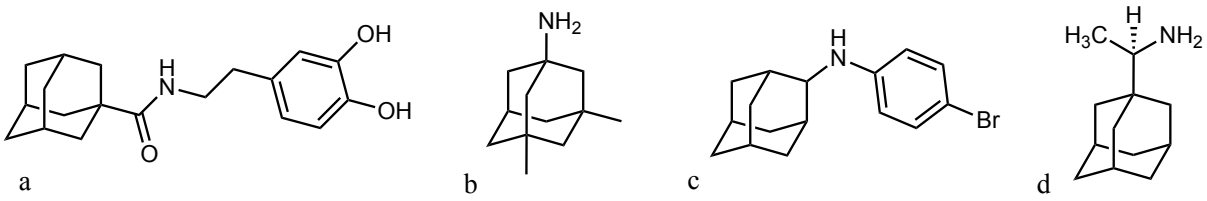

***Figure 5**: Adamantane in medicine: (a) dopamantine, (b) memantine, (c) bromantane, (d) rimantadine.*

I. 2 Functionalization of adamantane

I. 2.1 Adamantane reactivity

As explained in the previous section, adamantane is highly reactive compared to other hydrocarbons. It possesses six secondary and four tertiary carbons, which means that different positions of the backbone structure can be modified leading to functionalized adamantane with new properties. The most common reaction is certainly the C-H activation for the functionalization of the bridgehead positions. Indeed, these positions are really sensitive in electrophilic media and allow nucleophilic substitution at the saturated carbon atom following the S_N1 mechanism.[24] Compared to classic hydrocarbons composed of σ-bond, which are relatively inert, adamantane conformation is capable to stabilize the produced cations.[25] Indeed, one lob of the empty *p*-orbital extends into the adamantane cage leading to an overlapping by the three sp^3 bridgehead C-H orbitals resulting in a selective charge distribution to the bridgehead positions. This reactivity confirms that adamantane reacts like a system where all the carbons can interact together improving the stability of the charges. Even the dication 1,3-didehydroadamantane obtained from the 1,3-difluoroadamantane in a super acid solution shows high stability due to the three-dimensional aromaticity system (figure 6).[27,28]

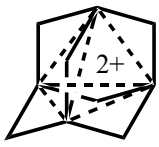

***Figure 6**: Adamantane three-dimensional aromaticity system.*

Moreover, the same effect was observed with radical anions, in this case the odd electron is located inside the molecular cavity of adamantane and spin-couple with the four bridgehead hydrogens.[26]

Another possibility developed for selective adamantane functionalization is the use of phase transfer catalysis (PTC). For example, halogenation reactions often lead to the production of mixtures. To avoid this lack of selectivity a nontraditional approach, combining radical chemistry initiated by single-electron transfer (SET) with phase transfer catalysis (figure 7),[29] has been developed. Due to the difference of concentration, the reactive species are confined into a small interphase zone, thus, the products are at lower concentration in the reactive region avoiding unselective over-functionalization (figure 7).

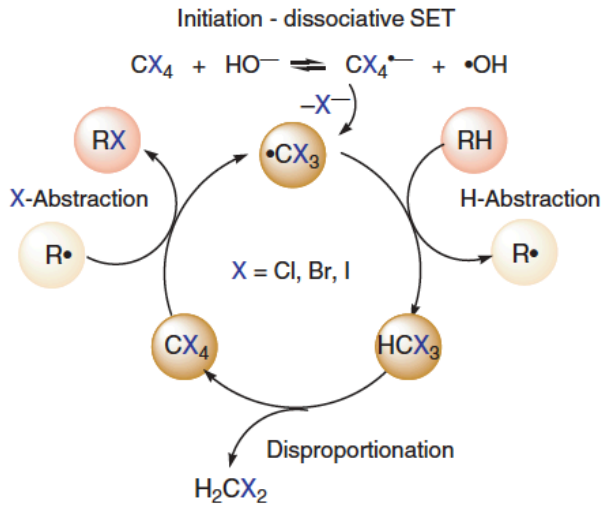

***Figure 7**: Phase transfer catalytic approach to alkane halogenation[29].*

The bridge position reactivity was also investigated. Poorly reactive compared to the bridgehead positions, the methylene positions of adamantane react under special conditions. Treatment of adamantane with 96% H_2SO_4 at 77 °C for 5 h gives adamantanone.[30] After investigation of the mechanism using D_2SO_4, it has been demonstrated that the mechanism involves an equilibrium between the 1- and 2-adamantyl cations *via* intermolecular hydride transfers. Apparently, it is a fast second order reaction. Starting with 1-hydroxyadamantane the reaction affords better yield (70-80%) of 2-adamantanone.[31] These experiments confirmed that the final product obtained depends on the concentration of 1-hydroxyadamantane and sulfuric acid, the temperature and the duration. Geluk and Schlatmann also studied the mechanism of the reaction confirming that it starts with an equilibrium between 1-hydroxyadamantane, adamantane and 1,3-dihydroxyadamantane called disproportionation reaction of 1-hydroxyadamantane (figure 8). They demonstrated that 1,3-dihydroxyadamantane is not involved in the formation of adamantanone. Then, adamantane can be re-oxidize to give 1-hydroxyadamantane followed by its isomerization to 2-hydroxyadamantane due to hydride transfer reaction (they isolated small amounts of secondary alcohol). Finally, oxidation of 2-

hydroxyadamantane gives the desired 2-adamantanone. This route of synthesis is the main one to synthesize adamantane derivatives functionalized on position 2.

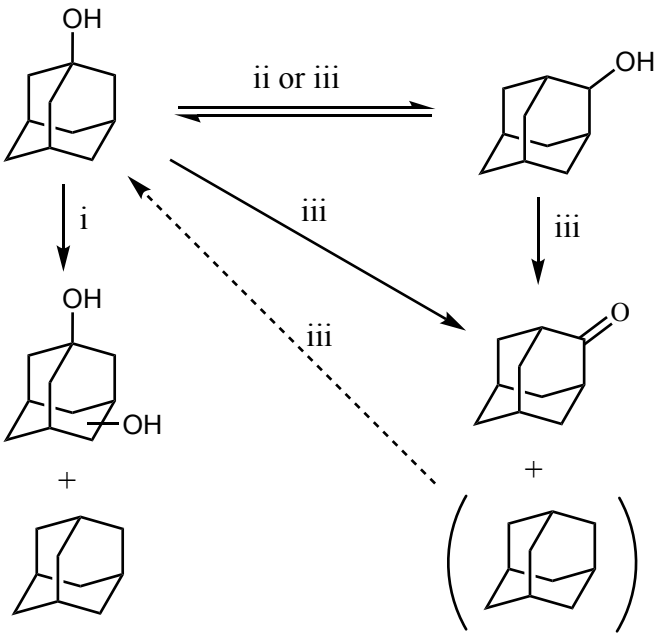

i: 70 % H_2SO_4 (aq); ii: conc H_2SO_4, rt; iii: conc H_2SO_4, heat

***Figure 8**: Mechanism of 2-adamantanone synthesis, an example of the bridge position functionalization.*

I. 2.2 Bridgehead position functionalization

During these last decades, the chemists were more focused on exploring the reactivity of the bridgehead positions. More reactive and more selective, they allow the synthesis of mono, bi, tri or even tetra substituted adamantane derivatives (figure 9).

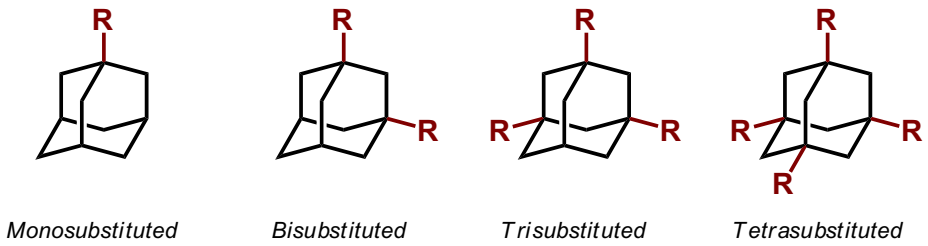

***Figure 9**: Adamantane bridgehead position polysubstituted derivatives.*

Both approaches (C-H activation or PTC protocol) are tools for the functionalization and multi-functionalization of adamantane. One of the most useful functionalization is halogenation, which allows to obtain reactive precursors for further reactions. Unfortunately, the reactivity of

each bridgehead position is strongly influenced by the substituents at the other bridgeheads especially with electron withdrawing groups. For example, for bromination of adamantane, we observe that, the introduction of each additional bromine decreases the reactivity of the system for the next bromination.[24] Thus, harsh conditions are required to produce tribomo- and tetrabromoadamantane (figure 10).

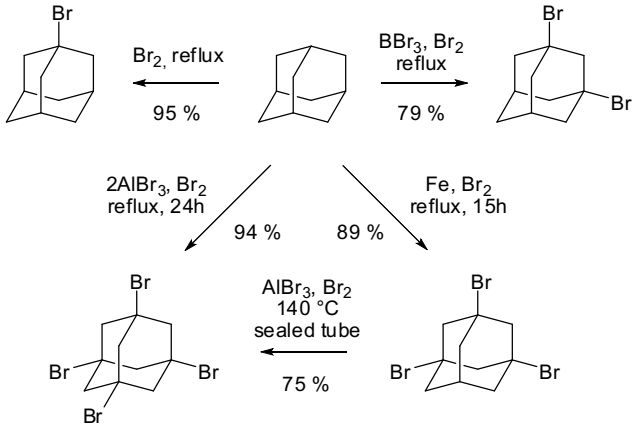

***Figure 10**: Multi-bromination of adamantane.*

Other strategies have been developed to obtain adamantane halides derivatives. Another example is the step-by-step synthesis. One hydroxyl group is introduced on the bridgehead position of adamantane carboxylic acid and then, replaced by fluorine.[32] The same step is repeated to obtain mono- di- or tri-fluorinated derivatives of adamantane carboxylic acid (figure 11).

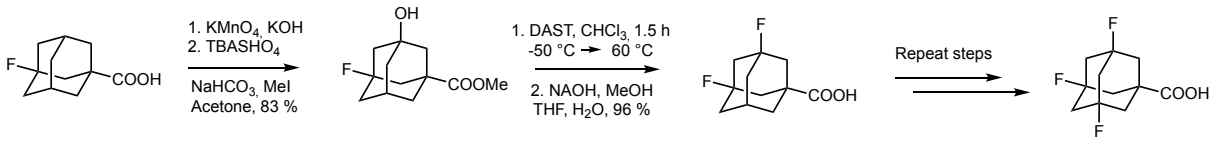

***Figure 11**: Adamantane fluorination using step-by-step strategy.*

The second possibility is a direct fluorination of adamantane using pentafluoride[33]. Playing with temperature and equivalent, selective preparation of 1-fluoroadamantane can be achieved with a final yield up to 90 %. In contrast, using an excess of iodine pentafluoride and carrying out the reaction a 75 °C leads to 1,3-difluoroadamantane selectively. Neither trifluorination nor reaction on bridge positions were observed. Finally, the tetrasubstituted was achieved by electrochemistry (figure 12)[34]. The use of Et_3N-5HF, as fluorine source and as electrolyte, has the advantage that oxidation potential is controlled and only the desired reaction occurs.

Moreover, functional groups, such as ester, cyano and acetoxy can tolerate the reaction conditions so that fluorination can be performed on functionalized adamantane.

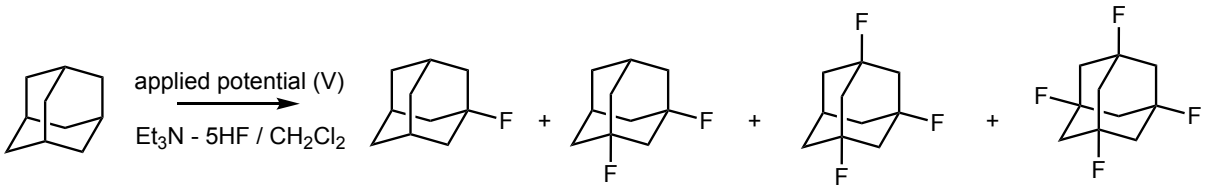

***Figure 12**: Adamantane selective fluorination by electrochemistry.*

Halogen exchange has been investigated using appropriate treatments. Boron tribromide seems to be the most useful reagent to replace fluorine by bromine. Indeed, even the tetrafluoroadamantane is transformed into tetrabromoadamantane in presence of BBr_3 at 70 °C. On the other hand, halogen exchange between bromine and fluorine was successfully achieved using ZnF_2 or AgF. In the case of monohalogenated derivatives the simplest way of synthesis is the utilization of the appropriate hydrogen halides (figure 13).[24]

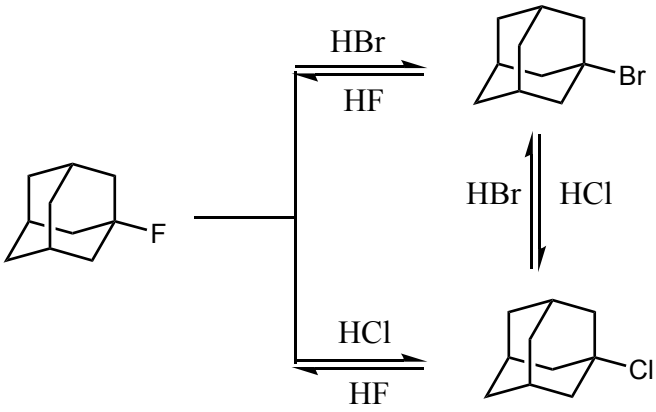

***Figure 13**:Halogen exchange on monohalogenated adamantane derivatives.*

The next step is the multi-functionalization of adamantane by halides leading to a pseudotetrahedral stereogenic center. The synthesis of polyhaloadamantanes has been done following multi-steps of phase transfer catalysis.[35] Using this approach, it is possible to add the desired halides one by one in the free bridgehead position, resulting into the desired tetrahaloadamantane. As expected, the yields obtained are quite low.

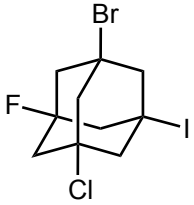

***Figure 14**: Polyhaloadamantane synthesized following PTC multi-steps.*

In parallel, in order to conjugate adamantane with biomolecules like amino acids, peptides, or sugars, various reactions of functionalization have been developed to obtain alkyl, amine, carboxylic acids, alcohols and nitro adamantane derivatives.[36] The other possibility is the introduction of alkyne or azide which can react with a high yield via copper catalyzed azide alkyne cycloaddition (CuAAC).[37] Starting from adamantane or its halogenated derivatives, and following the reactivity of adamantane in electrophilic media or using the PTC protocol, it results easy to selectively functionalize adamantane with the desired functional groups. For example, the alkylation using Grignard reaction involving a halogenoadamantane and an alkyl magnesium halide, is a possibility to alkylate adamantane with a good yield.[38] It must be noted that the alkylation mechanism involves, in general, an S_N2 mechanism, but in the case of adamantane derivative, it is incompatible. Ohno *et al*. described this mechanism as a S_Ni-like substitution, where the Grignard reagent acts both as a nucleophile and a Lewis acid.[38] In order to complete the reaction, the solvent must be a non-Lewis basic medium such as dichloromethane. These different possibilities to functionalize adamantane are the starting points of using adamantane like a building-block, rigid and easy for multi-functionalization.

I. 2.3 Adamantane as a building block

The (3+1) combination of functional groups is the most useful multi-functionalization of adamantane. Indeed, even if we lost a degree of symmetry, the C_3 symmetry still plays an important role in various artificial and natural recognition systems.[39] The binding sites of enzymes have often a pseudo C_3-symmetric geometry and in many cases, after binding of a given receptor to its substrate, a receptor ligand complex with a threefold geometry is observed.[40] C_3-symmetry also plays a role in other areas like asymmetric catalysis,[41] self-assembly[42] or molecular recognition.[43]

Different strategies are possible for multi-functionalization of adamantane to obtain a (3+1) building block (figure 15).[44] The first route involves the desymmerization of a tetrasubstituted adamantane derivative. The second route involves a trisubstituted intermediate which is then functionalized with the effector (B). Finally, the last route is exactly the opposite of route 2, the intermediate is a monosubstituted adamantane which is then converted into the desired product by adding the three ligands on the three bridgehead positions. The latter is not often used despite the fact that lots of commercially mono-substituted derivatives are available.

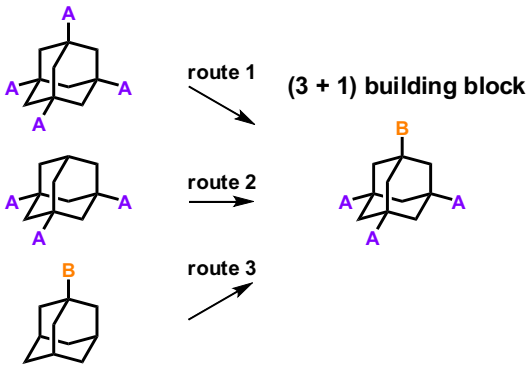

***Figure 15**: Routes of synthesis to adamantane (3+1) building blocks.*

The advantages of this design are the multivalency effect due to the three functionalized positions (positions A) and the free bridgehead position (position B), which can be modified to improve the characteristics of the molecule without affecting the threefold geometry of the scaffold. Following these approaches rigid and semi-rigid scaffolds based on adamantane have been synthesized.[44] The purpose is to attach rigid or flexible linkers to achieve the optimal geometry and spacing, depending on the application desired. For the synthesis of rigid structures, triphenyladamantane has been chosen as precursor. It is easy to obtain starting from commercial bromoadamantane[45] and it reacts via a retro-Friedel-Craft reaction. Then, the triphenyl groups are subjects of oxidative degradation,[46,47] leading to the intermediate tricarboxylic acid with an excellent yield. This tri-acid can be reduced to obtain the corresponding trialcohol (figure 16A). Another possibility is to use ethynyladamantane as precursor (figure 16B). Indeed, its synthesis is quick and starts from tribromoadamantane *via* radical reaction. Then, the compound can be used for chemoselective conjugaton with biomolecule *via* click chemistry. On the other hand, it can be also used as another precursor for rigid and semi-rigid analogs. For example, after deprotonation by lithium base (MeLi), it reacts with carbon dioxide forming a tricarboxylic acid derivative with a very good yield. Then it can be reduced by H_2 on Pd/C to give a semi-rigid triacid. Some other reagents can be used as electrophiles to quench the highly reactive species formed by the base, like formaldehyde, to give the corresponding trialcohols.

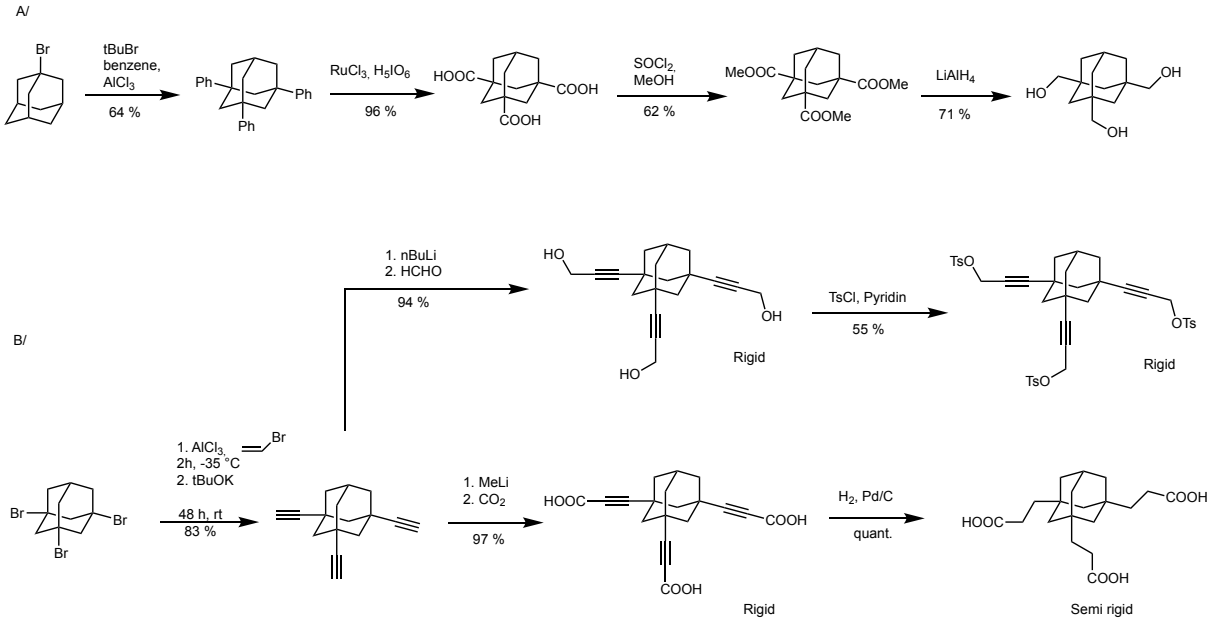

***Figure 16**: Synthesis of diverse tripodal rigid and semi-rigid adamantane-based building blocks.*

Depending on the desired applications, it could be interesting to optimize the rigidity and spacing of the scaffold, by introducing, for example, flexible linkers between the adamantane core and anchor groups. An additionally simple route of synthesis starts from commercially available tribromoadamantane (figure 17), which reacts *via* radical reaction with activated species (alkene functionalized with nitrile group). Then, the compound can be hydrolyzed to give the corresponding tricarboxylic acid or reduced to give the corresponding triamine. Both are easy to use for attaching some ligand using the classic peptide bond formation. Moreover, the tricarboxylic acid is a suitable starting material to obtain the trialcohol derivatives throughout esterification and reduction of the compound.

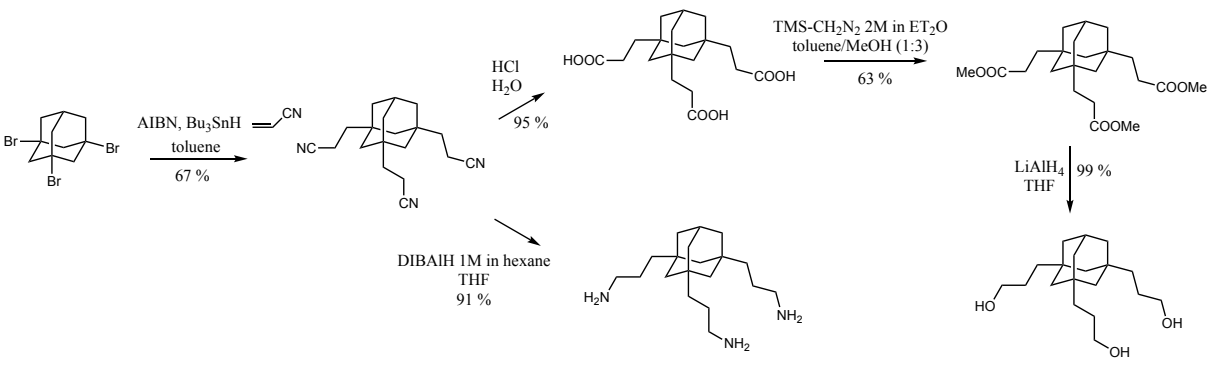

***Figure 17**: Synthesis of tripodal semi-rigid adamantane.*

Following these strategies, libraries of (3+1) building blocks have been synthesized and functionalized with chemical functions like cyano, amino, carboxylic acids, azido and alkyne groups with different spacer lengths to control the rigidity of the molecule depending on the desired applications.[48,44,49]

To finish, I wish to describe the aminoadamantane-1,3,5-tricarboxylic acid building block, which is the base of all my thesis work. The synthesis of the latest has been developed by our group.[50] It was developed on a five step process, starting from the commercially available bromoadamantane (figure 18), with a good yield and without need of silica gel column purification for each intermediate.

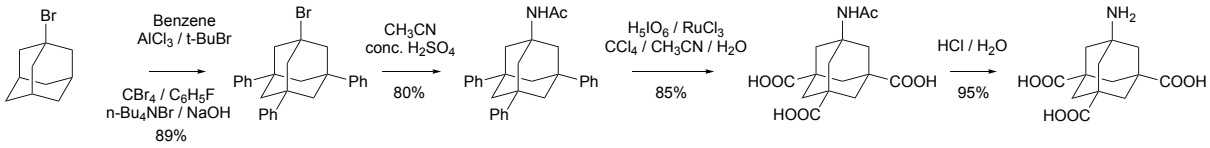

***Figure 18**: Synthesis of adamantane (3+1) building block.*

First bromoadamantane reacts by retro Friedel-Craft reaction with benzene in presence of a Lewis acid and *t*-butylbromide to give the 1,3,5-triphenyladamantane. Then, it is converted to 1-bromo-3,5,7-triphenyladamantane following the Schreiner protocol. The bromide derivative is a suitable substrate for the Ritter reaction with acetonitrile, leading to the corresponding *N*-acetylamide derivative. Oxidative degradation of phenyl groups by ruthenium catalysis allows the formation of a tricarboxylic acid derivative, which is finally hydrolyzed to obtain the (3+1) building block aminoadamantane-1,3,5-tricarboxylic acid. This practical approach affords a scaffold for complex structures with a C_3-symmetry, especially in the case of my thesis, for the synthesis of dendron-based on adamantane.

I. 3 Dendritic nanoparticles

I. 3.1 Introduction to nanoparticles

Following the definition from the international organization for standardization (ISO), nanoparticles are described like nano-objects with at least one dimension in nano-metric scale (less than 100 nm). Under this denomination, we can find different sort of nanoparticles like micelles, liposomes, nanoshells, quantum dots, polymers and dendrons/dendrimers.

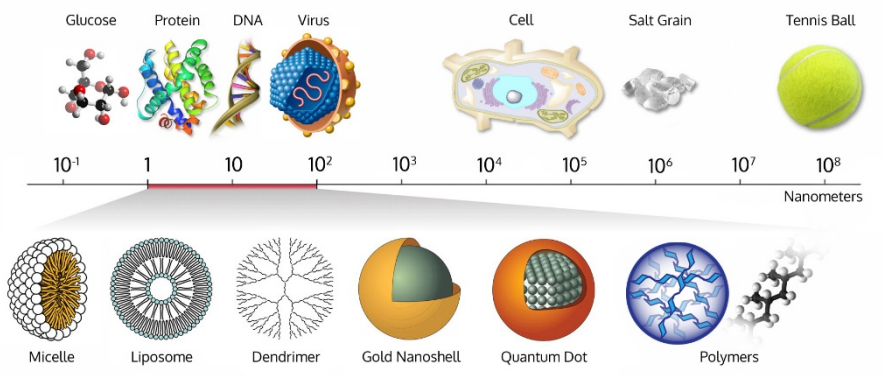

***Figure 19**: Representation of different classes of nanoobjects (whichlab.com).*

Nanoparticles are classified in two categories according to their origin: 1) natural, or 2) anthropogenic (produced by Humans). Anthropogenic nanoparticles are then further divided in two additional categories: the unintentional particles, like the particles produced by combustion of hydrocarbons (diesel), and the desired nanoparticles that are of synthetic origin. The development of this new class of nano-objects has opened new fields of applications commonly grouped under the term Nanotechnology. The interesting properties of these particles are due to two main parameters. First the high surface/volume ratio, which leads to a remarkably increased reactivity of the particles. Then their sizes, which endow unique characteristics. This combination gives to the nanoparticles different physicochemical characteristics, which impart unique properties. Nowadays, the nanoparticles find applications in lots of fields such as materials science, biology, medicine and food. This latest is currently under observation due to the famous E171. This white pigment made of titan dioxide nanoparticles showed an increased risk of chronic intestinal inflammation and carcinogenesis against orally exposed rats.[51] However, the nano-foods are promised to a bright future through interesting products like active oil emulsions (Shemen Industries), which inhibits cholesterol diffusion in blood. Or even, in their utilization as smart packaging for food storage, due to antibacterial properties to protect food. In nanomaterials, nanoparticles also find a large number of applications like self-cleaning

glass (TiO_2 nanoparticles react under UV and destroy dust), electrochromic glass and smart painting. For example, Ecopaint from British firm Millennium chemicals is a painting able to purify ambient air. The same trend is observed in other fields like informatics and more particularly in nanomedicine. An interesting application of nanoparticles have been developed in corneal transplantation. Indeed, due to immuno rejection after corneal transplantation, patients display a long-term graft failure. To treat this symptom, patients use steroids as immunosuppressive agents. However, steroid drops are rapidly cleared from the surface of the eyes and so, the treatment requires frequent dosage (once every 2 h). To improve the efficiency of steroid delivery, Scientist use poly(lactic-co-glycolic acid) nanoparticles, which are biodegradable and can provide sustained release of corticosteroid.[52] The results are impressive: sustained release for 15 days *in vitro* and sustained ocular drug levels for at least 7 days (as tested on rats). Moreover, no corneal allograft rejections were observed during the 9 weeks of the study. In our case, we are interested by dendritic nanoparticles and their applications especially in nanomedicine.

I. 3.2 Dendrons and dendrimers

Dendrons and dendrimers were discovered in the early 1980s[53], they are macromolecular hyperbranched compounds, made of series of branches around a central core.[54] Due to their sizes they are considered as nanoparticles. The properties of the dendrimers are linked to the chemical nature of their skeleton and their periphery. The most used are PPI (poly-(propylene imine)) and PAMAM (poly-(amidoamine)) dendrimers. Dendrons can be described as a branch of a dendrimer (Figure 20).

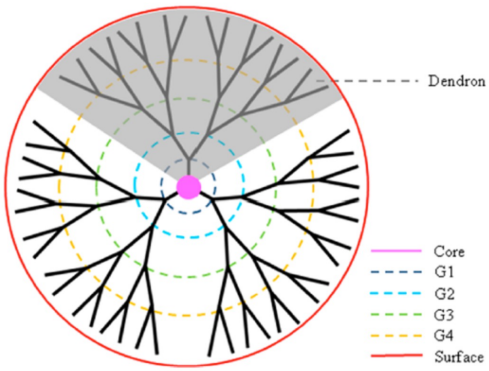

***Figure 20**: Representation of a dendron and dendrimer.*[55]

Both dendrons and dendrimers have advantages and disadvantages. Indeed, a dendron is less symmetrical and loses a part of the globular shape. However, the access to the focal point (at the core) allows its multi-functionalization.

Contrarily to other nanoparticles and nanomaterials like carbon nanotubes or graphene, dendrons and dendrimers can be synthesized following classic organic chemistry strategies. The synthesis of dendrimers can be achieved by two different ways (Figure 21). The first is called "divergent synthesis" (Figure 21a). In this case, each generation is added layer-by-layer. The second is the "convergent synthesis" (Figure 21b). In this top-down approach, different blocks of the final compound are synthesized separately before being attached to the central core in the final step.

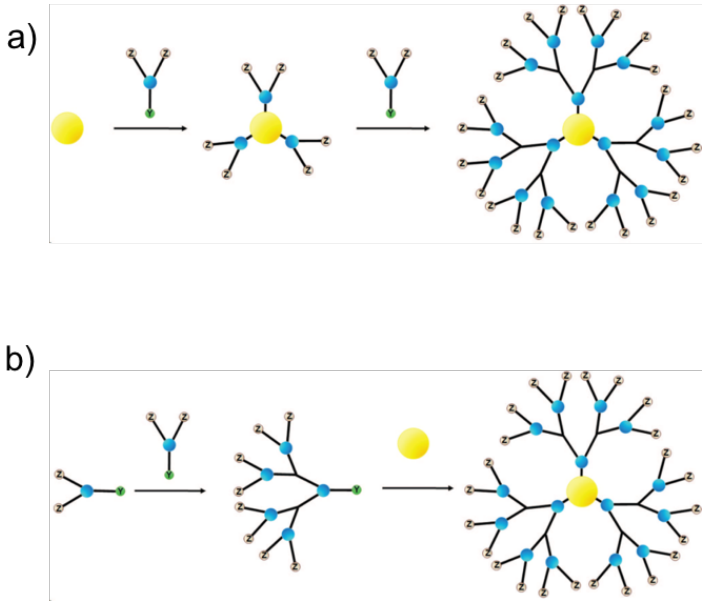

***Figure 21**: Dendrimer route of synthesis (a) divergent, (b) convergent. Adapted from literature.*[56]

Usually, convergent method is preferred, especially in the case of higher generation dendrimers where the divergent method showed lower yield and polydispersity.[57]

I. 3.3 Dendrons and dendrimers in nanomedicine

Dendrons and dendrimers have resulted very useful in nanomedicine,[58] mainly because of their size range (they are considered as nanoparticles) and their ability as vectors of therapeutic agents. Indeed, their relatively small size confers to dendrons unique characteristics. One of these characteristics is called EPR effect for enhanced permeability and retention (Figure 22). The EPR effect is a passive targeting of cancer cells that was observed for the first time by

Maeda and his colleagues in the 80's. As a matter of fact, they noticed a selective accumulation of macromolecules into tumor tissues (up to 200 times higher) compared to normal tissues such as skin, muscle, heart or kidney.[59] This phenomenon is actually due to angiogenesis, which is one of the most important features of tumors characterized by a sustained rapid growth and defective blood vessel architecture, leading to the formation of a large gap between endothelial cells and a lack of smooth muscle layers. Due to these characteristics, the nanoparticles can go through the cells and accumulate into the tumor.[60] Furthermore, the defective lymphatic function observed in tumor tissues has been shown to be in favor of the retention of the nanoparticles for long time.[61] This effect can be further increased using nanoparticle coated with hydrophilic polymers like PEG. Pegylated nanoparticles appear to be highly efficient in improving the pharmacokinetics, mainly because the coating allows them to escape an important body defense, which is the reticuloendothelial system (RES). In fact, the PEG coat improves the colloidal stability and prevents the uptake of the nanoparticles by the RES. It forms a protective hydrophilic layer on the surface of the nanoparticles, offers steric stabilization and prevents their self-interactions, thus avoiding the formation of aggregates. Finally, PEG coating reduces the uptake of the particles by macrophages and increases their the blood circulation time.[62,63]

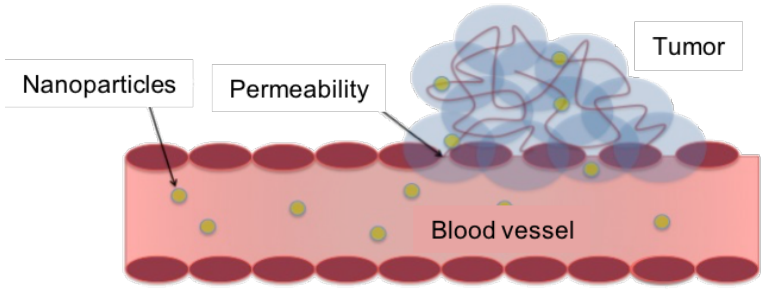

***Figure 22**: Representation of the enhance permeability and retention effect – a passive targeting of Npts. Adapted from literature.*[64]

Nevertheless, while the EPR effect has been well investigated in small animal models, clinical data is still missing. For example, Doxil® (a doxorubicin-loaded PEGylated liposome) failed to show drastic enhanced tumor accumulation over free doxorubicin, indicating that EPR concept is unreliable in human tumors.[65] Doxil® has been approved in 1995 by the FDA only five years after its development.[66] Its therapeutic efficacy was superior in ovarian cancers compared to standard therapies, while equivalent in metastatic breast cancer. Doxil® main advantage is the reduction of cardiotoxicity due to a decrease of doxorubicin exposure to

cardiomyocytes. However, the toxicity was increased for other therapies, especially the skin toxicity resulting from the extended circulation time of the drug. Thus, animal models used to study EPR in laboratories are certainly not sufficiently accurate and require reconsideration. Indeed, human cancers differ from murine tumor models in several aspects like the rate of development, the relative size of the host, the metabolic rate and the host's lifespan.

Luckily, another possibility for targeting cancer cells remains and is the active targeting. In this case, a dendron can be functionalized with a molecule or a biomolecule like a peptide, a sugar or an antibody with a strong affinity for the receptors over-expressed by cancer cells. Specific targeting is indeed quite important in medicine. It helps to decrease the potential side effects produced by a lack of selectivity of a molecule. Moreover, the selectivity allows to decrease the dose, meaning once more lower side effects.

Dendrons and dendrimers are also interesting for another property: their multivalent interaction. Multivalency or polyvalency is a naturally occurring phenomenon playing an important role in self-assembly of matter, in the recognition processes and signal transduction in a range of biological systems. It can be described like a multiple interaction between a host and his receptor, resulting in an addition of weaker connection to obtain a stronger, but still reversible interaction (Figure 23). This behavior can be explained by four different situations, the first being a binding event favoring a second and further binding (A), also described as the "chelate effect". The second situation is the recruitment of another receptor to form clusters (B). The third one is a binding of primary and secondary sites (C). The last possibility is a high local concentration meaning a high affinity toward a single receptor (D).

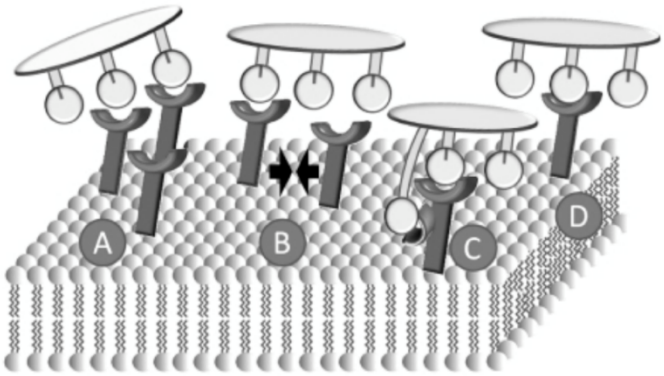

***Figure 23**: Representation of the multi-valency effect. Adapted from literature.*[67]

I. 3.4 Dendrons as nanovectors

Many molecules with potential activity are discovered every day. Unfortunately, most of them are not active *in vivo,* because of various reasons like instability, toxicity, short half-time circulation, low solubility or low permeability. One solution to overcome these hurdles is the vectorization. The idea of using biocompatible tools, loaded or functionalized with drugs (peptides, proteins, nucleic acids, etc.), in quantity enough to be efficient, able to pass through cell membranes and displaying no toxicity, has been proposed at the end of the 19th century by Paul Ehrlich.[68] Because of their intrinsic properties (size, shape) dendrons are interesting systems for vectorization of the drugs. They can be loaded using non-covalent interactions such as hydrogen bonds, ionic forces, van der Waals forces, π-stacking or hydrophobic interactions. In this case, the drug is located inside the dendron. This method is interesting for the delivery of hydrophobic drugs. Indeed, the interaction of dendrons with the molecular environments is controlled by their terminal groups. Thus, it allows to increase drug solubility. The two main disadvantages are the risk of drug release before reaching the target and the instability.

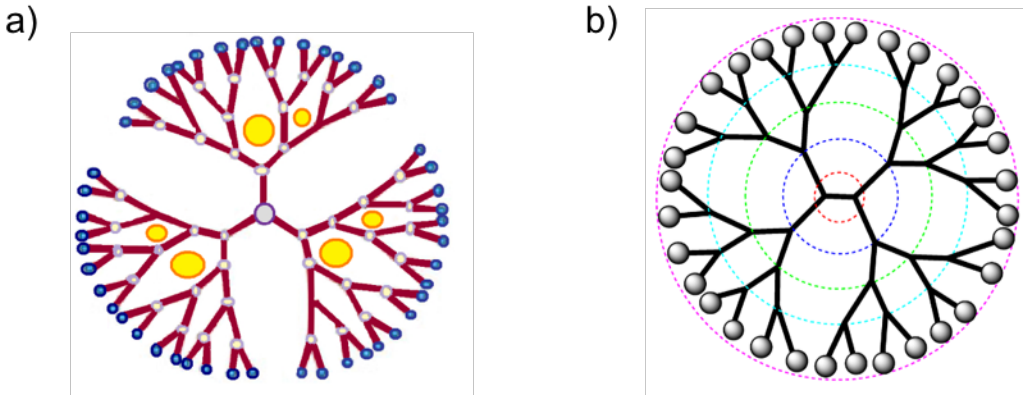

***Figure 24**: Functionalization of dendrimer: (a) non-covalently, (b) covalently. Adapted from literature.*[69]

Another possibility is the covalent functionalization. Covalently linking a drug allows to control the drug release thus reducing non-specific toxicity. Moreover, the molecules are more stable and stay longer in the bloodstream. The downside in this case, is the solubility. Indeed, the compound is attached on the periphery meaning that it will directly play a role in the particle solubility. Moreover, in the case of vectorization of drugs, the active molecules must be released after cellular uptake. For this purpose, different tools have been developed to control the drug release based on the differences between intra and extracellular conditions. For example, the

glutathione (GSH) is a natural reducing agent present in the cell and at high concentrations in cancer cells. This means that disulfide bonds can be reduced once inside the cytoplasm leading to the drug release. Different chemical functions sensitive to specific stimuli, such as photo-cleavable linkers, pH sensitive linkers, redox potential and enzymatic sensitivity, can be used to improve drug release. The functionalization of the dendrons or the dendrimers with polycationic derivatives is another alternative solution to complex DNA and use them for gene delivery. These different possibilities of functionalization make dendrons tunable since they can be functionalized to gain specific properties and thus be useful for many biomedical applications.

I. 3.5 Multi-functionalization of dendrons

As explained before, the dendrons can be described as a branch of the dendrimer. Their main advantage is the access to the focal point, which holds the possibility to functionalize selectively the periphery and the focal point resulting in multi-functionalization. If we take as an example the dendrons developed in our laboratory, we can observe that they have a protected amine at the focal point and a 3^n methyl ester functions on the periphery (with n = number of generation). Thus, the amine or the carboxylic acids can be selectively deprotected for further functionalization.

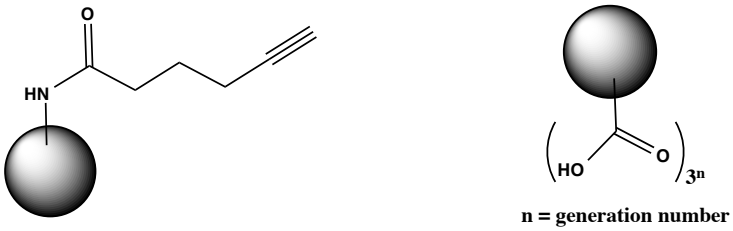

***Figure 25**: Dendron functionalization (focal point and periphery).*

For example, the amine can be functionalized with an alkyne group, which is known to be highly reactive with azide derivatives *via* CuAAc. With only one position available, the azide can be used to attach targeting groups (i.e. peptides, antibodies), fluorophores or lipophilic groups. In the periphery, where the number of positions is higher, it is instead more interesting to attach drugs to exploit the multivalency effect, cationic derivatives for gene delivery or sensitives linkers for drug delivery. Thus, dendrons can be easily multi-functionalized. The advantage of multi-functionalization is that it permits combinations of a therapeutic molecule

with a diagnostic component in a single particle. These particles are called theranostics (merging of therapy and diagnostics). Theoretically, a nanoparticle-based theranostics agent can release therapeutics to a diseased area and can utilize its imaging functions to make better diagnosis and supervise the therapeutic response.[70] These combined properties afford the possibility to personalize molecular medicine for example in cancer.[71,72]

I. 4 Adamantane to build dendritic nanoparticles

Dendrimers, as explained previously, are synthesized following classical organic synthesis, which allows molecular engineering. The main limit of the synthesis is the steric hindrance. To optimize the synthesis, different types of dendritic scaffolds have been developed.[58] The idea to use adamantane to build dendritic structures was conceived to explore and exploit the characteristics of its structure. The first dendtritic macromolecules based on adamantane were isolated in 1991 by G.R Newkome who described it like a "cascade polymers" reactions,[73] whereas actually, the appropriate term is "generation". Newkome used adamantane tetracarboxylic acid as the core. After activation of carbonyl with $SOCl_2$ to generate the corresponding tetraacyl chloride, he mixed it with di-*tert*-butyl-4-amino-2-[(*tert*-butoxycarbonyl)ethyl]heptanedioate and obtained the first generation dendrimer, protected in periphery as *tert*-butyl esters. The esters were easily hydrolyzed in acidic conditions to give the free acids. Then, using coupling agents in DMF and the previous amine, he obtained the second generation of the dendrimers. Finally, he developed a divergent synthesis of dendrimer using adamantane core based on a protection/deprotection strategy to control the growth of the dendrimer. Following this idea, different functional groups have been inserted on the adamantane core to control the reaction such as aminoacetoxy for Michael addition or azidoacetoxy for click chemistry, both combined with a protection/deprotection strategy.[57] Unfortunately the results showed the difficulty to obtain higher generation dendrimers and thus Newkome developed a two steps convergent method for this synthesis. The first step consisted in synthesizing dendritic segments using protection/deprotection steps. Then, the second step consisted in coupling the dendritic structures on the adamantane core using classical peptide bond synthesis.[57] The convergent synthesis allowed to obtain the first, second and third generation dendrimers based on an adamantane core.

In our laboratory, we are particularly interested in dendrons based on multifunctionalized adamantane. We developed a new synthetic strategy based on aminoadamantane-1,3,5-tricarboxylic acid as a building block and methyl-6-aminohenoate as a spacer. The main difference with previous dendrimers is the utilization of an adamantane derivative at each step (Figure 26).

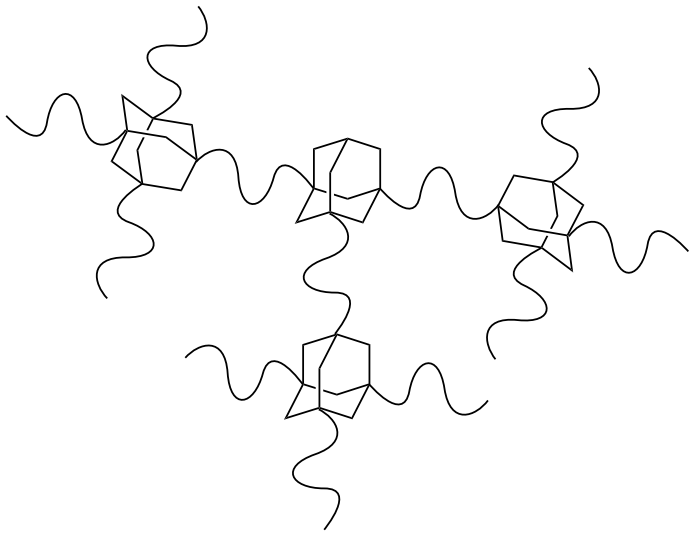

***Figure 26**: Illustration of dendrons made of adamantane.*

Usually, adamantane is only used as a core. In this case, adamantane is used for each ramification to obtain a novel type of adamandane-based dendrons called HYDRA*mers*.[50]
The name HYDRA*mers* was inspired by its structure which resembles the mythological nine-headed serpent-like beast, the hydra. Playing with orthogonal protection of the aminoadamantane using Boc-protection at the focal point, the three carboxylic acids selectively react with three methyl-6-aminohexanoate chains *via* peptide bonds formation providing the first generation dendron. The obtained dendron is fully protected (Boc at the focal point and methyl esters on periphery). This strategy allows to control the reaction and avoid side reactions. Then, the compound was split in two parts. The first one is Boc deprotected and the second one is hydrolyzed to give the corresponding three acid derivative. Both can react together leading to the formation of second generation adamantane-based dendrons. Finally, following a convergent synthesis, second and third generation adamantane-based dendrons have been isolated. Moreover, this selective protection strategy allows to easily and selectively functionalize the dendron. The cytotoxicity of these dendrons has been evaluated in cell lines and appeared low even at high concentrations (up to 100 μM). Moreover, the functionalization of the first and second generation HYDRA*mers*, with an anti-inflammatory drug (ibuprofen),

enhanced the anti-inflammatory activity of the drug *in vitro* in RAW 264.7 and primary macrophages.[74] The second generation dendrons have better anti-inflammatory potential than the first generation, and both are more efficient than ibuprofen alone. These results confirmed the potential of multivalency for therapeutic applications. More recently, our group developed polycationic adamantane-based dendrons of first and second generation (Figure 27 and 28).[75] These molecules were built from different adamantane scaffolds using short ethylene glycol chains as linkers to improve flexibility, biocompatibility and solubility in water. The first and second generation HYDRA*mers* were functionalized with cyanine 5 at the focal point, covalently linked *via* click chemistry. This labeling with a fluorescent dye allows cell imaging and the evaluation of cellular internalization. The periphery was functionalized with ammonium and guanidinium groups. The polycationic HYDRA*mers* displayed an improved biocompatibility compared to other polycationic dendrons. Moreover, the cellular uptake analysis provided a combination between active and passive uptake mechanisms dependent on cell types, dendron peripheral groups and dendron generations. However, in all cases, the HYDRA*mers* were well internalized by both phagocytic and nonphagocytic cells. Finally, these polycationic dendrons did not show cytotoxic effect compared to other polycationic carriers resulting very promising for biomedical applications.

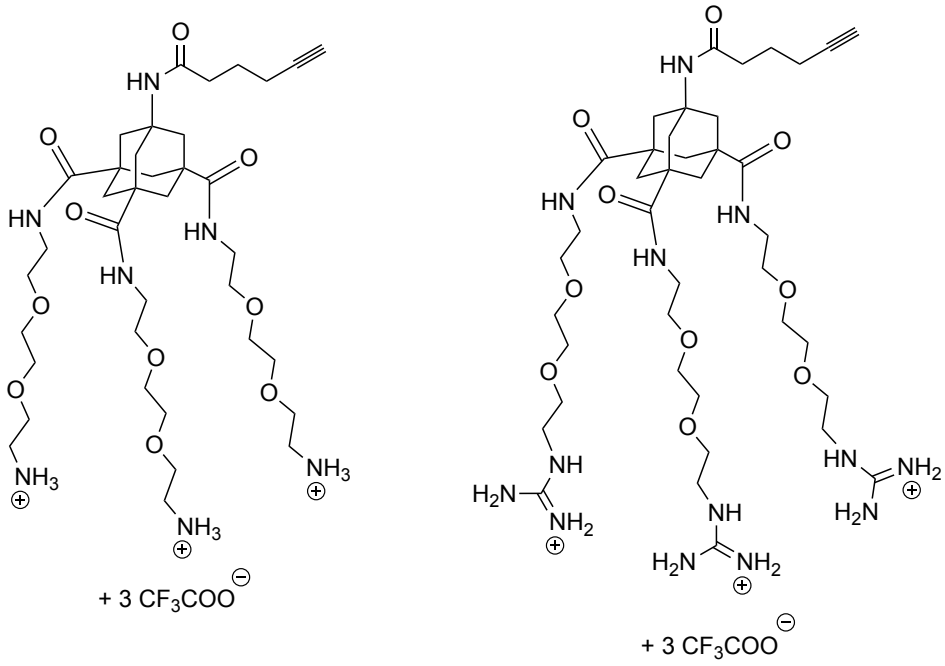

***Figure 27**: 1st generation adamantane based polycationic dendrons developed in our laboratory.*

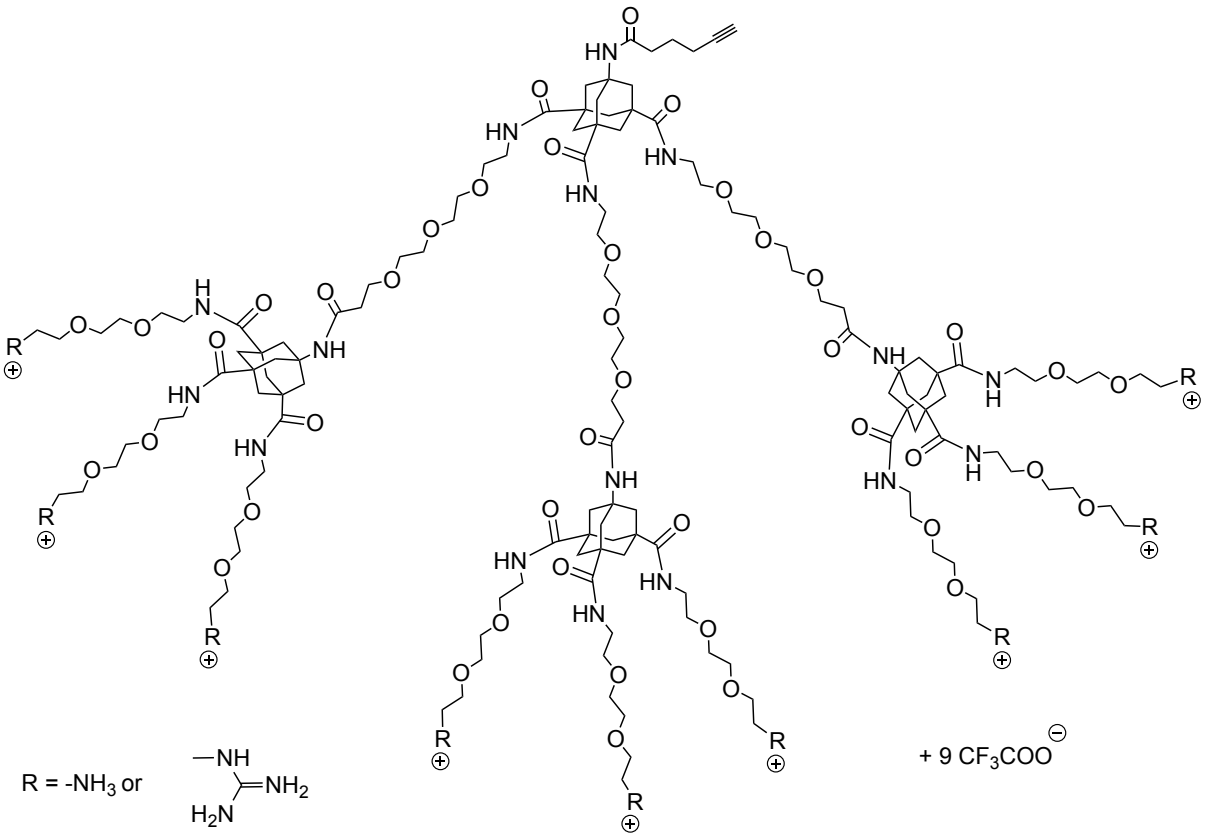

***Figure 28**: 2nd generation adamantane based polycationic dendrons developed in our laboratory.*

I. 4.1 Gene delivery

The interest in gene therapy has increased considerably this last years due to the promising treatment of many diseases.[76] Indeed, gene therapy allows introduction of foreign genomic materials into host cells to elicit a therapeutic benefit. During the last three decades, numerous viral and nonviral gene delivery systems have been developed.[77] Viral vectors, like retroviruses, adenoviruses and herpes viruses are common systems for gene therapy. Their genome is modified to disrupt their replication and make them safer. However, they still display a potential oncogenicity or are associated to immunogenic effect.[78] To solve this problem, nonviral vectors have been developed. Even if they are less efficient in gene transduction, they offer several advantages. Indeed, they are easy to produce, have no limitation for the transgenic DNA size and are less prone activate the immune system.[79] Among the nonviral delivery systems, chemical systems appear to be the most useful. Generally, they consist on nanometric complexes like liposome, micelles, positively charged dendrimers or cationic polymers. In the presence of a nucleic acid, which is negatively charged, they form a complex called polyplex. These complexes are stable enough to prevent DNA degradation and are easily internalized by

cells, often by endocytosis.[80] The mechanism of gene delivery by cationic system follows four steps. It starts with a nonspecific interaction between the particle and the cell surface. Then, the polyplex is internalized into endosomes. During the last steps, the DNA molecules are released and finally translocated into the nucleus for gene expression. Cationic polymers like PLL (poly-L-lysine), PAMAM or PEI[81] display a good transfection activity but are still associated to a potentially high cellular toxicity.[82] In our laboratory, they investigated dendrons as nanocarriers for gene delivery. Polycationic adamantane based dendrons were selected. They were able to form a polyplex with DNA called HYDRA*plex* and displayed a high cellular uptake without triggering cytotoxicity. Moreover, the focal point was functionalized, *via* click chemistry, with different azido-modified hydrophobic compounds in order to produce amphiphilic dendrons and improve DNA complexation and protection. Finally, we observed that, for DNA complexation, the second generation HYDRA*mers* are more efficient than the first generation, because of the number of positives charges. The functionalization of the focal point with cholesterol increases the HYDRA*mer* hydrophobicity leading to a better DNA binding and protection DNA.

These results were encouraging for the use of polycationic dendrons for gene delivery and confirmed the relationship between dendron generation, global hydrophobicity and periphery cationic functions with efficiency and toxicity.

I. 5 Self-assembly studies

Self-assembly can be described as the formation of an organized structure because of supra-molecular interactions generated without external interventions.[83] This phenomenon can occur with components, which range from the molecular to the macroscopic scale. The structures generated during the molecular self-assembly are usually in equilibrium. Nowadays self-assembly is ubiquitous in science and become a full field of study. Indeed, many applications such as the formation of molecular crystals,[84] lipid bilayers,[85] self-assembled monolayers,[86] protein folding[87] and even ligand/receptor interactions, are related to self-assembly.[88] Thus, the self-assembly defines the interactions between different or equal molecules or molecular segments. The driving force is the path from a less ordered state to a final more ordered state. Different parameters must be considered to generate ordered structures by self-assembly. One of these parameters is the reversibility, meaning that the components must have the possibilities to adjust their positions even after their association has started (Figure 29). Another criterion is the environment, which is controlled by solvents, concentration, temperature and pressure. To

allow self-assembly to occur, the compound must be mobile as well. In solution, thermal motion usually provides enough energy to the system.

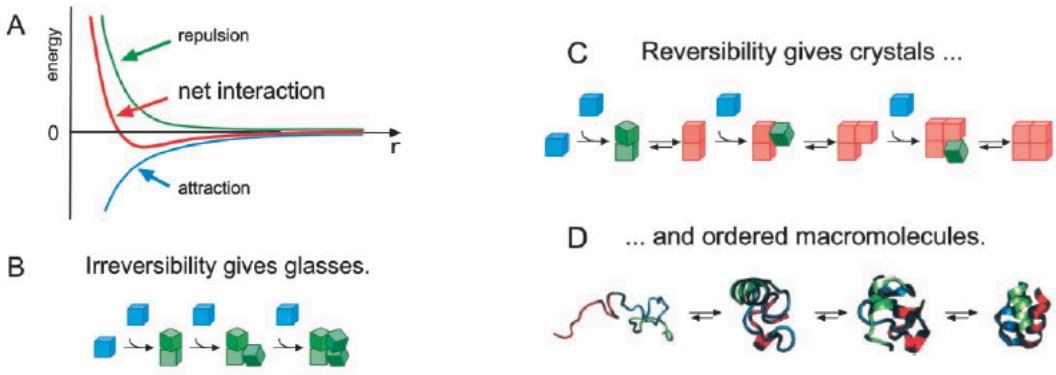

***Figure 29**: Self-assembly mechanisms. Adapted from literature.*[83]

In normal conditions, there is an equilibrium between attraction and repulsion of two entities (Figure 29). However, a strong attraction leads to aggregation (A). If this last one is irreversible, an aggregate with a disordered structure is formed (B). Otherwise, if the components can still interact, they will adjust their position to form an ordered structure, with a low energy level, to form a crystal (C) or, in the case of intramolecular self-assembly, provide ordered macromolecules (D).

I. 5.1 Self-assembly of nanoparticles

The aim of self-assembly is to control the morphology of nanoparticles. As explained before, self-assembly is an organization of molecules into an ordered structure, through colloidal stabilization, to avoid aggregation and flocculation. This observation is often associated to a thermodynamic equilibrium and can be achieved through direct interactions (weak interactions), but also by indirect methods using a template or an external field. Directed self-assembly allows the modulation of thermodynamic forces, they can be tuned using chemistry[89] and physics. Concerning the chemical aspects, the concept resembles to supramolecular chemistry. The particles are designed with functional groups, which self-interact to create an ordered system. In this case, the desired structure is obtained by specific interaction and it requires a high degree of control. For example, Xia *et al.* developed a method to synthesize monodispersed gold nanoparticles in water *via* silver (I) assisted citrate reduction (Figure 30). The authors modified the classic Turkevich method,[90] which requires a mix of $HAuCl_4$ with sodium citrate at high temperature to obtain gold nanoparticles. The first modification occurred

using an aqueous solution of citrate mixed, at room temperature, with gold precursors and then quickly added to boiling water. This allows to minimize the effect of citrate on buffer the pH of reaction and thus to guarantee the presence of the highly active auric ion $AuCl_3(OH)^-$. The second modification consists in using Ag^+ in trace amount that speeds up the nucleation and gold nanoparticle formation due to citrate oxidation catalysis activity.

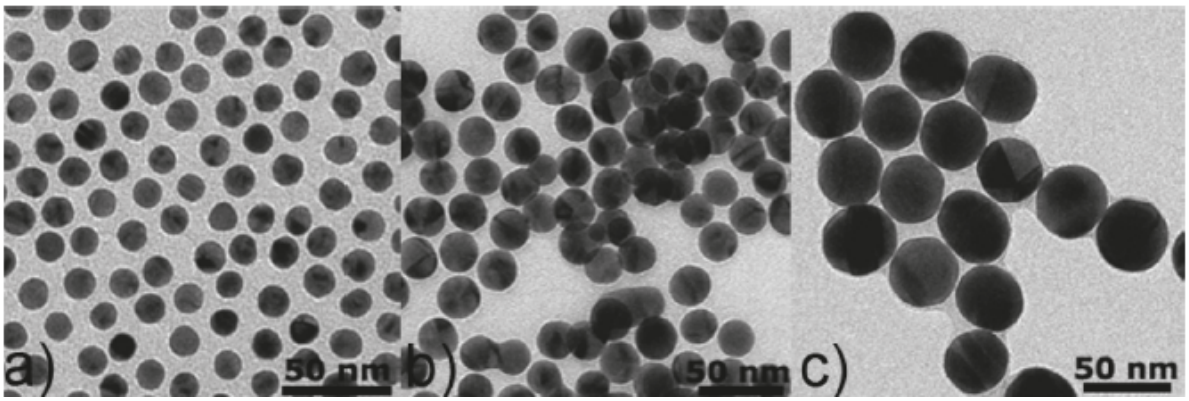

***Figure 30**: TEM images of quasi-spherical gold nanoparticles (From Xia et al).*[91]

Alternatively, it is possible to design particles with specific physical properties, sensitive to different stimuli such as magnetic or electric fields.[92] Indeed, among a variety of driving forces for self-assembly, electrostatic interactions play an important role due to their long-range nature but also because they are easy to control.[93] This is a possibility to induce self-organized nanostructures of nanoparticles dispersed in a non-conducting liquid. Another possibility is to use a template for direct self-assembly. This technique consists on using a surface modified in 1D, 2D or 3D containing active sites, which selectively induce the nanoparticle deposition.

Over the past few decades, self-assembly interest increased especially in nanomedicine. Controlling the particle structures and sizes allows a better use of them as vectors and a better internalization. Indeed, self-assembled particles display new physicochemical characteristics (size, shape, lipophilicity) compared to the single molecule. For example, self-assembled DNA nanostructures have been developed as bio-sensing materials.[94] Several other biologicals applications have been developed like drug delivery using self-assembled nanosized micelles[95] and more recently, magnetic drug delivery has been developed. This technique is based on superparamagnetic nanostructures which can be manipulated using magnetic field.[96]

I. 6 Foldamers

Molecular recognition plays an important role especially in biology. The molecular complementarity is at the base of several biological phenomena, which can be described as specific noncovalent interactions. These interactions that lead to function (information storage, catalysis, etc.) are possible because of the secondary structure of biopolymer backbones. Thus, the motivation for developing new molecules able to adopt a specific conformation is followed due to their potential biological applications. Currently, the field of foldamer focuses on creating mimetic structures of three major classes of biopolymer backbones, namely proteins, ribonucleic acids and polysaccharides.

Foldamers can be described like any oligomer that folds into a conformational ordered state in solution, where structures are stabilized by non-covalent interactions between nonadjacent monomeric units.[97] The origin of "foldamers" dates back to 1998 when Samuel Gellman described it like an artificial polymers with a specific and stable conformation, similar to that observed among natural proteins and nucleic acids.[98] Indeed, these medium sized molecules (500 to 5000 Da) adopt secondary structure including α-helix and β-sheets stabilized through weak interactions. Nowadays, these artificial molecules are designed to mimic proteins and other biopolymers and, thus, are developed for their biological activities.

Foldamers can be divided into two families following their backbones structures. The foldamers containing a backbone related to biopolymers are called "biotic" foldamers and the ones designed *via* bottom up approach and composed mainly of aromatic rich sequences are called "abiotic" foldamers.[99] We can also separate them in two additional classes, depending on their supramolecular interactions. The first one is single stranded foldamers, which only fold, like peptidomimetics. The second class is multiple-stranded foldamers that both associate and fold like nucleotidomimetics (Figure 31).[97]

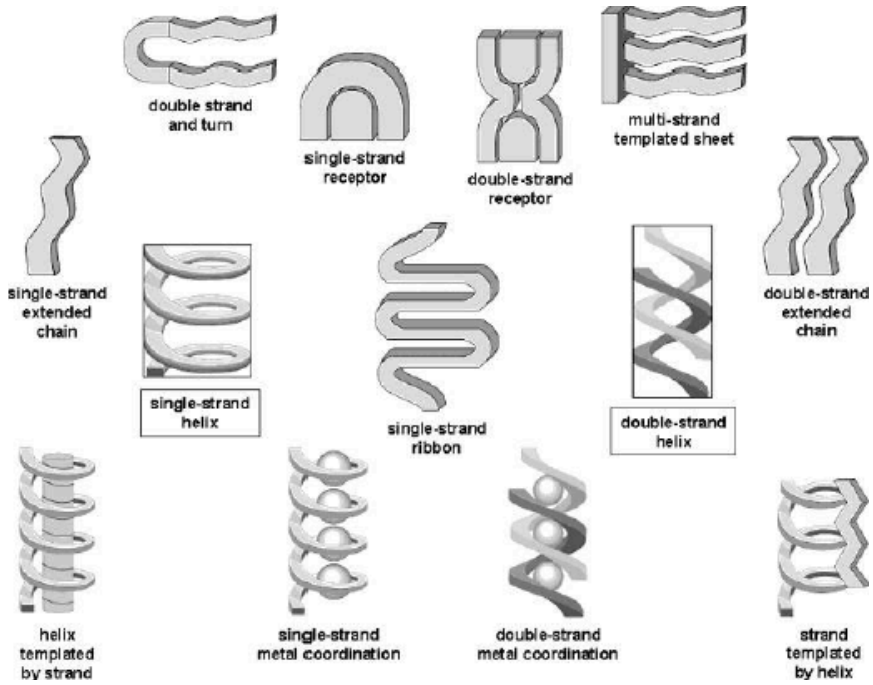

***Figure 31**: Illustration of different types of foldamer secondary structures. Adapted from literature.*[97]

I. 6.1 Peptidomimetic-based foldamers

We particularly focused on the peptidomimetics, which are part of single strand family. These foldamers are developed to mimicking peptide structures. They are classified in three types. The ones who mimic local topography of an amide bond called type-I-mimetics. The particularity of these molecules is their backbones, which often match atom by atom with the peptide. The type-II-mimetics are functionalized mimetics. They are non-peptide molecules, which bind peptide receptors but different antagonist subsites that parent peptide. Thus, they do not necessarily mimic the structure of the parent. Then, the type-III- mimetics, which possess novel templates unrelated to original peptides but containing functional groups to serve as topographical mimetics.

A simple route of synthesis of biotic peptidomimetic foldamers is to modify classical α-peptides or even to use non-natural amino acid to build β-peptides, γ-peptides or δ-peptides. One famous α-peptide derivative is the peptoid, for poly-N-substituted glycines. Peptoids have free C_α carbon because the pendant groups are attached to the amide nitrogen. This particular design imparts new characteristics to the peptide. The first is the lack of stereochemistry in the backbone and the second the absence of intramolecular H-bonds through carbonyl and amine.

This allows both *cis* and *trans* peptide bonds and thus a better diversity compared to α-peptides. Other examples of α-peptides family are azapeptide and azatide (Figure 32).[100] In this case, one α-carbon is replaced by a trivalent nitrogen atom, while when more α-carbons are replaced it leads to azatide.

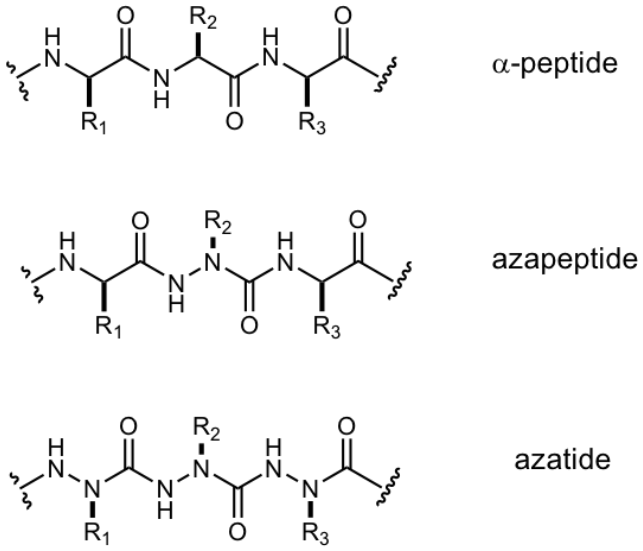

***Figure 32**: Biotic peptidomimetic foldamers.*

These derivatives have interesting characteristics because of the CO-N-N-CO torsion providing high stability. Indeed, the nitrogen lone pairs are almost perpendicular to one other. Thus, the conformational properties are mainly determined by hydrazine and urea constituents. Moreover, because of the N-N bond restricted rotation, azapeptides cannot adopt extended conformation which provides to azapeptides resistance against proteases.[101] β-Peptide family foldamers are also well represented. The interest on β-peptides is often due to their similarity of their backbones with α-peptide chain. They offer high flexibility and the possibility to form a rich variety of regular conformations. This family is not exclusively composed of β-peptides but also of α-aminoxy acids and hydrazino peptides. Following this ideas, γ-peptide and δ-peptide foldamers also have been synthesized like carbopeptoids, which use carbohydrate amino acids as backbone. Finally, a last possibility is to mix two classes of amino acids in a single peptide, for example combined α-and β-peptide in a sequence. To summarize peptidomimetics are foldamers designed with a specific spatial arrangement with the purpose to replace peptide substrates of enzymes or proteins receptors.[102]

I. 6.2 Foldamer applications

The diversity of sizes, shapes and the possible arrangements of non-natural monomers provide to foldamers properties that can be useful in therapeutics or materials chemistry. For example, they can also be combined with pharmacophore to find applications in medicinal chemistry.

The peptoids are easily synthesized by solid phase peptide synthesis. They display good water solubility and proteolitic enzymes do not degrade *N*-substituted polyglycines,[103] making them interesting for pharmaceutical applications. For example, cationic peptoids have been used to condense plasmid DNA into small particles, and protect it from nuclease degradation and efficiently mediate the transfection in several cell lines.[104] More recently, Mojsoska *et al*. synthesized two short cationic peptoids, which inhibit the growth of gram negative *E.coli*.[105] Dye leakage assays confirmed membrane damage but the killing effect of this peptoids is not totally attributed to leakage. Indeed, like anti-microbial peptide (AMP), peptoids may enter the cytoplasm and inhibits DNA, RNA or protein synthesis.[106] Some other examples of foldamers with antimicrobial activities have been published.[107] β-Peptides offer a large range of potential activity. As explained before, they fold into stable structures such as natural peptides and proteins. Moreover, β-peptides are completely stable to proteolytic degradation and thus, make them attractive as peptidomimetics. It have been demonstrated that β-peptides mimic α-peptide hormones,[108] they may inhibit cholesterol uptake,[109] they may be used as inhibitors of protein-protein interaction.[110] They also possess antimicrobial[107] and anti-proliferative properties.[111] Rueping *et al*. used β-peptides for cellular uptake studies.[112] Indeed due to their resistance towards enzymatic degradation, β-peptides are interesting for elucidating mechanism of internalization, to internalize non penetrating compounds or for diagnostic purpose. Abiotic foldamers also displayed biological functions, as it is the case for aromatic amide foldamers, which use their well-defined backbones to produce special binding domains or multiple-binding sites.[97] Then, Hamilton and co-workers synthesized different structures extended α-helix mimetics. These structures display high inhibition of protein-protein interactions.[113] Foldamers are involved in a large number of applications like mediating cell penetration, specific binding to various target including RNA, proteins, membranes and carbohydrates. They are good tools to extend our understanding of protein folding and functions. Furthermore, antibiotic resistance is now one of the most healthcare problems and AMPs provide a new approach to develop efficient antibiotics. AMPs play a central role in the innate immunity system of many organisms. They have been modified to improve their efficiency and selectivity for killing bacteria versus mammalian cells. Nowadays, drug design and structural biology combined with

high capacity of synthesis and screening methods are powerful strategies to develop efficient peptidomimetic drugs. We must realize that these structures are not just duplicates of the natural world, but provide an excellent foundation for the creation of new structures with new functions leading to new applications.

I. 7 Conclusion

Since its discovery in 1933, adamantane have been used in several applications, especially in medicine where its well defined structure and its symmetry afford an interesting scaffold. Highly reactive compare to other hydrocarbons, adamantane allows to change absorption, distribution, metabolism and excretion of molecule, to bind hydrophobic site in enzyme and act as an inhibitor. It also disrupts the transmembrane flow by affecting ion channels. Dendrons and dendrimers are nanoparticles particularly interesting for medicine where they can be used, for example as nanovector. The recent use of adamantane to design multi-functionalized dendrons providing to these nanoparticles interesting properties for biological applications.
Foldamers are artificial folded molecular architectures inspired by natural biopolymers. They introduced new tools and concepts to develop biologically active substances. Their properties are correlated to their shape because folding is the process selected by nature to control conformation of its molecular machinery and thus lead to biological applications like enzyme catalysis, information storage and molecular recognition. Inspired by peptide, polysaccharide and nucleic acid, foldamers offer an incredible diversity in term of synthesis and folding and thus in term of applications.

I. 8 Objectives of the thesis

My thesis is focused on the use of adamantane building block for different applications. First, I followed up the previous work of our laboratory aimed to use functionalized adamantane to build dendrons. My challenge was to synthesize different generation of adamantane-based dendrons but without any spacer between the adamantane cores to obtain smaller, more compact and rigid molecules. My work started with the multifunctionalization and characterization of adamantane building block with amine and carboxylic acid groups, which was then used for the synthesis of further dendron generations. Then I tried to synthesize a trimeric adamantane-based dendron conjugated with mannose to be tested as anti-inflammatory agent.

I also investigated the self-assembly of different adamantane derivatives in order to better understand the parameters involved in particles formation (functional groups, dendron generations, concentrations, solvents, etc.).

Then, in collaboration with the University of Copenhagen and the team of Prof. K. J. Jensen, I prepared an adamantane amino acid to build foldamers. This work includes the synthesis and characterization of different peptides by solid-phase protocols and the study of their folding properties.

I was also involved in the synthesis and characterization of a bioactive fluorescent molecule in order to elucidate its mechanism of storage and elimination in Drosophilia (Collaboration with the group of Dr. D. Ferrandon at IBMC, Strasbourg). The synthesis, characterization and results are presented in an Annex.

I. 9 References

(1) Reiser, J.; McGregor, E.; Jones, J.; Enick, R.; Holder, G. Adamantane and Diamantane; Phase Diagrams, Solubilities, and Rates of Dissolution. *Fluid Phase Equilibria* **1996**, *117* (1), 160–167.

(2) Fort, R. C.; Schleyer, P. von R. Adamantane: Consequences of the Diamondoid Structure. *Chem. Rev.* **1964**, *64* (3), 277–300.

(3) Landa, S.; Macháček, V. Sur l'adamantane, Nouvel Hydrocarbure Extrait Du Naphte. *Collect. Czechoslov. Chem. Commun.* **1933**, *5*, 1–5.

(4) Wei, Z.; Moldowan, J. M.; Paytan, A. Diamondoids and Molecular Biomarkers Generated from Modern Sediments in the Absence and Presence of Minerals during Hydrous Pyrolysis. *Org. Geochem.* **2006**, *37* (8), 891–911.

(5) Fang, C.; Xiong, Y.; Li, Y.; Chen, Y.; Liu, J.; Zhang, H.; Adedosu, T. A.; Peng, P. The Origin and Evolution of Adamantanes and Diamantanes in Petroleum. *Geochim. Cosmochim. Acta* **2013**, *120*, 109–120.

(6) Schleyer, P. von R.; Nicholas, R. D. Further Examples of the Adamantane Rearrangement. *Tetrahedron Lett.* **1961**, *2* (9), 305–309.

(7) Giruts, M. V.; Rusinova, G. V.; Gordadze, G. N. Generation of Adamantanes and Diamantanes by Thermal Cracking of High-Molecular-Mass Saturated Fractions of Crude Oils of Different Genotypes. *Pet. Chem.* **2006**, *46* (4), 225–236.

(8) Wei, Z.; Moldowan, J. M.; Peters, K. E.; Wang, Y.; Xiang, W. The Abundance and Distribution of Diamondoids in Biodegraded Oils from the San Joaquin Valley: Implications for Biodegradation of Diamondoids in Petroleum Reservoirs. *Org. Geochem.* **2007**, *38* (11), 1910–1926.

(9) von R. Schleyer, P. a simple preparation of adamantane. *J. Am. Chem. Soc.* **1957**, *79* (12), 3292–3292.

(10) Bingham, R. C.; Schleyer, P. v R. Recent Developments in the Chemistry of Adamantane and Related Polycyclic Hydrocarbons. In *Chemistry of Adamantanes*; Fortschritte der Chemischen Forschung; Springer, Berlin, Heidelberg, 1971; pp 1–102.

(11) Engler, E. M.; Farcasiu, M.; Sevin, A.; Cense, J. M.; Schleyer, P. V. R. Mechanism of Adamantane Rearrangements. *J. Am. Chem. Soc.* **1973**, *95* (17), 5769–5771.

(12) Nowacki, W.; Hedberg, K. W. An Electron Diffraction Investigation of the Structure of Adamantane. *J. Am. Chem. Soc.* **1948**, *70* (4), 1497–1500.

(13) Vijayakumar, V.; Garg, A. B.; Godwal, B. K.; Sikka, S. K. Pressure Induced Phase Transitions and Equation of State of Adamantane. *J. Phys. Condens. Matter* **2001**, *13* (9), 1961.

(14) Bazyleva, A. B.; Blokhin, A. V.; Kabo, G. J.; Charapennikau, M. B.; Emel'yanenko, V. N.; Verevkin, S. P.; Diky, V. Thermodynamic Properties of Adamantane Revisited. *J. Phys. Chem. B* **2011**, *115* (33), 10064–10072.

(15) Landa, S. Adamantane and its homologues http://www.currentscience.ac.in/Downloads/article_id_032_11_0485_0489_0.pdf (accessed Sep 13, 2016).

(16) McCall, D. W.; Douglass, D. C. Nuclear Magnetic Resonance in Solid Adamantane. *J. Chem. Phys.* **1960**, *33* (3), 777–778.

(17) Watanabe, K.; Kozawa, M.; Yano, E.; Namiki, T.; Nozaki, K.; Kon, J.; Hoshino, E.; Uraguchi, M.; Minagawa, T.; Yamamoto, Y. Resist Composition and Pattern Forming Process. US20010006752 A1, July 5, 2001.

(18) Morcombe, C. R.; Zilm, K. W. Chemical Shift Referencing in MAS Solid State NMR. *J. Magn. Reson. San Diego Calif 1997* **2003**, *162* (2), 479–486.

(19) Jeong, H. Y.; Lee, Y. K.; Talaie, A.; Kim, K. M.; Kwon, Y. D.; Jang, Y. R.; Yoo, K. H.; Choo, D. J.; Jang, J. Synthesis and Characterization of the First Adamantane-Based Poly(p-Phenylenevinylene) Derivative: An Intelligent Plastic for Smart Electronic Displays. *Thin Solid Films* **2002**, *417* (1), 171–174.

(20) Davies, W. L.; Grunert, R. R.; Haff, R. F.; Mcgahen, J. W.; Neumayer, E. M.; Paulshock, M.; Watts, J. C.; Wood, T. R.; Hermann, E. C.; Hoffmann, C. E. ANTIVIRAL ACTIVITY OF 1-ADAMANTANAMINE (AMANTADINE). *Science* **1964**, *144* (3620), 862–863.

(21) Maugh, T. H. Panel Urges Wide Use of Antiviral Drug. *Science* **1979**, *206* (4422), 1058–1060.

(22) Schwab, R. S.; England, A. C.; Poskanzer, D. C.; Young, R. R. Amantadine in the Treatment of Parkinson's Disease. *JAMA* **1969**, *208* (7), 1168–1170.

(23) Blanpied, T. A.; Clarke, R. J.; Johnson, J. W. Amantadine Inhibits NMDA Receptors by Accelerating Channel Closure during Channel Block. *J. Neurosci. Off. J. Soc. Neurosci.* **2005**, *25* (13), 3312–3322.

(24) Moiseev, I. K.; Makarova, N. V.; Zemtsova, M. N. Reactions of Adamantanes in Electrophilic Media. *Russ. Chem. Rev.* **1999**, *68* (12), 1001–1020.

(25) Schleyer, P. von R.; Fort, R. C.; Watts, W. E.; Comisarow, M. B.; Olah, G. A. Stable Carbonium Ions. VIII. The 1-Adamantyl Cation. *J. Am. Chem. Soc.* **1964**, *86* (19), 4195–4197.

(26) Bowers, K. W.; Nolfi, G. J.; Greene, F. D. Radical Anions of Adamantane and Hemamethylenetetramine. *J. Am. Chem. Soc.* **1963**, *85* (22), 3707–3707.

(27) Chan, M. S. W.; Arnold, D. R. Three-Dimensional Electron Delocalization: A Theoretical Study Based on the Pentacyclo[3.3.1.13,7.01,3.05,7]Decane System. *Can. J. Chem.* **1997**, *75* (2), 192–201.

(28) Olah, G. A.; Rasul, G.; Surya Prakash, G. K. Homoconjugation in the Adamantane Cage: DFT/IGLO Studies of the 1,3-Dehydro-5-Adamantyl Cation, Its Isoelectronic Boron Analogue 1,3-Dehydro-5-Boraadamantane, and Related Systems1,. *J. Org. Chem.* **2000**, *65* (19), 5956–5959.

(29) Schreiner, P. R.; Lauenstein, O.; Butova, E. D.; Gunchenko, P. A.; Kolomitsin, I. V.; Wittkopp, A.; Feder, G.; Fokin, A. A. Selective Radical Reactions in Multiphase Systems: Phase-Transfer Halogenations of Alkanes. *Chem. Weinh. Bergstr. Ger.* **2001**, *7* (23), 4996–5003.

(30) Adams, D. R.; Bailey, P. D.; Collier, I. D.; Leah, S. A. H.; Ridyard, C. The Mechanism for the Rearrangement of the Adamantly Cation. *Chem. Commun.* **1996**, *0* (3), 333–334.

(31) Geluk, H. W.; Schlatmann, J. L. M. A. A Convenient Synthesis of Adamantanone. *Chem. Commun. Lond.* **1967**, *0* (9), 426a–426a.

(32) Jasys, V. J.; Lombardo, F.; Appleton, T. A.; Bordner, J.; Ziliox, M.; Volkmann, R. A. Preparation of Fluoroadamantane Acids and Amines: Impact of Bridgehead Fluorine Substitution on the Solution- and Solid-State Properties of Functionalized Adamantanes. *J. Am. Chem. Soc.* **2000**, *122* (3), 466–473.

(33) Hara, S.; Aoyama, M. Direct Fluorination of Adamantanes with Iodine Pentafluoride. *Synthesis* **2008**, *2008* (16), 2510–2512.

(34) Aoyama, M.; Fukuhara, T.; Hara, S. Selective Fluorination of Adamantanes by an Electrochemical Method. *J. Org. Chem.* **2008**, *73* (11), 4186–4189.

(35) Schreiner, P. R.; Fokin, A. A.; Lauenstein, O.; Okamoto, Y.; Wakita, T.; Rinderspacher, C.; Robinson, G. H.; Vohs, J. K.; Campana, C. F. Pseudotetrahedral Polyhaloadamantanes as Chirality Probes: Synthesis, Separation, and Absolute Configuration. *J. Am. Chem. Soc.* **2002**, *124* (45), 13348–13349.

(36) Shokova, E. A.; Kovalev, V. V. Adamantane Functionalization. Synthesis of Polyfunctional Derivatives with Various Substituents in Bridgehead Positions. *Russ. J. Org. Chem.* **2012**, *48* (8), 1007–1040.

(37) Fournier, D.; Hoogenboom, R.; Schubert, U. S. Clicking Polymers: A Straightforward Approach to Novel Macromolecular Architectures. *Chem. Soc. Rev.* **2007**, *36* (8), 1369–1380.

(38) Ohno, M.; Shimizu, K.; Ishizaki, K.; Sasaki, T.; Eguchi, S. Cross-Coupling Reaction of Tert-Alkyl Halides with Grignard Reagents in Dichloromethane as a Non-Lewis Basic Medium. *J. Org. Chem.* **1988**, *53* (4), 729–733.

(39) Moberg, C. C3-Symmetrie in Der Asymmetrischen Katalyse Und Der Chiralen Erkennung. *Angew. Chem.* **1998**, *110* (3), 260–281.

(40) Eckert, D. M.; Kim, P. S. Mechanisms of Viral Membrane Fusion and Its Inhibition. *Annu. Rev. Biochem.* **2001**, *70*, 777–810.

(41) Bringmann, G.; Pfeifer, R.-M.; Rummey, C.; Hartner, K.; Breuning, M. Synthesis of Enantiopure Axially Chiral C3-Symmetric Tripodal Ligands and Their Application as Catalysts in the Asymmetric Addition of Dialkylzinc to Aldehydes. *J. Org. Chem.* **2003**, *68* (18), 6859–6863.

(42) van Gestel, J.; Palmans, A. R. A.; Titulaer, B.; Vekemans, J. A. J. M.; Meijer, E. W. "Majority-Rules" Operative in Chiral Columnar Stacks of C3-Symmetrical Molecules. *J. Am. Chem. Soc.* **2005**, *127* (15), 5490–5494.

(43) Kim, S.-G.; Kim, K.-H.; Kim, Y. K.; Shin, S. K.; Ahn, K. H. Crucial Role of Three-Center Hydrogen Bonding in a Challenging Chiral Molecular Recognition. *J. Am. Chem. Soc.* **2003**, *125* (45), 13819–13824.

(44) Maison, W.; Frangioni, J. V.; Pannier, N. Synthesis of Rigid Multivalent Scaffolds Based on Adamantane. *Org. Lett.* **2004**, *6* (24), 4567–4569.

(45) NEWMAN, H. Facile Syntheses of 1,3-Diphenyl-, 1,3,5-Triphenyl-, and 1,3,5,7-Tetraphenyladamantane from 1-Bromoadamantane. *Synthesis* **1972**, *1972* (12), 692–693.

(46) Denis, J. N.; Greene, A. E.; Serra, A. A.; Luche, M. J. An Efficient, Enantioselective Synthesis of the Taxol Side Chain. *J. Org. Chem.* **1986**, *51* (1), 46–50.

(47) Carlsen, P. H. J.; Katsuki, T.; Martin, V. S.; Sharpless, K. B. A Greatly Improved Procedure for Ruthenium Tetroxide Catalyzed Oxidations of Organic Compounds. *J. Org. Chem.* **1981**, *46* (19), 3936–3938.

(48) Fleck, C.; Franzmann, E.; Claes, D.; Rickert, A.; Maison, W. Synthesis of Functionalized Adamantane Derivatives: (3 + 1)-Scaffolds for Applications in Medicinal and Material Chemistry. *Synthesis* **2013**, *45* (11), 1452–1461.

(49) Nasr, K.; Pannier, N.; Frangioni, J. V.; Maison, W. Rigid Multivalent Scaffolds Based on Adamantane. *J. Org. Chem.* **2008**, *73* (3), 1056–1060.

(50) Lamanna, G.; Russier, J.; Ménard-Moyon, C.; Bianco, A. HYDRAmers: Design, Synthesis and Characterization of Different Generation Novel Hydra-like Dendrons Based on Multifunctionalized Adamantane. *Chem. Commun. Camb. Engl.* **2011**, *47* (31), 8955–8957.

(51) Bettini, S.; Boutet-Robinet, E.; Cartier, C.; Coméra, C.; Gaultier, E.; Dupuy, J.; Naud, N.; Taché, S.; Grysan, P.; Reguer, S.; Thieriet, N.; Réfrégiers, M.; Thiaudière, D.; Cravedi, J.-P.; Carrière, M.; Audinot, J.-N.; Pierre, F. H.; Guzylack-Piriou, L.; Houdeau, E. Food-Grade TiO_2 Impairs Intestinal and Systemic Immune Homeostasis, Initiates Preneoplastic Lesions and Promotes Aberrant Crypt Development in the Rat Colon. *Sci. Rep.* **2017**, *7*, srep40373.

(52) Pan, Q.; Xu, Q.; Boylan, N. J.; Lamb, N. W.; G. Emmert, D.; Yang, J.-C.; Tang, L.; Heflin, T.; Alwadani, S.; Eberhart, C. G.; Stark, W. J.; Hanes, J. Corticosteroid-Loaded Biodegradable Nanoparticles for Prevention of Corneal Allograft Rejection in Rats. *J. Controlled Release* **2015**, *201*, 32–40.

(53) Tomalia, D. A.; Baker, H.; Dewald, J.; Hall, M.; Kallos, G.; Martin, S.; Roeck, J.; Ryder, J.; Smith, P. A New Class of Polymers: Starburst-Dendritic Macromolecules. *Polym. J.* **1985**, *17* (1), 117–132.

(54) Sahoo, S. K.; Labhasetwar, V. Nanotech Approaches to Drug Delivery and Imaging. *Drug Discov. Today* **2003**, *8* (24), 1112–1120.

(55) Wu, L.; Ficker, M.; Christensen, J. B.; Trohopoulos, P. N.; Moghimi, S. M. Dendrimers in Medicine: Therapeutic Concepts and Pharmaceutical Challenges. *Bioconjug. Chem.* **2015**, *26* (7), 1198–1211.

(56) Medina, S. H.; El-Sayed, M. E. H. Dendrimers as Carriers for Delivery of Chemotherapeutic Agents. *Chem. Rev.* **2009**, *109* (7), 3141–3157.

(57) Akiyama, H.; Miyashita, K.; Hari, Y.; Obika, S.; Imanishi, T. Synthesis of Novel Polyesteramine Dendrimers by Divergent and Convergent Methods. *Tetrahedron* **2013**, *69* (33), 6810–6820.

(58) Astruc, D.; Boisselier, E.; Ornelas, C. Dendrimers Designed for Functions: From Physical, Photophysical, and Supramolecular Properties to Applications in Sensing, Catalysis, Molecular Electronics, Photonics, and Nanomedicine. *Chem. Rev.* **2010**, *110* (4), 1857–1959.

(59) Matsumura, Y.; Maeda, H. A New Concept for Macromolecular Therapeutics in Cancer Chemotherapy: Mechanism of Tumoritropic Accumulation of Proteins and the Antitumor Agent Smancs. *Cancer Res.* **1986**, *46* (12 Pt 1), 6387–6392.

(60) Greish, K. Enhanced Permeability and Retention (EPR) Effect for Anticancer Nanomedicine Drug Targeting. *Methods Mol. Biol. Clifton NJ* **2010**, *624*, 25–37.

(61) Fang, J.; Nakamura, H.; Maeda, H. The EPR Effect: Unique Features of Tumor Blood Vessels for Drug Delivery, Factors Involved, and Limitations and Augmentation of the Effect. *Adv. Drug Deliv. Rev.* **2011**, *63* (3), 136–151.

(62) Wang, M.; Thanou, M. Targeting Nanoparticles to Cancer. *Pharmacol. Res.* **2010**, *62* (2), 90–99.

(63) Gabizon, A.; Shmeeda, H.; Barenholz, Y. Pharmacokinetics of Pegylated Liposomal Doxorubicin: Review of Animal and Human Studies. *Clin. Pharmacokinet.* **2003**, *42* (5), 419–436.

(64) Jhaveri, A. M.; Torchilin, V. P. Multifunctional Polymeric Micelles for Delivery of Drugs and SiRNA. *Front. Pharmacol.* **2014**, *5*.

(65) Danhier, F. To Exploit the Tumor Microenvironment: Since the EPR Effect Fails in the Clinic, What Is the Future of Nanomedicine? *J. Control. Release Off. J. Control. Release Soc.* **2016**, *244* (Pt A), 108–121.

(66) Barenholz, Y. Doxil®--the First FDA-Approved Nano-Drug: Lessons Learned. *J. Control. Release Off. J. Control. Release Soc.* **2012**, *160* (2), 117–134.

(67) Caminade, A.-M.; Turrin, C.-O.; Laurent, R.; Ouali, A.; Delavaux-Nicot, B. *Dendrimers: Towards Catalytic, Material and Biomedical Uses*; Wiley, 2011.

(68) Winau, F.; Westphal, O.; Winau, R. Paul Ehrlich--in Search of the Magic Bullet. *Microbes Infect.* **2004**, *6* (8), 786–789.

(69) Escobar-Chávez, J. J.; Rodríguez-Cruz, I. M.; Domínguez-Delgado, C. L.; Torres, R. D.-; Revilla-Vázquez, A. L.; Aléncaster, N. C. Nanocarrier Systems for Transdermal Drug Delivery. **2012**.

(70) Nagaich, U. Theranostic Nanomedicine: Potential Therapeutic Epitome. *J. Adv. Pharm. Technol. Res.* **2015**, *6* (1), 1.

(71) Bendtzen, K. Personalized Medicine: Theranostics (Therapeutics Diagnostics) Essential for Rational Use of Tumor Necrosis Factor-Alpha Antagonists. *Discov. Med.* **2013**, *15* (83), 201–211.

(72) Penet, M.-F.; Chen, Z.; Kakkad, S.; Pomper, M. G.; Bhujwalla, Z. M. Theranostic Imaging of Cancer. *Eur. J. Radiol.* **2012**, *81* (0 1), S124–S126.

(73) Newkome, G. R.; Nayak, A.; Behera, R. K.; Moorefield, C. N.; Baker, G. R. Chemistry of Micelles Series. 22. Cascade Polymers: Synthesis and Characterization of Four-Directional Spherical Dendritic Macromolecules Based on Adamantane. *J. Org. Chem.* **1992**, *57* (1), 358–362.

(74) Lamanna, G.; Russier, J.; Dumortier, H.; Bianco, A. Enhancement of Anti-Inflammatory Drug Activity by Multivalent Adamantane-Based Dendrons. *Biomaterials* **2012**, *33* (22), 5610–5617.

(75) Grillaud, M.; Russier, J.; Bianco, A. Polycationic Adamantane-Based Dendrons of Different Generations Display High Cellular Uptake without Triggering Cytotoxicity. *J. Am. Chem. Soc.* **2014**, *136* (2), 810–819.

(76) Ginn, S. L.; Alexander, I. E.; Edelstein, M. L.; Abedi, M. R.; Wixon, J. Gene Therapy Clinical Trials Worldwide to 2012 - an Update. *J. Gene Med.* **2013**, *15* (2), 65–77.

(77) Nayerossadat, N.; Maedeh, T.; Ali, P. A. Viral and Nonviral Delivery Systems for Gene Delivery. *Adv. Biomed. Res.* **2012**, *1*.

(78) Gardlík, R.; Pálffy, R.; Hodosy, J.; Lukács, J.; Turna, J.; Celec, P. Vectors and Delivery Systems in Gene Therapy. *Med. Sci. Monit. Int. Med. J. Exp. Clin. Res.* **2005**, *11* (4), RA110-121.

(79) Hirai, H.; Satoh, E.; Osawa, M.; Inaba, T.; Shimazaki, C.; Kinoshita, S.; Nakagawa, M.; Mazda, O.; Imanishi, J. Use of EBV-Based Vector/HVJ-Liposome Complex Vector for Targeted Gene Therapy of EBV-Associated Neoplasms. *Biochem. Biophys. Res. Commun.* **1997**, *241* (1), 112–118.

(80) Vercauteren, D.; Rejman, J.; Martens, T. F.; Demeester, J.; De Smedt, S. C.; Braeckmans, K. On the Cellular Processing of Non-Viral Nanomedicines for Nucleic Acid Delivery: Mechanisms and Methods. *J. Control. Release Off. J. Control. Release Soc.* **2012**, *161* (2), 566–581.

(81) Boussif, O.; Lezoualc'h, F.; Zanta, M. A.; Mergny, M. D.; Scherman, D.; Demeneix, B.; Behr, J. P. A Versatile Vector for Gene and Oligonucleotide Transfer into Cells in Culture and in Vivo: Polyethylenimine. *Proc. Natl. Acad. Sci. U. S. A.* **1995**, *92* (16), 7297–7301.

(82) Yu, T.; Liu, X.; Bolcato-Bellemin, A.-L.; Wang, Y.; Liu, C.; Erbacher, P.; Qu, F.; Rocchi, P.; Behr, J.-P.; Peng, L. An Amphiphilic Dendrimer for Effective Delivery of Small Interfering RNA and Gene Silencing in Vitro and in Vivo. *Angew. Chem. Int. Ed Engl.* **2012**, *51* (34), 8478–8484.

(83) Whitesides, G. M.; Boncheva, M. Beyond Molecules: Self-Assembly of Mesoscopic and Macroscopic Components. *Proc. Natl. Acad. Sci. U. S. A.* **2002**, *99* (8), 4769–4774.

(84) Maginn, S. J. Crystal Engineering: The Design of Organic Solids by G. R. Desiraju. *J. Appl. Crystallogr.* **1991**, *24* (3), 265–265.

(85) Chayen, J. Micelles, Monolayers and Biomembranes. M. N. Jones and D. Chapman. Wiley–Liss, New York and Chichester. Xii + 252 Pages, £36.75 (1995). *Cell Biochem. Funct.* **1996**, *14* (1), 75–75.

(86) Kumar, A.; Abbott, N. L.; Biebuyck, H. A.; Kim, E.; Whitesides, G. M. Patterned Self-Assembled Monolayers and Meso-Scale Phenomena. *Acc. Chem. Res.* **1995**, *28* (5), 219–226.

(87) Grantcharova, V.; Alm, E. J.; Baker, D.; Horwich, A. L. Mechanisms of Protein Folding. *Curr. Opin. Struct. Biol.* **2001**, *11* (1), 70–82.

(88) Bongrand, P. Ligand-Receptor Interactions. *Rep. Prog. Phys.* **1999**, *62* (6), 921.

(89) Chen, X.; Huang, X.; Kong, L.; Guo, Z.; Fu, X.; Li, M.; Liu, J. Walnut-like CdS

Micro-Particles/Single-Walled Carbon Nanotube Hybrids: One-Step Hydrothermal Route to Synthesis and Their Properties. *J. Mater. Chem.* **2009**, *20* (2), 352–359.

(90) Turkevich, J.; Stevenson, P. C.; Hillier, J. A Study of the Nucleation and Growth Processes in the Synthesis of Colloidal Gold. *Discuss. Faraday Soc.* **1951**, *11* (0), 55–75.

(91) Xia, H.; Bai, S.; Hartmann, J.; Wang, D. Synthesis of Monodisperse Quasi-Spherical Gold Nanoparticles in Water via Silver(I)-Assisted Citrate Reduction. *Langmuir* **2010**, *26* (5), 3585–3589.

(92) Tanase, M.; Silevitch, D. M.; Hultgren, A.; Bauer, L. A.; Searson, P. C.; Meyer, G. J.; Reich, D. H. Magnetic Trapping and Self-Assembly of Multicomponent Nanowires. *J. Appl. Phys.* **2002**, *91* (10), 8549–8551.

(93) Lu, W.; Salac, D. Patterning Multilayers of Molecules via Self-Organization. *Phys. Rev. Lett.* **2005**, *94* (14), 146103.

(94) Chhabra, R.; Sharma, J.; Liu, Y.; Rinker, S.; Yan, H. DNA Self-Assembly for Nanomedicine. *Adv. Drug Deliv. Rev.* **2010**, *62* (6), 617–625.

(95) Messina, P. V.; Besada-Porto, J. M.; Ruso, J. M. Self-Assembly Drugs: From Micelles to Nanomedicine. *Curr. Top. Med. Chem.* **2014**, *14* (5), 555–571.

(96) Kralj, S.; Makovec, D. Magnetic Assembly of Superparamagnetic Iron Oxide Nanoparticle Clusters into Nanochains and Nanobundles. *ACS Nano* **2015**, *9* (10), 9700–9707.

(97) Hill, D. J.; Mio, M. J.; Prince, R. B.; Hughes, T. S.; Moore, J. S. A Field Guide to Foldamers. *Chem. Rev.* **2001**, *101* (12), 3893–4012.

(98) Gellman, S. Foldamers: A Manifesto. *Acc. Chem. Res.* **1998**, *31*, 173–180.

(99) Claudia, T.; Ivan, H.; J, A. D.; Ferenc, F. Foldamers. *Eur. J. Org. Chem.* **2013**, *17* (2347494), 3408–3409.

(100) Han, H.; Janda, K. D. Azatides: Solution and Liquid Phase Syntheses of a New Peptidomimetic. *J. Am. Chem. Soc.* **1996**, *118* (11), 2539–2544.

(101) Perona, J. J.; Craik, C. S. Structural Basis of Substrate Specificity in the Serine Proteases. *Protein Sci. Publ. Protein Soc.* **1995**, *4* (3), 337–360.

(102) Ripka, A. S.; Rich, D. H. Peptidomimetic Design. *Curr. Opin. Chem. Biol.* **1998**, *2* (4), 441–452.

(103) L. Bolt, H.; L. Cobb, S. A Practical Method for the Synthesis of Peptoids Containing Both Lysine-Type and Arginine-Type Monomers. *Org. Biomol. Chem.* **2016**, *14* (4), 1211–1215.

(104) Murphy, J. E.; Uno, T.; Hamer, J. D.; Cohen, F. E.; Dwarki, V.; Zuckermann, R. N. A Combinatorial Approach to the Discovery of Efficient Cationic Peptoid Reagents for Gene Delivery. *Proc. Natl. Acad. Sci. U. S. A.* **1998**, *95* (4), 1517–1522.

(105) Mojsoska, B.; Carretero, G.; Larsen, S.; Mateiu, R. V.; Jenssen, H. Peptoids Successfully Inhibit the Growth of Gram Negative E. Coli Causing Substantial Membrane Damage. *Sci. Rep.* **2017**, *7*.

(106) Mojsoska, B.; Jenssen, H. Peptides and Peptidomimetics for Antimicrobial Drug Design. *Pharm. Basel Switz.* **2015**, *8* (3), 366–415.

(107) Liu, D.; DeGrado, W. F. De Novo Design, Synthesis, and Characterization of Antimicrobial β-Peptides. *J. Am. Chem. Soc.* **2001**, *123* (31), 7553–7559.

(108) Gademann, K.; Kimmerlin, T.; Hoyer, D.; Seebach, D. Peptide Folding Induces High and Selective Affinity of a Linear and Small β-Peptide to the Human Somatostatin Receptor 4. *J. Med. Chem.* **2001**, *44* (15), 2460–2468.

(109) Werder, M.; Hauser, H.; Abele, S.; Seebach, D. β-Peptides as Inhibitors of Small-Intestinal Cholesterol and Fat Absorption. *Helv. Chim. Acta* **1999**, *82* (10), 1774–1783.

(110) Kritzer, J. A.; Stephens, O. M.; Guarracino, D. A.; Reznik, S. K.; Schepartz, A. β-Peptides as Inhibitors of Protein–protein Interactions. *Bioorg. Med. Chem.* **2005**, *13* (1), 11–16.

(111) Gademann, K.; Seebach, D. Synthesis of Cyclo-β-Tripeptides and Their Biological in Vitro Evaluation as Antiproliferatives against the Growth of Human Cancer Cell Lines. *Helv. Chim. Acta* **2001**, *84* (10), 2924–2937.

(112) Rueping, M.; Mahajan, Y.; Sauer, M.; Seebach, D. Cellular Uptake Studies with B-Peptides. *ChemBioChem* **2002**, *3* (2-3), 257–259.

(113) Zhang, D.-W.; Zhao, X.; Hou, J.-L.; Li, Z.-T. Aromatic Amide Foldamers: Structures, Properties, and Functions. *Chem. Rev.* **2012**, *112* (10), 5271–5316.

Chapter II: Design and synthesis of 1st and 2nd generation adamantane-based dendrons

II. 1 Introduction

Dendrons can be described like wedge-shaped dendrimer sections. They are hyperbranched molecular nanostructures with well-defined shapes and monodispersed structures.[1] These nanoparticles have the advantage to be synthesized using simple organic chemistry,[2,3] resulting monodispersed, macromolecular, polymeric architectures. Dendrons are composed of three different parts, the focal point, the branches and the dendritic surface. Each component plays a role in the dendron characteristics and thus can be modified to tune the properties (e.g. molecular weight, chemical composition, polarity, shape, stability, hydrodynamic diameter, etc.). The main difference between dendrons and dendrimers is the access of the focal point. Indeed, the focal point is the core of the dendrimer and thus, it is totally integrated into its structure. Meanwhile, the architecture of the dendron makes the focal point accessible to other molecules. For this reason, the functional group at the focal point is usually different than the groups on periphery, allowing an orthogonal functionalization of these positions and so allowing the preparation multi-functional dendrons.

The varied characteristics of dendrons imparted them a broad range of applications in supramolecular chemistry, especially in medicine where they can be used as drug delivery systems, gene transfection agents and imaging probes. By manipulating their shapes, weights and chemical compositions they are promising candidates to solve problems of biocompatibility, toxicity, pharmacokinetics or organ-specific targeting.[4] Moreover, another advantage of dendrons is the multivalency effect,[5] which consists of multiple surface groups at the dendron's periphery to promote higher binding affinity for ligand/receptor interactions. Combined with the EPR effect due to the particles size,[6] dendrons can be described like ideal nanocarriers for the delivery of bioactive materials into cells.[7]

Today a wide range of different dendritic families exists, but the first that became commercially available were PPI (poly(propyleneimine))[8] and PAMAM (poly(amido-amine))[9] dendrimers. Polycationic dendrimers based on polyamines have been commonly used for gene delivery. Although their good transfection activity, they displayed problematic toxicity against cells dependent on the concentration used.[10] The cytotoxicity behavior of cationic dendrimers is widely explained by the favored interactions between negatively charged cell membranes and the positively charged dendrimer surface, enabling these last one to adhere and damage the cell

membrane, causing cell lysis. To overcome this toxicity issues, dendrimers are modified on their surface by different agents such as carbohydrates, acetates or PEG. Indeed, PEG-based nanocarriers have high solubility in water and displayed low cytotoxicity with enhanced permeability and retention.

Our group is particularly interested on adamantane-based dendrons as multivalent scaffolds. Using adamantane core to build dendrons offers multiple advantages. Because of their well-defined 3D conformation and reactivity, it is easy to functionalize the four bridgehead positions to obtain multifunctional building blocks. This is the starting point of dendron synthesis with a tripodal arrangement, giving rise to the arborescent structure with less sterical hindrance between the attached entities. Following this idea, different generation of adamantane-based dendrons have been synthesized. Functionalized with multiple ibuprofen units, first and second generation of adamantane based dendrons displayed an enhanced anti-inflammatory activity *in vitro*.[11] The higher anti-inflammatory activity can be attributed to a higher availability of the multivalent ibuprofen compared to ibuprofen alone.

Then, our group also designed different generation of polycationic adamantane-based dendrons.[12] Tri- and tetraethylene glycol chains have been used as flexible and water compatible branching units. The periphery was functionalized with polyammonium and polyguanidinium groups. Moreover, the focal point was functionalized with an alkyne group to attach a fluorescent probe by CuAAC. Compared to classical polycationic vectors, which often displays cellular toxicity, none of these dendritic structures showed significant cytotoxicity effects on different cell line (RAW 264.7 and HeLa).

In this chapter, I describe the synthesis and characterization of different generation adamantane-based dendrons. These dendrons have been designed without linkers, meaning that they are more rigid and dense (compact). As a consequence, the solubility is mainly dependent of the peripheral groups of the dendrons. Different functional group have been used to functionalized the periphery or/and the focal point of adamantane based dendrons. Then, using transmission electron microscopy (TEM) I analyzed the morphology of the different adamantane dendrons and I tried to understand the role of the functional groups in the self-assembly capacity. Moreover, controlling the morphology of the nanoparticles allows to use them in specific applications, for example for drug delivery, and to correlate the morphology to the mechanisms of cell internalization and to their biological efficacy.

II. 2 Results and Discussion

II. 2.1 Synthesis of first generation adamantane dendrons

Following the previous work done in our Lab, I synthesized (3+1) tetrasubstituted adamantane building blocks (Scheme 1). I started from the commercial 1-bromoadamantane **1**, obtained by C-H activation of adamantane in electrophilic media.[13] 1-Bromoadamantane reacts with benzene in a Friedel-Craft reaction in the presence of aluminium chloride as Lewis acid and *t*-butylbromide, to give 1,3,5-triphenyladamantane **2** with a yield up to 75%. The second step consists on bromination of the last bridgehead position. Triphenyladamantane **2** is converted to 1-bromo-3,5,7-triphenyladamantane **3** with 89% yield following a PTC (phase transfer catalysis) protocol. The bromide derivative obtained is suitable to Ritter reaction with acetonitrile leading to the *N*-acetylamide-3-5-7-triphenyladamantane **4** (80% yield). The fourth step is an oxidative degradation of the three phenyl groups catalyzed by ruthenium with an excess of periodic acid leading to the formation of the *N*-acetylamide-3-5-7-tricarboxylicadamantane acid **5**. This step is difficult and the yield observed can change from 20 to 85%. Finally, compound **5** is hydrolyzed to give the unprotected 1-amino-3,5,7-tricarboxylicadamantane acid **6**. This compound corresponds to the (3+1) building block but also to the first generation dendron without linkers and protecting groups. Moreover, this compound is obtained without any purification step.

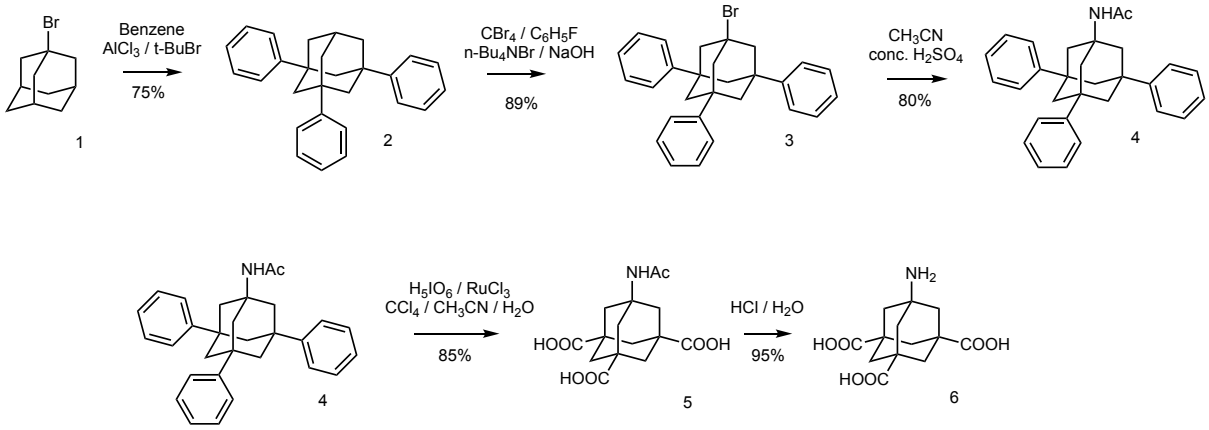

***Scheme 1**: Synthesis of adamantane (3+1) building block, the first generation dendron.*

The 1-amino-3,5,7-tricarboxylicadamantane acid **6** corresponds to the starting building block for the construction of further molecules like functionalized first generation dendrons and precursors for the synthesis of the second generation adamantane-based dendrons.

I started with a classic Boc protection of the free amine to obtained the corresponding carbamate compound (Scheme 2). The Boc group offers different advantages, first it can be an orthogonal protection (Boc is acid-labile), then it is stable towards most nucleophiles and bases, which allows further reactions on the other free functional groups.

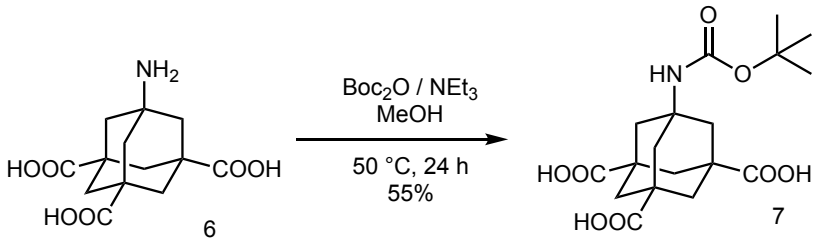

***Scheme 2**: Boc protection of amino-3,5,7-tricarbocylicadamantane acid.*

The yield obtained is relatively low for a Boc protection of primary amine. This is due to the particular low reactivity of adamantane. We observed that the free amine is more reactive when the carboxylate groups are esterified. For this reason, I decided to change strategy and to esterify the tricarboxylic acid intermediate to form trimethylaminoadamantane-1,3,5-tricarboxylate **8** with a yield of 75%. From compound **8**, two different amine protections have been used (Scheme 3). The first one is the coupling with 5-hexaynoic acid activated with *N*-(3-dimethylaminopropyl)-*N'*-ethylcarbodiimide hydrochloride (EDC×HCl) and 1-hydroxybenzotriazole (HOBt) to give the corresponding alkyne derivative **9** with 50 % yield. The presence of an alkyne moiety which protect the amine group also allows further functionalization through CuAAC with the desired azide modified molecules. The second reaction performed is the benzyl carbamate protection. This is carried out by mixing compound **8** with *N*-(benzyloxycarbonyloxy)succinimide (Cbz-OSu) and trimethylamine (NEt_3) to give carboxybenzyl (Cbz) derivative **11** with 45 % yield. As Boc protecting group, benzyl carbamate is an orthogonal protection and it can be selectively removed by hydrogenation catalyzed Pd/C or Ni. Moreover, the absorbance of benzyl group in UV is helpful to follow the reactions by TLC. To recover the free acid groups, basic hydrolysis is performed on both compound **9** and **11** to obtain the corresponding tricarboxylic acid derivatives **10** and **12** with a yield close to 95 %. All compounds were fully characterized by NMR, FT-IR and mass spectrometry.

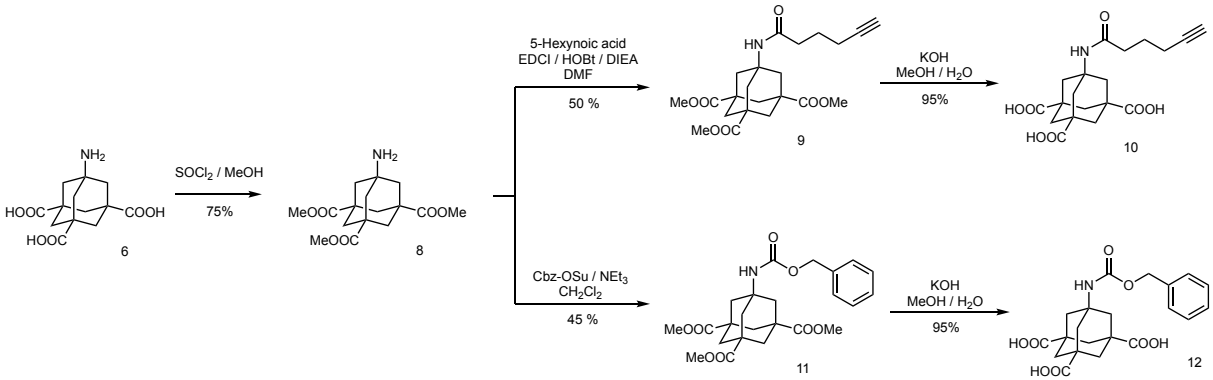

***Scheme 3**: Functionalization of 1st generation adamantane dendrons.*

II. 2.2 Synthesis of second generation adamantane dendrons

We first explored the spatial structure of the desired 2nd generation adamantane dendron by computer modeling. Figure 1 shows the importance of adamantane 3D conformation to reduce sterical hindrance between all adamantane moieties and confirms the possibility to reach the second generation adamantane dendrons without spacers.

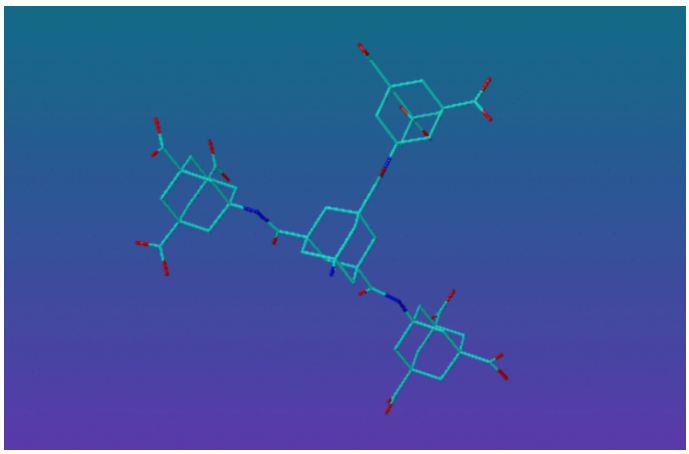

***Figure 1**: Computer simulation of 2nd generation adamantane-based dendrons.*

To synthesize the 2nd generation adamantane dendrons (G2), I started from 1-amino-3,5,7-tricarboxylicadamantane acid **6** and used a protection/deprotection strategy. Compound **6** was separated in two parts. The first part is protected at the focal point. Indeed, the free amine is Boc protected to give intermediate **7**. The second part is protected at the periphery. The three carboxylic acid groups are esterified to give the corresponding three methyl ester derivatives **8**. Coupling **7** with three equivalents of compound **8** gives the second generation fully protected

adamantane dendron **13** (Scheme 4). Different conditions have been tested during the coupling: the best yield was obtained with 2-(1*H*-benzotriazol-1-yl)-1,1,3,3-tetramethyluronium hexafluorophosphate (HBTU) as coupling agent and NEt_3 as a base to give compound **13** with 75 % yield. Then, Boc protecting group on compound 13 is easily and selectively removed using trifluoroacetic acid (TFA) in DCM to form the 2nd generation adamantane dendrons **14** with the free amine at the focal point. This latest can be functionalized or use for further generation synthesis through convergent synthesis (see 3rd generation synthesis).

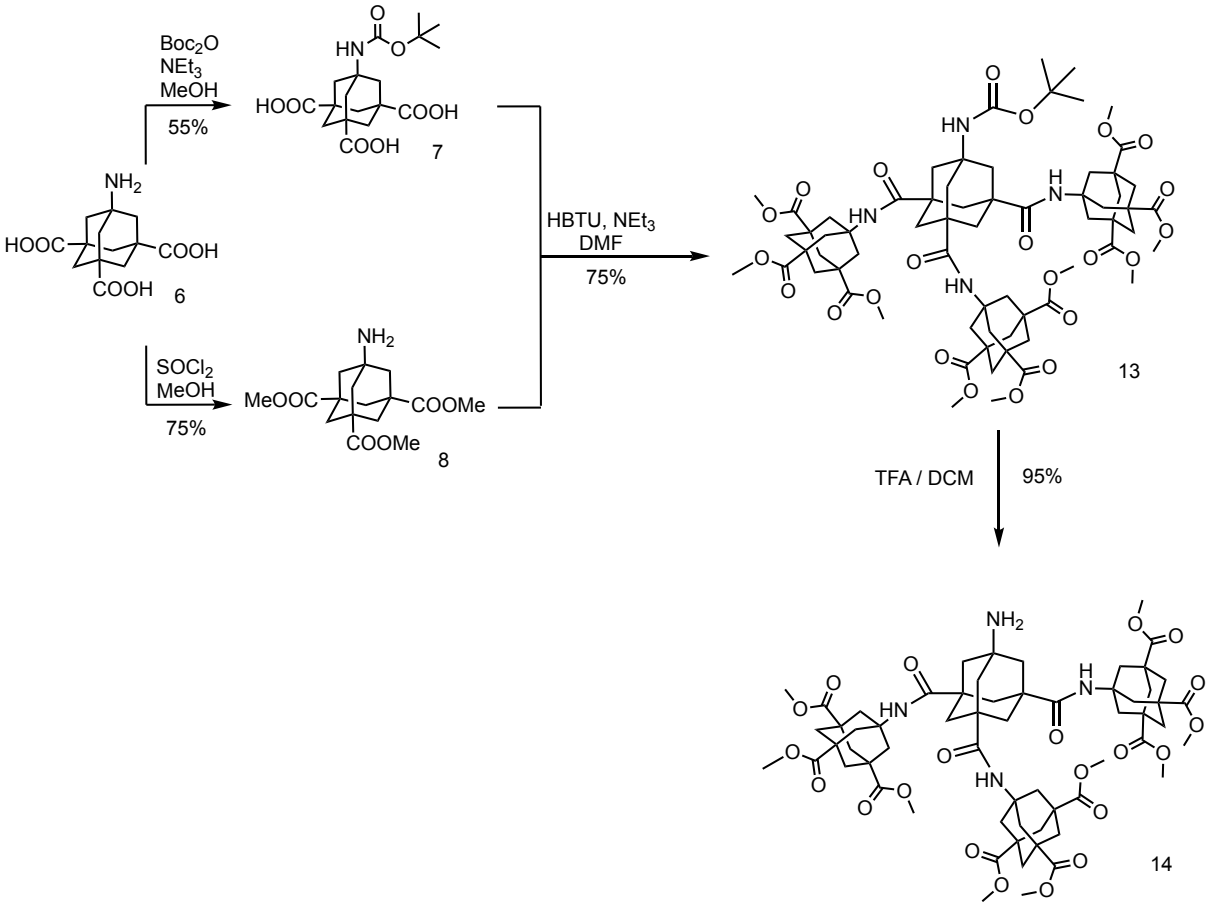

***Scheme 4**: 2nd generation of adamantane based dendrons synthesis.*

The 2nd generation adamantane-based dendrons were fully characterized and the ^{1}H NMR allows to easily follow the Boc deprotection with the disappearance of the characteristic peak of *t*-butyl at 1.4 ppm (Figure 2).

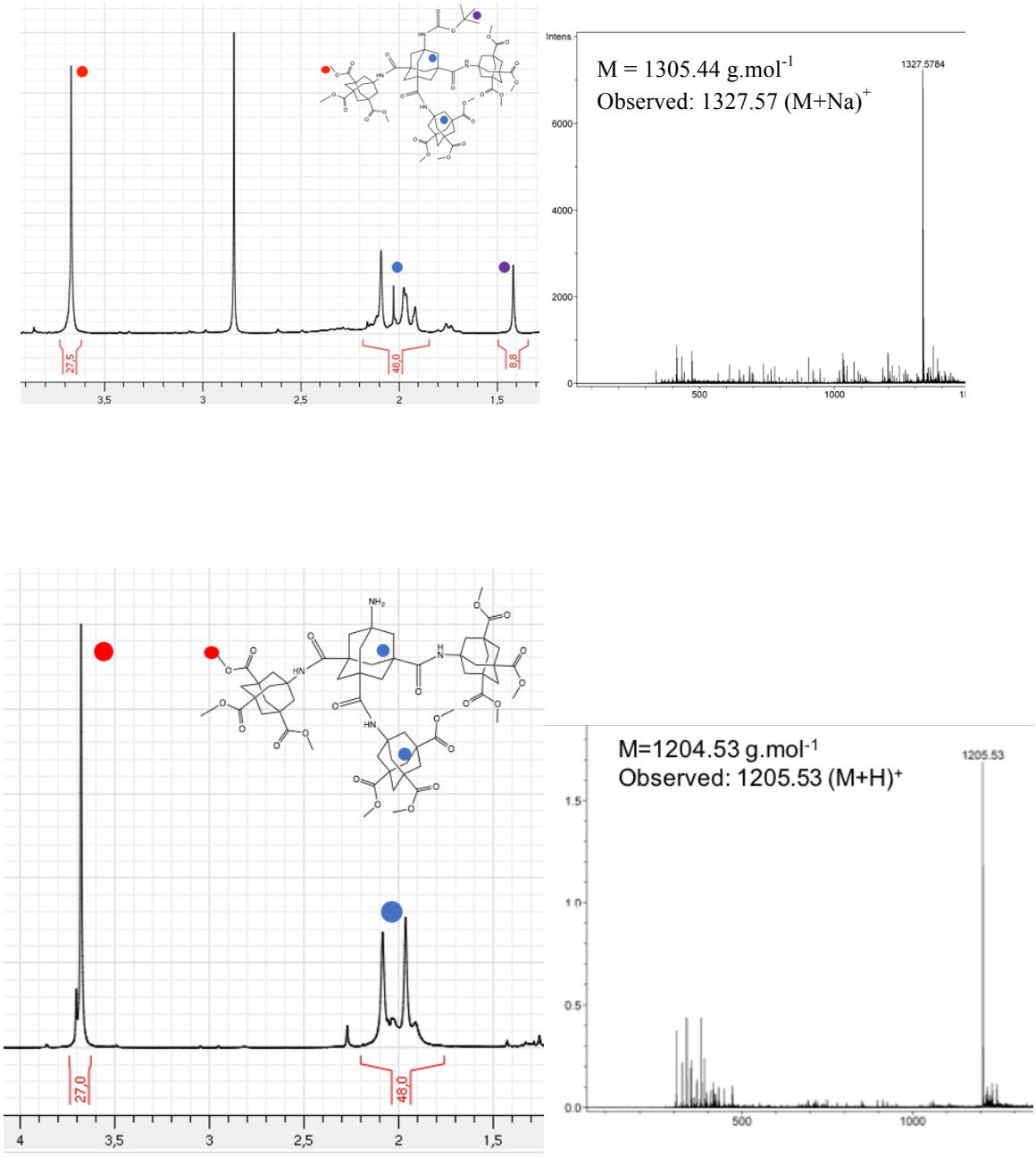

***Figure 2**: [1]H NMR and mass spectrometry characterizations of 2nd generation adamantane-based dendrons (Boc protected (top) and deprotected (bottom)).*

The key step was the coupling between Boc-protected compound **7** and the esterified amine **8**. For this purpose, I tried different conditions summarized in Table 1. All experiments were performed under inert gas such as argon or nitrogen and in an aprotic polar solvant (DMF), during 72 h with an excess of free amine, inspired by protocol of previous work did in the Lab.[12]

***Table 1**: Conditions tested for the second generation dendron synthesis.*

Solvent	Coupling agents	Base	Temperature	Yield
DMF	EDC / HOBt	DIEA	65 °C	5 %
DMF	EDC / HOBt	NEt_3	65 °C	15 %
DMF	TSTU	DIEA	65 °C	< 5 %
DMF	TSTU	NEt_3	65 °C	< 5 %
DMF	HBTU	NEt_3	65 °C	75 %

The amide bond formation consists of two consecutive steps: first the carboxyl moiety is activated, then the activated carboxylate reacts with the nucleophile, the free amine derivative. I first tried to couple compound **7** and **8** using the carbodiimide. I first selected EDC×HCl. This coupling agent has been designed for coupling in polar solvent such as DMF and less polar solvent like methylene chloride. To avoid a possible side effect (O-N migration leading to N-acyl urea which is not reactive), I used HOBt additive. It allows to enhance the reactivity and reduce both epimerization and O-N migration. As a base, DIEA is one of the most use because of his sterical hindrance, however I obtained better result with NEt_3 which is more nucleophilic. In view of the low yield obtained (5 and 15%, respectively). I decided to try other coupling reagents such as uronium derivatives. I first used *N,N,N′,N′*-tetramethyl-O-(N-succinimidyl)uronium tetrafluoroborate (TSTU), but I never isolated the desired compound (yield <5 %). Then, I tested 2-(1H-benzotriazol-1-yl)-1,1,3,3-tetramethyluronium hexafluorophosphate (HBTU). This is one of the most common coupling reagents, working both in solid phase reactions and in solution.[14] Combined with NEt_3, I successfully synthesized the second generation-based adamantane dendrons with 75 % yield.

In parallel, I also attempted to synthesize the 2nd generation adamantane dendrons with the Cbz-protected amine derivative instead of Boc. Indeed, I selected Cbz-protected adamantane **12** to react with the triester protected adamantane derivative **8** to give the desired fully protected 2nd generation dendron **16**. Then the Cbz is selectively removed by hydrogenation catalyzed by palladium on charcoal. The synthesis occurs in two step. Firstly, compound **12** is activated and then reacts with the free amine **8** through an amidation reaction. I tried to activate the three acids *in situ* with oxalyl chloride to form the highly reactive species **15**, which can then react with the free amine **8**. Unfortunately, this test was never conclusive and I never isolated the desired compound **16** (Scheme 5).

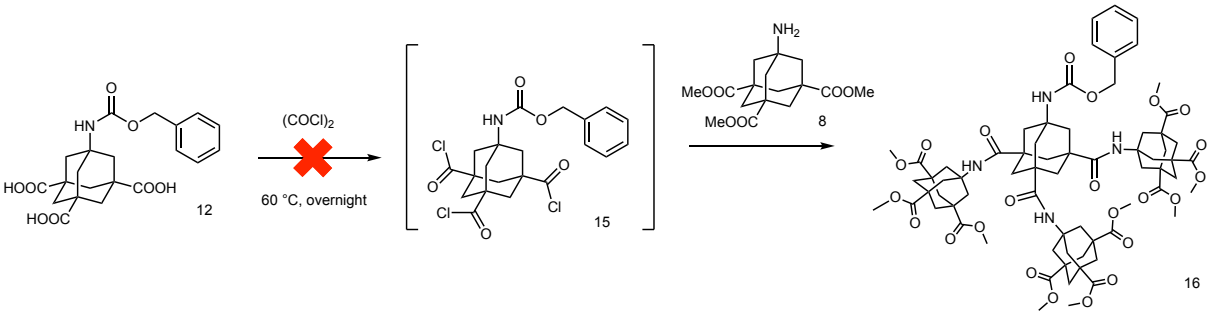

***Scheme 5**: Synthesis of 2nd generation adamantane-based dendrons using oxalyl chloride.*

Thus, I decided to try the same condition used for the Boc-protected adamantane derivative, namely, activation of the three acid groups with HBTU in presence of NEt_3 (Scheme 6). Following this procedure, I isolated the desire Cbz-protected 2nd generation adamantane dendron. However, the yield obtained was quite low (35 % compared to 75 % with Boc protected derivative). Then the selective hydrogenation of compound **16** affords almost quantitatively the desired unprotected 2nd generation dendron **14**.

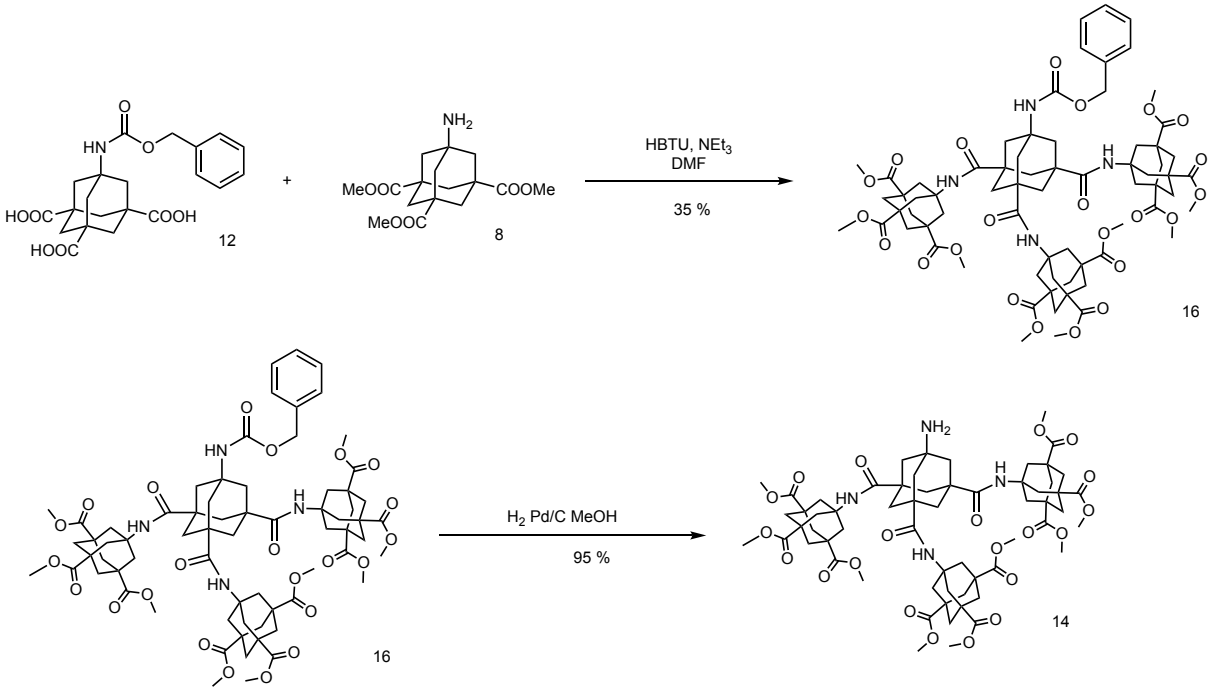

***Scheme 6**: Synthesis of 2nd generation of adamantane-based dendrons using peptide coupling reagents.*

Because of the multiple step to isolated the Cbz-adamantane derivative, I can conclude that, the best route to prepare 2nd generation dendrons is HBTU with NEt_3 on Boc-protected derivatives.

II. 2.3 Third generation dendron synthesis

As in the case of the second generation dendron synthesis, the first step was the computer simulation to assess the 3D structure of the third generation adamantane-based dendron (Figure 3). Molecular modelling shows that the sterical hindrance between the adamantane moieties is increasing causing an enhancement of density close to the core. Nevertheless, this simulation confirmed that the well-defined conformation of adamantane likely allows to achieve the third generation dendrons.

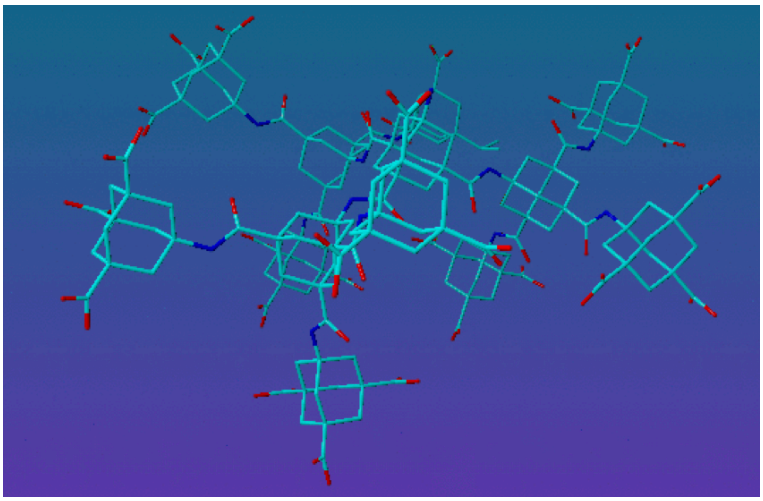

***Figure 3**: Computer simulation of 3rd generation adamantane-based dendrons.*

For the preparation of third generation dendrons, I followed the same type of procedure based on protection/deprotection, activation and amidation used to obtain the second generation dendrons. For this purpose, I started by the deprotection of the 2nd generation adamantane dendrons (Cbz or Boc protected) to give the 2nd generation adamantane dendrons with the free amine at the focal point, and still protected by methyl ester groups on periphery (compound **14**). Then compound **14** should reacts through convergent synthesis with Boc-protected-tricarboxylic acid adamantane derivatives **6** to give the fully protected 3rd generation dendron **17** (Scheme 7).

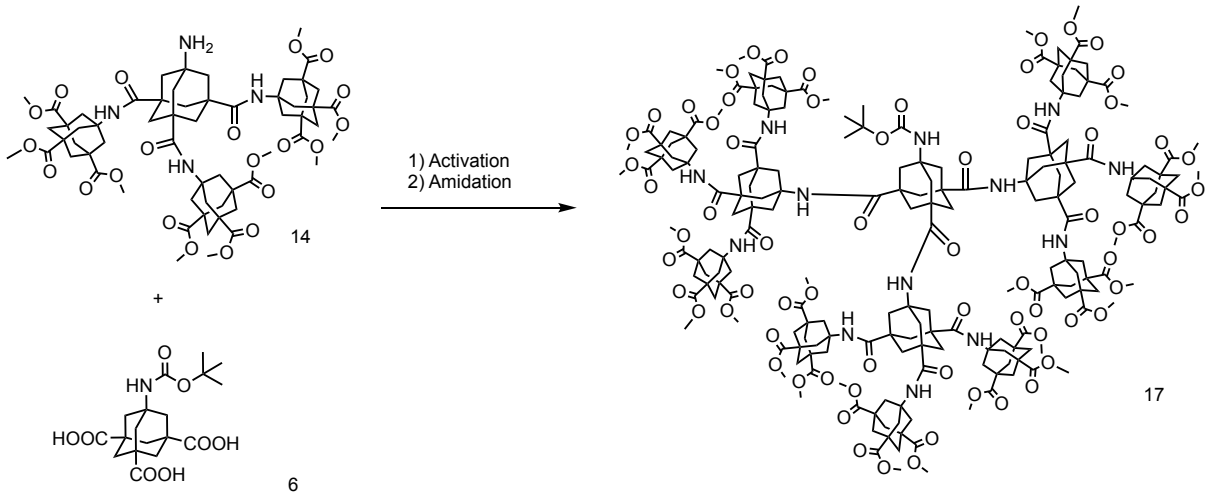

***Scheme** 7: Synthesis of the 3rd generation adamantane-based dendrons.*

I first started using the same conditions, which gave the best results for the synthesis of the second generation, namely, HBTU with NEt_3 in dry DMF under inert atmosphere (Ar) at 65 °C for three days, but unfortunately, in this case, the reaction does not occur. Thus, I tried different conditions to enhance the activation of the three carboxylic acid groups and to improve the amine nucleophilicity (Table 2).

***Table 2**: Tests for the synthesis of the 3rd generation adamantane-based dendrons*

Solvent	Coupling agents / Reagents	Base	Temperature	Time	Yield
DMF	HBTU	NEt_3	65 °C	72 h	n.d
DMF	COMU	DIEA	25 °C	5 h	n.d
DMF	COMU	DIEA	65 °C	72 h	n.d
DMF	COMU	NEt_3	65 °C	72 h	n.d
DCM	Oxyma / DIC	-	65 °C – MW	2 h	n.d
DMF	Oxyma / DIC	-	65 °C – MW	2 h	n.d
DCM	$SOCl_2$	NEt_3	r.t	5 h	n.d
Pyridine	$(COCl)_2$	-	50 °C	5 h	n.d

For this purpose, I selected as new coupling agent 1-[1-(cyano-2-ethoxy-2oxoethyliddeneaminooxy)-dimethylamino-morpholino]-uronium hexafluorophosphate (COMU). This new type of uronium coupling reagents is first safer and more effective than benzotriazole based uronium reagents such as HBTU (Figure 4). Indeed, COMU differs in its iminium moiety and leaving group. The presence of both morpholino group and oxime derivative influences the solubility, the stability and the reactivity of the reagents.[15] Moreover, COMU works in the presence of only one equivalent of base, the morpholino group is hydrogen bond acceptor and the oxyma moiety guarantee a lower risk of explosion compared to benzotriazole derivatives.[16] A further characteristic of the oxyma is the *O*-form present during the coupling compared to benzotriazole derivatives where the *N*-form is predominant and less reactive (Figure 5).

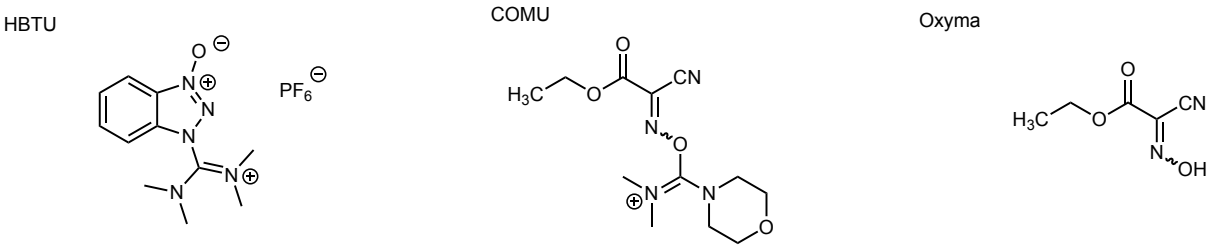

***Figure 4**: Molecular structures of HBTU, COMU and Oxyma.*

***Figure 5**: O-form (COMU) versus N-form (benzotriazole) activation.*

Another advantage of COMU is the water solubility of the by-products, which can be easily removed. In order to validate the use of COMU, I first tried it in activation of 5-hexaynoic **18** acid to functionalize the focal point of the first generation dendron **8**. I isolated the desired alkyne derivative **9** with a yield of 65 % (scheme 8) compare to 50 % with the classical EDC/HOBt combination. Moreover, the reaction is performed for 24 h against 48 h confirming that COMU is a better coupling reagent than EDC/HOBt and stable, even at 60 °C.

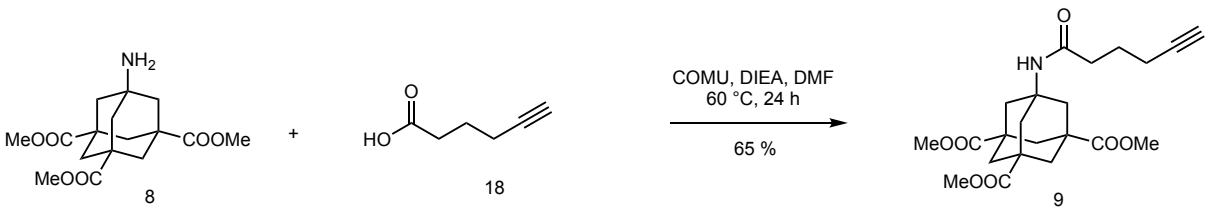

***Scheme 8**: Test reaction using COMU to functionalize amino-adamantane derivative.*

Then I tested COMU in the synthesis of 2nd generation dendrons in mild conditions (25 °C, DMF, 3 h) with DIEA as a base, and under inert atmosphere. I isolated the second generation dendrons with a yield of 45 % confirming the potential of COMU as a coupling agent. Newt step was to use COMU for the synthesis of the third generation dendrons employing different tertiary bases (NEt_3 and DIEA) and conditions (time and temperature). Unfortunately, I never isolated the desired compound using COMU. Considering that I obtained good yield for the synthesis of the second generation adamantane based dendrons, I concluded that the activation specie does exist but it does not allow to couple the derivatives **6** and **14**. The problem is likely due to the low nucleophilicity of the amine. To solve this problem, I decided to use the microwave. This technology is applied in solid phase peptide synthesis (see Chapter 3) and it has become one of the most widely used tools for the synthesis of difficult peptide sequences.[17] I selected DIC/oxyma in conjunction with DMF or DCM as the solvent, and heated the mixture by microwave (100 W) during 2 h. Again, I did not isolate the desired 3rd generation dendrons. I also tried to use 4-dimethylaminopyridine (DMAP) as catalyst with the same negative result. Finally, I decided to try a new approach with less sterical hindered and highly reactive reagents, through acyl chloride intermediates. First, I followed the procedure established by Leggio et al. who used thionyl chloride for the synthesis of secondary and tertiary amides.[18] I mixed the Boc-protected triacid derivative with the second generation free amine adamantane derivative and added the thionyl chloride. The reaction was performed in DCM with an excess of NEt_3 at room temperature for 5 h. Unfortunately, the reaction does not occur even when increasing the temperature (50 °C). Then, I selected an alternative using oxalyl chloride and pyridine (Scheme 9). The idea is to use pyridine as a solvent, as activator of the acid and as a base to neutralized the HCl formed during the reaction.

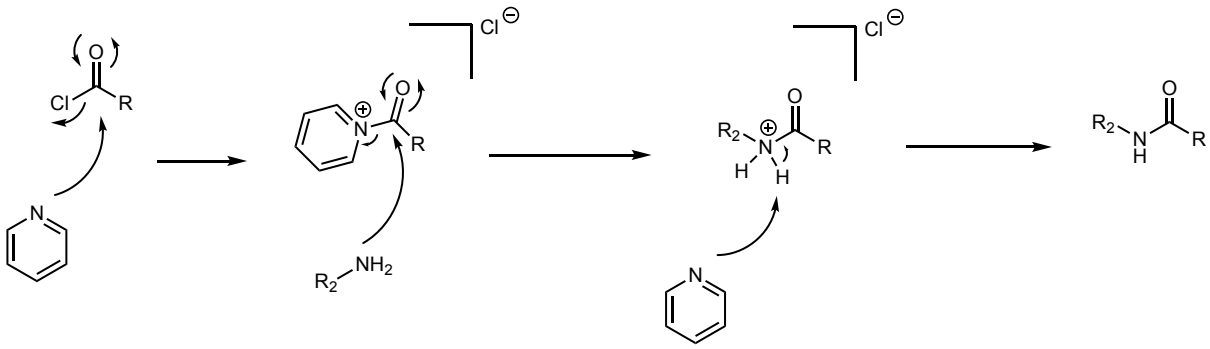

***Scheme 9**: Mechanism of peptide bond formation in pyridine with oxalyl chloride activation.*

To conclude, I have never succeeded in isolating the 3rd generation adamantane-based dendrons despite all the different trials. However, lots of parameters can be modified (temperature, pressure, coupling agents, and solvent) to find the best combination and isolate the desired compound. What it remains still unclear is the fact that I did not isolate either a truncated derivative **17** with only one or two branches.

II. 2.4 Self-assembly studies

The interest on self-assembly is important especially in nanomedicine allowing a better understanding of nanoparticles cell internalization and thus improving its use as nanovectors. Indeed, the morphology of the particles and their self-assembly capacity will endow them of unique properties such as size, shape, solubility and stability in physiological conditions. These parameters are directly linked to the pharmacokinetics properties of the particles (absorption, distribution, metabolism, elimination and toxicity). Moreover, when loaded with drugs, dendrons could protect them from degradation and improve its cell internalization, which is usually size and solubility dependent. Thus, controlling the morphology of the particles is fundamental to use them as carriers.

Using transmission electron microscopy (TEM), it is possible to analyze the morphology of the particles. In our Lab, we already observed interesting morphology of functionalized dendrons. For example, first and second generation of adamantane-based dendrons, containing triethylene glycol (TEG) as a spacer, and functionalized in the periphery (with ammonium or guanidinium) and at the focal point (with cholesterol) have been used to complex plasmid DNA.[19] Different nitrogen/phosphate (N/P) ratios have been tested and, unfortunately, relatively low transfection performance were observed. TEM analysis provided explanation for the low biological activity. Indeed, while the dendrons alone display to self-assemble in small particles (Figure 6A), when

they are used to complex plasmid DNA, the so called *Hydraplexes* displayed the formation of homogeneous and very dense nanorods. (Figure 6B). The functionalization with cholesterol rendered the polycationic more hydrophobic, leading to strongly binding and protection of pDNA. However, due to their size spanning several micrometers, the gene transfection resulted very limited.

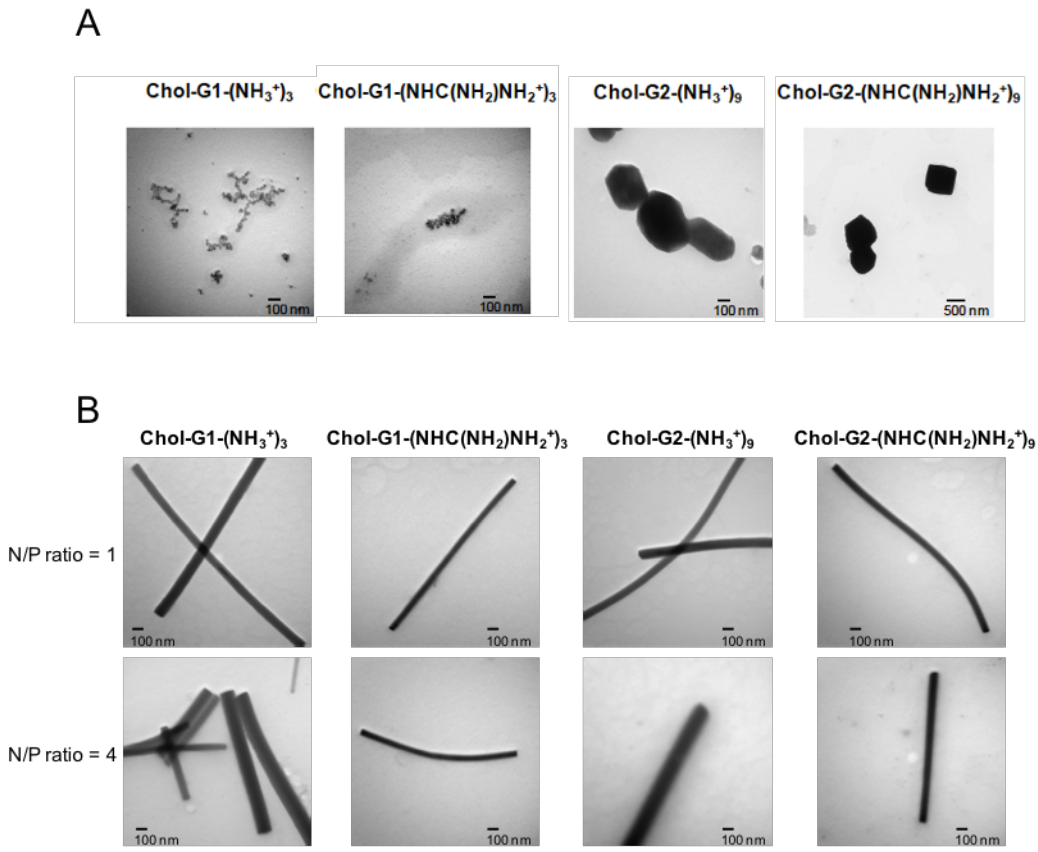

***Figure 6**: TEM images of cholesterylated* HYDRAmers (A) and *HYDRAplexes* (B) *at 1 and 4 N/P ratios.*[19]

II. 2.4.1 TEM analysis of adamantane-based dendrons with spacers

I decided to use TEM and investigate the morphology of a series of different functionalized adamantane based dendrons, synthesized during my thesis together with some dendrons that where available as previously synthesized in our Lab. For this purpose, the particles are solubilized in the appropriate solvent at the desired concentration. After 30 min of self-assembly, 10 μL of solution are deposited to a carbon grid. After evaporation of the solvent, the particles are analyzed by TEM. The morphology of the particles observed depends on several parameters including solvent, temperature, concentration and the intrinsic characteristics of the molecules. I started with functionalized based dendrons with spacers previously synthesized in our laboratory. The synthesis of these compounds was reported in a previous thesis. Firstly, I selected an adamantane derivative protected at the focal point with a Cbz group and functionalized at the periphery by the Boc protected amino acid histidine (Figure 7). Moreover, to study the impact of the solvent and the concentration, I analyzed different samples with different concentration and solvent mixture proportion by TEM. Then other functionalized dendrons have been analyzed to better understand the role of functional groups on the self-assembly process. I started with functionalized based dendrons with spacers previously synthesized in our laboratory. The synthesis of these compounds was reported in a previous thesis. Firstly, I selected an adamantane derivative protected at the focal point with a Cbz group and functionalized at the periphery by the Boc protected amino acid histidine (Figure 7). Moreover, to study the impact of the solvent and the concentration, I analyzed different samples with different concentration and solvent mixture proportion.

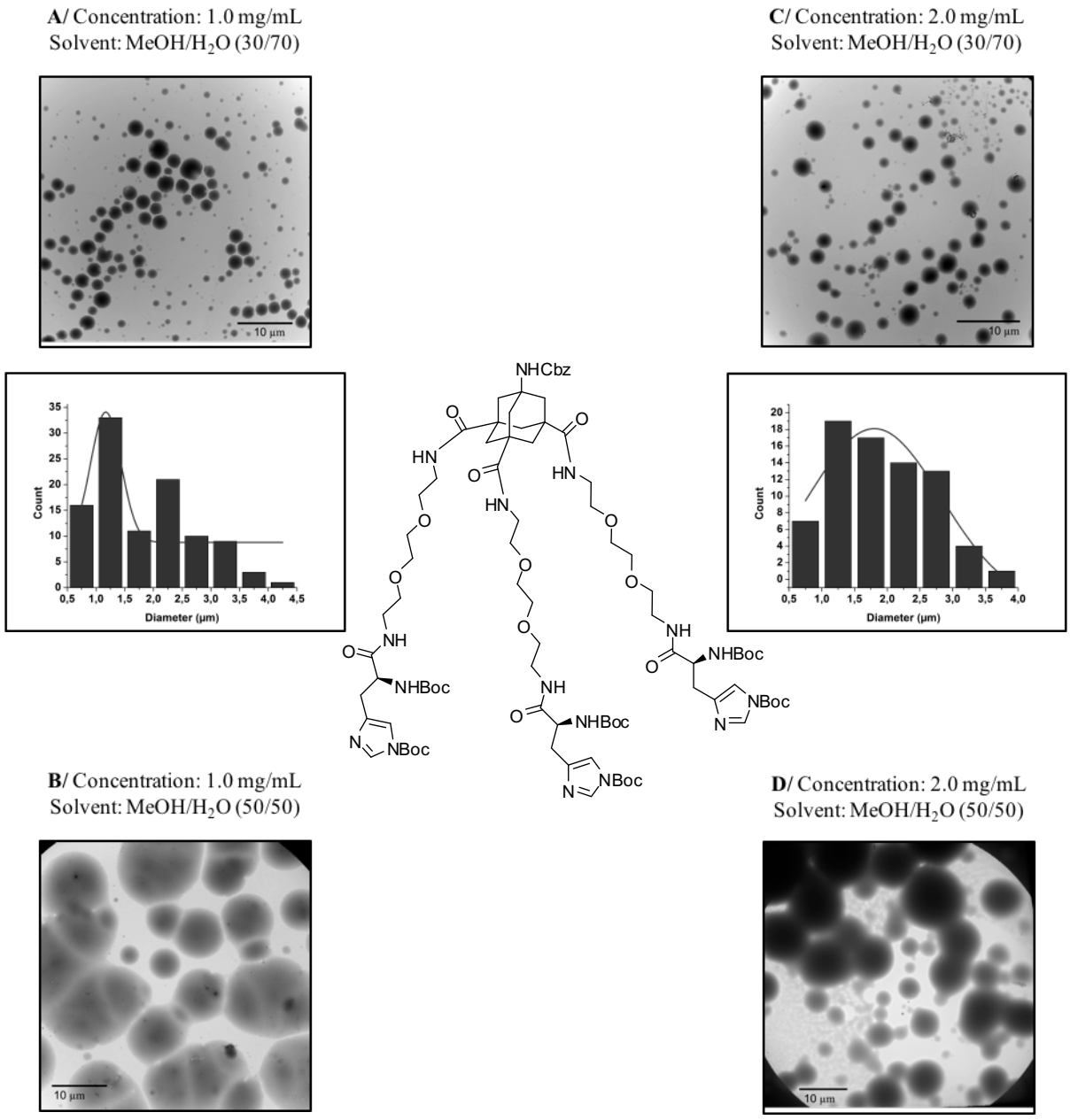

Figure 7: *TEM images of Cbz and histidine protected adamantane 1st generation dendrons at different concentrations and/or solvents. Polydispersity of A (n=104) and C (n=95).*

As shown in Fig. 7 we can observe that generally the histidine functionalized dendrons self-assemble forming spherical particles. However, the assemble morphology is strongly affected by the solvent as shown in Figure 7A and 7B. Indeed, using 30 % methanol (Fig 7A), we observe formation of spherical particles, highly dense with an average diameter size of 1.25 µm, while when the proportion of methanol increase until 50 % (Fig 7B), the molecules do not self-assemble. The self-assembly process is enhanced by the dendrons intermolecular

interactions and hampered by the dendron-solvent interactions. Most probably, when the concentration of methanol is too high the dendrons are better solubilized by the solvent mixture and so they do not form any evident self-assemble in solution. Meanwhile, a lower concentration of methanol enhances the dendrons-dendrons interaction and so favour the spherical assembly formation. A similar effect is observed when I increased the dendron concentration (Figure 7C and 7D). Indeed, when we compare Figure 7A and 7C, both conditions lead to spherical particle formation (30 % methanol). However, the particle size increased from 1.25 to 1.75 µm meaning that the concentration influence their size. Even at 50 % methanol (Figure 7D), the increase of the concentration induces some particle formation. However, they are bigger (12 µm), and not well-defined, more similar to aggregates than to self-assembled particles.

Then, I analyzed another Cbz-protected derivative where the periphery is functionalized with a benzyl-protected tyrosine (Figure 8).

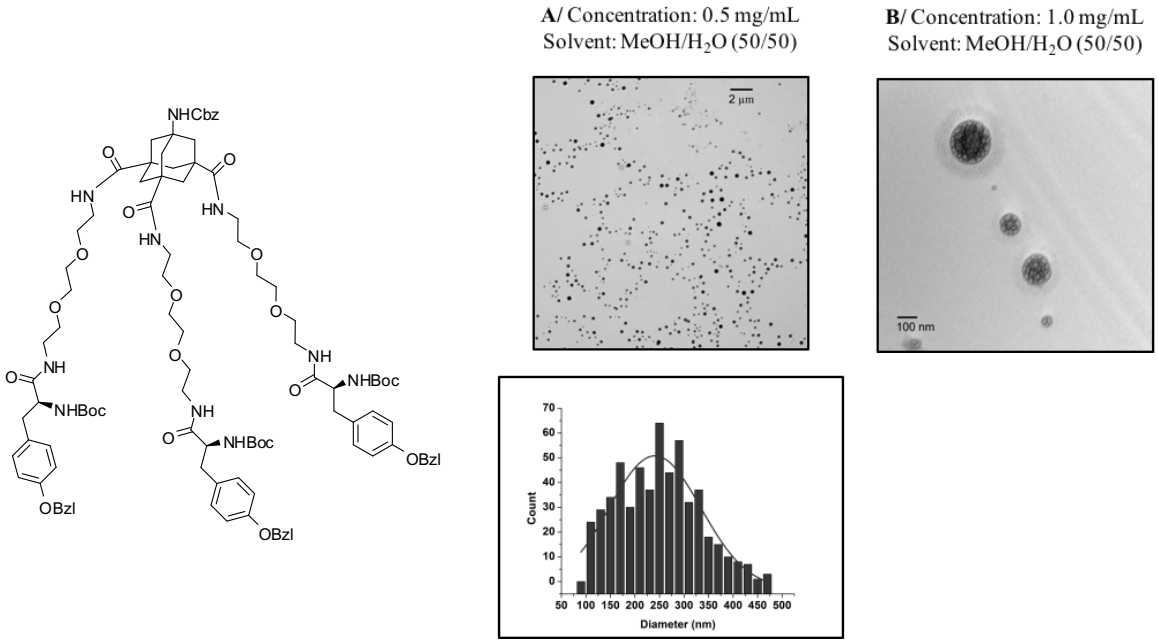

***Figure 8**: TEM images of Cbz and tyrosine protected adamantane 1st generation dendrons at different concentrations. Polydispersity (n=541).*

Because of the low solubility of this molecule in water, I performed the analysis only in methanol/water mixture (1:1). Once again, the tendency of the molecule it to self-assemble to form spherical nano-object. If we compare the Figure 8B with Figure 7B (C=1.0 mg/mL and solvent 1:1 methanol/water), in the former the particles clearly self-assembled. However, they are not well-defined and quite small (less than 150 diameter length). Moreover, these particles seem to be porous. Then, I analyzed the same molecules more diluted (C=0.5 mg/mL) and obtained well-defined and homogenous particles with an average diameter size of 250 nm. These experiments confirm first the importance of the combination solvent/concentration, and second the role of the functional groups on the periphery, which impact on the solubility and on the self-assembly ability of the molecules.

II. 2.4.2 TEM analysis of adamantane-based dendrons without spacers

Subsequently, I focused my attention on the analysis by TEM of the functionalized adamantane derivatives without spacers. In particular, I studied the 1st and the 2nd generation adamantane dendrons, functionalized or not at the focal point (amine) and at the periphery (carboxylic acids). First, I started with the Boc protected tricarboxylic acid derivative **7**. In this case, I also performed SEM measurements to confirm the 3D morphology (Figure 9).

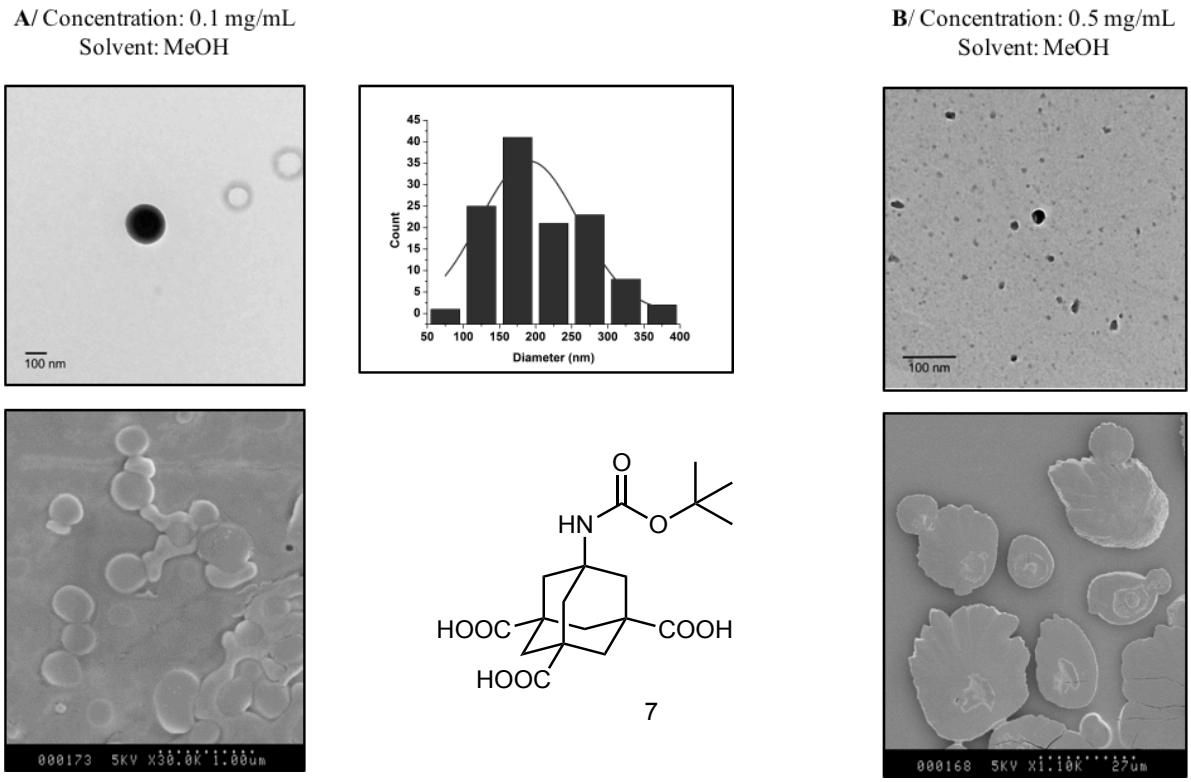

***Figure 9**: TEM and SEM images of Boc protected adamantane-based dendron 7. Polydispersity of A (n=122).*

In the TEM images, we observe the formation of spherical particles at 0.1 mg/mL. They are well defined and highly dense with an average diameter of 190 nm. The same concentration on SEM surface also leads to the formation of spherical particle but less well defined and with a bigger average size (around 300 nm). Moreover, on SEM the particles look to strongly interact together. However, tilt SEM analysis allows to confirm the spherical shape of the self-assembled particles. The difference observed in TEM and SEM can be explained by the interaction with the solid support. Indeed, in TEM the deposit is done on a carbon grid, more hydrophobic than the silicon dioxide wafer, which is used for SEM analysis. When the concentration increase up to 0.5 mg/mL, in both case (TEM and SEM), I observed the loss of the spherical shape. The particles seem to aggregate especially in SEM. To determine the importance of the Boc protecting group at the focal point, I analyzed another derivative where the Boc group is replaced by an alkyne group (Figure 10). In this case, we observe a clear difference in the morphology. Indeed, at 0.5 mg/mL the particles self-assemble into spheres with an average diameter of 115 nm and they are well dispersed, while when the concentration increases to 1.0 mg/mL, the particles self-assemble totally differently to form highly dense and quite well defined sheets.

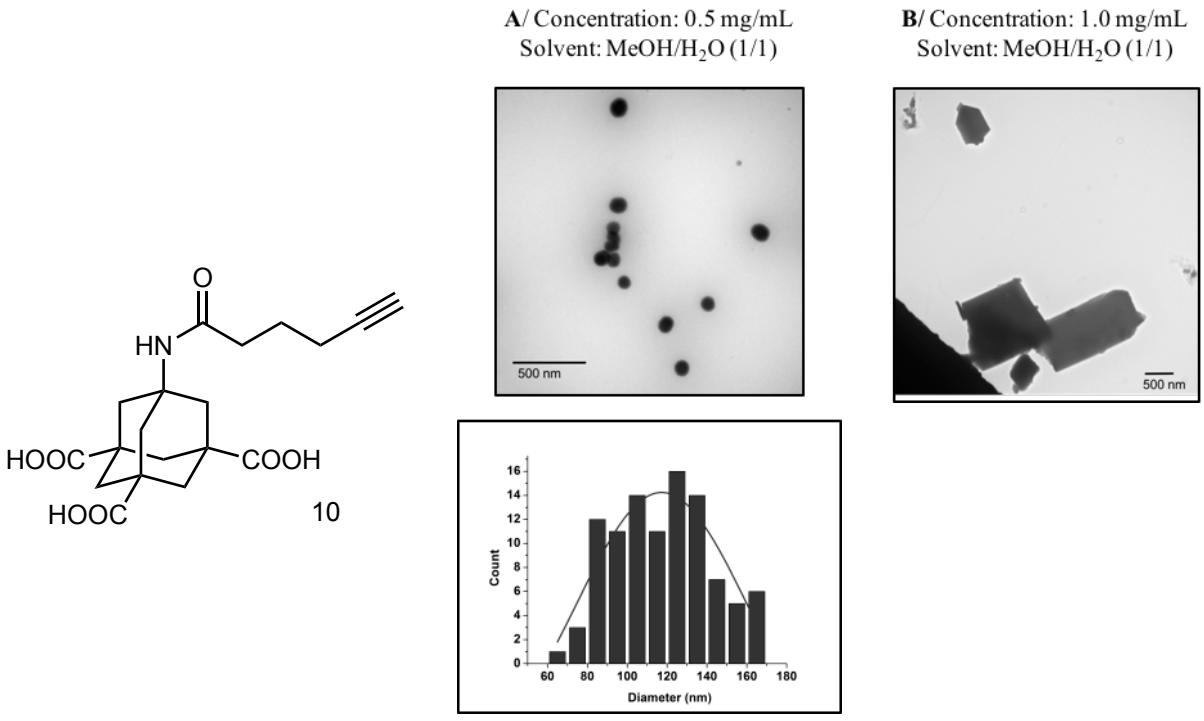

***Figure 10**: TEM images of alkyne protected first generation adamantane-based dendron **10**. Polydispersity of A (n=101)*

The same alkyne derivative with ester groups protecting the carboxylic acids adopted different supramolecular structures (Figure 11). Even at low concentration (0.1 mg/mL), I never observed the formation of spherical particles. Instead, I could see small rods (1-2 µm in length). When I increased the concentration, the particles self-assemble and form long ribbons of several micron length, confirming that both focal point and periphery functional groups play an important role in dictating the self-assembly behavior.

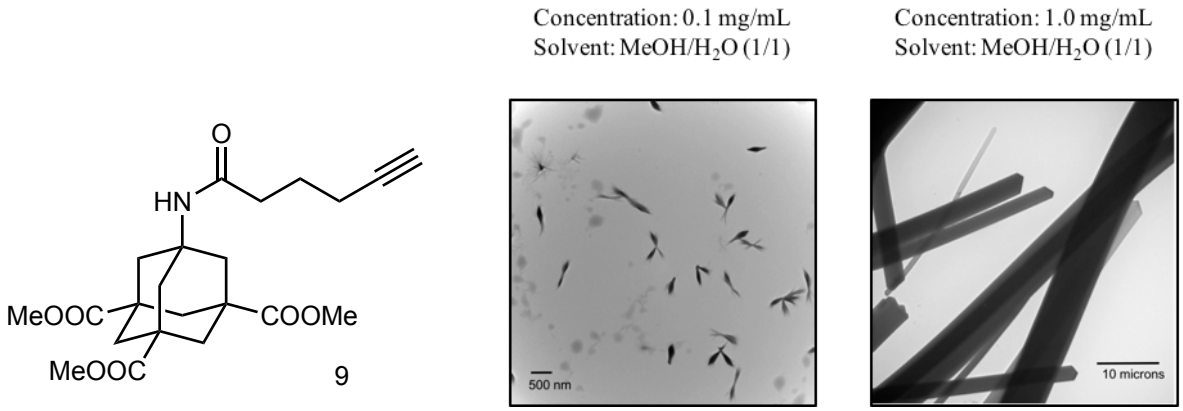

***Figure 11**: TEM images of alkyne-triester protected first generation adamantane-based dendron **9**.*

I also synthesized a first generation adamantane-based dendron with a lipophilic group at the focal point (see Chapter 3 for details). Because of the hydrophobic properties of the molecule, the compound is not soluble in water and poorly soluble in methanol. Only one concentration was analyzed, the 0.1 mg/mL (Figure 12). We can observe the formation of not well defined spherical particles with a diameter closed to 100 nm. The same type of self-assembled particles were obtained previously with cholesterylated admantane based dendrons confirming the role of lipophilic groups at the focal point on the self-assembly process.[19]

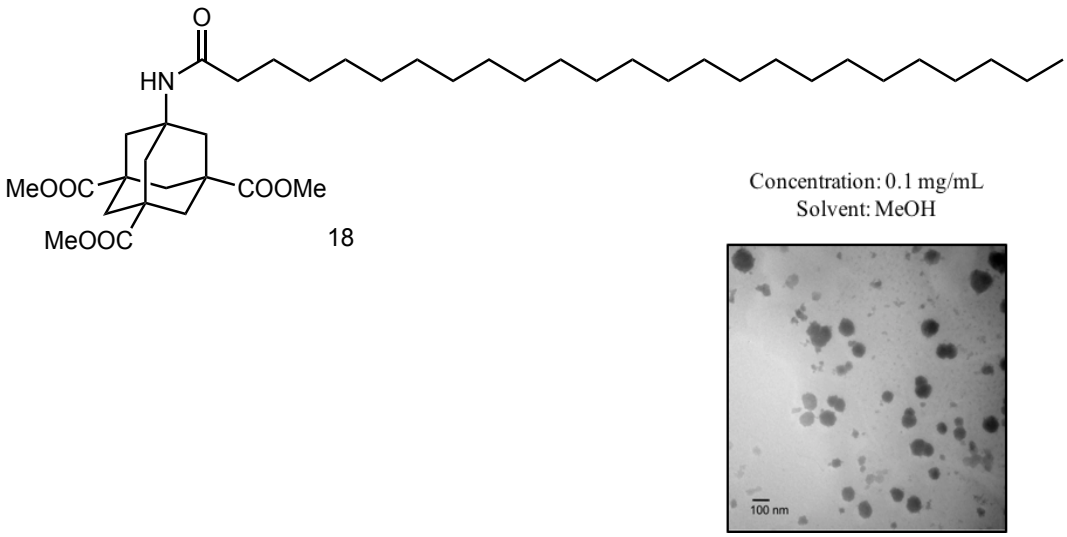

***Figure 12**: TEM images of hexacosanyl triester functionalized adamantane first generation based dendron **18**.*

Finally, I analyzed the second generation adamantane-based dendrons, Boc protected (Figure 13) and with the free amine (Figure 14).

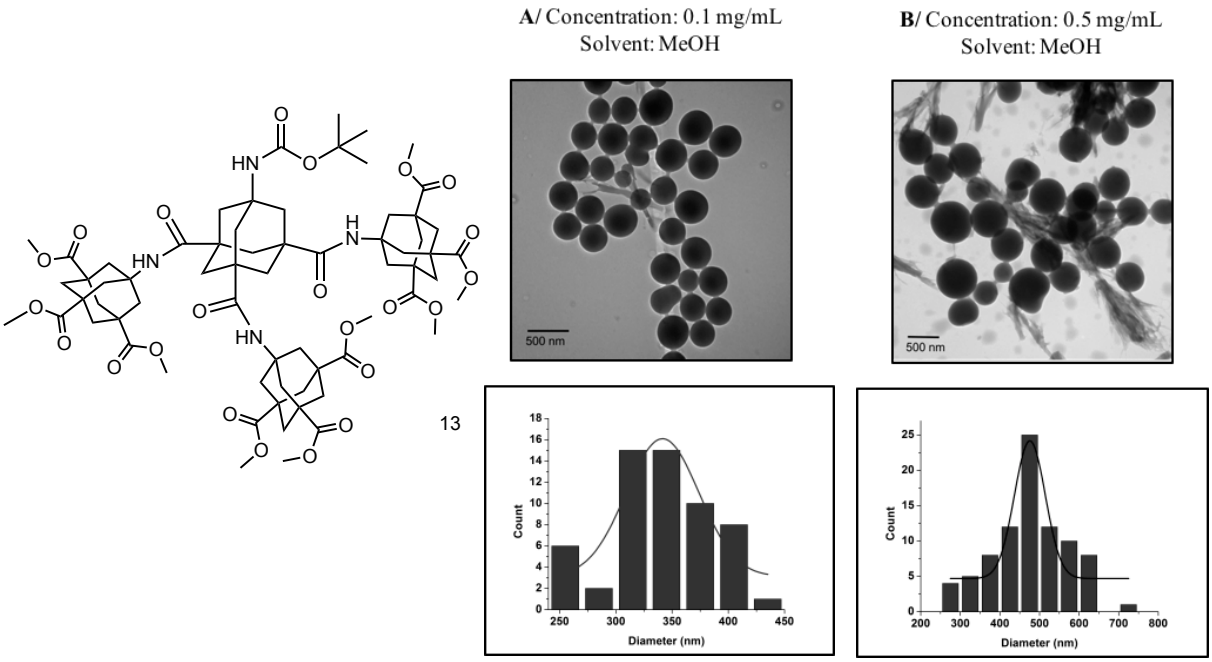

Figure 13: *TEM images of 2nd generation adamantane-based dendron Boc protected* ***13****. Polydispersity of A (n=89), of B (n=97).*

In both cases, the size of the particles increase with the concentration. The Boc protected derivative self-assembles in well-defined spherical particles with an average size of 340 nm at 0.1 mg/mL, and 475 nm at 0.5 mg/mL (Figure 13). In the case of the deprotected derivative (Figure 14), we can observe that the particles are less dense and less well defined. Even if some spherical particles are observed at 0.1 mg/mL, when the concentration increases to 0.5 mg/mL, there is tendency to form bigger particles (1.2 μm diameter length), which seem to interact in pairs. Moreover, it looks like that changing the molecule properties due to the lack of protecting group at the focal point completely change the self-assembly process.

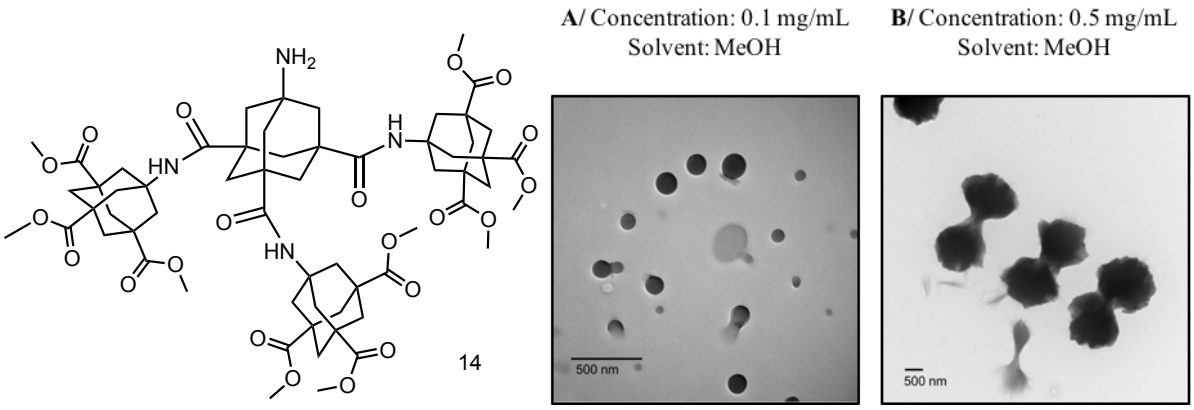

***Figure 14**: TEM images of 2nd generation adamantane-based dendron deprotected **14**.*

These results confirm the importance of the functional groups, the concentration and the solvent in the self-assembly process. The spacers do not affect the morphology but play a role in the solubility. As expected, the focal point and the periphery play a more important role in the self-assembly, certainly because the functional groups at these positions interact with the solvent and with other molecules leading to the formation of the particles. TEM is a powerful but also limited technique. We only observe images in two dimensions, as TEM is based on transmitted electrons. A possible solution is to use scanning electronic microscopy. SEM is based on scattered electrons and thus provides three-dimensional pictures. Nevertheless, SEM has a lower resolution. Thus, the best would be their combination. Another limitation of these techniques is that the compounds are dried on a surface, which likely affects the self-assembly process. To complete theses analyses, it would be interesting to study the particles using cryogenic transmission electron microscopy (cryo-TEM). Cryo-TEM maintains the sample at low temperature using liquid helium and allows imaging in vitreous ice, which is more representative of the particles assembly in solution. Finally, dynamic light scattering (DLS) could be interesting to measure the size distribution profile of the particles in suspension at different temperature and confirm the self-assembly of the particles in solution.

II. 3 Conclusion & Perspectives

In this chapter, I described the synthesis of a series of 1st and 2nd generation adamantane-based dendrons. I optimized the synthetic steps leading to the formation of aminotricarboxylic acid (3+1) building block. This compound is the key molecule for the synthesis of further generation adamantane dendrons or for the multi-functionalization of the first generation. I also described the different experiments done to synthesized the 3rd generation of adamantane dendrons. Despite, my effort I never succeeded to isolate the desired compound.

The TEM analysis of functionalized adamantane allows to observe the morphology of the nanoparticles obtained by the self-assembly of the different dendrons. I proved the important role of both the focal point and the periphery in the self-assembly processes to form these nanoparticles. Playing with different groups, I observed the formation of different shapes, mainly spherical. I also observed formation of sheet and ribbons in some case. These analyses confirmed that the self-assembly depends on several parameters including concentration and solvent.

The future work will be to achieve the synthesis of the 3rd generation adamantane-based dendrons, by using microwave which is a promising technique to improve peptide bond yields. Subsequently, the different generations of adamantane dendrons could be functionalized and explored for biological applications.

II.4 References

(1) Abbasi, E.; Aval, S. F.; Akbarzadeh, A.; Milani, M.; Nasrabadi, H. T.; Joo, S. W.; Hanifehpour, Y.; Nejati-Koshki, K.; Pashaei-Asl, R. Dendrimers: Synthesis, Applications, and Properties. *Nanoscale Res. Lett.* **2014**, *9* (1), 247.

(2) van der Poll, D. G.; Kieler-Ferguson, H. M.; Floyd, W. C.; Guillaudeu, S. J.; Jerger, K.; Szoka, F. C.; Fréchet, J. M. Design, Synthesis, and Biological Evaluation of a Robust, Biodegradable Dendrimer. *Bioconjug. Chem.* **2010**, *21* (4), 764–773.

(3) Newkome, G. R.; Shreiner, C. Dendrimers Derived from 1 → 3 Branching Motifs. *Chem. Rev.* **2010**, *110* (10), 6338–6442.

(4) Lee, C. C.; MacKay, J. A.; Fréchet, J. M. J.; Szoka, F. C. Designing Dendrimers for Biological Applications. *Nat. Biotechnol.* **2005**, *23* (12), 1517–1526.

(5) Welsh, D. J.; Smith, D. K. Comparing Dendritic and Self-Assembly Strategies to Multivalency--RGD Peptide-Integrin Interactions. *Org. Biomol. Chem.* **2011**, *9* (13), 4795–4801.

(6) Matsumura, Y.; Maeda, H. A New Concept for Macromolecular Therapeutics in Cancer Chemotherapy: Mechanism of Tumoritropic Accumulation of Proteins and the Antitumor Agent Smancs. *Cancer Res.* **1986**, *46* (12 Pt 1), 6387–6392.

(7) Tian, W.; Ma, Y. Theoretical and Computational Studies of Dendrimers as Delivery Vectors. *Chem. Soc. Rev.* **2012**, *42* (2), 705–727.

(8) de Brabander-van den Berg, E. M. M.; Meijer, E. W. Poly(Propylene Imine) Dendrimers: Large-Scale Synthesis by Hetereogeneously Catalyzed Hydrogenations. *Angew. Chem. Int. Ed. Engl.* **1993**, *32* (9), 1308–1311.

(9) Tomalia, D. A.; Baker, H.; Dewald, J.; Hall, M.; Kallos, G.; Martin, S.; Roeck, J.; Ryder, J.; Smith, P. A New Class of Polymers: Starburst-Dendritic Macromolecules. *Polym. J.* **1985**, *17* (1), 117–132.

(10) Lv, H.; Zhang, S.; Wang, B.; Cui, S.; Yan, J. Toxicity of Cationic Lipids and Cationic Polymers in Gene Delivery. *J. Control. Release Off. J. Control. Release Soc.* **2006**, *114* (1), 100–109.

(11) Lamanna, G.; Russier, J.; Dumortier, H.; Bianco, A. Enhancement of Anti-Inflammatory Drug Activity by Multivalent Adamantane-Based Dendrons. *Biomaterials* **2012**, *33* (22), 5610–5617.

(12) Grillaud, M.; Russier, J.; Bianco, A. Polycationic Adamantane-Based Dendrons of Different Generations Display High Cellular Uptake without Triggering Cytotoxicity. *J. Am. Chem. Soc.* **2014**, *136* (2), 810–819.

(13) Fleck, C.; Franzmann, E.; Claes, D.; Rickert, A.; Maison, W. Synthesis of Functionalized Adamantane Derivatives: (3 + 1)-Scaffolds for Applications in Medicinal and Material Chemistry. *Synthesis* **2013**, *45* (11), 1452–1461.

(14) Adam, S. HBTU: A Mild Activating Agent of Muramic Acid. *Bioorg. Med. Chem. Lett.* **1992**, *2* (6), 571–574.

(15) El-Faham, A.; Subirós Funosas, R.; Prohens, R.; Albericio, F. COMU: A Safer and More Effective Replacement for Benzotriazole-Based Uronium Coupling Reagents. *Chem. Weinh. Bergstr. Ger.* **2009**, *15* (37), 9404–9416.

(16) Wehrstedt, K. D.; Wandrey, P. A.; Heitkamp, D. Explosive Properties of 1-Hydroxybenzotriazoles. *J. Hazard. Mater.* **2005**, *126* (1–3), 1–7.

(17) Vanier, G. S. Microwave-Assisted Solid-Phase Peptide Synthesis Based on the Fmoc Protecting Group Strategy (CEM). *Methods Mol. Biol. Clifton NJ* **2013**, *1047*, 235–249.
(18) Leggio, A.; Belsito, E. L.; Luca, G. D.; Gioia, M. L. D.; Leotta, V.; Romio, E.;

Siciliano, C.; Liguori, A. One-Pot Synthesis of Amides from Carboxylic Acids Activated Using Thionyl Chloride. *RSC Adv.* **2016**, *6* (41), 34468–34475.

(19) Grillaud, M.; Garibay, A. P. R. de; Bianco, A. Polycationic Adamantane-Based Dendrons Form Nanorods in Complex with Plasmid DNA. *RSC Adv.* **2016**, *6* (49), 42933–42942.

Chapter II: Experimental Section

General experimental details

Chemicals and Solvents

All the starting materials, chemicals, and anhydrous solvents were obtained from commercial suppliers (Sigma-Aldrich, Acros Organics and Alfa Aeasar laboratories). All solvent used for the synthesis were analytical grade. When anhydrous conditions were required, high quality commercial dry solvent were used. Water was purified using Millipore filter system MilliQ® equipped with Biopak® filter.

Characterization Methods and Instrumentation

Thin layer Chromatography (TLC): TLC was conducted on pre-coated aluminium plates with 0.25 mm *Macherey-Nagel* silica gel with fluorescent indicator UV254.

Column Chromatography**:** Chromatographic purifications were carried out with silica gel (Merck Kieselgel 60, 40-60 μm, 230-400 mesh ASTM).

Nuclear Magnetic Resonance: ^{1}H-NMR and ^{13}C-NMR spectra were recorded in deuterated solvents using Bruker Avance I – 300 MHz and Bruker Avance III – 400 MHz. Chemical shifts are reported in ppm using the residual signal of deuterated solvent as reference (TMS = 0). Coupling constants *J* are reported in Hertz (Hz), and the splitting patterns are designated as *s* (singlet), *d* (doublet), *t* (triplet), *td* (triplet of doublet), *q* (quartet), *p* (pentet), *m* (multiplet), and *br* (broad).

Infrared Spectroscopy: IR spectra were measured on a Perkin–Elmer Spectrum One ATR-FTIR spectrometer.

ESI Mass Spectrometry: Mass spectra were recorded on a Thermo Fisher Finnigan LCQ Advantage Max Instrument.

High resolution ESI Mass Spectrometry: MS experiments were performed on a Bruker Daltonics microTOF spectrometer (Bruker Daltonik GmgH, Bremen, Germany) equipped with an orthogonal electrospray (ESI) interface. Calibration was performed using Tunning mix (Agilent Technologies).

Transmission Electron Microscopy: TEM analyses were performed on a Hitachi H7500 microscope with an accelerating voltage of 80 kV. The samples were dispersed in solvent at the desire concentration and were briefly sonicated. Then, samples were let in solution for 30 min. Ten microliters of the solution were drop-casted onto a carbon-coated copper grid (Formvar/Carbon 300 Mesh, Cu from Delta Microscopies) and left for evaporation under ambient conditions.

Scanning Electron Microscopy: SEM analysis were performed on a Hitachi S-800 scanning electronic microscope. The samples were dispersed in solvent at the desired concentration and shortly sonicated. Then, they were kept in solution for 30 min. 20 microliters of the solution were dropped onto a silica wafer. After solvent evaporation, the samples were metalized with gold-palladium deposition using SCD030 Balzers device and analyzed.

Microwave heating: MW experiments were performed using a CEM Discover SP microwave synthesizer (power: 100 W regulated with the temperature).

Synthesis and characterization data

Adamantane-based building block

1,3,5-triphenyladamantane (2)

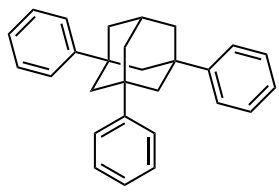

Aluminum chloride (0.93 g, 6.97 mmol) was added at 0°C to a solution of bromoadamantane (15.0 g, 69.72 mmol), *t*-butylchloride (15.75 mL, 139.4 mmol) in 100 mL of benzene. The reaction mixture was stirred at 0 °C for 1.5 h and then at rt for 1.5 h. The reaction was stopped by addition of HCl 1 M, 25 mL and filtered through sintered glass. The precipitate was recrystallized in chloroform overnight at 60 °C and filtered through sintered glass (washed with hot chloroform). The solvent of the filtrate was evaporated *in vacuo* and the solid obtained was washed with Et_2O (2×20 mL) to yield **2** as a white powder (19.0 g, 52.1 mmol, 75 %). ^{1}H NMR ($CDCl_3$, 400 MHz) δ: 7.43 (*t*, J = 7.7 Hz, 6H, Ar*H*), 7.33 (*t*, J = 7.7 Hz, 6H, Ar*H*), 7.03 (*t*, J = 7.7 Hz, 3H, Ar*H*), 2.54 (*p*, J = 3.8 Hz, 1H, C*H*-$(CH_2)_3$), 2.11 (*s*, 6H, CH_2), 2.01 (*d*, J = 3.5 Hz, 6H, 3xCH_2-CH).

1-bromo-3,5,7-triphenyladamantane (3)

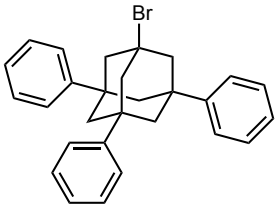

Compound **2** (5.05 g, 13.8 mmol), CBr_4 (27.57 g, 83.1 mmol), *n*-tetrabutylammonium bromide (1.33 g, 4.65 mmol) were solubilized in fluorobenzene (100 mL). 100 mL of a solution of sodium hydroxide 50 % was added and the mixture was stirred at 90 °C for 72 h. The fluorobenzene is removed *in vacuo* and AcOEt (150 mL) is added. The organic phase is washed with saturated aqueous solutions NH_4Cl (2 × 100 mL), $NaHCO_3$ (2×100 mL) and brine. The organic phase was dried over magnesium sulfate and concentrated under *vacuo* to give compound **3** with 89% yield. ^{1}H NMR ($CDCl_3$, 400 MHz) δ: 7.26 (*t*, J = 7.4 Hz, 6H, Ar*H*), 7.21 (*t*, J = 7.4 Hz, 6H, Ar*H*), 7.09 (*t*, J = 7.4 Hz, 3H, Ar*H*), 2.47 (*s*, 6H, CH_2), 2.00 (*s*, 6H, CH_2). MS (ESI) m/z: 444.42 $[M+H]^+$.

1,3,5-triphenyl-7-actetylaminoadamantane (4)

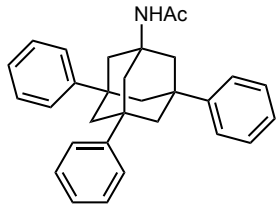

To a suspension of 1-bromo-3,5,7-triphenyladamantane (2.5 g, 5.6 mmol) in 200 mL of acetonitrile was added concentrated sulfuric acid (3.6 mL, 67.2 mmol). The mixture was refluxed 24 h and the solvent was removed under *vacuo*. The reaction mixture was poured into ice water and the product was extracted with ethyl acetate (3×120 mL). The combined organic layers were dried over magnesium sulfate, filtered and evaporated to give the acetamide **4** as a white solid (1.9 g, 4.5 mmol, 80% yield). ^{1}H NMR ($CDCl_3$, 400 MHz) δ: 7.33 (*t*, J = 7.9 Hz, 6H, Ar-*H*), 7.24 *(t*, J = 7.9 Hz, 6H, Ar-*H*), 7.12 (*t*, J = 7.9 Hz, 3H, Ar-*H*), 5.50 (*s*, 1H, N*H*), 2.2 (*s*, 6H, 3xCH_2), 2.01 (*s*, 6H, 3xCH_2), 1.88 (*s*, 3H, CH_3); ^{13}C NMR ($CDCl_3$, 75 MHz) δ: 169.78 (*C*=O) 148.37 (*C*=C), 128.37 (*C*=C), 126.21 (*C*=C), 124.95 (*C*-N), 54.86 (*C*H_2), 47.26 (*C*H_2), 45.27 (C_q), 39.73 (C_q), 24.57 (*C*H_3-C); MS (ESI) m/z: 284.3 $[M+H]^+$.

1,3,5-tricarboxylic-7-acetylamidoadamantane acid (5)

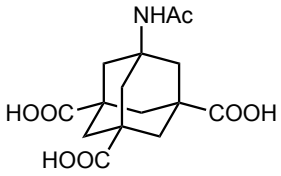

$RuCl_3×H_2O$ (0.27 g, 1.3 mmol) was added to a solution of 1,3,5-triphenyl-7-actetylaminoadamantane **4** (1.6 g, 3.8 mmol) and periodic acid (39.0 g, 171 mmol) in 100 mL of CCl_4/MeCN/H_2O (3/2/3), kept at 0 °C. The resulting mixture was stirred at rt for 72 h. Then the reaction mixture is poured into ice water and the excess of oxidant was destroyed by sodium sulfite addition. The aqueous layer was acidified with 2 N HCl to reach pH 1. Then, compound is extracted with ethyl acetate (3×200 mL). The combined organic layers were dried on magnesium sulfate, filtrated and the solvent was removed under *vacuo*. The powder obtained was finally washed with diethyl ether to give **5** as a lightly brown powder. (1.0 g, 3.2 mmol, 85%). ^{1}H NMR (DMSO-d_6, 300 MHz) δ: 12.51 (*s,br*, 3H, COO*H*), 1.95 *(s*, 6H, 3xCH_2), 1.75 (*s*, 3H, CH_3), 1.70-1.82 (*m*, 6H, 3xCH_2); ^{13}C NMR (DMSO)d_6, 75 MHz) δ: 176.58 (*C*=O), 169.12 (*C*=ONH), 51.58 (*C*-N), 41.90 (*C*H_2), 40.70 (*C*H_2), 38.52 (C_q), 23.62 (*C*H_3-C); MS (ESI) m/z: 326,2 $[M+H]^+$.

1-amino-3,5,7-tricarboxylicadamantane acid (6)

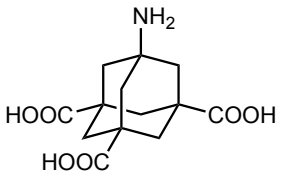

A solution of 1,3,5-tricarboxylic-7-acetylamidoamantane acid **5** (1.2 g, 3.7 mmol) in a mixture of water (20 mL) and concentrated HCl (5 mL) was refluxed for 24 h. After cooling to rt, the solution was washed with ethyl acetate (2×25 mL) and the aqueous phase was evaporated and the product was solubilized in 2 mL MeOH and precipitated by adding diethyl ether to give compound **6** as a white powder (1.0g, 3.5 mmol, 95% yield). ^{1}H NMR (DMSO-d_6, 300 MHz) δ: 12.33 (*br*, 3H, COO*H*), 8.40 (*br*, 2H, NH_2), 1.85 (*s*, 6H, 3xCH_2), 1.71-1.86 (*m*, 6H, 3xCH_2); ^{13}C NMR (DMSO-d_6, 75 MHz) δ: 175.74 (*C*=O), 51.88 (*C*-N), 41.82 (*C*H_2), 39.71 (*C*H_2), 37.98 (C_q). MS (ESI) m/z 284.3 $[M+H]^+$.

1st generation dendron derivative

1,3,5-tricarboxylic-7-(*tert*-butoxycarbonylamino)adamantane acid (7)

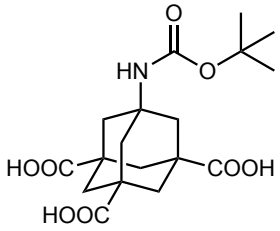

To a solution of **6** (1.4 g, 5.1 mmol) in methanol (70 mL) were added NEt_3 (3.5 mL, 25.6 mmol) and Boc_2O (3.3 g, 15.3 mmol). The solution was stirred at 50 °C for 24 h and a second addition of Boc_2O (1.6 g, 7.6 mmol) with NEt_3 was added again. After 24 h at 50 °C, the solvent was removed by *vacuo* and reaction mixture was solubilized in water, acidified with HCl 1N to pH 1 and extracted with ethyl acetate (3×50 mL). The combined organic layers were dried over magnesium sulfate, filtered and concentrated to give compound **7** as a white solid (1.07 g, 2.8 mmol, 55% yield). ^{1}H NMR ($CDCl_3$, 400 MHz) δ: 12.45 (*br s*, 3H, COO*H*), 6.71 (*br s*, 1H, N*H*), 1.86 (*s*, 6H, 3xCH_2), 1.68-1.83 (*m*, 6H, 3xCH_2), 1.37 (*s*, 9H, 3xCH_3); ^{13}C NMR ($CDCl_3$, 75 MHz) δ: 176.57 (*C*=O), 153.96 (*C*=ONH), 77.53 (*C*-O), 50.66 (*C*-N), 41.93 (CH_2), 40.91 (CH_2), 38.39 (C_q), 28.20 (CH_3-C). MS (ESI) m/z: 284.2 $[M+H\text{-}Boc]^+$.

Trimethyl aminoadamantane-1,3,5-tricarboxylate (8)

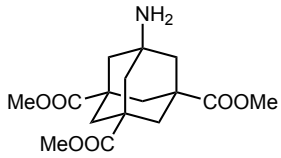

Thionyl chloride (3.7 mL, 50.4 mmol) was added at 0°C to a solution of aminoadamantane-1,3,5-tricarboxylic acid (1.20 g, 4.2 mmol) in 20 mL of MeOH. The reaction mixture was stirred at rt for 24 h and the solvent was evaporated *in vacuo*. The crude product was purified by column chromatography on silica gel (eluant: AcOEt/MeOH/Net_3 90/8/2) to give **8** as a white solid (1.04 g, 3.2 mmol, 75%). The free amine was used for the next step without further purification. ^{1}H NMR ($CDCl_3$, 500 MHz) δ: 8.22 (*br s*, 2H, NH_2), 3.70 (*s,* 9H, 3xCH_3), 2.10-1.90 (*m*, 12H, 6xCH_2); ^{13}C NMR ($CDCl_3$, 75 MHz) δ: 174.60 (*C*=O), 53.18 (COOCH_3), 52.50 (*C*-N), 42.76 (CH_2), 39.74 (CH_2), 38.04 (C_q). FT-IR (neat, ν/cm^{-1}): 3545, 3418, 2960, 1719, 1679, 1557, 1454, 1436, 1295, 1236, 1203, 1175, 1128, 1039. MS (ESI, m/z): 326.2 $[M+H]^+$. MS (ESI) m/z: 326.16 $[M+H]^+$.

Trimethyl hexynamidoadamantane-1,3,5-tricarboxylate (9)

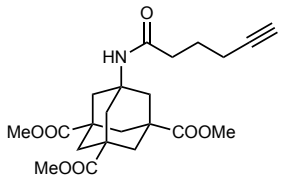

To a solution of 5-hexynoic acid (25.6 mg, 0.23 mmol) in 5 mL of dry DMF were added COMU (94.1 mg, 0.22 mmol) and DIEA (50 µL, 0.27 mmol). The resulting mixture was stirred at r.t under an argon atmosphere for 2 min. Then a solution of Trimethyl aminoadamantane-1,3,5-tricarboxylate **8** (71.2 mg, 0.22 mmol) in 5 mL of dry DMF was added and the reaction was stirred at 65°C under an argon atmosphere for 24 h. After addition of AcOEt (100 mL), the organic phase was washed with saturated aqueous NH_4Cl solution (2×100 mL), saturated aqueous $NaHCO_3$ solution (2×100 mL) and brine (1×100 mL), dried over $MgSO_4$ and filtered. The solvent was removed *in vacuo* and the crude product was purified by column chromatography on silica gel (eluant: CH_2Cl_2/MeOH 95:05) to give **9** as a yellow solid (0.335 g, 0.80 mmol, 65% yield). ^{1}H NMR ($CDCl_3$, 400 MHz) δ: 5.50 (*br s*, 1H, N*H*), 3.64 (*s*, 9H, 3x CH_3), 2.26-2.18 (*m*, 4H, COCH_2, CH_2C≡C*H*), 2.10 (*s,* 6H, 3xCH_2), 2.02-1.88 (*m*, 7H, 3xCH_2, C≡C*H*), 1.78 (*p*, J = 7.2 Hz, 2H, $CH_2CH_2CH_2C{\equiv}CH$); ^{13}C NMR ($CDCl_3$, 100 MHz) δ: 175.23 (*C*=O), 171.71 (*C*=ONH), 83.44 (*C*≡CH), 69.26 (C≡*C*H), 52.51 (CH_2), 52.07 (COOCH_3), 42.86 (CH_2), 41.03 (CH_2), 38.55 (CH_2), 35.63 (CH_2), 23.91 (C_q), 17.65 (C_q). FT-IR (neat, ν/cm^{-1}): 3676, 3290, 2971, 2901, 1721, 1644, 1531, 1454, 1433, 1248, 1208, 1039. MS (ESI, *m/z*): 442.2 $[M+Na]^+$.

1,3,5-Tricarboxylic hexynamidoadamantane acid (10)

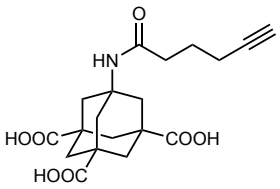

To a solution of trimethyl hexynamidoadamantane-1,3,5-tricarboxylate **9** (0.320 g, 0.76 mmol) in 10 mL of MeOH/H_2O (1:1) was added KOH (0.256 g, 4.56 mmol) and the reaction mixture was stirred at 60°C for 24 h. Then the solution was diluted with H_2O (50 mL), acidified with 2 N HCl to pH 1 and extracted with AcOEt (3×60 mL). Drying of the combined organic layers over $MgSO_4$ and evaporation of the solvent yielded **10** as a colorless solid (0.268 g, 0.71 mmol, 95% yield). ^{1}H NMR (CD_3OD, 400 MHz) δ: 2.29-2.17 (*m*, 4H, COCH_2, CH_2C≡CH), 2.11 (*s*, 6H, 3 CH_2), 2.01-1.87 (*m*, 7H, 3 CH_2, C≡C*H*), 1.77 (*p*, J = 7.2 Hz, 2H, $CH_2CH_2CH_2C$≡CH); ^{13}C NMR (CD_3OD, 75 MHz) δ: 178.97 (*C*=O), 175.13 (*C*=ONH), 84.24 (*C*≡CH), 70.27 (C≡*C*H), 53.70 (*C*H_2), 43.91 (*C*H_2), 42.03 (*C*H_2), 40.07 (*C*H_2), 36.55 (*C*H_2), 25.96 (C_q), 18.62 (C_q). FT-IR (neat, ν/cm^{-1}): 3671, 3362, 3281, 2967, 2901, 1697, 1628, 1534, 1454, 1408, 1249, 1194. MS (ESI): 400.1 $[M+Na]^+$.

Trimethyl (benzyloxycarbonylamino)adamantane-1,3,5-tricarboxylate (11)

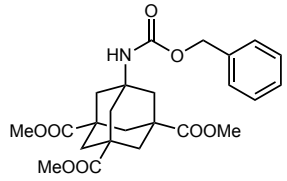

Trimethyl aminoadamantane-1,3,5-tricarboxylate **8** (0.900 g, 2.77 mmol) was dissolved in a mixture of 20 mL CH_2Cl_2 and Et_3N (1.2 mL, 8.31 mmol). Then a solution of *N*-(benzyloxycarbonyloxy)succinimide (1.381 g, 5.54 mmol) in 10 mL of CH_2Cl_2 was added at 0°C and the reaction mixture was stirred at 37°C for 24 h. After addition of CH_2Cl_2 (200 mL), the organic phase was washed with saturated aqueous NH_4Cl solution (2×200 mL) and brine (1×200 mL), dried over $MgSO_4$ and filtered. The solvent was removed *in vacuo* and the crude product was purified by column chromatography on silica gel (eluant: cyclohexane/AcOEt 6:4) to give **11** as a white solid (0.57 g, 1.24 mmol, 45% yield). ^{1}H NMR ($CDCl_3$, 400 MHz) δ: 7.40-7.29 (*m*, 5H, Ar*H*), 5.04 (*s*, 2H, ArCH_2), 4.78 (br *s*, 1H, N*H*), 3.68 (*s*, 9H, 3x CH_3), 2.07 (*s*, 6H, 3 CH_2), 2.03-1.92 (*m*, 6H, 3 CH_2); ^{13}C NMR ($CDCl_3$, 75 MHz) δ: 175.17 (*C*=O), 154.19 (*C*=ONH), 136.29 128.45 128.05 128.00 (4x Ar*C*), 66.21 (Ar*C*H_2), 52.02 (COO*C*H_3), 51.56 (*C*H_2), 42.85 (*C*H_2), 41.15 (C_q), 38.45 (C_q). FT-IR (neat, ν/cm^{-1}): 3676, 3342, 2972, 2901, 1719, 1697, 1529, 1455, 1431, 1234, 1210, 1039. MS (ESI, *m/z*): 482.2 $[M+Na]^+$.

1,3,5-Tricarboxylic (benzyloxycarbonylamino)adamantane acid (12)

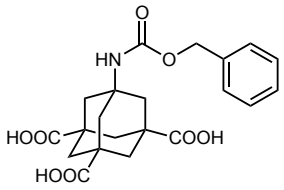

To a solution of trimethyl (benzyloxycarbonylamino)adamantane-1,3,5-tricarboxylate **11** (0.700 g, 1.52 mmol) in 20 mL of MeOH/H_2O (1:1) was added KOH (0.512 g, 9.12 mmol) and the reaction mixture was stirred at 60°C for 24 h. Then the solution was diluted with H_2O (80 mL), acidified with 2 N HCl to pH 1 and extracted with AcOEt (3×100 mL). Drying of the combined organic layers over Na_2SO_4 and evaporation of the solvent yielded **12** as a white solid (0.572 g, 1.37 mmol, 92% yield). ^{1}H NMR (CD_3OD, 400 MHz) δ: 7.36-7.25 (*m*, 5H, Ar*H*), 5.03 (*s*, 2H, ArCH_2), 2.05 (*s*, 6H, 3 CH_2), 2.00-1.83 (*m*, 6H, 3 CH_2); ^{13}C NMR (CD_3OD, 75 MHz) δ: 179.16 (*C*=O), 156.97 (*C*=ONH), 138.51 129.64 129.13 129.03 (4x Ar*C*), 67.12 (Ar*C*H_2), 52.88 (*C*H_2), 44.18 (*C*H_2), 42.55 (C_q), 40.23 (C_q). FT-IR (neat, ν/cm^{-1}): 3332, 3028, 2950, 2917, 2871, 2633, 1692, 1524, 1456, 1272, 1244, 1196, 1100, 1018. MS (ESI, *m/z*): 440.1 $[M+Na]^+$.

2nd generation dendron derivative

Boc and methyl ester protected 2nd generation adamantane-based dendron (13)

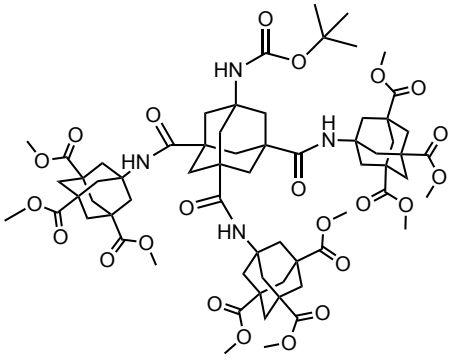

Boc protected tricarboxylic acid adamantane **7** (15 mg, 0.039 mmol), HBTU (147.9 mg, 0.39 mmol) and NEt_3 (55 µL, 0.39 mmol) were solubilized in DMF (5 mL) and triester free amine adamantane **8** (57.30 mg, 0.176 mmol) was added. The mixture was stirred at 60 °C for 72 h and ethyl acetate (150 mL) was added. The organic phase was washed with saturated aqueous NH_4Cl solution (2×100 mL), saturated aqueous $NaHCO_3$ solution (2×100 mL) and brine (1×100 mL), dried over $MgSO_4$ and filtered. The solvent was removed *in vacuo* and the crude product was purified by column chromatography on silica gel (eluant: AcOEt/Cyclohexane 60/40) to give **13** as a white solid (38.1 mg, 0.029 mmol, 75% yield). ^{1}H NMR ($CDCl_3$, 300 MHz) δ: 5.49 (*s*, 3H, N*H*CO), 4.58 (*s*, 1H, N*H*CO), 3.67 (*s*, 27H, 9xCH_3), 2.17-1.87 (*m*, 48H, CH_2), 1.41 (*s*, 9H, 3xCH_3); ^{13}C NMR ($CDCl_3$, 125 MHz) δ: 175.83 (*C*=O), 166.10 (*C*=ONH), 155.28 (*C*=O Boc), 51.36 (*C*-O), 43.78 (CH_2), 42.84 (*C*H_2), 40.33 (*C*H_2), 38.35 (*C*H_2), 37.58 (*C*H_2), 27.50 (C_4), 14.26 (C_4); FT-IR (neat, ν/cm^{-1}): 3690, 3511, 2903, 2861, 1780, 1710, 1501, 1482, 1261, 1240, 1098. MS (ESI, *m/z*): 1328.58 $[M+Na]^+$.

Free amine ester protected 2nd generation adamantane-based dendron (14)

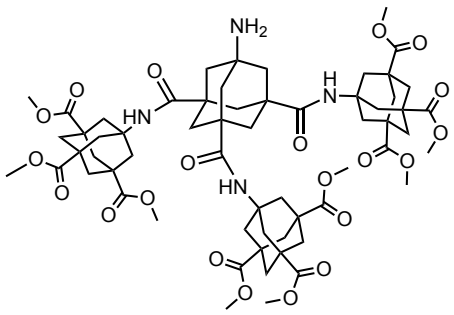

Boc-ester protected 2nd generation dendrons **13** (20 mg, 0.015 mmol) was solubilized in 5 mL of DCM/TFA (1/1) for 1 h at rt. The solvent volume is reduced in *vacuo* and the compound is precipitated with diethyl ether to give **14** as white solid (17.55 mg, 0.014). ^{1}H NMR ($CDCl_3$, 400 MHz) δ: 3.69 (*s*, 27H, 9xCH_3), 2,12-1.84 (*br*, 48H, CH_2). ^{13}C NMR ($CDCl_3$, 125 MHz) δ:175.52 (*C*=O), 159.34 (*C*=ONH), 53.38 (*C*-NH), 52.26 (*C*-NH), 43.83 (H_3C-O), 42.83 (*C*H_2), 40.39 (*C*H_2), 39.33 (*C*H_2), 38.46 (*C*H_2), 29.71 (C_4), 14.91 (C_4). FT-IR (neat, ν/cm^{-1}): 3400, 2982, 2853, 1744, 1625, 1501, 1493, 1252, 1196, 1105, 1002. MS (ESI, *m/z*): 1205.53 $[M+H]^+$.

Chapter III: Adamantane-Based Dendrons for Trimerization of Mannose

III. 1 Introduction

Dendrons (wedge-shaped dendrimers sections) have unique properties due to their molecular architectures and chemical composition. Thereby, they are particularly attractive for biomedical applications,[1] such as cell targeting,[2] therapeutics[3], diagnosis and imaging[4]. As explained before (cf. Chapter I), dendrons structures can display on their periphery a desired repeated motif, the multiple copies of a recognition element promote higher binding affinity for ligand/receptor interactions[5] this effect is called multivalency. Multivalency is widely exploited in nature[6] and leads to enhanced biological activity (i.e. binding affinity or catalytic activity). In our laboratory, we already demonstrated the potential of multivalent adamantane-based dendrons. For example, Lamanna *et al.* coupled ibuprofen to first and second generation adamantane dendrons and observed an increased anti-inflammatory activity of the drug *in vitro*.[7] Indeed, Ibuprofen functionalized dendrons were more effective to reduce the production of both TNFα and IL6 proteins than ibuprofen alone. Moreover, second generation displays better anti-inflammatory potential than the first generation confirming the potential of multivalency effect in therapeutic applications.

Toll-like receptors (TLRs) serve at the first line of defense against invading pathogens such as bacteria and viruses. Expressed in monocytes, macrophages and dendritic cells (DCs), they activate the host defense system by rapidly triggering a local inflammation.[8] However, a deregulated response of TLR signaling results in tissue damage and contributes to the pathogenesis of chronic inflammatory diseases like atherosclerosis,[9] auto-immune colitis,[10] diabetes[11] or Alzheimer disease.[12] TLR4, one of the TRLs, is directly involved in the response to bacterial infection. Indeed, it recognizes the lipopolysaccharide (LPS) present in the outer membrane of Gram negative bacteria. LPS interacts with its corresponding binding protein (LPB), with the cluster differentiation CD14 and the myeloid differentiation protein (MD-2). Then, it is presented in a monomeric form to TLR4 resulting in a dimerization of TLR4 (Figure 1). Then, the TLR4 dimer recruits downstream adaptor proteins, which initiate the intracellular signaling cascade until translocation of transcription factors to the nucleus and biosynthesis of pro-inflammatory cytokines and interferons. In this context, interfering in TLR4 signaling is a therapeutic approach actively studied. Moreover, it has been recently observed a possible link between TLR4 and breast cancer oncogenesis.[13] Mannoside glycolipid conjugates (MGCs) displays interesting potential as TLR antagonist. These water-soluble compounds already

demonstrated antiviral activity[14] and have been recently used as anti-inflammatory drugs on TLR4 mediated signaling.[15] In our Unit, Flasher *et al.* designed MGCs and examined their effects on LPS-induced inflammatory reactions in human monocytes and DCs (Figure 1). They demonstrated the importance of mannose heads and lipid chains to selectively block TLR4 mediated activation of human monocytes and dendritic cells by LPS. Indeed, when the mannose residues are replaced with sugars such as galactose or sialic acid, the conjugates are totally inactive. Moreover, MGCs inhibit signaling through TLR4 without competing with LPS, induce rapid cell internalization and disrupt the localization of TLR4 and CD14. Thus, the efficiency of MGCs is most likely interference with early membrane events involving CD14 and TLR4.

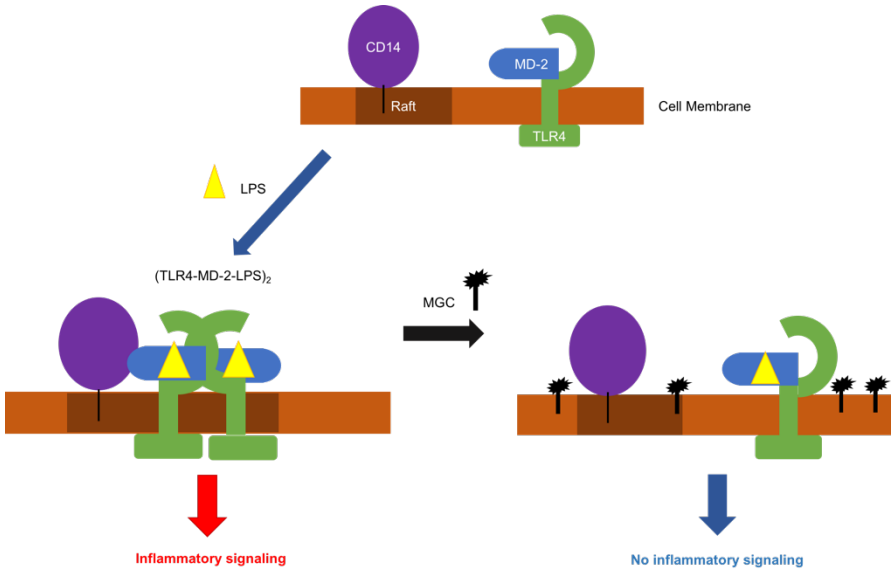

***Figure 1**: Possible mechanism of MGCs as TLR antagonist. Adapted from literature.*[15]

Based on this previous finding, we were interested to develop a therapeutic molecule interfering with TLR4 receptor and which display anti-inflammatory activity. We designed a mannoside-glycolipid adamantane-based dendrons, combining multivalency and C_3-symmetric cores, which plays an important role in molecular recognition.[16] The arborescent structure of adamantane scaffold offers a rigid tripodal structure and a low steric hindrance. Moreover, mannose motifs will be linked through triethylene glycol spacers to confer a certain flexibility and to modulate the solubility of functionalized dendrons. Indeed, the influence of the linker in multivalent interactions has been demonstrated (attachment of viruses to target cells or the binding of antibodies to pathogens).[17]

III.2 Results and Discussion

III. 2.1 Design of mannoside-glycolipid adamantane-based dendrons

We designed two different compounds based on adamantane dendrons. The first one (Figure 2A) is a 1st generation of adamantane dendron functionalized with both sugar heads and a lipid chain. Indeed, Flacher *et al.* demonstrated the importance of both lipid chain and sugar heads in the inflammatory properties of mannoside glycolipid conjugates (MGCs).[15] Thus, we designed a dendron functionalized at the focal point with a lipidic chain (hexacosanoic acid) and with mannose at the periphery (Figure 2A). This dendron will be used as reference, as being composed of both lipid chain and mannose heads we expect to observe an anti-inflammatory activity. Moreover, the mannoses will be anchored using polyethylenglycol chain in order to improve the flexibility and the solubility of the final compound. The second compound designed (Figure 2B) follows the same idea. However, the main difference is at the focal point where the lipid chain is replaced by the fluorophore nitrobenzoxadiazole (NBD). The adamantane-NBD conjugate must be enough hydrophobic to display an anti-inflammatory activity. Then, the NBD attached *via* click chemistry will allow to perform the studies of cellular uptake.

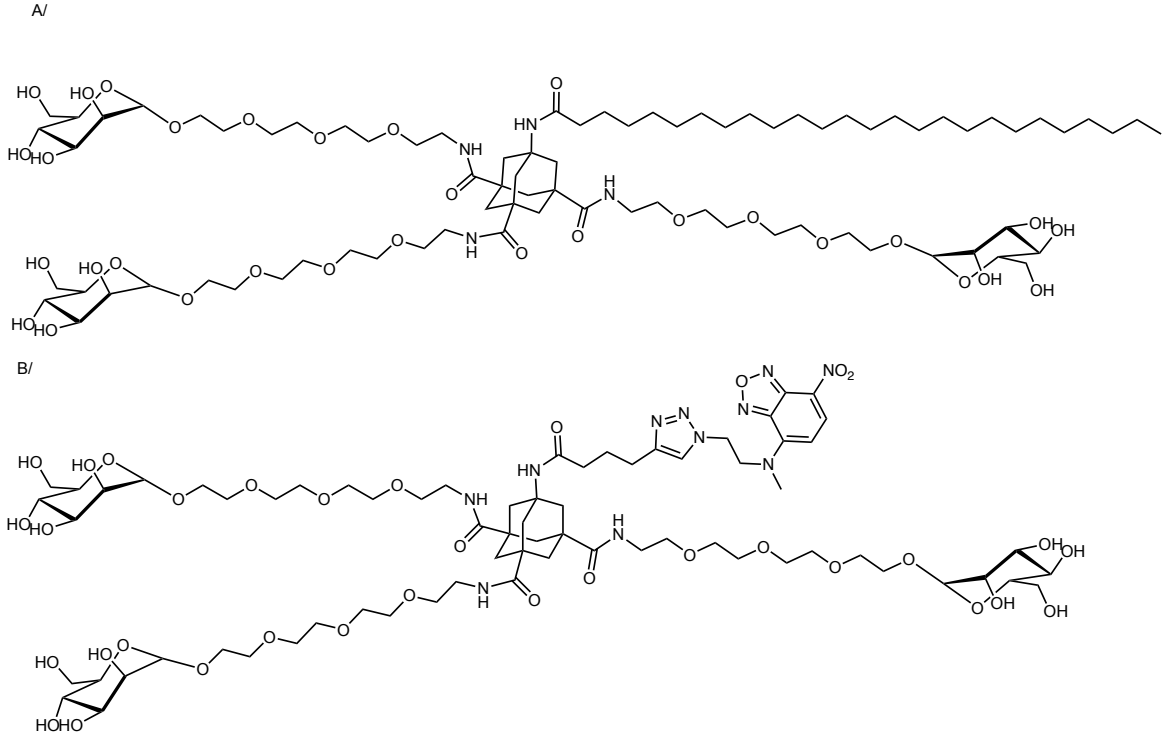

***Figure 2**: Designed mannoside glycolipid conjugates based on adamantane.*

III. 2.2 Synthesis of adamantane based dendron trimerized with mannose

The synthesis of mannose-glycolipid adamantane dendrons is composed of four different steps. Following a retro-synthetic approach, I divided the molecule in three parts. The first step is the preparation of the fluorophore, which will be attached to the adamantane dendron *via* click chemistry. The second part concerns the adamantane core. The (3+1) functionalized adamantane building block plays a role of scaffold to anchor mannose derivatives on periphery and a lipid chain or a fluorophore probe at the focal point. The third part is PEGylated mannose. Mannose is functionalized with a tetraethyleneglycol chain (TEG) and anchored to the adamantane core through peptide bonds to obtain the desired adamantane based dendron trimerized with a mannose motif.

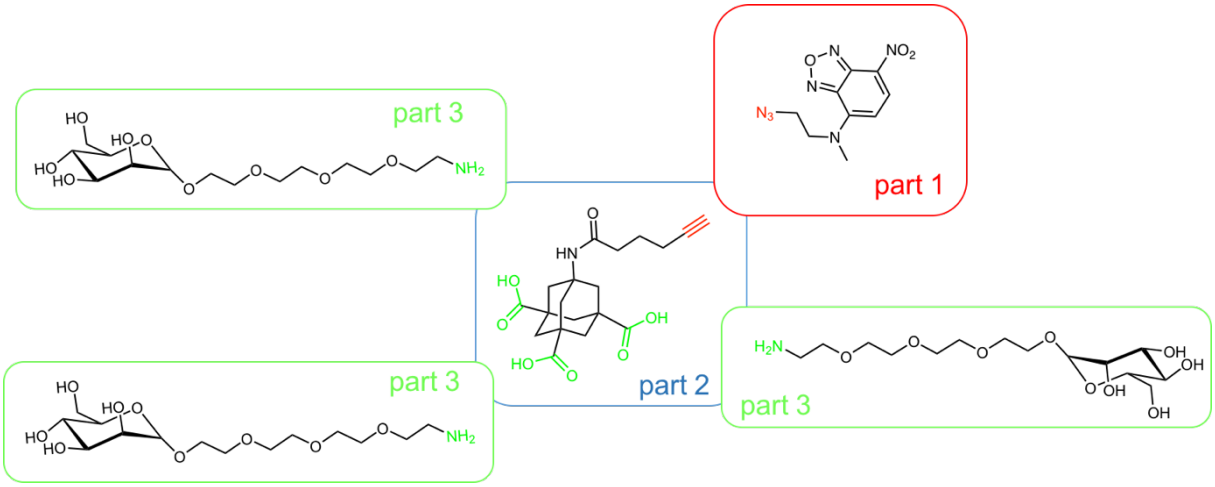

***Figure 3**: Retro-synthetic approach for the synthesis of MGC based on adamantane.*

Step 1: Synthesis of azido-NBD

I selected NBD as probe for imaging as it offers several advantages. It is commercially available and it is a small molecule (MW 199.55 g/mol) that allows to avoid sterical hindrance problem. NBD is also quite hydrophobic, which is mandatory to observe anti-inflammatory property of the final compound. Its spectral properties make it a good candidate as probe (λ_{ex} = 464-470 nm, λ_{em} = 512-530 nm in aqueous solution). These values depend on the molecule and the environment. Indeed, NBD adducts are highly environmental sensitive. Nowadays, NBD is widely used to label biomolecules such as peptides, proteins or drugs.

For conjugation to the adamantane via click chemistry, it is necessary to insert an azido group on NDB. The synthesis of azido functionalized NBD started from the commercial 4-chloro-7-nitro-2,1,3-benzoxadiazole (NBD-Cl) **1** which is refluxed with an excess of 2-

(methylamino)ethanol **2** in ethanol for 2 h (Scheme 1). After filtration, the crude orange product was recrystallized from ethanol to give the desired 2-[methyl-(7-nitro-2,1,3-benzoxadiazol-4-yl)amino]ethanol (NBD-Aminol) **3** as an orange solid (Yield: 89 %). Then compound **3** is solubilized in pyridine and reacted with 4-toluenesulfonyl chloride during 3 h. The crude product is purified by column chromatography to give **4** as an orange powder (Yield: 85%). Tosylated compound **4** can then reacts *via* SN_2 mechanism with sodium azide. The reaction is performed in DMF under inert atmosphere for 5 h at 60 °C. Azido functionalized NBD **5** is purified by column chromatography leading to a red powder with 80 % yield. All compounds were characterized by NMR and mass spectrometry.

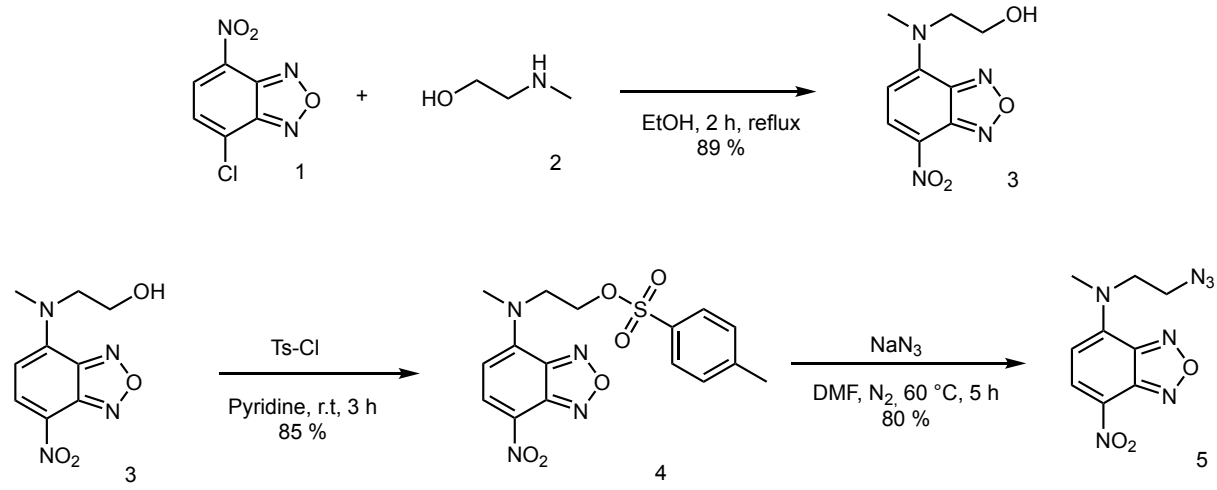

***Scheme 1**: Synthesis of azido-NBD probe **5**.*

Step 2: Synthesis of adamantane scaffolds

Following the procedure described in Chapter II, compound **12** has been synthesized starting from bromoadamantane. After, esterification of the periphery, the focal point was functionalized with hexaynoic acid using COMU in presence of DIEA at 60 °C for 24 h. The alkyne derivative **14** is obtained with a yield of 65 %. Final hydrolysis of the esters give the desired (3+1) adamantane building block that can be selectively functionalized *via* click chemistry at the focal point (with compound **5**) or *via* peptide bonds at the peripheral groups. The details of the synthesis are described in Chapter II experimental part.

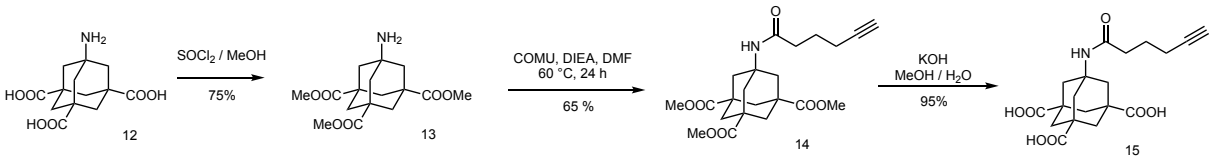

***Scheme 2**: Synthesis of alkyne functionalized adamantane dendron **15**.*

The second synthesis concerns the functionalization of the free amine with a lipid chain. I selected the hexacosanoic acid (also called cerotic acid). Mostly found in beeswax, it is composed of 24 long-chain saturated carbons. Due to the high hydrophobic properties of the molecule, the main issue was to avoid the formation of micelles or even liposomal-like structure during the coupling reactions. In order to increase the nucleophilicity of the adamantane amino group, the three carboxylic acids on adamantane have been esterified to give the corresponding methyl ester derivatives **13** (see Chapter II for details).

Different coupling agents have been tried for the amide bond formation (Table 1). I first started with HBTU because it gave the best result for the synthesis of the second generation adamantane-based dendron (see Chapter II). Unfortunately, the reaction did not occur. The same result was observed with another benzotriazol-uronium salt called HATU. HATU is commonly used in peptide synthesis, especially for difficult sequences. I also tried third generation uranium agent COMU (described in Chapter II), but I never isolated the desire compound. Due to the difficulty to solubilize hexacosanoic acid, I tried the reaction in chloroform but once again it did not work. Finally, microwave heating in combination with DIC, Oxyma as coupling agents and catalytic DMAP in 1:1 DCM/DMF allowed to obtain the desired compound. Indeed, using these conditions I isolated the compound **16** after only 30 min at 60 °C (Scheme 4). Moreover, catalytic DMAP was used to increase the final yield to 64 %.

***Table 1:** Conditions tested for the functionalization of adamantane with the lipid chain.*

Solvent	Coupling agents	Conditions	Yield
DMF	HBTU	N_2, NEt_3, 60 °C, 24 h	n.d
$CHCl_3$	HBTU	N_2, NEt_3, 60 °C, 24 h	n.d
DMF	COMU	N_2, DIEA, 60 °C, 24 h	n.d
DMF	HATU / HOAt	N_2, DIEA, 30 °C, 72 h	< 5 %
DMF / DCM	Oxyma - DIC	DMAP, 70 °C (MW), 30 min	64 %

Finally, I tried to hydrolyzed compound **16** to give the corresponding three carboxylate acid derivative **17**. However, the reaction is more difficult due to the high hydrophobicity of the molecule. The saponification reaction is not possible in MeOH/water (1/1). Even using *t*-BuOH as solvent to improve the solubility, the hydrolysis of methyl ester groups did not occur. Other tests are still in progress.

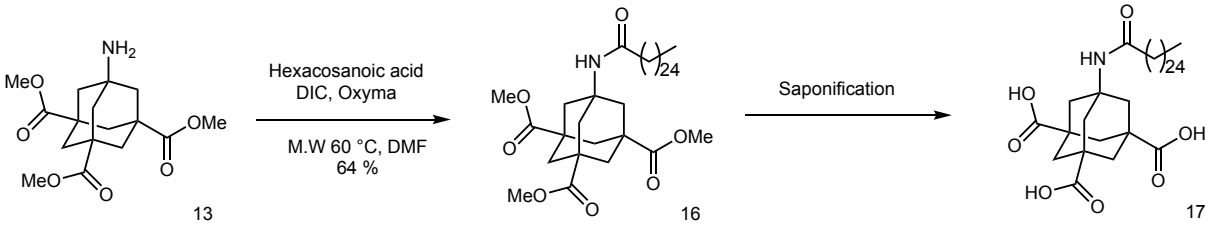

Scheme 3: *Synthesis of lipid functionalized adamantane **17**.*

Step 3: Synthesis of PEGylated mannose

The synthesis of PEGylated mannose starts with 2,3,4,6-tetra-*O*-acetyl-alpha-D-mannopyranosyltrichloroacetimidate **18**. The four hydroxyl groups are protected with acetyl groups to avoid side reactions. Indeed, acetate is stable against reductant agents such as H_2, stable in acidic condition (excepted at high temperature) and stable against tertiary amine (DIEA, NEt_3) which are used during the amidation reactions. Then, acetyl groups are easily removed in presence of strong nucleophiles like sodium methoxide. The anomeric position of the mannose derivative is activated with a trichloroacetimidate group, which is obtained by reaction of the mannose with trichloroacetonitrile after deprotonation of the hydroxyl with a strong base. Trichloroacetimidate is a leaving group often used for sugar activation during glycosidation reactions.[18] Thus, compound **18** is reacted with azido-dPEG$_4$-OH **19** which has been chosen as a linker to provide flexibility and tune the solubility of the final compounds. A similar approach was previously adopted by Flecher et *al*. The reaction occurs with broron trifluoride diethyl etherate activation (Scheme 5).[19] Moreover, the anchimeric assistance of the acetate in position 2 allows to obtain mainly the α-acetal product **20** in good yield (60%). Then, azido-dPEG$_4$- 2,3,4,6-tetra-*O*-acetyl-alpha-D-mannopyranose **20** is reduced with H_2 on Pd/C leading to the corresponding free amine **21**. The reaction is easily followed by infrared spectrophotometry: the azide stretching vibration at 2160-2120 cm^{-1} disappears after the hydrogenolysis.

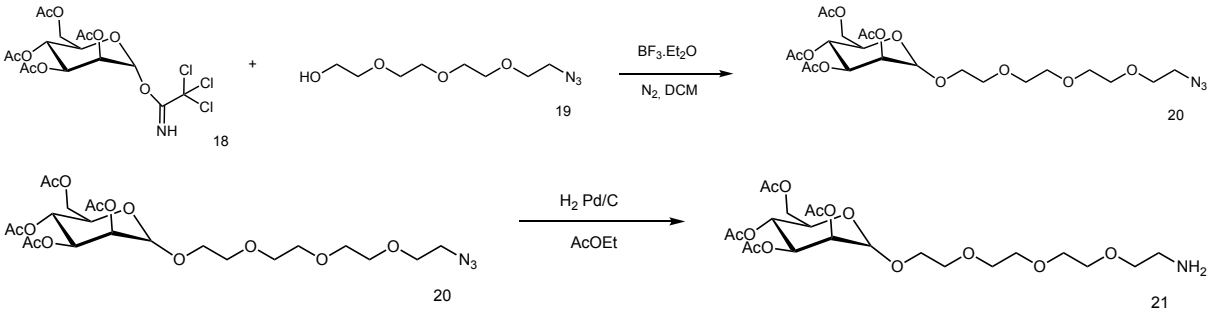

Scheme 4: *Synthesis of azido **20** and amino **21** PEGylated mannoses.*

Step 4: Synthesis of trimers

The last step consists in linking all the different components together, and to remove the protecting acetate groups on mannose. Unfortunately, due the unexpected difficulties encountered during the synthesis and the lack of time I did not yet succeeded to hydrolyze compound **16** and perform the coupling with the mannose derivative (Scheme 5).

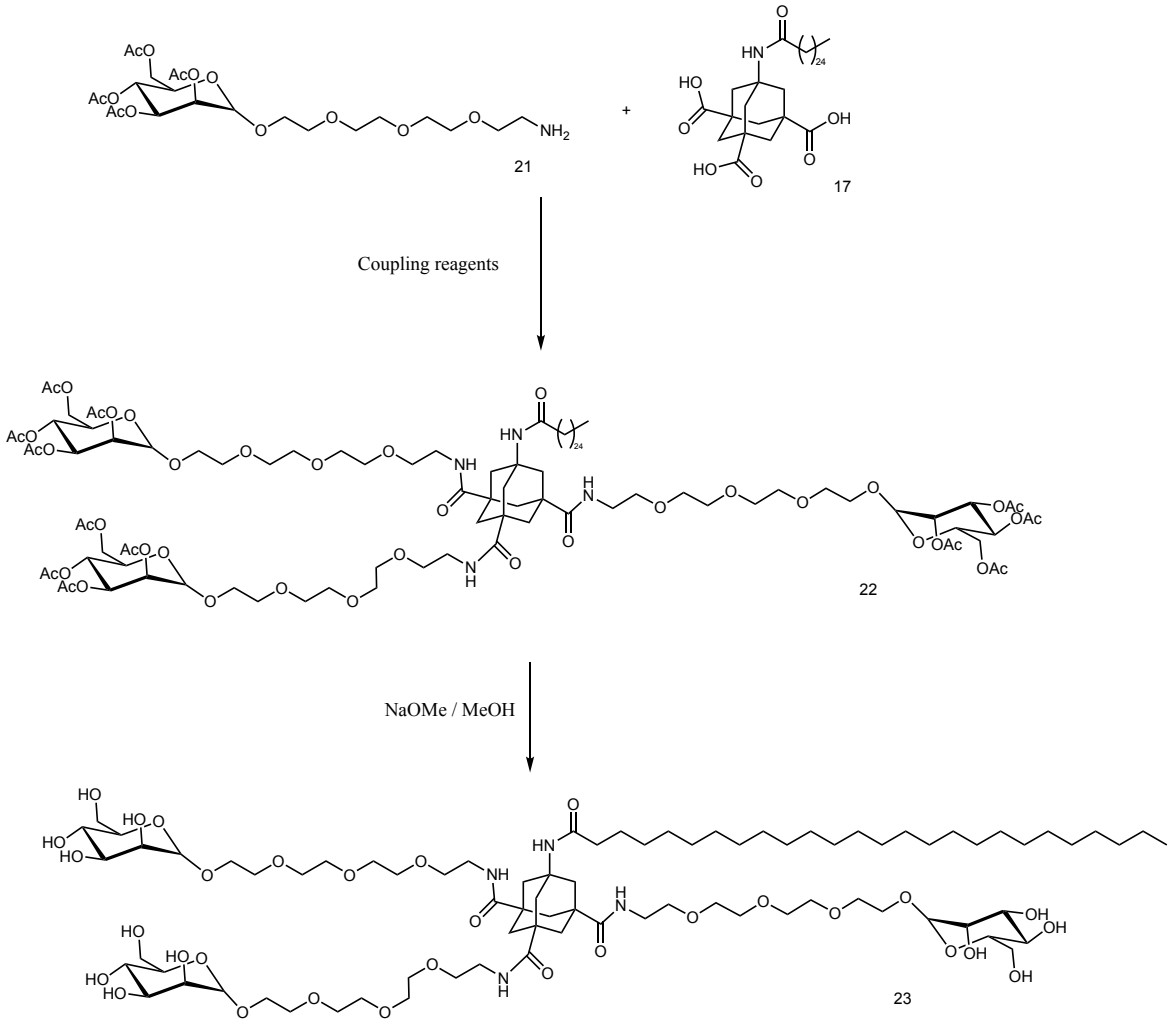

Scheme 5: *Synthesis strategy to obtain the desired MGC based on adamantane **23**.*

For the synthesis of NBD-mannoside adamantane dendrons **26** (Scheme 6), I tried to couple the alkyne derivative **15** with the amino-PEG-mannose **21** using HBTU, HOBt as coupling agents in the presence of NEt_3. However, TLC and LC-MS analysis were not conclusive. As a consequence, I could not achieve the synthesis of the final product **26**, again for the lack of time. I am however illustrating all the steps in Scheme 7.

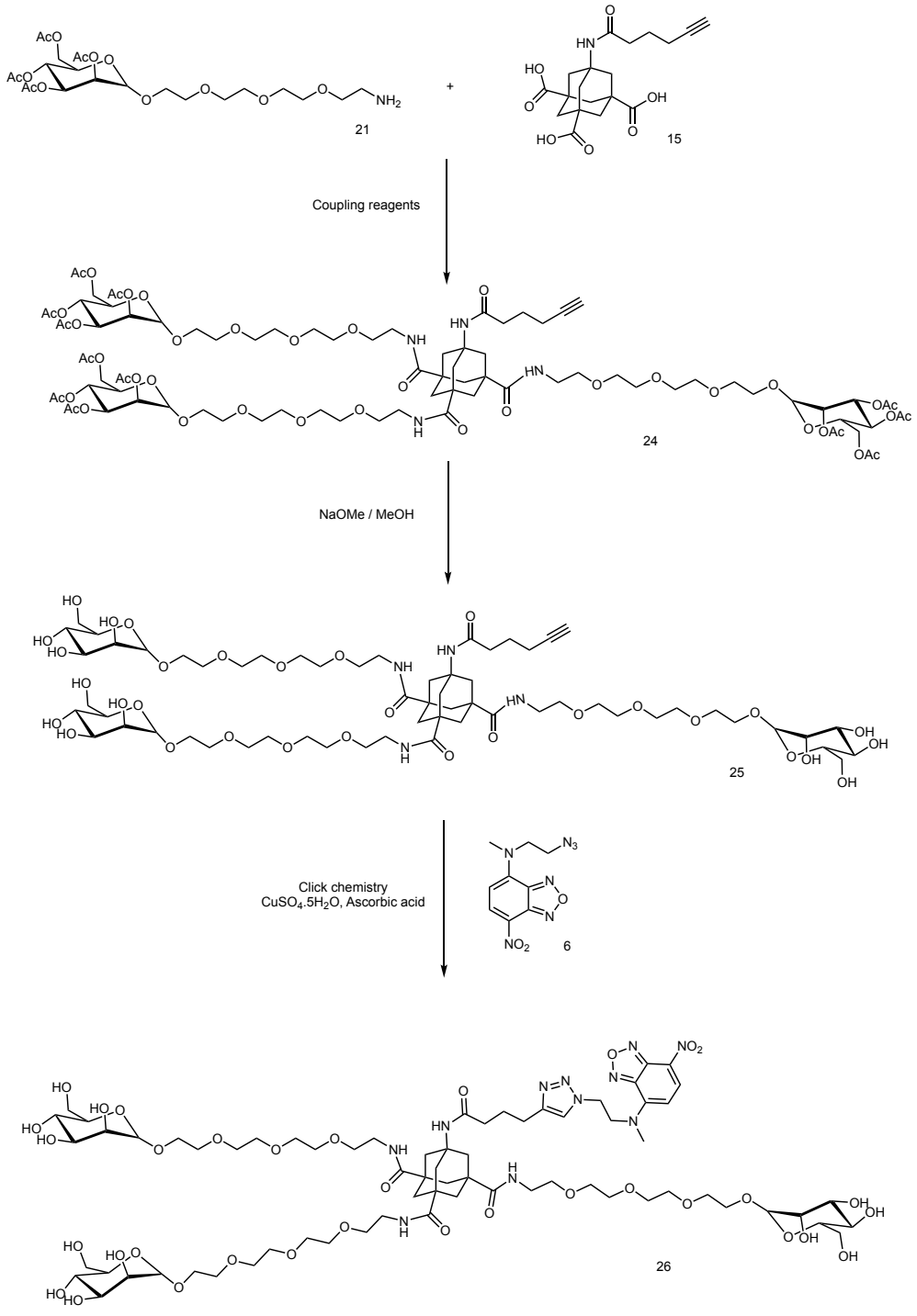

Scheme 6: *Synthesis strategy to obtain the desired NBD-mannoside adamantane dendrons* ***26****.*

II.3 Conclusion & Perspectives

In this chapter, I designed two adamantane-based dendrons which display three mannose motifs at the periphery and differ at the focal point. Indeed, one is functionalized with a lipid chain and will be use as reference, while the second one is functionalized with a fluorochrome. The idea was first to check the anti-inflammatory effect of the dendrons, then to determine a possible mechanism using confocal microscopy. Unfortunately, due to the lack of time, the syntheses of the final compounds were not achieved. Moreover, one of the main problem met was the solubility of the lipid derivatives. Indeed, the tendency of lipid chains to form micelles certainly affected the reactions. A solution could be to determine the critical micellar concentration to improve the reactions conditions.[20]

In perspective, two problems must be solved. The first one is the hydrolysis of the C_{24}-adamantane triester derivative. Another possibility would be to use the 7-amino-1,3,5-tricarboxylicadamantane acid for the *N*-acylation instead of the triesterified compound. The second issue is the coupling step between functionalized adamantane triacid and amino PEGylated mannose to achieve the formation of the desired dendrons. Then, the final steps were not performed but they are well described in the literature. From a biological point of view, both dendrons will be tested *in vitro*. If both display anti-inflammatory activity, confocal microcopy will be performed on the NBD derivative. Indeed, cell imaging allows to determine more precisely the dendron localization and thus, the possible mechanism of interaction of the glycolipid conjugate with TLR4.

II.4 References

(1) Mintzer, M. A.; Grinstaff, M. W. Biomedical Applications of Dendrimers: A Tutorial. *Chem. Soc. Rev.* **2011**, *40* (1), 173–190.

(2) Lee, C. C.; MacKay, J. A.; Fréchet, J. M. J.; Szoka, F. C. Designing Dendrimers for Biological Applications. *Nat. Biotechnol.* **2005**, *23* (12), 1517–1526.

(3) Medina, S. H.; El-Sayed, M. E. H. Dendrimers as Carriers for Delivery of Chemotherapeutic Agents. *Chem. Rev.* **2009**, *109* (7), 3141–3157.

(4) Kesharwani, P.; Jain, K.; Jain, N. K. Dendrimer as Nanocarrier for Drug Delivery. *Prog. Polym. Sci.* **2014**, *39* (2), 268–307.

(5) Rolland, O.; Turrin, C.-O.; Caminade, A.-M.; Majoral, J.-P. Dendrimers and Nanomedicine: Multivalency in Action. *New J. Chem.* **2009**, *33* (9), 1809–1824.

(6) Mahon, C. S.; Fulton, D. A. Mimicking Nature with Synthetic Macromolecules Capable of Recognition. *Nat. Chem.* **2014**, *6* (8), 665–672.

(7) Lamanna, G.; Russier, J.; Dumortier, H.; Bianco, A. Enhancement of Anti-Inflammatory Drug Activity by Multivalent Adamantane-Based Dendrons. *Biomaterials* **2012**, *33* (22), 5610–5617.

(8) Akira, S.; Takeda, K. Toll-like Receptor Signalling. *Nat. Rev. Immunol.* **2004**, *4* (7), 499–511.

(9) Triantafilou, M.; Gamper, F. G. J.; Lepper, P. M.; Mouratis, M. A.; Schumann, C.; Harokopakis, E.; Schifferle, R. E.; Hajishengallis, G.; Triantafilou, K. Lipopolysaccharides from Atherosclerosis-Associated Bacteria Antagonize TLR4, Induce Formation of TLR2/1/CD36 Complexes in Lipid Rafts and Trigger TLR2-Induced Inflammatory Responses in Human Vascular Endothelial Cells. *Cell. Microbiol.* **2007**, *9* (8), 2030–2039.

(10) Arranz, A.; Juarranz, Y.; Leceta, J.; Gomariz, R. P.; Martínez, C. VIP Balances Innate and Adaptive Immune Responses Induced by Specific Stimulation of TLR2 and TLR4. *Peptides* **2008**, *29* (6), 948–956.

(11) Devaraj, S.; Dasu, M. R.; Rockwood, J.; Winter, W.; Griffen, S. C.; Jialal, I. Increased Toll-like Receptor (TLR) 2 and TLR4 Expression in Monocytes from Patients with Type 1 Diabetes: Further Evidence of a Proinflammatory State. *J. Clin. Endocrinol. Metab.* **2008**, *93* (2), 578–583.

(12) Zhou, X.; Yuan, L.; Zhao, X.; Hou, C.; Ma, W.; Yu, H.; Xiao, R. Genistein Antagonizes Inflammatory Damage Induced by β-Amyloid Peptide in Microglia through TLR4 and NF-KB. *Nutr. Burbank Los Angel. Cty. Calif* **2014**, *30* (1), 90–95.

(13) Ahmed, A.; Redmond, H. P.; Wang, J. H. Links between Toll-like Receptor 4 and Breast Cancer. *Oncoimmunology* **2013**, *2* (2), e22945.

(14) Dehuyser, L.; Schaeffer, E.; Chaloin, O.; Mueller, C. G.; Baati, R.; Wagner, A. Synthesis of Novel Mannoside Glycolipid Conjugates for Inhibition of HIV-1 Trans-Infection. *Bioconjug. Chem.* **2012**, *23* (9), 1731–1739.

(15) Flacher, V.; Neuberg, P.; Point, F.; Daubeuf, F.; Muller, Q.; Sigwalt, D.; Fauny, J.-D.; Remy, J.-S.; Frossard, N.; Wagner, A.; Mueller, C. G.; Schaeffer, E. Mannoside Glycolipid Conjugates Display Anti-Inflammatory Activity by Inhibition of Toll-like Receptor-4 Mediated Cell Activation. *ACS Chem. Biol.* **2015**, *10* (12), 2697–2705.

(16) Gibson, S. E.; Castaldi, M. P. C3 Symmetry: Molecular Design Inspired by Nature. *Angew. Chem. Int. Ed Engl.* **2006**, *45* (29), 4718–4720.

(17) Kane, R. S. Thermodynamics of Multivalent Interactions: Influence of the Linker. *Langmuir ACS J. Surf. Colloids* **2010**, *26* (11), 8636–8640.

(18) Schmidt, R. R. New Methods for the Synthesis of Glycosides and Oligosaccharides—Are There Alternatives to the Koenigs-Knorr Method? [New Synthetic Methods (56)]. *Angew. Chem. Int. Ed. Engl.* **1986**, *25* (3), 212–235.

(19) Huang, Y.; Shaw, M. A.; Mullins, E. S.; Kirley, T. L.; Ayres, N. Synthesis and Anticoagulant Activity of Polyureas Containing Sulfated Carbohydrates. *Biomacromolecules* **2014**, *15* (12), 4455–4466.

(20) Basu Ray, G.; Chakraborty, I.; Moulik, S. P. Pyrene Absorption Can Be a Convenient Method for Probing Critical Micellar Concentration (Cmc) and Indexing Micellar Polarity. *J. Colloid Interface Sci.* **2006**, *294* (1), 248–254.

Chapter III: Experimental Section

General experimental details

Chemicals and Solvents

All the starting materials, chemicals, and anhydrous solvents were obtained from commercial suppliers (Sigma-Aldrich, Acros Organics and Alfa Aeasar laboratories). The amino-PEG-azide provides from Quanta biodesign whereas mannopyranosyltrichloroacetimidate provides from Glentham. All solvent used for the synthesis were analytical grade. When anhydrous conditions were required, high quality commercial dry solvent were used. Water was purified using Millipore filter system MilliQ® equipped with Biopak® filter.

Characterization Methods and Instrumentation

Thin layer Chromatography (TLC): TLC was conducted on pre-coated aluminum plates with 0.25 mm *Macherey-Nagel* silica gel with fluorescent indicator UV254.

Column Chromatography**:** Chromatographic purifications were carried out with silica gel (Merck Kieselgel 60, 40-60 μm, 230-400 mesh ASTM).

Nuclear Magnetic Resonance: ^{1}H-NMR and ^{13}C-NMR spectra were recorded in deuterated solvents using Bruker Avance I – 300 MHz and Bruker Avance III – 400 MHz. Chemical shifts are reported in ppm using the residual signal of deuterated solvent as reference (TMS = 0). Coupling constants *J* are reported in Hertz (Hz), and the splitting patterns are designated as *s* (singlet), *d* (doublet), *t* (triplet), *td* (triplet of doublet), *q* (quartet), *p* (pentet), *m* (multiplet), and *br* (broad).

ESI Mass Spectrometry: Mass spectra were recorded on a Thermo Fisher Finnigan LCQ Advantage Max Instrument.

Microwave heating: MW heating were performed using a CEM Discover SP microwave synthesizer (power: 100 W regulated with the temperature).

Synthesis and characterization data

Synthesis of azido-nitrobenzoxidiazol

2-[methyl-(7-nitro-2,1,3-benzoxadiazol-4-yl)amino]ethanol[1] (3)

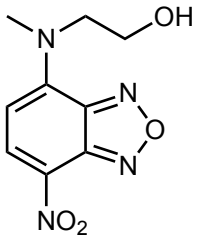

4-Chloro-7-nitro-2,1,3-benzoxadiazole (NBD-Cl) (30 mg, 0.15 mmol) was refluxed with an excess of 2-(methylamino)ethanol (36 µL, 0.45 mmol). After 2 h, the mixture was cooled to rt, filtered and washed with cold ethanol. The resulting orange solid was recrystallized from ethanol to give NBD-aminol compound **3** (32 mg, 0.13 mmol, 88 %). The intermediate was quickly characterized and used for next step. ^{1}H NMR (Acetone, 300 MHz) δ: 8.46 (*d*, J = 8.5 Hz, 1H, Ar-*H*), 6.45 (*d*, J = 8.5 Hz, 1H, Ar-*H*), 4.33 (*br s*, 1H, O-*H*), 4.12 (*t*, J = 5.5 Hz, 2H, CH_2), 3.97 (*q*, J = 5.5 Hz, 2H, CH_2). MS (ESI) *m/z*: 239.07 $[M+H]^+$.

Toluenesulfonyl-nitrobenzoxidiazol (4)

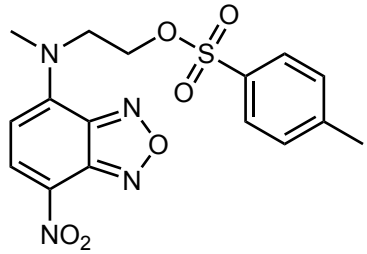

NBD-aminol **3** (31 mg, 0.13 mmol) was diluted in pyridine and cooled at 0 °C. *p*-Toluenesulfonyl chloride (240 mg, 1.3 mmol) was added and the ice bath was removed after 10 min. After 3 h at rt, the solvent was removed under vacuum. The crude product was solubilized in chloroform and wash with saturated aqueous solutions ($NaHCO_3$ and NH_4Cl). The organic layer was concentrated and the obtained residue was purified by column chromatography (eluant: ethyl acetate/cyclohexane (4:6)) to give toluensulfonylated NBD **4** (44 mg, 0.11 mmol, 85 %).^{1}H NMR ($CDCl_3$, 400 MHz) δ: 8.41 (*d*, J = 8.5 Hz, 1H, Ar-*H*), 7.64 (*d*, J = 8.5 Hz, 2H, Ar-*H*) 7.22 (*d*, J = 8.5 Hz, 2H, Ar-*H*), 6.10 (*d*, J = 8.5 Hz, 1H, Ar-*H*), 4.43 (*d,* J = 4.0 Hz, 2H, CH_2), 3.39 (*d,* J = 4.0 Hz, 2H, CH_2), 3.43 (*s*, 3H, CH_3), 2.38 (*s*, 3H, CH_3). MS (ESI) *m/z*: 393.09 $[M+H]^+$.

Azido-nitrobenzoxidiazol (5)

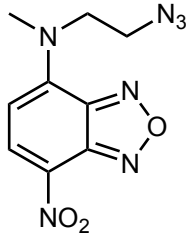

Toluenesulfonyl-nitrobenzoxidiazol **4** (44 mg, 0.11 mmol) was dissolved in DMF and flashed with azote. Sodium azide (36 mg, 0.55 mmol) was added and the mixture was heating at 60 °C. After 5 h, the mixture was cooled down and extracted with ethyl acetate. The organic layer was washed and solvent was removed under vacuum. The crude obtained was purify by column chromatography (eluant: ethyl acetate) to give compound **5** (23 mg, 0.09 mmol, 80 %). ^{1}H NMR ($CDCl_3$, 400 MHz) δ: 8.46 (*d*, J = 8.5 Hz, 1H, Ar-*H*), 6.18 (*d*, J = 8.5 Hz, 1H, Ar-*H*), 4.34 (*t*, J = 6.2 Hz, 2H, CH_2), 3.74 (*t*, J = 6.2 Hz, 2H, CH_2), 3.48 (*s*, 3H, CH_3). ^{13}C NMR ($CDCl_3$, 100 MHz) δ: 145.6, 140.4, 137.2, 132.1, 125.6, 96.8, 61.8, 42.9. MS (ESI) *m/z*: 264.08 $[M+H]^+$.

Synthesis of adamantane scaffolds

Trimethylhexynamidoadamantane-1,3,5-tricarboxylate acid (15)

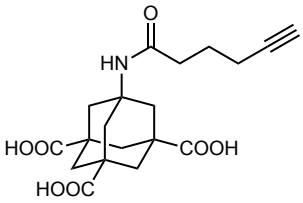

Synthesis and characterization of compound **15** is described in Chapter II experimental part.

1,3,5-trimethyl-7-hexacosanamidoadamantane-1,3,5-trocarboxylate (16)

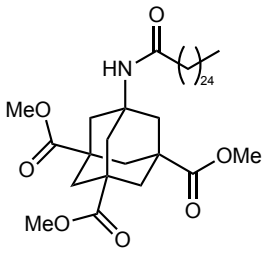

Trimethylaminoadamantane-1,3,5-tricarboxylate **15** (80 mg, 0.25 mmol) was solubilized in dry DMF. Hexacosanoic acid (390 mg, 1.0 mmol), DIC (155 µL, 1.0 mmol) and Oxyma (142 mg, 1.0 mmol) previously solubilized in DMF were added. A catalytic amount of DMAP (5.0 mg, 0.025 mmol) was added and the mixture was heated using MW at 70 °C. After 30 min, the gel obtained was solubilized in DCM. The organic layer was washed with saturated aqueous solution ($NaHCO_3$ and NH_4Cl), dried and concentrated under vacuum. The crude product obtained was purified by column chromatography (eluant: ethyl acetate/cyclohexane (1/3)) to give compound **16** as a white powder (110 mg, 0.16 mmol, 64 %). ^{1}H NMR ($CDCl_3$, 400 MHz) δ: 5.19 (*s*, 1H, N*H*), 3.66 (*s*, 9H, CH_3), 2.13 (*s*, 6H, CH_2), 2.08 (*t*, J = 7.0 Hz, 2H, COCH_2), 2.05-1.92 (*br*, 6H, CH_2), 1.29-1.21 (*br s*, 44H, CH_2), 0.88 (*t*, J = 7.0 Hz, 3H, CH_3). MS (ESI) *m/z*: 676.44 $[M+H]^+$.

Synthesis of PEGylated mannose

2,3,4,6-Tetra-O-acetyl-alpha-D-manopyranosyl-PEG_4-azide (20)

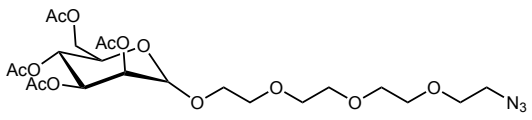

2,3,4,6-tetra-O-acetyl-alpha-D-mannopyranosyltrichloroacetimidate **18** (170 mg, 0.35 mmol) was solubilized in freshly distilled DCM in a round bottom flask previously flashed with N_2/vacuum (3 times). PEG-azide (227 mg, 1.04 mmol) was added and the mixture was cooled at 0 °C. $BF_3 \times Et_2O$ (43.7 µL, 0.35 mmol) was added dropwise and the mixture was stirred overnight at rt. NEt_3 was added to stop the reaction and the organic phase was washed with saturated NH_4Cl, water, dried and concentrated under vacuum. The crude obtained was purified by column chromatography (eluant: ethyl acetate/cyclohexane (1:1)) to give compound **20** (115 mg, 0.20 mmol, 60 %). ^{1}H NMR ($CDCl_3$, 400 MHz) δ: 5.65-5.29 (*br m*, 4H, C*H*), 4.57-4.11 (*br m*, 4H, CH_2), 3.90-3.60 (*br m*, 10H, CH_2), 3.40 (*t*, 2H, CH_2), 2.17 (*s*, 3H, CH_3), 2.11 (*s*, 3H, CH_3), 2.07 (*s*, 3H, CH_3), 2.01 (*s*, 3H, CH_3). MS (ESI) *m/z*: 566.97 $[M+H_2O]^+$.

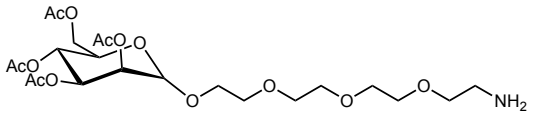

2,3,4,6-Tetra-*O*-acetyl-alpha-D-manopyranosyl-PEG_4-azide **20** (100 mg, 0.18 mmol) was solubilized in DCM. The round bottom flask was flashed with N_2 and vacuum (3 times). Then, palladium on charcoal (10 mg) was added and the nitrogen is replaced by hydrogen (bubbling). After 15 h, the mixture was filtered on celite pad and concentrated under vacuum. The compound was precipitated from DCM using Et_2O. IR analysis confirmed the reduction of the azide to amino. MS (ESI) *m/z*: 524.14 $[M+H]^+$. ^1H NMR ($CDCl_3$, 300 MHz) δ: 5.47–5.18 (*br*, 6H, C-*H*), 4.36-3.53 (*br*, 16H, CH_2), 2.15 (*s*, 3H, CH_3), 2.09 (*s*, 3H, CH_3), 2.03 (*s*, 3H, CH_3), 1.98 (*s*, 3H, CH_3).

References

(1) Katzenstein, J. M.; Janes, D. W.; Hocker, H. E.; Chandler, J. K.; Ellison, C. J. Nanoconfined Self-Diffusion of Poly(Isobutyl Methacrylate) in Films with a Thickness-Independent Glass Transition. *Macromolecules* **2012**, *45* (3), 1544–1552.

Chapter IV: Foldamers containing Adamantane

IV. 1 Introduction

Foldamers can be described like non-natural folded polymers. Indeed, the main characteristic of foldamers is their secondary structure, which included α-helix and ß-sheets. These types of structures are stabilized through non-covalent interactions (hydrogen bonding, π-stacking, hydrophobic interactions, solvophobic effects, van der Waals forces and electrostatic interactions).[1] As explained in the Introduction, foldamers can be divided in two families depending on their backbone structures (i.e. biotic and abiotic foldamers) and separated in two classes depending on their supramolecular interactions (i.e. single or multiple stranded foldamers).[2] We are particularly interested in peptidomimetic-based foldamers, which are designed to mimick natural peptide conformations. Indeed, peptide foldamers are a rich source of diversity.[3] They are easy to synthesize, generally through classical peptide synthesis technique like solid phase peptide synthesis (SPPS). Several parameters can be modified to change the intramolecular interaction of a peptide leading to the folding event. We can for example incorporate non-natural amino acids, use *D*-amino acids in place of *L*-amino acids, modify the sequences or even change the building blocks used. This latest is a promising possibility to tune the interaction strength and it led to the creation of news peptide foldamer family like ß-peptides, γ-peptides, azapeptides and aminoxy acid containing oligomers. For example, ß-peptides are the closest derivatives of the natural α-peptides. A methylene group is introduced between the α-carbon and the amide bond. Apparently small, this change offers higher flexibility and thus, additional variables affecting the secondary structure. Moreover, due the additional carbon atom in the backbone, the side chain can be attached on the first or second carbon leading to ß^2 and ß^3 amino acids (Figure 1). Similarly to β-peptides, γ- peptides have been designed and synthesized to bind natural α-peptide receptors, confirming the potential therapeutic applications of this type of foldamers.[4]

ß^3-amino acid ß^2-amino acid

***Figure 1**: representation of ß^3 and ß^2 amino acids.*

Another possibility is the combination of different monomer types in a single sequence. All new combinations lead to a specific pattern and thus to novel secondary structures, practically designing limitless numbers of different sequences. For example, αß-peptides using ß-residue with a five membered-ring adopt helical secondary structures (11-helix or 14/15 helix) in solution (Figure 2).[5]

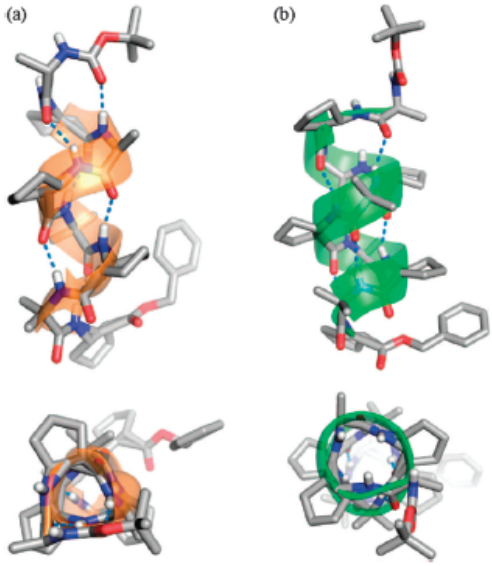

***Figure 2**: Molecular structures of αß-peptide helices obtained by X-ray: (a) 11-helix (orange), (b) 14/15-helix (green). Adapted from literature.[4]*

In this study, we combined the remarkable structure and chemical properties of adamantane to design new biomimetic scaffolds. The four bridgehead positions of adamantane allow control of the functional groups, which enables the design of polyfunctional building blocks for foldamer synthesis. Indeed, following appropriate protections steps, it is possible to obtain adamantane-based amino acids that can be used for solid phase synthesis of novel foldamers incorporating the adamantane moiety into their backbones. The aim is to exploit the rigid and well-defined structure of adamantane to induce a specific conformation. By conformational studies, it is possible to describe their capacity to fold into new structures that can be exploited for applications in materials science and biology. The interest in foldamers, especially for biological applications, considerably increased because of the similarity between foldamers and natural peptides and proteins. Furthermore, they are easily synthesized, display resistance to hydrolysis and their pharmacokinetic properties make them good candidate as new drugs. Their tunable molecular conformations provide to foldamers intrinsic properties, which can play a role in recognition and inhibition of several targets such as: bacterial cell membranes,[6] protein-RNA interaction,[7] protein-protein interactions,[8] and lectins.[9]

IV.2 Results and Discussion

IV. 2.1 Design and synthesis of γ- amino acid based on adamantane

In order to synthesize peptide foldamers incorporating the adamantane moiety, we designed a non-natural γ-amino acid based on adamantane (Figure 3). Two of the bridgehead positions are functionalized with a carboxylic acid and an amino group, respectively, leading to the desired γ-amino acid. Moreover, the two other bridgehead positions are functionalized with protected methyl esters. These protecting groups allow to control the peptide synthesis and avoid side-reactions. However, they can be removed at the end of the synthesis to obtain a fully deprotected peptide.

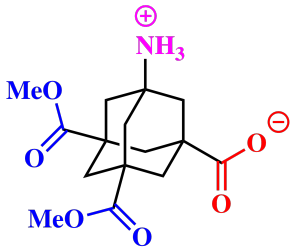

***Figure 3**: 3-Amino-5,7-bis(methocarbonyl)adamantane-1-carboxylic acid for peptide synthesis.*

Synthesis of adamantane γ- amino acid

The synthesis of functionalized adamantane starts with the commercial and inexpensive compound 1-bromoadamantane **1**. In previous chapter, I described the synthetic route to obtain the (3+1) adamantane building block **5** in five steps and without need of silica gel column purification for each intermediate (Scheme 1).

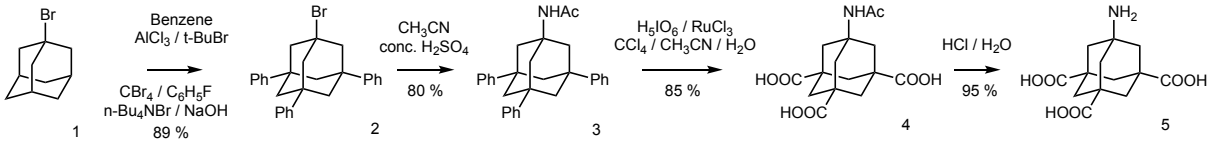

***Scheme 1**: Synthetic route to obtain functionalized (3+1) adamantane.*

From compound **5** to the desired protected amino acid **7**, two synthetic routes are possible. The first one is a selective esterification of two acid groups. However, I did not retain this possibility due to the lack of selectivity of the reaction. Thus, I selected the second possibility which is composed of two steps (Scheme 2 and 3). Firstly, I performed an esterification of the three carboxylic groups leading to the corresponding tri-esterified derivatives **6**. After purification, compound **6** undergoes a hydrolysis with a slight excess of potassium hydroxide allowing to

isolate mainly the mono-hydrolyzed product **7**, which corresponds to the designed γ- amino acid (Scheme 2). The protocol consists in mixing the tri-ester derivative **6** with a slight excess of potassium hydroxide in a methanol/water mixture (1/1) at 50 °C. The reaction can be followed by liquid chromatography coupled to mass spectrometry (LC-MS). Then, the mixture is neutralized with HCl 6N and concentrated under vacuum. The unreacted triester **6** can be recycled by extraction using hot acetonitrile (ACN) and used in a new hydrolysis reaction. Moreover, the little amount of side compounds formed (Scheme 2, **7a** and **7b**) are easily removed after *N*-acylation.

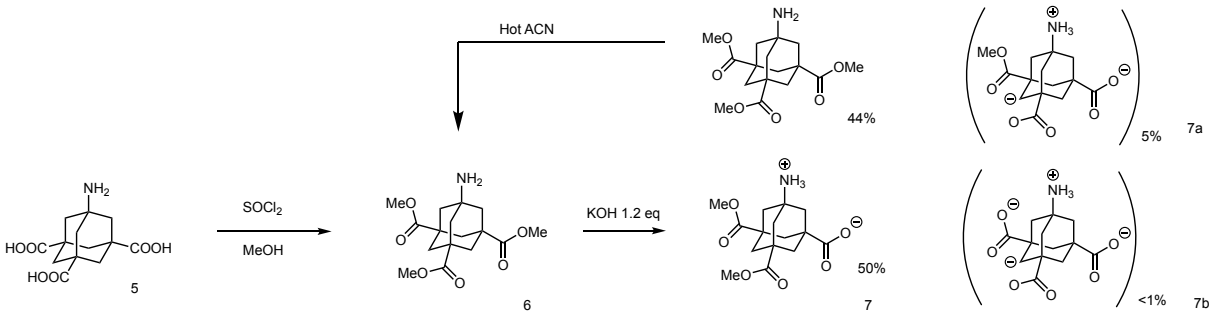

***Scheme 2**: Synthesis of 3-amino-5,7-bis(methocarbonyl)adamantane-1-carboxylic acid **7** from the tri-carboxilic acid **6** derivative.*

Then, in order to use compound **7** in SPPS, the free amino group has to be protected. The Fmoc strategy is the most commonly used in SPPS. I first tried to protect the free amine with a Fmoc protecting group leading to compound **8**. Following the procedures found in the literature,[10] different conditions have been tested (Table 1).

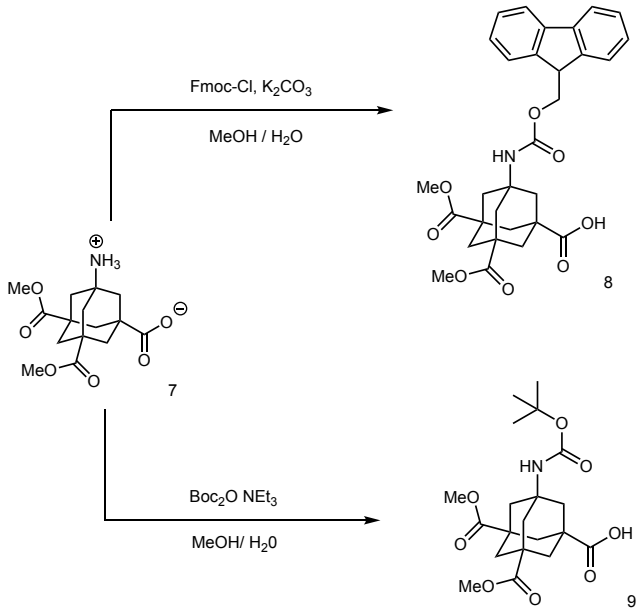

***Scheme 3**: Synthesis of Boc and Fmoc protected adamantane γ-amino acid.*

Table 1: *Conditions tested for the synthesis of Fmoc protected γ- amino acid.*

Solvent	Reagent	Base	Conditions	Yield
DMF	Fmoc-OSu	DIEA / DMAP	37 °C, overnight	< 5%
Dioxane / Water	Fmoc-Cl	Na_2CO_3	r,t overnight	24%
Dioxane / Water	Fmoc-OSu	Na_2CO_3	r,t overnight	< 6%
Dioxane / Water	Fmoc-Cl	K_2CO_3	r,t overnight	30%

Unfortunately, the results obtained confirmed the low nucleophilicity of the amino group on adamantane. Indeed, Fmoc-chloride and Fmoc-*N*-hydroxysuccinimide ester (*O*-Su) have been tested as reactant. Only trace of product were isolated. Then, different inorganic bases were tested, and potassium carbonate allows to obtain a better but still low yield than sodium carbonate (30% against 24%). In addition to the low yield observed, the reaction was not reproducible and the yield decreased when increasing the reaction scale to hundred milligrams. That is why, we changed our strategy and decided to use a Boc protecting group in place of Fmoc. Once again, different conditions have been tested leading to the formation of Boc protected γ-amino acid **9** (Table 2).

Table 2*: Conditions tested for the synthesis of Boc-protected γ- amino acid.*

Solvent	Reagent	Base	Conditions	Yield
MeOH	Boc_2O	NEt_3	60 °C, 48 h	30%
MeOH	Boc_2O	NEt_3	40 °C, 48 h	55%
THF	Boc_2O	NEt_3	50 °C	n.d

While the reaction does not occur in THF, I observed better yield in methanol, which is the solvent used for the Boc protection of the dendron building block described in Chapter II. It is interesting to notice the effect on the temperature. Indeed, when the temperature rises, the yield decreases. This is certainly due to the instability of the reactant at high temperature. I found a good compromise in performing the reaction at 40 °C for 48 h. In this case, the heat provides enough energy to the system (especially to the free amine) and the Boc anhydride displays an acceptable stability. Using this condition, I isolated compound **9** in 55% yield, even with a larger scale, which allows to synthesis several hundred milligrams of product.

IV. 2.2 Computational studies

In parallel to the synthesis of the protected building block, our collaborator Dr. Niels Johan Cristensen at the University of Copenhagen performed preliminary computational studies to understand the potential folding of peptides incorporating adamantane moiety in their backbones (Figure 4). The study was made on a sequence composed of glycine alternated with adamantane amino acid and with a tyrosine at the N-terminus: (H-(D,L)Tyr-Ada(Me)$_2$-Gly-Ada(Me)$_2$-Gly-Ada(Me)$_2$-OH*)*. First, we observed that the peptides adopt a favored conformation: this is not an α-helix but the peptide seems to fold. Then, we observed that the last tyrosine residue, depending on its own chirality (L or D), might induce a preferential right or left turn during the folding. For this reason, we decided to build each alternated peptide with L- or D-tyrosine at the *N*-terminus. Moreover, we also designed a homopeptide made of five adamantane residues directly connected, to study the importance of adamantane into the peptide backbone and observe if a particular conformation is adopted by this sequence.

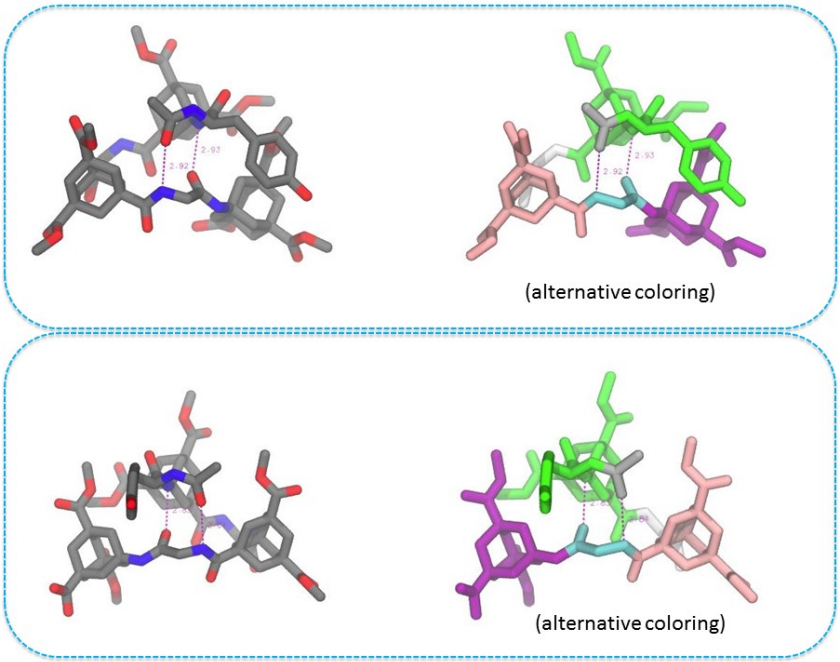

Figure 4: *Preferential folding of the peptide H-(D,L)Tyr-Ada(Me)$_2$-Gly-Ada(Me)$_2$-Gly-Ada(Me)$_2$-OH. D-tyrosine-containing peptide (top) forms a left turn while L-tyrosine-containing peptide (bottom) forms a right turn.*

Designed and synthesized peptide sequences:

1) H-(L,D)Tyr-Gly-Ada-Gly-Ada-Gly-Ada-Gly-OH (alternated peptide)
2) H-(L)Tyr-Gly-Ada-Ada-Ada-Ada-Ada-Gly-OH (homopeptide)

Differently from the computational studied, both sequences start with a glycine at the *C*-terminus and include an additional glycine before the N-terminal tyrosine. Indeed, we decided to add an initial achiral amino acid to have a short spacer before the incorporation of the first bulky adamantane γ- amino acid onto the resin and to determine the initial loading of the resin, a Fmoc derivative was necessary. Then, in the case of the alternated peptide, L- or D-tyrosine is attached to observe if this chiral amino acid is able to induce a preferential conformation during the folding. For the homopeptide, due to a lack of γ-amino acid, only the L-tyrosine was attached to observe if it plays again a role in the folding. The presence of the tyrosine also helps during the purification steps (strong absorbance in UV) and for the calculation of the exact concentration of the peptides in solution.

IV. 2.3 Set up and optimization

Synthesis strategy

The coupling of two admantane building blocks will likely be almost as difficult as coupling the natural amino acid Aib (α-amino isobutyric acid). Additionally the *N*-acylation of the γ-amino acid, to prepare the Boc and Fmoc protected amino acid, confirmed the low nucleophilicity of the amino group on adamantane. To overcome these difficulties, the synthesis of the peptides can be achieved using controlled microwave heating in solid phase. The concept of SPPS was introduced in 1963 by Robert Bruce Merrifield,[11] for which he was awarded the 1984 Nobel Prize in chemistry. Indeed, this methodology has been for decades the primary source of synthetic peptides in a laboratory scale. The protocol of solid phase synthesis, or more precisely matrix assisted synthesis, is described in three steps (Figure 5). The first building block is anchored to a matrix (resin). Then, repeated cycle of reactions (deprotection and coupling) are performed. Finally, the product is cleaved from the matrix and deprotected at the same time. However, by playing with the protecting groups, linkers, and reagents, the peptide can be also released from the support in a fully protected form.

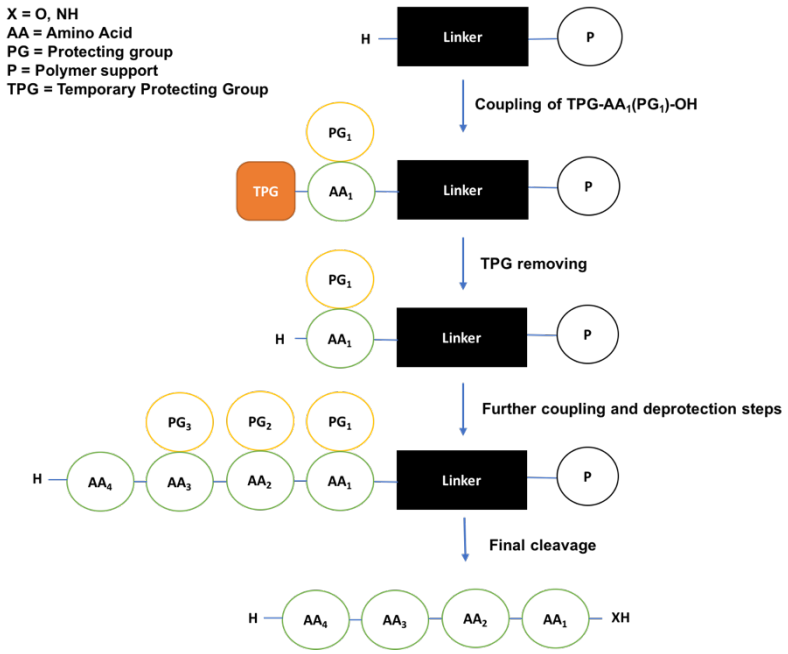

***Figure 5**: Principle of solid phase peptide synthesis.*

Several parameters must be considered in SPPS and they play a significant role in the peptide final yield (resin, linker, protecting group, solvent, coupling agents, temperature, MW, etc.). The first parameter is the choice of the resin. Indeed, the physicochemical properties of the resin are directly linked to the peptide final yield. Resins are characterized by the swelling capacity, the kinetics (reactivity) and the loading. The most common resins for SPPS are made on polystyrene (PS), typically with 1% cross-linking. The Merrifield resin is often used as a starting point to produce many other resins. It is a chloromethyl-polystyrene resin that can be synthesized by chloromethylation of polystyrene or even by copolymerization. Another important class of resins is obtained from a polystyrene core onto which PEG chains have been attached. These resins called TentaGel are developed by Rapp Polymere company in Germany. They provide higher purity of synthesized peptides, especially with long sequences or peptide that are prone to aggregate. Some others resins are available like aminomethyl polystyrene and more recently, free polystyrene resins have been developed such as PEGA (copolymerization of PEG chains with *N,N*-dimethylacrylamide).[12,13] This kind of resins display high permeability and allow synthesized proteins up to 35-70 kDa.

The second parameter is the linker. Lynkers are bifunctional molecules, which are anchored to the solid support and to the growing peptide. Thus, they play a role of protecting group at the *C*-terminus and determine the cleavage conditions.

In order to incorporate the adamantane building block into the peptide backbone and because of its high sterical hindrance, we selected: TentaGel resin (Loading = 0.29 mmol·g^{-1}) and 4-hydroxymethylbenzoic acid (HMBA) as linker. This combination of resin/linker display good swelling capacity and quite low initial loading compare to other resins. Moreover, it is commonly used in Fmoc strategy and the cleavage is effected using a strong nucleophile like sodium hydroxide.

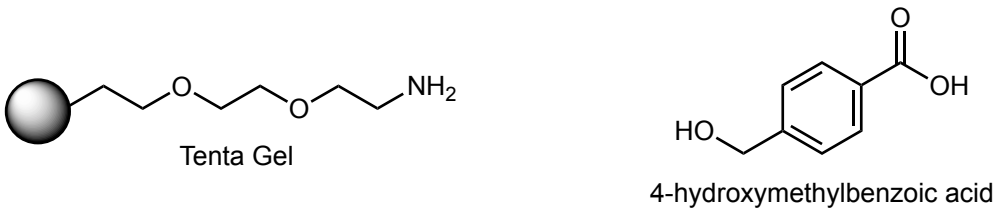

***Figure 6**: Representation of TentaGel resin and 4-hydroxymethylbenzoic acid linker.*

Fmoc versus Boc protocol

The third parameter concerns the choice of the temporary protecting groups. These protecting groups allow to control the peptide sequence. Thus, they must be stable against the coupling conditions but quickly and selectively removed after the coupling to continue the peptide synthesis. The most commonly used protecting groups are fluoren-9-ylmethyloxycarbonyl (Fmoc) and *tert*-butoxycarbonyl (Boc).

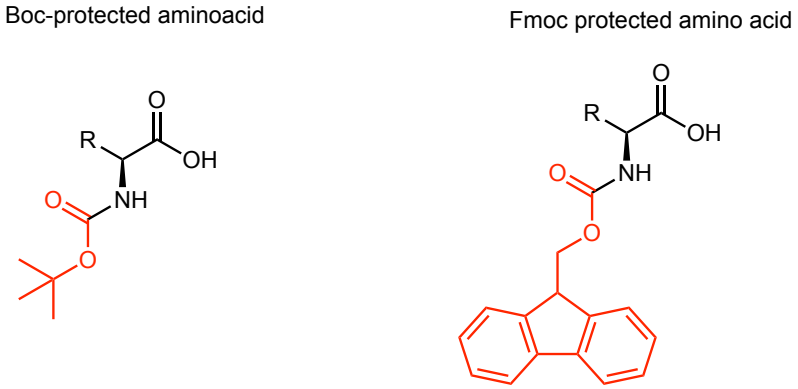

***Figure 7**: Representation of Boc- and Fmoc-protected amino acids.*

Each *N*-α-protecting group will define the overall strategy for SPPS (Fmoc vs Boc strategy). The chemical conditions for removal of the temporary protecting group will define the linker and the side chain protecting groups, which must be stable in these conditions. Boc is easily

removed in acidic condition (TFA 50% in DCM). However, Boc strategy requires special equipment because of the final cleavage which is performed using HF which is highly corrosive and toxic. For this reason, Fmoc strategy is usually preferred in SPPS. Fmoc is usually removed by piperidine (20% in DMF), which first reacts as a base and then as nucleophilic scavenger. More safer and strongly active in UV, the Fmoc residual product allows to determine the loading of the resin and thus, to determine the incorporation yield of each amino acid. Because of the low nucleophilicity of the adamantane γ-amino acid, I only synthesized Boc-protected derivative in large scale. However, due to the use of HF in Boc strategy and the requirement of specialized apparatus to handle it, we decided to combine Boc and Fmoc strategies. Moreover, the use of adamantane to prepare peptide and homopeptide by SPPS represented a real challenge and it has never been reported before. Thus, the importance of using Fmoc-protected amino acids is important because it allows to determine the loading of the resin after each coupling by spectrophotometrically analysis following the Beer-Lambert law (see Experimental section).

Stability of amino-adamantane-diester

Before starting the peptide synthesis, I checked the stability of the Boc-protected adamantane amino acid **10** in the coupling and deprotection conditions.

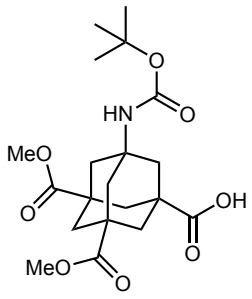

10

Figure 8: *Boc-protected adamantane γ- amino acid.*

Indeed, mixing Boc and Fmoc strategies needed to initially check the stability of compound **10**. It must be stable in basic condition (Fmoc removal) and against strong nucleophiles (cleavage conditions). Moreover, the Boc must be remove selectively without affecting the protecting groups (esters). Thus, different conditions have been tested, and LC-MS analysis allowed to quickly determine what happened (Table 3).

***Table 3**: Stability of the Boc-protected adamantane γ- amino acid.*

Conditions	Observation (LC-MS)
TFA 100 % - 1 h	Boc and ester are removed
NaOH 0.05M – 30 min	Esters partially hydrolyzed
TFA 50 % - 30 min	Boc selectively removed
20 % piperidine in DMF – 30 min	Nothing happens
Sodium methoxide (0.05M) in MeOH	Mix (due to free acid)

While 100 % TFA during one hour leads to a loss of selectivity because we observed that ester groups are hydrolyzed in this condition, using 50 % of TFA during 30 min allows to selectively remove the Boc protecting groups without affecting the methyl esters. Then sodium hydroxide at 0.05 M, which is commonly used for the final cleavage (with TentaGel – HMBA combination) displays a partially hydrolysis of the ester groups. A solution was to use sodium methoxide as strong nucleophile for the final cleavage. Indeed, even if it reacts with the ester groups it will regenerate the same methyl ester. I also tested 20 % piperidine in DMF, which is the routinely mixture to remove Fmoc temporary protecting group. Neither Boc group or esters were sensitive to this condition meaning that the Boc-protected γ- amino acid can be use in a Fmoc/Boc strategy.

Set up and optimization

In order to save the precious protected amino acid **10**, I decided to perform the set up using the Boc-protected free acid derivative **11**. This latest is easily synthesized by *N*-acylation of the 7-aminoadamantane-1,3,5-tricarboxylic acid (described in Chapter II).

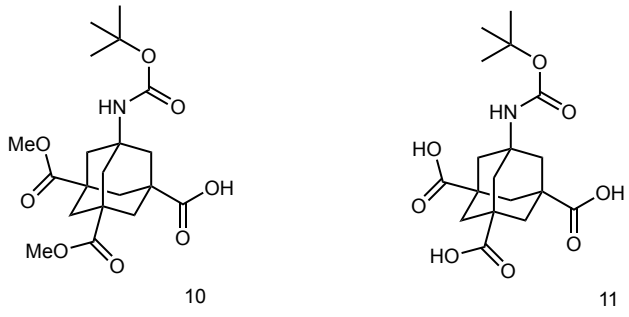

***Figure 9**: Boc protected amino acid with and without ester protecting groups.*

Moreover, the reactions are followed by Kaiser test, which allows to detect free terminal amino groups in SPPS.[14] This very sensitive test is based on the reactivity of ninhydrin with primary amines. Indeed, ninhydrin reacts with the deprotected *N*-terminal group of the peptide-resin to produce an intense blue color. Thus, it allows to determine if the coupling reactions are completed.

Resin/linker preparation and first amino acid incorporation

I first started by attaching the linker to the resin. TentaGel S-NH_2 resin reacts with HMBA (linker) *via* classical peptide bond synthesis using HBTU, HOBt as coupling reagents and *N,N*-diisopropylethylamine (DIEA) as a base. As explained before, the first amino acid moiety is anchored to the linker *via* ester bond. This reaction requires an excess of amino acid (10 eq). For this purpose, I chose Fmoc-Glycine-OH. It allowed to save the precious adamantane amino acid and to avoid sterical hindrance problems. Moreover, due to the presence of the Fmoc temporary protecting group, a loading test can be performed. The reaction is performed by adding Fmoc-Glycine-OH (10 eq), DIC (5 eq) and a catalytic amount of 4-(dimethylamino)pyridine (DMAP) in a DMF/DCM mixture (9/1). This step is repeated twice in order to obtain a maximum incorporation of glycine, with a yield of 71 % (Loading = 0.205 $mmol \cdot g^{-1}$).

Incorporation of adamantane amino acid into a peptide sequences

After glycine insertion, I tried to insert the adamantane derivative **11** (Figure 11). First, the Fmoc temporary protecting group of glycine was removed using 20 % piperidine in DMF during 30 min. Kaiser test confirmed the efficiency of the deprotection. Then, using a mixture of 1-[bis(dimethylamino)methylene]-1H-1,2,3-triazolo[4,5-b]pyridinium 3-oxide hexafluoro-phosphate (HATU) (3 eq), 1-hydroxy-7-azabenzotriazole (HOAt) (3 eq) and N,N-diisopropylethylamine **(**DIPEA) (5.4 eq) in DMF for 2 h at room temperature we observed that adamantane derivative was easily inserted in the growing peptide (negative Kaiser test). While usually amino acids are added with an excess (4 eq), we decreased the amount of adamantane amino acid until 1.5 equivalent. Which will allow to save a large amount of this precious amino acid.

Incorporation of the other amino acids after the first adamantane amino acid

Thus, adamantane is easily inserted into the peptide backbone confirming the good reactivity of the activated carboxylic acid. However, the challenge is the quite low nucleophilicity of the amino group on adamantane. First of all, the Boc temporary group is removed selectively by TFA 50% in DCM for 30 min. Once again, Kaiser test allows to follow the deprotection (even if in this case, I observed the formation of brown color compared to usual blue/dark violet). This is certainly because I am using a γ-amino acid, thus, Kaiser test is not adapted for such amino acids). Then, I coupled Fmoc-Glycine-OH on adamantane free amine. Four eq of Fmoc-Glycine- have been used for each coupling, and proportional amounts of coupling reagents were added (Table 4). All reactions were followed by Kaiser test and loading test using the Fmoc titration before and after the glycine insertion. These two techniques were used at indicative title as they are sensitive to different parameters, especially the loading test which depends of the resin dryness, volume of piperidine and amount of resin (less than 5 mg), thus explaining why we could observe a yield sometimes higher than 100%.

***Table 4**: Incorporation of Fmoc-Glycine-OH (4eq) onto adamantane peptide.*

	Test 1	Test 2	Test 3	Test 4
Boc deprotection	✔	✔	✔	✔
Coupling reagents	HATU / HOAt / DIPEA	DIC / Oxyma	HATU / HOAt / DIPEA + MW	DIC / Oxyma + DMAP + MW
Loading test (mmol/g & yield)	0.11 / 54%	0.049 / 24%	0.14 / 69%	0.23 / 105%
Repeat reaction	0.13 / 63%	0.07 / 33%	0.16 / 78%	-
Repeat reaction	-	0.14 / 68%	-	-

These results illustrated in Table 4 confirm the low nucleophilicity of the free amine on adamantane, whatever the coupling reagents used at room temperature. However, we observe a significant better yield when the reactions were performed under microwave heating at 65 °C during only 10 min in the presence of catalytic DMAP. So, I selected DIC, ethyl 2-cyano-2-(hydroxyimino) acetate (Oxyma) as coupling reagents with microwave heating at 65 °C, for 10 min in DMF. In order to decrease the potential side reactions, I also tested the conditions without DMAP (Table 5).

***Table 5**: Fmoc-Glycine-OH addition on adamantane under microwave heating.*

	Test 1	Test 2
Remove Boc	TFA 50%, rt, 30 min	TFA 50%, rt, 30 min
Coupling conditions	MW (65 °C – 10 min)	MW (65 °C – 10 min)
Coupling reagents	DIC, Oxyma	DIC, Oxyma
Amino acid	Fmoc-Gly-OH (4eq)	Fmoc –Gly (2 x 1 eq)
Results	Kaiser test: still a bit brown Loading: 0.157 – 69%	Kaiser test: negative Loading (0,23 – 100%)
Repeated reaction	Kaiser test: negative Loading: 102%	- -

I found that DMAP was not necessary. Moreover, the reaction is complete using only 2 eq of protected amino acid in two step (2×1 eq each). This result is particularly interesting for the synthesis of the homopeptide because it allows to save a large amount of protected adamantane γ-amino acid.

Cleavage tests

After the addition of an amino acid with a phenyl group like phenylalanine or tyrosine (easier to detect in HPLC) (Figure 10), different cleavage tests have been performed, followed by Kaiser test. The cleavage is performed in two steps. Firstly, the deprotection of the Fmoc temporary protecting group of the last amino acid incorporated. Secondly, the cleavage of the peptide from the resin. Thus, after cleavage from the resin, we should recover the resin/linker with an alcohol function meaning that Kaiser test must be negative.

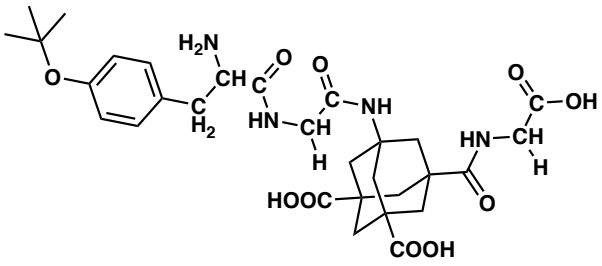

***Figure 10**: First SPPS synthesized peptide used for cleavage tests.*

I tried to cleave the peptide with sodium hydroxide 0.5 M in dioxane water (1:1) and with sodium methoxide 0.25 M in methanol, both at room temperature for 30 min. The Kaiser test confirmed that the cleavage was completely achieved using sodium methoxide but it did not occur with sodium hydroxide. LC-MS analysis after sodium methoxide cleavage confirmed the presence of the expected compound and a little amount of +1 and +2 glycine residues. This

observation means that the free acids of adamantane derivative **11** certainly reacts with the free glycine on the resin. Then, to better understand what is happening with sodium hydroxide, I synthesized a simple peptide without adamantane derivative (H-Tyr-Gly-Phe-Gly-OH) and, in this case, sodium hydroxide 0.5 M worked perfectly to cleave the peptide from the solid support confirming the impact of adamantane on the peptide. These results confirmed that compound **11** is not suitable to build peptide and it requires protecting group on the adamantane. In addition, sodium hydroxide cannot be used to cleave a peptide containing adamantane while sodium methoxide is a good option.

IV. 2.4 Peptide synthesis test incorporating Boc-amino-adamantane acid diester

In order to validate the set up when the Boc-amino adamantane acid diester is used, I first synthesized a small peptide incorporating the adamantane derivative (H-Tyr-Gly-Ada-Gly-OH). Using only 1.5 eq of Boc-protected adamantane derivative **10** and MW heating during the glycine addition on adamantane, I obtained a final loading of 75 %. Then, I focused on the cleavage of the peptide. The purpose was to find a way to obtain the fully deprotected peptide (adamantane side chain deprotected and COOH at the *C*-terminus). However, once again, only sodium methoxide showed good results (Table 6). Moreover, the cleavage with sodium methoxide led to two compounds (Figure 11) with the *C*-terminus as free acid or as methyl ester. Note that the *t*-Bu and Fmoc protecting groups were removed before the cleavage test.

***Table 6**: Cleavage conditions tested.*

Test	Conditions	Kaiser test	Observations
NaOMe 0.25 M	30 min / r.t	Negative	2 peak in HPLC (50/50) COOMe and COOH at *C*-terminus and adamantane is still protected
NaOMe 0.5 M	30 min / r.t	Negative	
NaOMe 0.5 M fresh	30 min / r.t	Negative	2 peaks in HPLC but 75 / 25 for COOMe
NaOH 0.25 M	30 min / r.t	Positive	n.d
NaOH 0.5 M	30 min / r.t	Positive	n.d
NaOH 0.5 M in MeOH	30 min / r.t	Positive	n.d
LiOH 0.5 M in THF	30 min / r.t	Positive	n.d
LiOH 1 M in MeOH	1 h / 50 °C	Positive	n.d

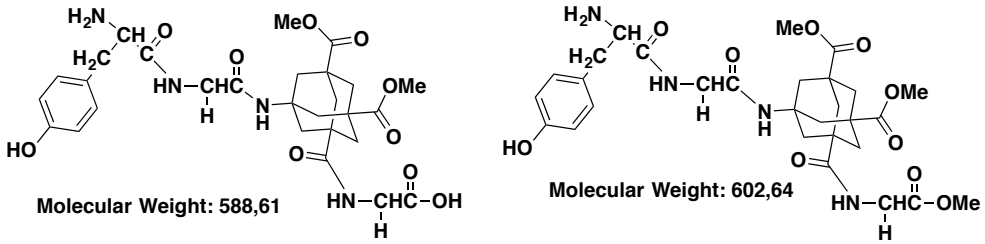

***Figure 11**: Peptide isolated after sodium methoxide cleavage.*

Unfortunately, sodium and lithium hydroxides are not able to cleave the peptide when adamantane derivative is into the backbone. Even at higher temperature and concentration, or by changing the solvent, the cleavage reaction did not occur. On the other hand, using sodium methoxide I achieved the expected peptides (keeping the protecting group on adamantane) but with a main difference at the *C*-terminus (COOH vs COOMe). I decided to use this protocol to cleave, then separate the two compounds, in order to keep the COOH derivative and hydrolyze with NaOH the methylester group from the second peptide to obtain a fully deprotected peptide (Figure 12).

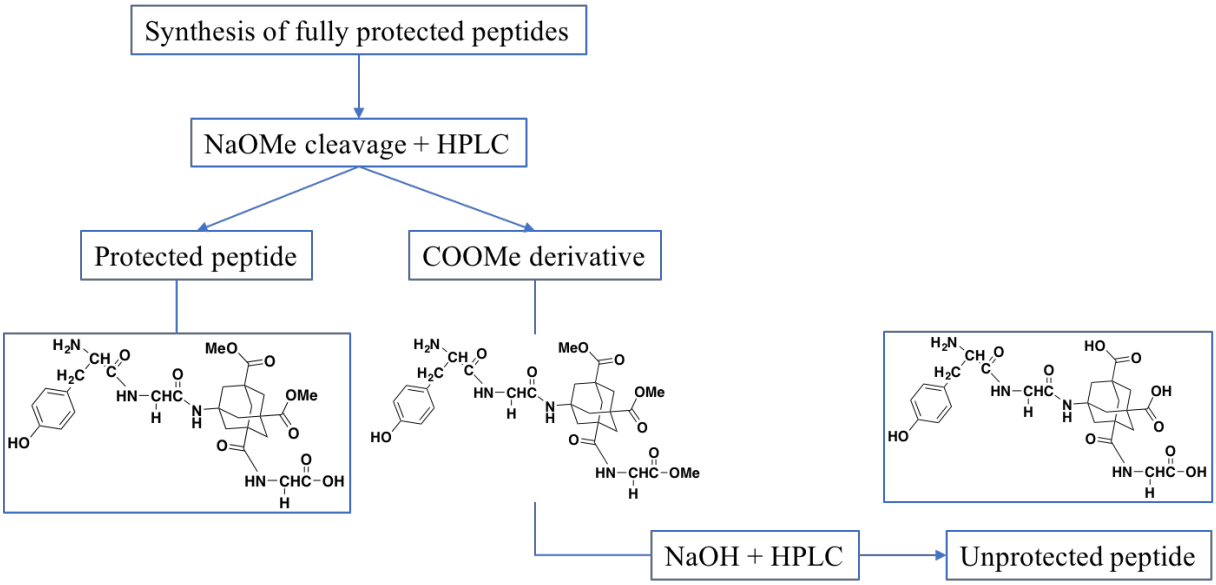

***Figure 12**: Strategy used to synthesize protected and fully protected peptides.*

IV. 2.5 Synthesis of the long peptides

After the optimization procedures described above, I successfully synthesized, purified and characterized by mass spectrometry (Figure 13A and 13B) the alternated peptides, with and without protecting groups on adamantane and with a final L- or D-tyrosine at the end of the sequence (Table 7).

***Table 7**: Alternated peptides sequences synthesized.*

Alternated peptides sequences:
H-L-Tyr-Gly-Ada(Me)$_2$-Gly-Ada(Me)$_2$-Gly-Ada(Me)$_2$-Gly-OH
H-L-Tyr-Gly-Ada-Gly-Ada-Gly-Ada-Gly-OH
H-D-Tyr-Gly-Ada(Me)$_2$-Gly-Ada(Me)$_2$-Gly-Ada(Me)$_2$-Gly-OH
H-D-Tyr-Gly-Ada-Gly-Ada-Gly-Ada-Gly-OH

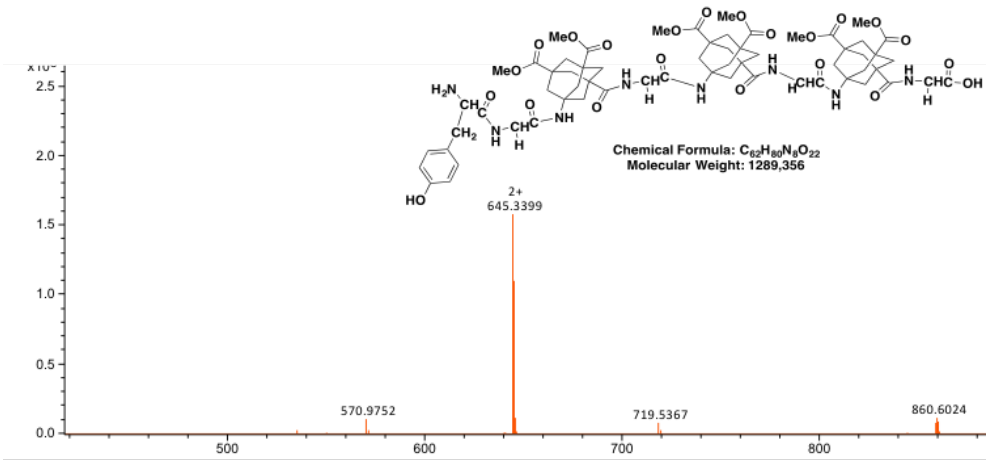

***Figure 13A**: Mass spectrum of the protected alternated peptide.*

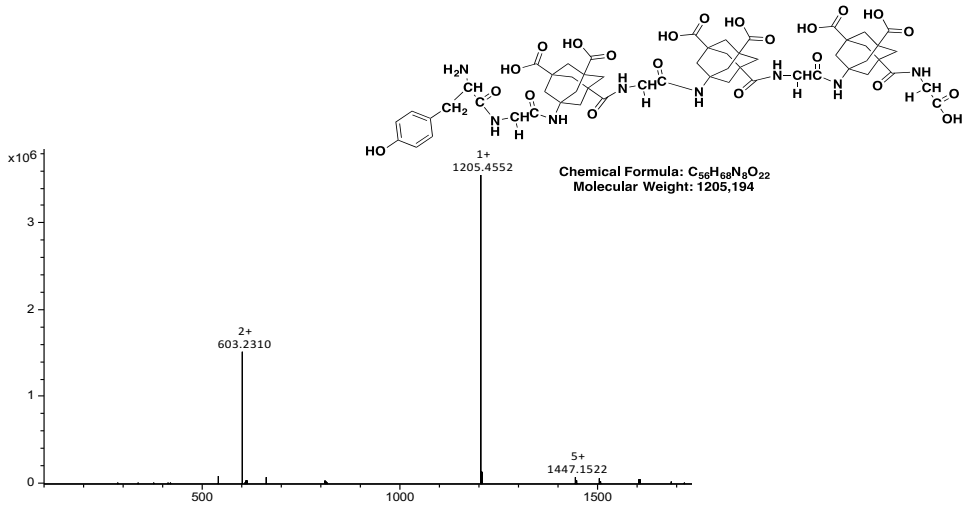

***Figure 13B**: Mass spectrum of the deprotected alternated peptides.*

I also synthesized the homopeptide (H-Tyr-Gly-Ada(Me)$_2$-Ada(Me)$_2$-Ada(Me)$_2$-Ada(Me)$_2$-Ada(Me)$_2$-Gly-OH). Unfortunately, in this case, I did not isolate the hydrolyzed compound (obtaining only the fully unprotected peptide). Indeed, I observed more side reactions during this synthesis and the crude mixture was less pure. I isolated different compounds but only fragments or unknown peptide (mass of +29 Da, while I expected a mass of +14 Da due to the methyl ester at the *C*-terminus). Even after hydrolysis of the protected peptide, I still observed a mass of +29 Da.

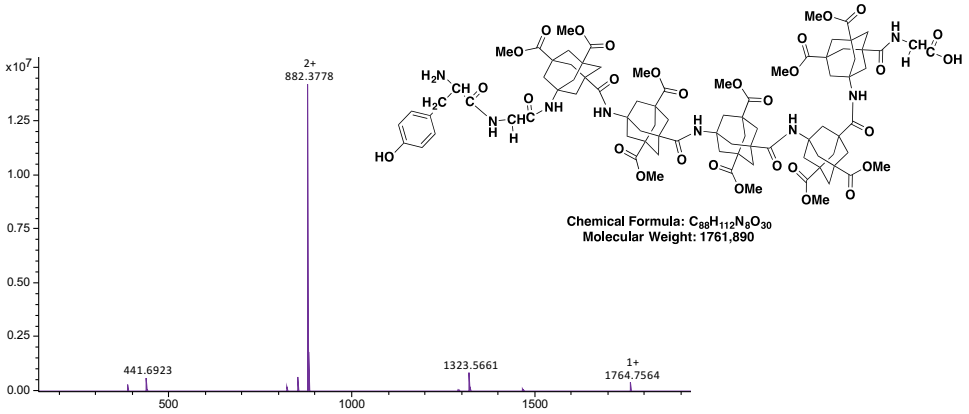

***Figure 14**: Mass spectrum of the homopeptide.*

IV. 2.6 Folding studies

After the synthesis of the different peptides I started to study their folding. To obtained information on the peptide structure, I used circular dichroism analysis. This technique is based on the differential absorption of left and right handed circularly polarized light when it passes through an absorbing optically active medium and thus it is a common method to study chiral molecules like proteins and peptides. In natural protein, chirality is provided firstly by the type of amino acid (L) (excepted glycine). Then, the folding of a peptide into an organized structure (secondary structure) like an α helix is another source of chirality. This type of chirality is the most adopted in Nature. It is possible to observe a signal in CD only at specific wavelengths, which correspond to molecule absorption bands. Under 240 nm, the absorption is due to peptide bonds and thus, provides information on secondary structure. Between 260 and 320 nm, the absorption is due to lateral chains of amino acids. The signal will depend on the relative position of each amino acids, their environment, their mobility and their quantities. This signal can be used like a digital print of the molecule.

UV titration and CD

Using CD, it is possible to measure the ellipticity of each solution containing the synthesized peptide. The ellipticity is giving in mdeg. To obtain values independent of the concentration, a mathematic transformation is used (see Experimental section). The precise concentration of each sample (following its weight and solubilization in the appropriate solvent) was determined by UV titration using the Beer-Lambert law and the optical properties of the tyrosine (Figure 15).

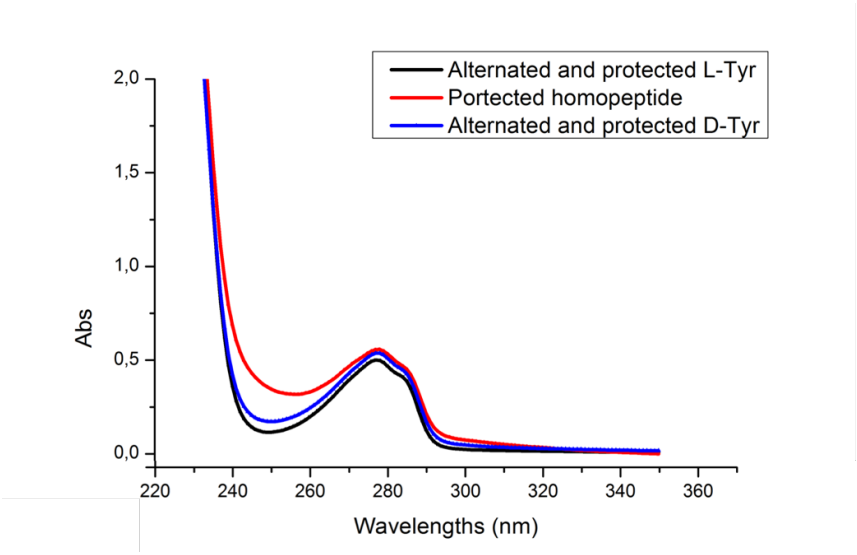

Figure 15: *Examples of UV titration using the tyrosine optical properties.*

Folding studies of peptides incorporating adamantane into the backbone

I started by study the folding of the peptides in methanol. The circular dichroism was first measured in mdeg and then converted into deg·cm^2·decagram^{-1}specific ellipticity. The different alternated protected and deprotected peptides and the homopeptide analyzed are

H-L-Tyr-Gly-Ada(Me)$_2$-Gly-Ada(Me)$_2$-Gly-Ada(Me)$_2$-Gly-OH (1)
H-D-Tyr-Gly-Ada(Me)$_2$-Gly-Ada(Me)$_2$-Gly-Ada(Me)$_2$-Gly-OH (2)
H-L-Tyr-Gly-Ada-Gly-Ada-Gly-Ada-Gly-OH (3)
H-D-Tyr-Gly-Ada-Gly-Ada-Gly-Ada-Gly-OH (4)
H-L-Tyr-Gly-[Ada(Me)$_2$]$_5$-Gly-OH (5)

These peptides display an interesting and unexpected signal in CD. Indeed, we can observe a specific signal in the range 200-240 nm which correspond to the peptide bond contributions. These signals mean that a specific conformation is adopted by the peptides. Moreover, as excepted, the signals were symmetric when I analyzed L- or D- tyrosine-containing peptides (Figure 16), confirming than the tyrosine induces an opposite chirality into the folded structure. However, the spectra obtained do not correspond to an α-helix or a ß-sheet thus, likely being another type of turn.

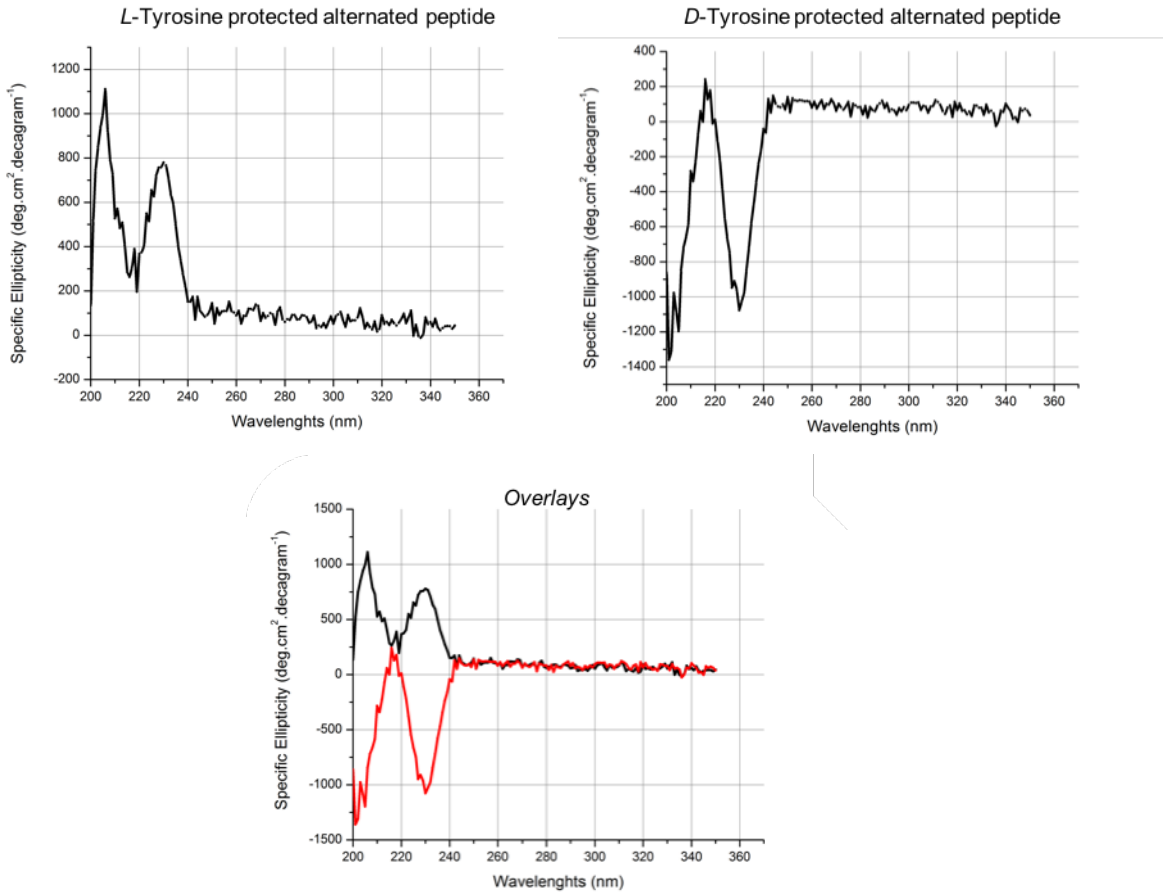

Figure 16: *Specific ellipticity in methanol of L-Tyr (1), D-Tyr (2), and overlays of protected alternated peptide.*

The same analysis was done with the unprotected alternated peptide. Only the D- derivative was first analyzed but it does not fold in methanol (Figure 17). The L-tyrosine fully unprotected was difficult to purify after hydrolysis (the compound came in the injection peak with the salt).

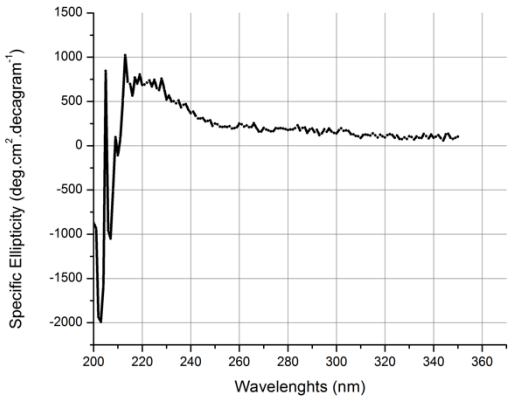

Figure 17*: Specific ellipticity in methanol of the unprotected D-Tyr-unprotected peptide (4).*

The fully protected homopeptide was also analyzed by CD in methanol, but any favorised conformations were observed (figure 18).

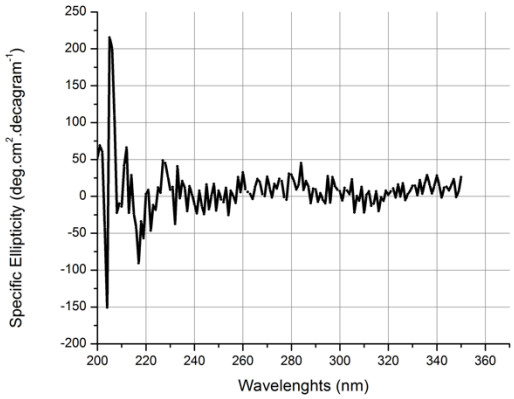

***Figure 18**: Ellipticity of the protected homopeptide (5) in methanol.*

Then, I measured the ellipticity of the peptides in trifluoroethanol (TFE), which is often used to induce a folding. Once again, a clear signal was observed for the alternated protected peptides with L- and D-tyrosine (Figure 19).

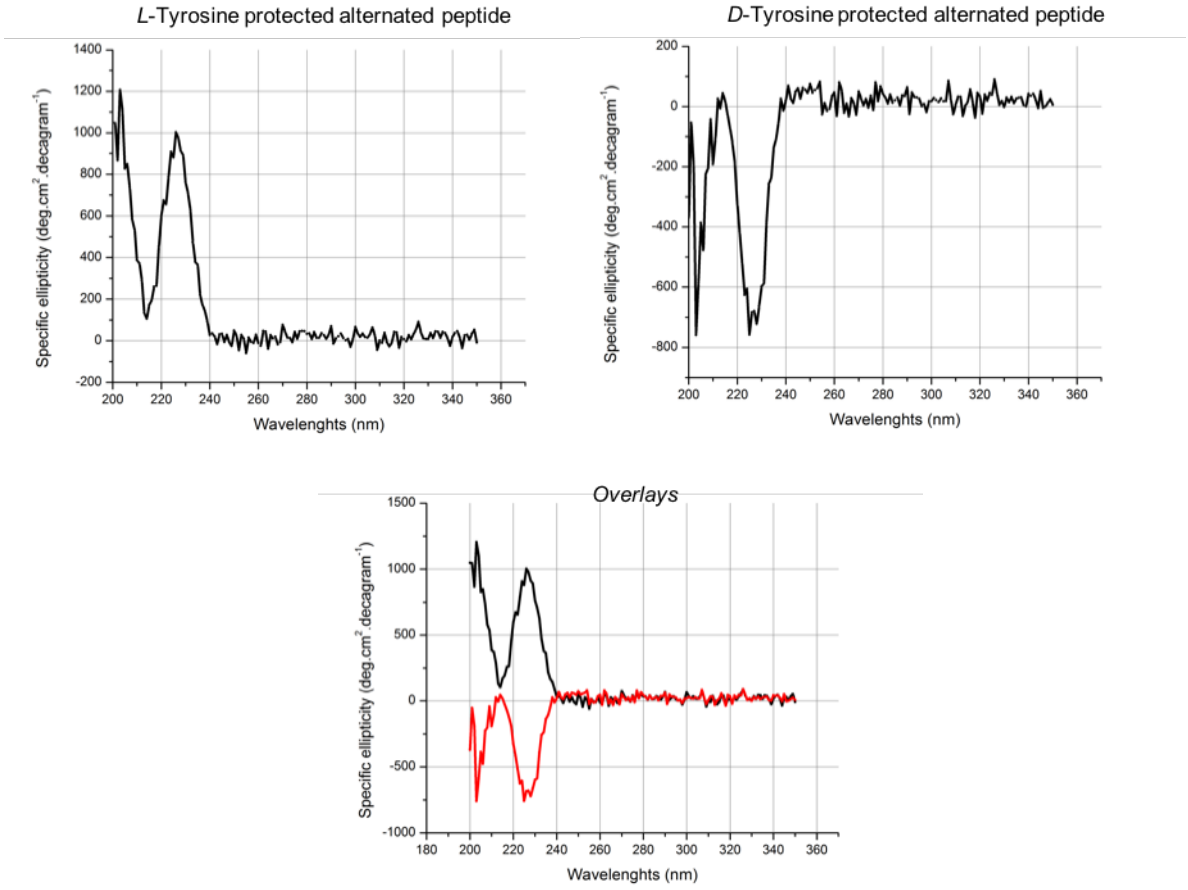

***Figure 19**: Specific ellipticity in TFE of L-Tyr (1), D-Tyr (2) and overlays of protected alternated peptides.*

The alternated unprotected peptides were not able to fold in TFE, likely due to their lack of solubility. Indeed, no CD signals were observed. Moreover, in TFE also the homopeptide adopts a favored conformation which provide a CD signal, confirming its capacity to adopt an ordered secondary structure.

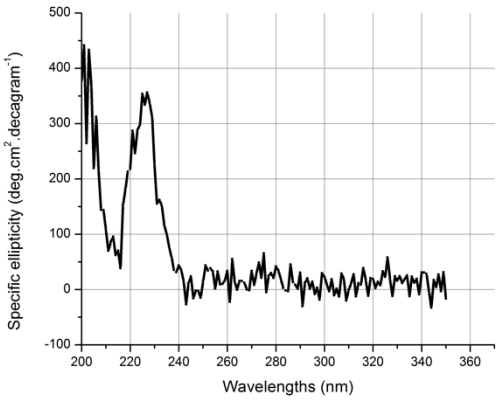

Figure 20: *Specific ellipticity of homopeptide (5) in TFE.*

IV. 3 Conclusions & Perspectives

In this chapter, I described the synthesis of an adamantane γ- amino acid starting from 1-bromoadamantane. I developed a synthesis which allows to obtain the γ- amino acid protected with two methyl esters. Then, the free amino group was Boc-protected for its use in SPPS.

During my visiting period in the Lab of Professor Knud Jensen at the University of Copenhagen, I developed a robust protocol to incorporate adamantane derivatives (with microwave assistance) in a growing peptide on SPPS, while using the minimum amount of protected amino acid derivative. Using a Fmoc and Boc mixed strategy, I developed selective deprotection of each temporary protecting group without affecting the resin, the linker or the other protecting groups. Thus, I synthesized the desired peptides and developed a cleavage protocol and a work-up, which gave us the possibility to obtain peptides with or without protecting groups (esters) on the adamantane.

Then, I studied the folding of each peptide using circular dichroism in methanol and trifluoroethanol. I observed that adamantane incorporated into peptide backbone plays a role in the peptide folding. Moreover, the presence of L- or D-tyrosine induces a specific chiral conformation during the folding, notably with the protected alternated peptides.

In perspective, it will be interesting to study the folding of the peptides in another medium like water with calcium (which can interact with carboxylate groups), or in PBS. I also tried to

obtain crystal in order to perform X-rays diffraction, without success. Therefore, more attempt should be made to get crystals. To finish, NMR could be interesting to confirm the conformation in solution, however it requires a larger amount of materials.

This project combine unique expertise on design and synthesis of novel adamantane building block, with the ability to use precise microwave heating to assemble sterically hindered monomers into oligomers. The outcomes are novel foldamers with new properties.

IV. 4 References

(1) Hill, D. J.; Mio, M. J.; Prince, R. B.; Hughes, T. S.; Moore, J. S. A Field Guide to Foldamers. *Chem. Rev.* **2001**, *101* (12), 3893–4012.

(2) Claudia, T.; Ivan, H.; J, A. D.; Ferenc, F. Foldamers. *Eur. J. Org. Chem.* **2013**, *17* (2347494), 3408–3409.

(3) Martinek, T. A.; Fülöp, F. Peptidic Foldamers: Ramping up Diversity. *Chem. Soc. Rev.* **2012**, *41* (2), 687–702.

(4) Seebach, D.; Beck, A. K.; Bierbaum, D. J. The World of Beta- and Gamma-Peptides Comprised of Homologated Proteinogenic Amino Acids and Other Components. *Chem. Biodivers.* **2004**, *1* (8), 1111–1239.

(5) Crystallographic Characterization of Helical Secondary Structures in α/β-Peptides with 1:1 Residue Alternation http://pubs.acs.org/doi/pdf/10.1021/ja800355p (accessed Oct 18, 2017).

(6) Patil-Sen, Y.; Dennison, S. R.; Snape, T. J. Functional Foldamers That Target Bacterial Membranes: The Effect of Charge, Amphiphilicity and Conformation. *Bioorg. Med. Chem.* **2016**, *24* (18), 4241–4245.

(7) Gelman, M. A.; Richter, S.; Cao, H.; Umezawa, N.; Gellman, S. H.; Rana, T. M. Selective Binding of TAR RNA by a Tat-Derived β-Peptide. *Org. Lett.* **2003**, *5* (20), 3563–3565.

(8) Bautista, A. D.; Appelbaum, J. S.; Craig, C. J.; Michel, J.; Schepartz, A. Bridged Beta(3)-Peptide Inhibitors of P53-HDM2 Complexation: Correlation between Affinity and Cell Permeability. *J. Am. Chem. Soc.* **2010**, *132* (9), 2904–2906.

(9) Kaszowska, M.; Norgren, A. S.; Arvidson, P. I.; Sandström, C. Studies on the Interactions between Glycosylated Beta3-Peptides and the Lectin Vicia Villosa by Saturation Transfer Difference NMR Spectroscopy. *Carbohydr. Res.* **2009**, *344* (18), 2577–2580.

(10) Marecek, J.; Song, B.; Brewer, S.; Belyea, J.; Dyer, R. B.; Raleigh, D. P. A Simple and Economical Method for the Production of 13C,18O-Labeled Fmoc-Amino Acids with High Levels of Enrichment: Applications to Isotope-Edited IR Studies of Proteins. *Org. Lett.* **2007**, *9* (24), 4935–4937.

(11) Merrifield, R. B. Solid Phase Peptide Synthesis. I. The Synthesis of a Tetrapeptide. *J. Am. Chem. Soc.* **1963**, *85* (14), 2149–2154.

(12) Auzanneau, F. I.; Meldal, M.; Bock, K. Synthesis, Characterization and Biocompatibility of PEGA Resins. *J. Pept. Sci. Off. Publ. Eur. Pept. Soc.* **1995**, *1* (1), 31–44.

(13) Meldal, M. Pega: A Flow Stable Polyethylene Glycol Dimethyl Acrylamide Copolymer for Solid Phase Synthesis. *Tetrahedron Lett.* **1992**, *33* (21), 3077–3080.

(14) Kaiser, E.; Colescott, R. L.; Bossinger, C. D.; Cook, P. I. Color Test for Detection of Free Terminal Amino Groups in the Solid-Phase Synthesis of Peptides. *Anal. Biochem.* **1970**, *34* (2), 595–598.

Chapter IV: Experimental Section

General experimental details

Chemicals and Solvents

All the starting materials, chemicals, and anhydrous solvents were obtained from commercial suppliers (Sigma-Aldrich, Acros Organics and Alfa Aeasar laboratories). All solvent used for the synthesis were analytical grade. When anhydrous conditions were required, high quality commercial dry solvent were used. Water was purified using Millipore filter system MilliQ® equipped with a Biopak® filter.

Characterization Methods and Instrumentation

Thin layer chromatography (TLC): TLC was conducted on pre-coated aluminum plates with 0.25 mm *Macherey-Nagel* silica gel with fluorescent indicator UV254.

Column chromatography: Chromatographic purifications were carried out with silica gel (Merck Kieselgel 60, 40-60 μm, 230-400 mesh ASTM).

Nuclear Magnetic Resonance: ^{1}H-NMR and ^{13}C-NMR spectra were recorded in deuterated solvents using Bruker Avance I – 300 MHz and Bruker Avance III – 400 MHz. Chemical shifts are reported in ppm using the residual signal of deuterated solvent as reference (TMS = 0). Coupling constants *J* are reported in Hertz (Hz), and the splitting patterns are designated as *s* (singlet), *d* (doublet), *t* (triplet), *td* (triplet of doublet), *q* (quartet), *p* (pentet), *m* (multiplet), and *br* (broad).

ESI Mass Spectrometry: Mass spectra were recorded on a Thermo Fisher Finnigan LCQ Advantage Max Instrument.

High Resolution ESI Mass Spectrometry: MS experiments were performed on a Bruker Daltonics microTOF spectrometer (Bruker Daltonik GmgH, Bremen, Germany) equipped with an orthogonal electrospray (ESI) interface. Calibration was performed using Tunning mix (Agilent Technologies).

Ultra Performance Liquid Chromatography Mass Spectrometry: UPLC-MS experiments were performed on a RSLC Dionex Ultimate 3000 (thermo) coupled to QTOF Impact HD (Brucker) on a kinete 2.6 μm EVO 100 Å, C18 column (50×2.1 mm, Phenomenex).

Reverse Phase High Pressure Liquid Chromatography: RP-HPLC were performed on Dionex Ultimate 3000 system with preparative C18 column (Phenomenex Gemini, 110 Å, 5 μm C18 particles, 21×100 mm). The following solvent system was used: solvent A, water containing 0.1 % TFA, solvent B, acetonitrile containing 0.1 % TFA. Gradient elution was applied at a flow rate of 15 mL/min.

UV-Vis-NIR Spectroscopy - UV-Vis-NIR spectra were recorded using a Varian Cary 5000 spectrophotometer, using 1 cm path quartz glass cuvettes.

Circular Dichroism: Circular dichroism spectra have been recorded with J-810 Jasco spectropolarimeter. Each spectrum was recorded at 1 nm resolution after 8 accumulations from 190 to 350 nm. In all CD measurements, the temperature of the samples is maintaining at 25°C.

Microwave heating: Microwave device used was Biotage® initiator and Biotage® Initiator Peptide Workstation.

Synthesis and characterization data

Synthesis of protected adamantane amino acid

Trimethyl aminoadamantane-1,3,5-tricarboxylate (6)

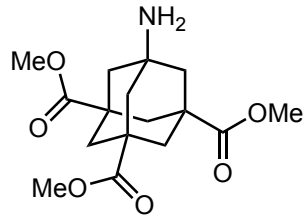

The synthesis of trimethyl aminoadamantane-1,3,5-tricarboxylate **6** from the commercially and cheap 1-bromoadamatane is described in the experimental section of Chapter II.

3-amino-5,7-bis(methoxycarbonyl)adamantane-1-carboxylic acid (7)

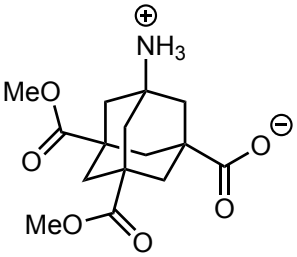

A potassium hydroxide (327 mg, 5.8 mmol) solution in water (50 mL) was added to a solution of trimethyl aminoadamantane-1,3,5-tricarboxylate **6** (1.20 g, 3.8 mmol) in methanol (50 mL) and the mixture was stirred at 60 °C for at least 3 h. LC-MS and TLC analysis allowed to follow the reaction. pH was adjusted to 7 using HCl 6N (1.0 mL) and the solvent was removed under vacuum. The crude product obtained was washed with hot acetonitrile (to remove the starting material **6**) and dried under vacuum to give the desired amino acid **7** as a white powder (560 mg, 1.9 mmol, 50 %). The bis-deprotected and fully-deprotected derivatives represent less than 5 % of the compound (as found by LC-MS), they will be totally removed after *N*-acylation by column chromatography. ^{1}H NMR (MeOD, 400 MHz) δ: 3.67 (*s*, 6H, 2xCH_3), 2.02-1.56 (*br s,*12H, 6xCH_2); ^{13}C NMR ($CDCl_3$, 75 MHz) δ: 175.61 (*C*=O), 173.72 (*C*=O), 52.21 (COO*C*H_3), 52.10 (*C*-N), 43.86 (*C*H_2), 37.94 (*C*H_2), 36.05 (C_q). MS (ESI) *m/z*: 312.32 $[M+H]^+$.

***3-N*-Fmoc-5,7-bis(methoxycarbonyl)adamantane-1-carboxylic acid (8)**

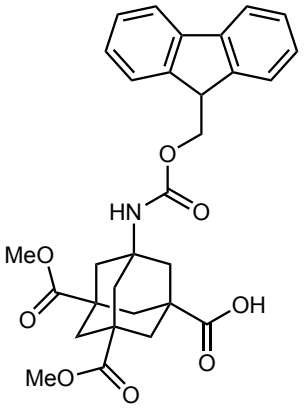

3-Amino-5,7-bis(methoxycarbonyl)adamantane-1-carboxylic acid **7** (42 mg, 0.136 mmol) and potassium carbonate (56.5 mg, 0.41 mmol) were solubilized in water (3 mL) and cooled at 0 °C. Dioxane (1 mL) was added (partial precipitation was observed). Fmoc-chloride (106 mg, 0.41 mmol) in dioxane (1.5 mL) was added dropwise with vigorous stirring. After 6 h at rt, the dioxane was removed under vacuum. The aqueous phase was acidified with HCl 6N to reach pH 2-3 and the compound was extracted using AcOEt (4×20 mL). The combined organic phases were drid on magnesium sulfate, filtered and concentrated to give **8** as a white powder (32 mg, 0.061 mmol, 44 %). ^{1}H NMR ($CDCl_3$, 300 MHz) δ: 7.76 (*d*, J = 9.8 Hz, 2H, Ar-*H*), 7.56 (*d*, J = 9.8 Hz, 2H, Ar-*H*), 7.39 (*t*, J = 9.8 Hz, 2H, Ar-*H*), 7.32 (*t*, J = 9.8 Hz, 2H, Ar-*H*), 4.72 (*s*, 1H, N*H*), 4.38 (*br*, 2H, CH_2), 4.19 (*t*, 1H, C*H*), 3.67 (*s*, 6H, 2xCH_3), 2.21-1.86 (*br s,*12H, 6xCH_2); MS (ESI) *m/z*: 556.20 $[M+Na]^+$.

***3-N*-Boc-5,7-bis(methoxycarbonyl)adamantane-1-carboxylic acid (9)**

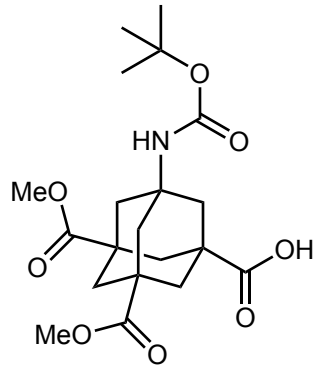

3-Amino-5,7-bis(methoxycarbonyl)adamantane-1-carboxylic acid **7** (60 mg, 0.19 mmol) was solubilized in MeOH (25 mL). NEt_3 (134 µL, 0.96 mmol) and Boc_2O (126 mg, 0.58 mmol) were added. Mixture was stirred at 50 °C. After 24 h, a second addition of Boc_2O (30 mg, 0.13 mmol) and NEt_3 (30 µL, 0.21 mmol) was done and the mixture was stirred for another 24 h at 50 °C. Then, methanol was removed under vacuum and acidic water was added. The compound was extracted with AcOEt (3×25 mL). The combined organic phases were dried on $MgSO_4$, filtered, and concentrated. The compound was purified by column chromatography on silica gel (eluant: AcOEt/cyclohexane (3/7)) to give **9** as a white powder (38 mg, 0.09 mmol, 49 %). ^{1}H NMR ($CDCl_3$, 300 MHz) δ: 3.69 (*s*, 6H, 2xCH_3), 2.12-1.95 (*br,*12H, 6xCH_2), 1.41 (*s*, 9H, 3xCH_3); ^{13}C NMR ($CDCl_3$, 75 MHz) δ: 178.21 (*C*=O) 176.57 (*C*=O), 154.12 (*C*=ONH), 77.82 (*C*-O), 51.24 (*C*-N), 42.19 (*C*H_2), 40.91 (*C*H_2), 38.39 (C_q), 27.10 (*C*H_3-C). FT-IR (neat, *v*/cm^{-1}) :3202, 2991,1722, 1698, 1511, 1390, 1312, 1251, 1102. MS (ESI) *m/z*: 434.18 $[M+Na]^+$.

Solid Phase Peptide Synthesis and Cleavage

Loading test protocol

Loading test was used to determine the resin loading. This technique is based on the absorbance of the fluorenyl group of the Fmoc-protecting group according to the Beer-Lambert law:

$$A = \varepsilon(\lambda) \cdot l \cdot C$$

With "*A*" is the Absorbance (no unit)

"ε" is the molar attenuation coefficient at λ nm

"*C*" is the molar concentration of those species

"*l*" is the pathlength

or $C = n / V$ and $n = L$ (loading) × m (mass of the resin) thus:

$$\frac{A = \varepsilon(\lambda) \cdot l. \cdot L \cdot m}{V}$$

If we selected 1 cm as pathlength, 3 mL as volume used and ε = 5253 $L \cdot mol^{-1} \cdot cm^{-1}$ for λ_{max} = 292 nm we can simplify the loading determination by:

$$L = \frac{A}{m \cdot 1.75}$$

With "*L*" is the loading of the resin in $mmol \cdot g^{-1}$

"*A*" is the Absorbance measured at λ= 292 nm.

"*m*" is the mass of the resin (dried) in mg.

Preparation of the Resin+linker (RL)

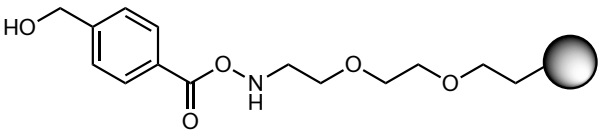

Tentagel-NH_2 resin (L=0.29 mmol/g, 345 mg, 0.1 mmol) was put into a syringe equipped with a teflon filter and connected to vacuum. After washing with DCM (3 times) and DMF (3 times), a solution of 4-hydroxymethylbenzoic (30.5 mg, 0.2 mmol) activated with HBTU (68.3 mg, 0.18 mmol) and HOBt (27 mg, 0.2 mmol) in the presence of DIPEA (63 µL, 0.36 mmol) in DMF (2.5 mL) was added. The mixture was stirred at room temperature overnight. After removing the solution, the resin was washed (DCM ×3, DMF ×3) to give the desired resin+linker. The reaction was followed by Kaiser test. To avoid further side reactions, the remaining free amine were capped with anhydride acetic (25 %) in DMF during 15 min.

Fmoc-Glycine-RL (first amino acid incorporation)

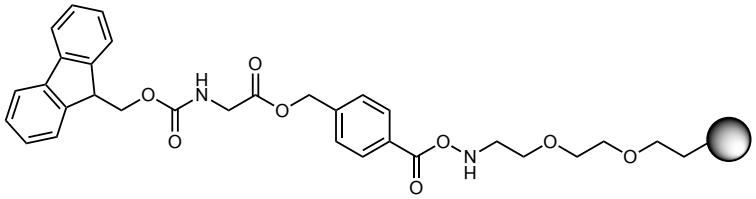

The resin-linker (RL) prepared before was swollen with DMF and DCM several times. A solution containing Fmoc-Glycine-OH (297 mg, 1.0 mmol) activated with DIC (78 μL, 0.5 mmol) and a catalytic amount of DMAP (1.22 mg, 0.01 mmol) in DMF / DCM (1/9) (5 mL) was added. The mixture was stirred at rt for 2 h. After removing the solution, the same protocol was repeated a second time. After 2 h, the resin was dried under vacuum. Kaiser test and loading test confirmed the progress of the reaction (reaching a yield up to 83 %).

Peptides incorporating adamantane amino acid starting from Fmoc-Glycine-RL

H-L-Tyr-Gly-Ada(Me)$_2$-Gly-Ada(Me)$_2$-Gly-Ada(Me)$_2$-Gly-OH and
H-D-Tyr-Gly-Ada(Me)$_2$-Gly-Ada(Me)$_2$-Gly-Ada(Me)$_2$-Gly-OH

Step	Residue added	Coupling agents	Procedure
1	Boc-Ada(Me)$_2$-OH (1.5 eq)	HATU (3.0 eq), HOAt (3.0 eq), DIPEA (5.4 eq) in DMF	- Fmoc deprotection (20 % piperidine in DMF) – 30 min - Washing (DCM and DMF 3x) - Coupling reaction (2 h, rt) - Washing (DCM and DMF
2	Fmoc-Gly-OH (4.0 eq)	DIC (4.0 eq), Oxyma (4.0 eq) in DMF	- Boc deprotection (TFA 50 % in DCM - 30 min) - Washing (DCM and DMF 3x) - Coupling reaction (MW heating 65 °C, 10 min) - Washing (DCM and DMF 3x) - Repeat reaction second time
3	Repeat step **1** and **2**		
4	Repeat step **1** and **2**		
5	Fmoc-L-Tyr-OH or Fmoc -D- Tyr-OH (4.0 eq)	HBTU (3.9 eq), HOBt (4.0 eq)	- Fmoc deprotection (20% piperidine in DMF) – 30 min - Washing (DCM and DMF 3x) - Coupling reaction (MW heating 65 °C, 10 min) - Washing (DCM and DMF 3x) - Repeat reaction second time
6	Cleavage		- NaOMe 0.5 M in MeOH (30 min, rt) - Neutralization with acetic acid (8.75 M, 115 μL)
7	Purification		RP-HPLC

Purified peptides were characterized by mass spectrometry and lyophilized to be store as white powder. MS (QTF) *m/z*: 645.34 $[M+2H]^{2+}$.

H-L-Tyr-Gly-Ada-Gly-Ada-Gly-Ada-Gly-OH and
H-D-Tyr-Gly-Ada-Gly-Ada-Gly-Ada-Gly-OH

L and D-tyrosine alternated and protected peptides were obtained by basic hydrolysis of the corresponding fully protected peptides (Ada-esterified and C-terminus esterified). The fully protected peptides were mixed with NaOH (0.5 M, 5.4 mL) and heated at 75 °C by MW during 50 min. Acetic acid (155 μL) was added to neutralize the solution. The crude compounds were purified by RP-HPLC to isolated the L or D-tyrosine alternated peptides subsequently lyophilized to obtain them as white powder. MS (QTF) *m/z*: 1205.45 $[M+H]^+$.

H-Tyr-Gly-Ada(Me)$_2$-Ada(Me)$_2$-Ada(Me)$_2$-Ada(Me)$_2$-Ada(Me)$_2$-Gly-OH

The fully protected homopeptide was synthesized by SPPS starting from Fmoc-Glycine-HMBA-TentaGel (described above).

Step	Residue added	Coupling agents	Procedure
1	Boc-Ada(Me)$_2$-OH (1.5 eq)	HATU (3.0 eq), HOAt (3.0 eq), DIPEA (5.4 eq) in DMF	- Fmoc deprotection (20 % piperidine in DMF) – 30 min - Washing (DCM and DMF 3x) - Coupling reaction (2 h, rt) - Washing (DCM and DMF 3x)
2	Repeat step **1** four times.		
3	Fmoc-Gly-OH 4. eq)	DIC (4.0 eq), Oxyma (4.0 eq) in DMF	- Boc deprotection (TFA 50 % in DCM - 30 min) - Washing (DCM and DMF 3x) - Coupling reaction (MW heating 65 °C, 10 min) - Washing (DCM and DMF 3x) - Repeat reaction second time
4	Fmoc-L-Tyr-OH (4.0 eq)	HBTU (3.9 eq), HOBt (4.0 eq)	- Fmoc deprotection (20 % piperidine in DMF) – 30 min - Washing (DCM and DMF 3x) - Coupling reaction (MW heating 65 °C, 10 min) - Washing (DCM and DMF 3x) - Repeat reaction second time
5	Cleavage		- NaOMe 0.5 M in MeOH (30 min, rt) - Neutralization with acetic acid (8.75 M, 115 μL)
6	Purification		- RP-HPLC

The final peptide was lyophilized and stored as a white powder. MS (QTF) *m/z*: 882.38 $[M+2H]^{2+}$.

UV titration for circular dichroism measurements:

UV titration was used to determine precisely the concentration of each peptide analyzed by CD. It allows to calculate the specific ellipticity of the compound (see Chapter IV) which is independent of the concentration and allows a more rigorous comparison of the results.

$$A_{280} = \varepsilon_{280} \cdot l \cdot C$$

$$A_{280} = \varepsilon_{280} \cdot l \cdot C_m / M$$

$$C_m = A_{280} \cdot M / \varepsilon_{280} \cdot l$$

With:

"A_{280}" is the absorption at 280 nm

"ε_{280}" is the molar attenuation coefficient at 280 nm (1280 for tyrosine) in $L \cdot mol^{-1} \cdot cm^{-1}$

"l" is the path length of the cuvette (cm)

"C" is the molar concentration in $mol \cdot L^{-1}$

"C_m" is the mass concentration in $g \cdot L^{-1}$

and "M" the molecular mass of the molecule in $g \cdot mol^{-1}$

In methanol:

	L-Tyr alternated protected	D-Tyr alternated protected	D-Tyr alternated unprotected	Homopeptide protected
Absorbance at 280 nm	0.542	0.501	0.492	0.551
Molecular weight (g/mol)	1289.3	1289.3	1205.1	1761.89
Concentration (mg/mL)	0.55	0.50	0.46	0.75

In trifluoroethanol:

	L-Tyr alternated protectide	D-Tyr alternated protected	Homopeptide protected
Absorbance at 280 nm	0.535	0.534	0.571
Molecular weight (g/mol)	1289.3	1289.3	1761.89
Concentration (mg/mL)	0.54	0.54	0.78

Circular dichroism analysis:

Using the UV titration, we can determine the specific ellipticity of each petitde in $deg \cdot cm^2 \cdot decagram^{-1}$:

$$\{\Psi\} = \theta / (100*C'*l)$$

with:

"$\{\Psi\}$" is the specific ellipiticity in $deg \cdot cm^2 \cdot decagram^{-1}$

"θ" is the ellipiticity measured in mdeg

"C'" is the concentration in $g \cdot mL^{-1}$

and "l" the path length of the cell (cm)

Chapter V: Conclusion and Perspectives

The work of my thesis was based on the utilization of adamantane in diverse structures such as dendrons or peptides, aimed for biomedical applications. The bridgehead positions of adamantane selectively react to give a wide range of multifunctional derivatives. These tuned building blocks could be precursors of more complex structures. Moreover, the rigidity and the well-defined 3D conformation of adamantane provide to these structures pertinent properties, especially in the biological field.

In the first part of this work, I designed, synthesized and characterized first and second generation adamantane-based dendrons with the particularity that no linker has been used between the adamantane moieties. Starting from the commercial 1-bromoadamantane, I improved the five steps synthesis to obtained the (3+1) adamantane building block. Then, I developed optimal conditions to synthesize 2nd generation adamantane-based dendrons with high yield. However, the same conditions did not work for further generation dendrons thus, the 3rd generation has not been isolated yet. I would like to underline the interesting results obtained to improve the amine nucleophilicity using microwave. Thus, exploring microwave heating is certainly the best way to lead to the 3rd generation adamantane dendrons. Moreover, transmission electron microscopy was used to study the self-assembly of different functionalized adamantane dendrons confirming the importance of the group at the focal point in the self-assembly process leading to different particle morphology. Indeed, spherical particles are usually observed, but certain types of functional groups like alkyne can induce ribbons. Using scanning electronic microscopy on one derivative, I observed that the support of deposition plays also an important role in the self-assembly process, additionally to the concentration, solvent and temperature. More analysis must be done, in particular using dynamic light scattering, which could give precise information on the particle size in solution.

In a second part of my work, I focused on TLR4 receptor, which is involved in inflammatory response after bacterial infection. I designed 1st generation dendrons that may interfere with TLR4 and thus avoid the biosynthesis of pro-inflammatory molecules such as cytokines like interferon. I designed and attempted to prepare two dendrons with mannoses heads on the periphery anchored to adamantane *via* polyethyleneglycol chains. This design allows to improve intrinsic characteristic (solubility, flexibility) which play a main role in the multivalency effect. The two dendrons differ in their focal point. The first one is inspired from the literature and it is functionalized with a lipid chain, while the second one is functionalized with a fluorophore attached via click chemistry. The idea was to use a hydrophobic probe to

obtain an active molecule and the possibility to do cell imaging. Unfortunately, the synthesis of the final products has not been achieved due to different synthesis challenges that I encountered during the different steps.

In a last part, in collaboration with the University of Copenhagen and the team of Prof. Knud J. Jensen, I worked on the incorporation of adamantane into a peptide backbone. I developed the synthesis of an adamantane γ-amino acid protected with two methyl esters. This amino acid has been protected with Boc for solid phase peptide synthesis. During my visiting period in the group of Prof. Jensen, I developed a robust protocol to incorporate adamantane moiety in a growing peptide while using the minimum amount of compound. Mixing Boc and Fmoc strategy, I developed selective deprotection of Boc group and a selective deprotection of Fmoc without affecting the resin, the linker or any protecting group on the amino acid side chains. I also developed cleavage conditions combined with an appropriate work-up, which allow to obtain fully protected or fully deprotected peptides. Finally, using circular dichroism I analyzed the secondary structure of the peptides and correlated the results with those obtained by computer simulation. Adamantane is able to induce a specific folding, and the peptides likely adopt a helical conformation. Using L- or D-tyrosine as C-terminal amino acid residue the peptides turn right and left, respectively. These results should help to design novel types of foldamers, which can be used, for example, in biological applications. In perspective, it will be interesting to synthesize more compound to perform more analysis (NMR, X-rays diffractions) to fully elucidate these structures.

To finish, in collaboration with Dr. Ferrandon (CNRS) and his team, I designed and synthesized a fipronil labelled with fluorescein to confirm their hypothesis that fipronil induces a novel host defense in *Drosophilia melanogaster* model.

Different strategies have been investigated for the synthesis of the desired derivative and finally the solution was provided by click chemistry. Finally, this conjugate allowed to confirm by confocal microscopy that fipronil induce a novel host defense in *Drosophilia melanogaster enterocytes*.

Annexe:
Design and synthesis of fipronil functionalized with fluorescein for cellular imaging

I. Introduction

Fipronil or (5-amino-1-[2,6-dichloro-4-(trifluoromethyl)-phenyl]-4-(trifluoromethylsufinyl)-1-*H*-pyrazole-3carbonitrile) is a phenyl pyrazole insecticide used to protect crops with good selectivity between insects and mammals.[1] It became recently famous due to the egg scandal (millions of eggs have been contaminated with fipronil despite being banned by the European Union for use on animals destined for human consumption), its toxicity effect has been investigated (i.e. against honeybees). In 2011, Vidau *et al.* showed that sublethal doses of fipronil highly increased mortality of honeybees previously infected by the microsporidian parasite *N.ceranae*.[2] However, uninfected honeybees exposed to fipronil were significantly less affected (mortality or behavior), meaning that uninfected honeybees would be able to respond to insecticides by enhancing detoxification process whereas infected honeybees cannot. In these studies, the activities of 7-ethoxycoumarine-O-deethylase (ECOD) and glutathione-S-transferase (GST), proteins implicated in insect detoxification, have been assessed. While ECOD activity remained unchanged, GST activity was enhanced in midgut and fat body, in contrast with the enhancement of infected honeybee susceptibility to fipronil. This means that GST would not be involved in detoxification process of fipronil. In 2013, the metabolic fate and the elimination of fipronil in rats was investigated using radiolabeled fipronil.[3] This study revealed that fipronil is slowly metabolized and excreted in these animals. Indeed, excepted in feces, no traces of parent compound were found in the analyzed samples. However, the highest level of radioactivity was found in adipose tissue and adrenals.

The group of Dr. Ferrandon at the CNRS in Strasbourg (IBMC, UPR 9022) is working on the effects of insecticides on *Drosophilia*. They recently observed that exposure to fipronil triggers a novel host defense in *Drosophilia melanogaster enterocytes*. Their hypothesis is called “lipid purge”. Indeed, they observed the formation of lipid vesicles, which are expulsed after exposure to fipronil. Thus, it looks like fipronil is able to induce this lipidic purge. To study this novel host defense in *Drosophilia*, and more precisely to understand the mechanism of the lipidic purge, our Lab was involved in the design and synthesis of a fipronil labelled with fluorescein. Therefore, I have contributed to the synthesis and characterization of the fluorescent molecule.

II. Results and discussion

II.1 Synthesis of fipronil fluoresceinisothiocyanate (Fipro-FITC)

In order to be used as probe for cellular imaging, the first idea was to directly functionalize fipronil with fluorescein isothiocyanate through thiourea bond (Figure 1).

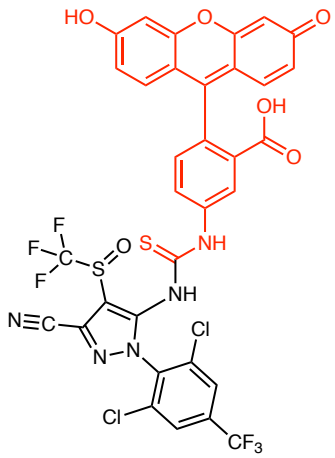

Figure 1: *Fipronil functionalized with fluorescein through a thiourea bond.*

The preparation of this compound was already reported in the literature[4]. The synthesis (Scheme 1) was initially performed by our engineer Jean-Baptiste Madinier. Fluorescein isothiocyanate (FITC) **2** reacts with fipronil **1** in basic condition (triethylamine) at 40 °C for one night to give the expected fluorescent conjugate **3** with 49 % yield.

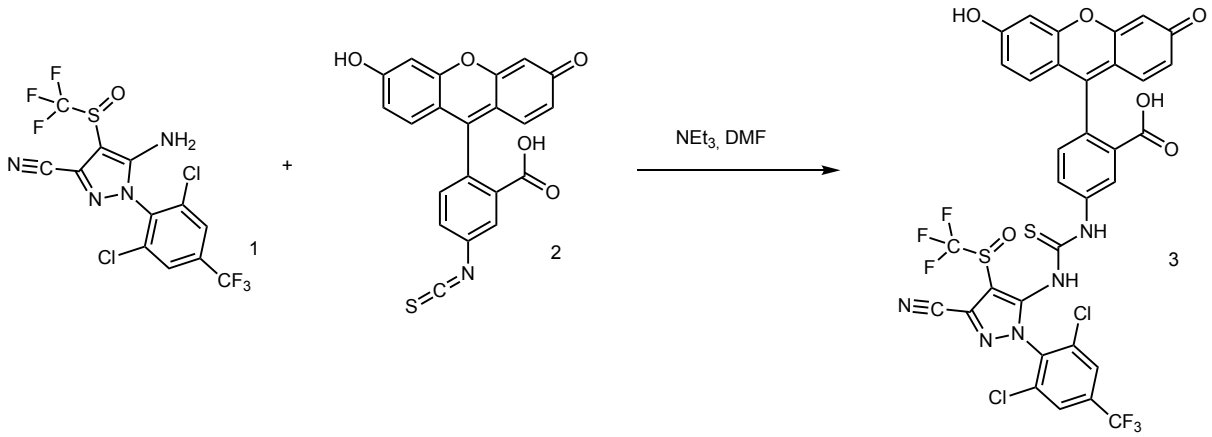

Scheme 1*: Synthesis of the fipronil functionalized with fluorescein through a thiourea bond.*

The desired compound **3** was characterized by ^{1}H and ^{13}C NMR in different deuterated solvent and by LC-MS. First, NMR in DMSO-d_6 displayed unexpected signals in the aromatic area. This may be due to cis-trans equilibrium around the thiourea bond and to the possible formation

of the lactone on the fluorescein moiety. To avoid these equilibria, I performed the NMR analysis at increasing the temperature (20, 50 and 70 °C) (Figure 2). These tests confirmed the exchange, but I still observed undefined peaks. However, when the NMR is performed in deuterated methanol (Figure 3), the signal is better defined and the integration of the peaks perfectly corresponds to the protons of the molecule **3**, meaning that solvent certainly plays a role in the conformation of the molecule.

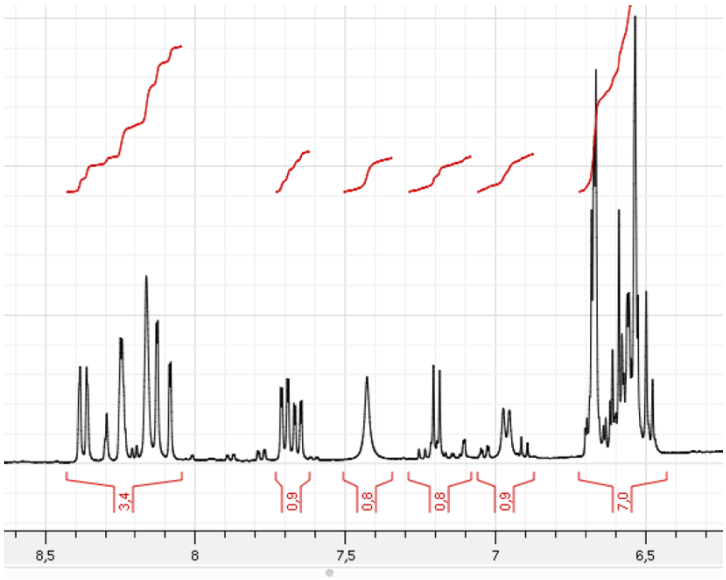

***Figure 2**: ^{1}H NMR of compound **3** in DMSO-d_6 at 50 °C.*

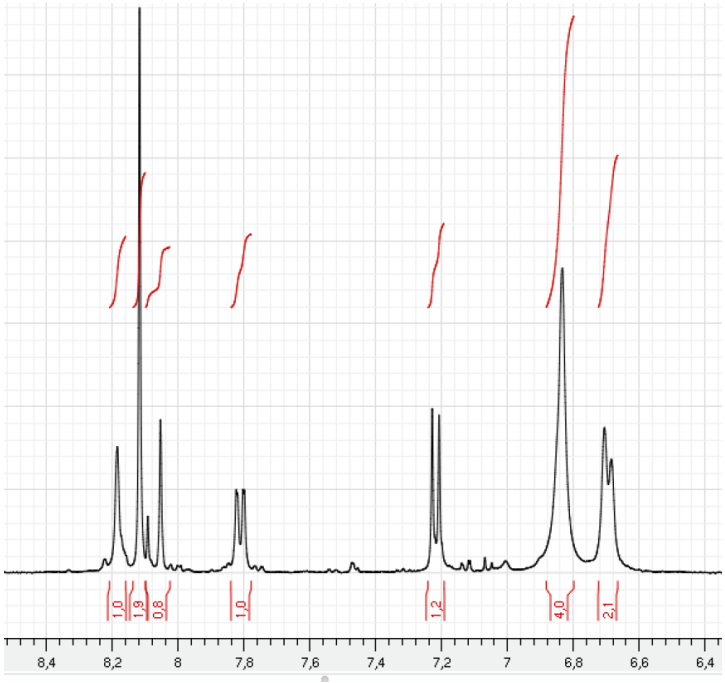

***Figure 3**: ^{1}H NMR of compound **3** in MeOD at 20 °C.*

Moreover LC-MS analysis confirmed the synthesis of the desired compound (*m/z* = 827.8 $[M+H]^+$). Unfortunately, to be administered to *Drosophila*, the compound should be stable at 29 °C for many hours. Surprisingly, we observe after one night at room temperature that the compound in solution is unstable. It is probably photo- and temperature sensitive. I compared then the stability of the compound in solution at 4 °C and at room temperature. The compound is not at all stable in solution at room temperature and a bit more stable at 4 °C (Figure 4).

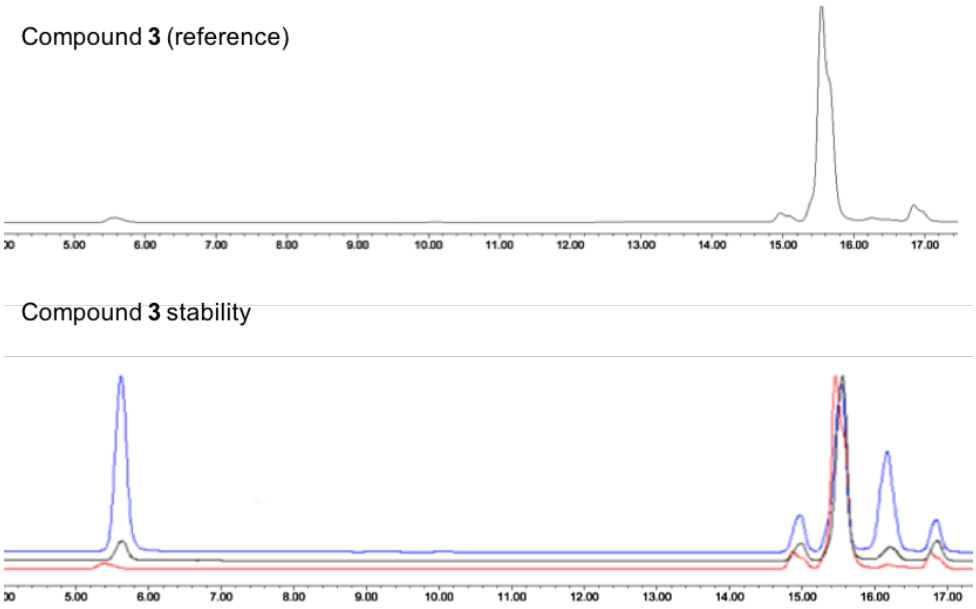

***Figure 4**: HPLC chromatograms showing the stability of the compound **3**: in red the compound stored in the fridge, in black the compound in solution at 4 °C (starts to degrade) and in blue the compound at rt in solution is highly degraded.*

Even when stored as a powder in the fridge compound **3** displays a certain level of degradation. The degraded product has been isolated by HPLC and analyzed by LC-MS. The main product at 5.79 min corresponds to a mass of *m/z* = 348.2 identified as aminofluorescein confirming the low stability of the thiourea bond (Figure 5).

We can clearly conclude that the product reported in reference does not correspond to the desired product and that the authors did not carefully studied the stability in different conditions. One can wonder what they really tested in their biological system.

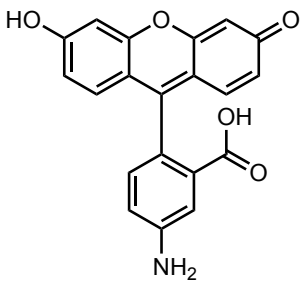

***Figure 5**: Amino-fluorescein which is formed after compound **3** degradation.*

II.2 Synthesis of fipronil-fluorescein *via* formation of a peptide bond

Due to the low stability of the thiourea bond, we then designed a new fipronil derivative. We decided to insert a peptide bond between the amino group in the fipronil moiety and the carboxylic function on fluorescein, which should be more stable at different temperatures. We made several attempts to obtain the compound **5** (Figure 6).

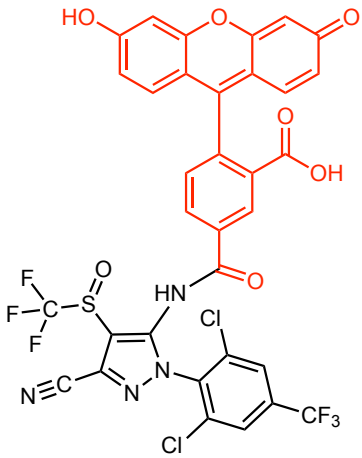

***Figure 6**: Fipronil functionalized with fluorescein through a peptide bond.*

We performed a synthesis following a pre-activation of carboxyfluorescein **4** with DIC and NHS to obtain the actived ester. Then, this ester was reacted with the amino group of fipronil in the presence of trimethylamine (TEA) to form the desired compound **5** (Scheme 2).

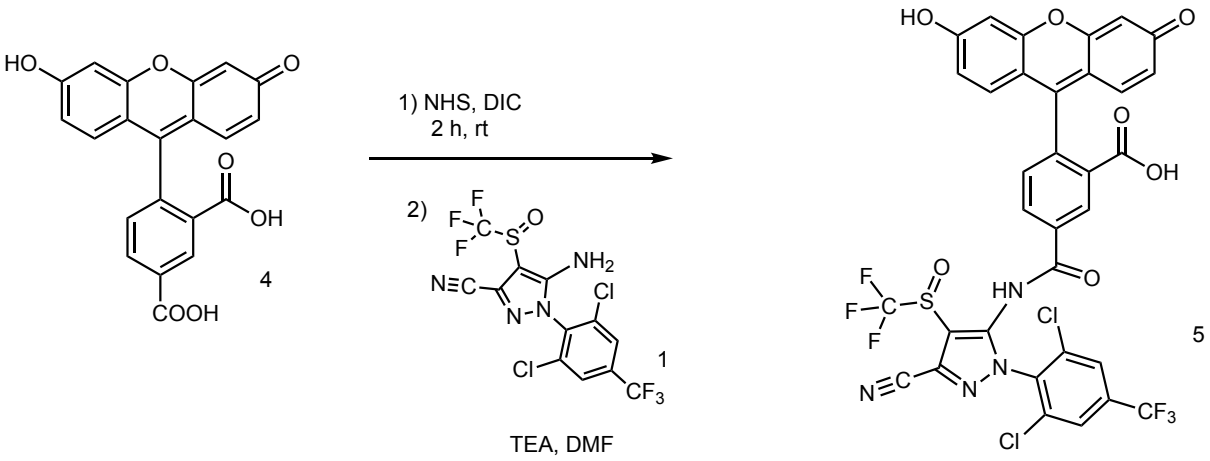

***Scheme 2**: Synthesis of the fipronil functionalized with fluorescein through peptide bond.*

The reaction was initially tested using 4(5)-carboxyfluorescein and followed by HPLC (Figure 7).

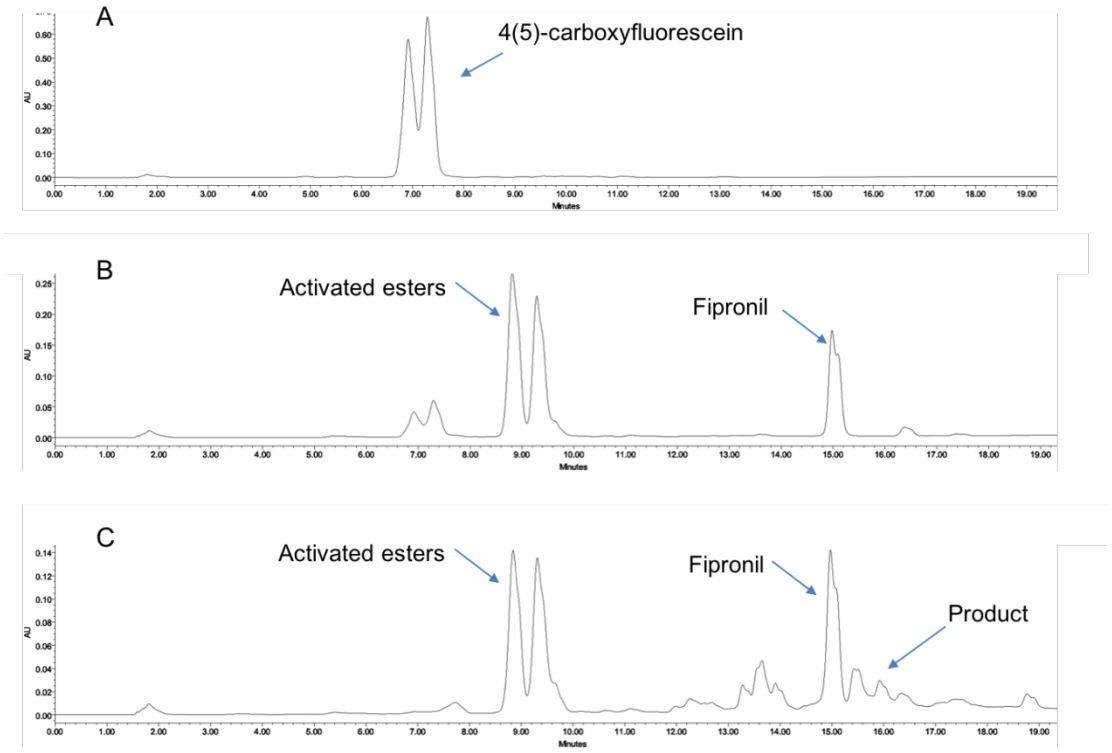

***Figure 7**: HPLC chromatograms at 254 nm of 4(5)-carboxyfluorescein (A), the reaction mixture after addition of fipronil t=0 (B), and the reaction mixture after 3 h at room temperature (C).*

HPLC analysis confirmed the activation of the 4(5)-carboxyfluorescein. Indeed, a shift of 2 min (from 6.9 and 7.1 to 8.9 and 9.1 min, respectively) is observed confirming the formation of the activated compound. However, after addition of fipronil and triethylamine, the reaction does not occur. Indeed, few peaks appeared at 13.5 and 16.0 min but with very low intensity. After 3 h, LC-MS analysis showed a peak at *m/z* = 794.8 corresponding to the desired product. However, even after one night and heating (up to 40 °C) the reaction did not proceed further and the main peaks observed were still the activated fluorescein at 8.9 and 9.1 min and the starting fipronil at 15.0 min.

Additionally to the low yield, we were not able to isolate a reasonable amount of compound **5**. The difficulties met can be attributed to two factors: 1) the low reactivity of the amino group of fipronil. Indeed, the electron lone pair of the nitrogen is not highly nucleophilc due to the conjugation on pyrazole ring. 2) the sterical hindrance. All the aromatic groups present considerably decreased the degree of freedom of the intermediates formed. As a consequence, we decided to try another approach to solve these problems.

II. 3 Synthesis of fipronil-fluorescein *via* click chemistry

In view of the difficulties to synthesize the desired compound, we decided to use third strategy using click chemistry. The strategy is based on the synthesis of the precursors functionalized with azide and alkyne groups, which can react together *via* Huisgen cycloaddition to form the fluorescent fipronil (Figure 8).

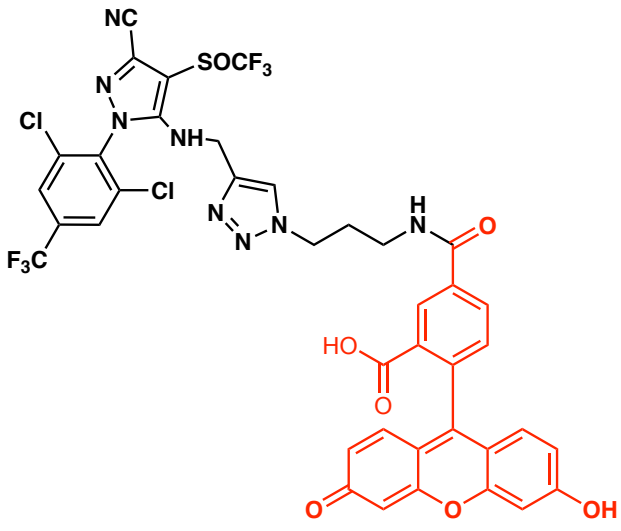

***Figure 8**: Fipronil functionalized with fluorescein through a triazole ring.*

Fipronil functionalization

The first step was to functionalize the fipronil with an alkyne group (Scheme 3). The synthesis is done by mixing fipronil (1 eq) with propargyl bromide (1.1 eq) in the presence of potassium hydroxide (2.2 eq) following a procedure described in the literature.[5]

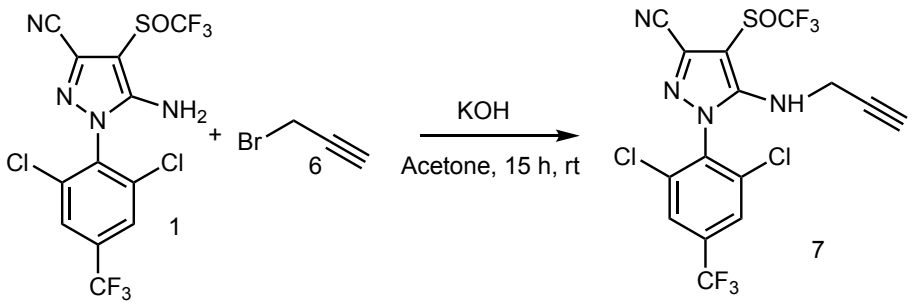

***Scheme 3**: Synthesis of propargyl-fipronil 7.*

However, following this procedure I have isolated the di-alkylated derivative **8**, which was confirmed by NMR and LC-MS (*m/z* = 512.97 $[M+H]^+$).

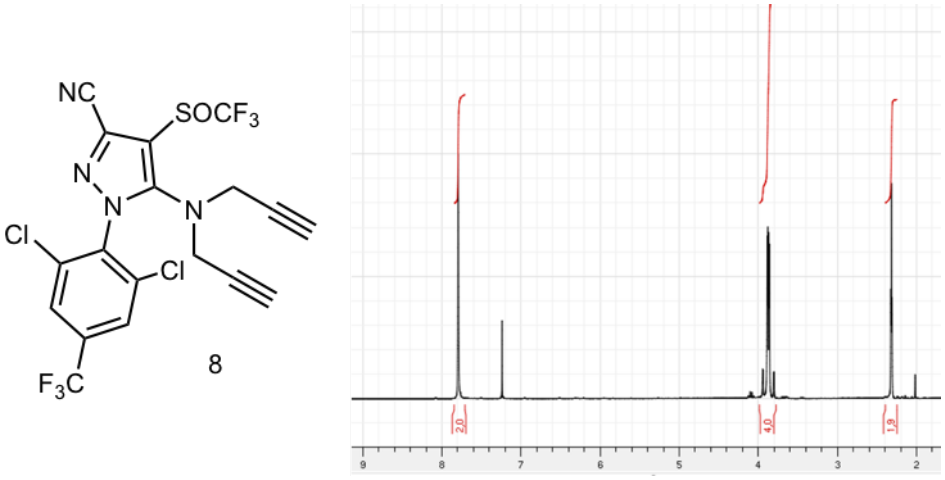

***Figure 9**: ^{1}H NMR of compound **8** in MeOD at 20 °C.*

To solve this problem, I improved the published protocol. I increased the dilution and decreased the amount of propargyl bromide to 0.9 eq and the temperature to 0 °C during the addition of this last one. Moreover, propargyl bromide is diluted in acetone and added dropwise along 15 min. The reaction is followed by TLC and HPLC. After one night at room temperature, the

compound is extracted with ethyl acetate, washed with saturated aqueous solution, filtered and concentrated under vacuum. The residue obtained was purified by column chromatography leading to the desired mono-alkylated compound **7** as a white powder with 50 % yield.

Fluorescein functionalization

For the click approach, the fluorescein must be functionalized with an azide group. We selected azidopropylamine **10** to react with fluorescein **9** *via* peptide bond to give the desired functionalized fluorescein-azide **11** (Scheme 4).

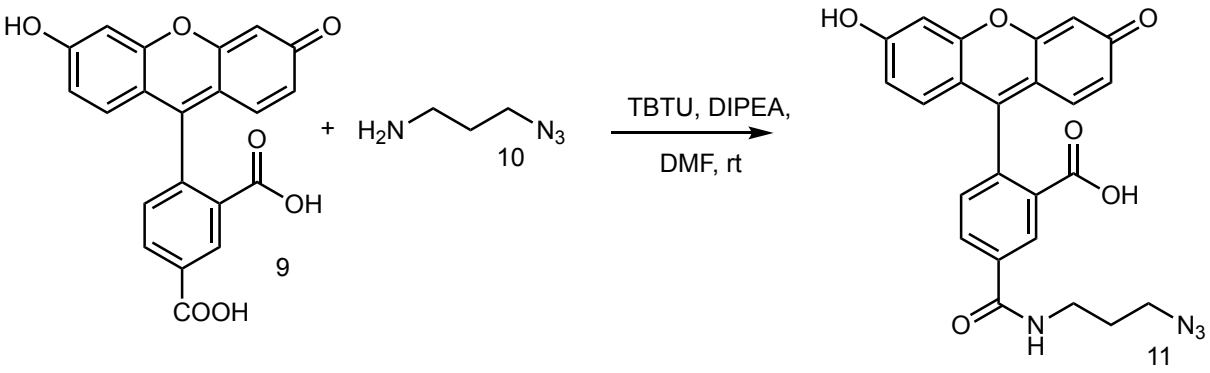

***Scheme 4**: Synthesis of fluorescein azide **11**.*

The synthesis of this compound is also described in the literature.[6] The reaction was followed by TLC and HPLC, and after 24 h the reaction is stopped. I discovered that the work-up reported in the literature did not work (addition of 10 % aqueous NaOH followed by diethyl ether extraction). Thus, I modified the work-up. I acidified the mixture to reach pH = 2 using HCl 6 N and extracted the compound with ethyl acetate. The organic layer was washed, dried and concentrated under vacuum. Unfortunately, TLC analysis displayed a strong affinity of the compound with silica, thus, I decided to purify it by preparative HPLC. The difficulty to dilute the compound in a water miscible solvent forced me to add more DMF resulting an important loss of the compound in the injection peak. Thus, I isolated the desired compound with a 20 % yield.

Click chemistry of fipronil-alkyne with Fluorescein-azide

The last step to obtained the desired fipronil-fluorescein conjugate consists on the Huisgen cycloaddition between the two precursors previously synthesized (Scheme 5).

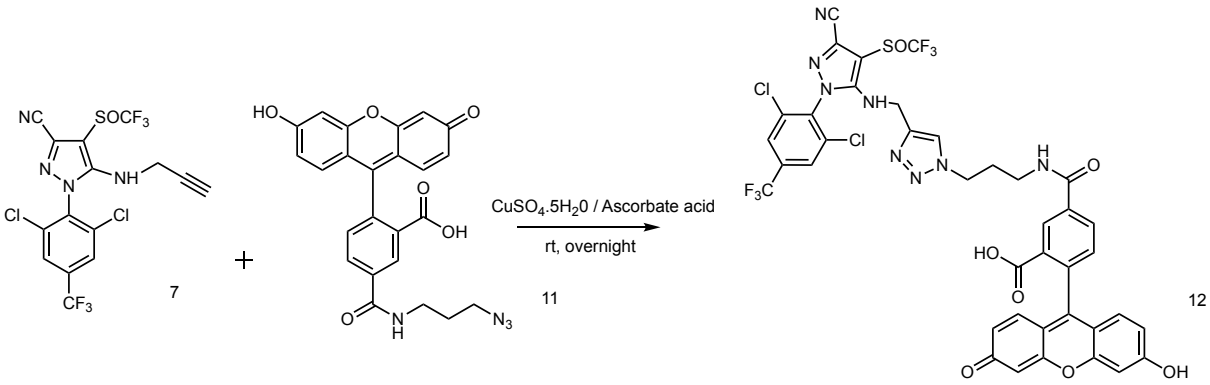

***Scheme 5**: Synthesis of fipronil-fluorescein conjugate.*

The reaction was performed using 1 eq of each compound in the presence of a catalytic amount of copper (0.4 eq), previously activated by ascorbic acid (0.8 eq) in 1:1 THF/water. After one night at room temperature, LC-MS analysis confirmed the formation of the desired conjugate. The crude was purified by silica gel column to give compound **12** with 85 % yield.

II. 4 Biological tests

The group of Dr. Ferrandon studied the effect of fipronil on *Drosophilia melanogaster enterocytes.* Using confocal images of *Drosophilia* intestine after exposure, they confirmed that fipronil induces the lipidic purge (Figure 10). Indeed, after 3 h exposure the lipid droplets started to aggregate, and at 6 h the endothelial cells start to eject the lipid droplets. Finally, after 8 h, all the lipid droplets are ejected in the intestine lumen. The lipidic purge occurs.

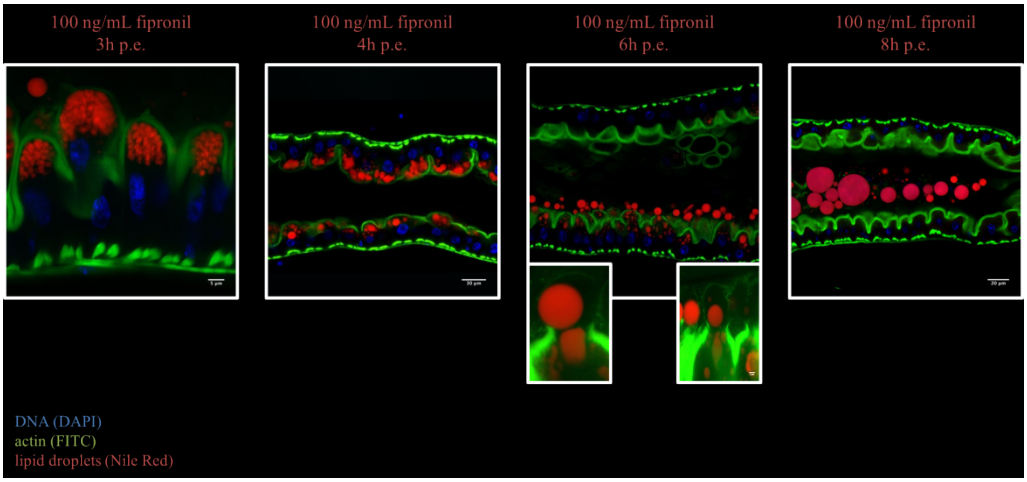

***Figure 10**: Drosophilia intestine after fipronil exposure at 29 °C, after 3 h the lipids start to agglomerate to form droplets (first panel from left). At 6 h endothelial cells start to eject the lipid droplets (third panel from left) until 8 h when all the lipid droplets have been ejected in the intestine lumen (fourth panel from left).*

In order to determine the localization of the fipronil, the same experiment was performed with the fipronil-fluorescein conjugate. In this case, they observed that the fluorescent molecule is co-localized with the lipid droplet meaning that the conjugate is inside the lipid droplets. This result confirmed the idea that lipid purge is a type of primitive protective immune system in *Drosophilia melanogaster*.

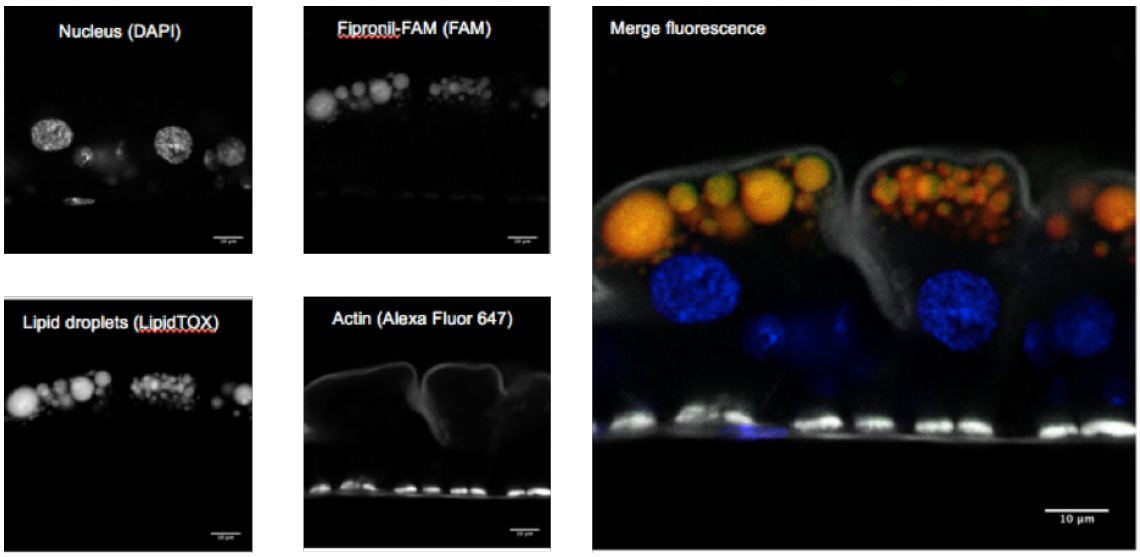

***Figure 11**: Drosophilia intestine 5 h after exposure at 29 °C to fipronil-fluorecein. The merge fluorescence panel displays co-localization of the fipronil-fluorescein conjugate with the lipid droplets confirming that the conjugate is located into these vesicles.*

III. Conclusion

We designed, synthesized and characterized a fipronil labelled with fluorescein *via* click chemistry. This conjugate was administrated to *Drosophilia* and confocal microscopy has been used to follow the conjugate allowing a precise localization of the pesticide in *Drosophilia* intestine. These experiments confirmed that exposure to fipronil triggers a novel host defense in *Drosophilia melanogaster enterocytes*: the lipidic purge.

IV. References

(1) Hainzl, D.; Casida, J. E. Fipronil Insecticide: Novel Photochemical Desulfinylation with Retention of Neurotoxicity. *Proc. Natl. Acad. Sci. U. S. A.* **1996**, *93* (23), 12764–12767.

(2) Vidau, C.; Diogon, M.; Aufauvre, J.; Fontbonne, R.; Viguès, B.; Brunet, J.-L.; Texier, C.; Biron, D. G.; Blot, N.; El Alaoui, H.; Belzunces, L. P.; Delbac, F. Exposure to Sublethal Doses of Fipronil and Thiacloprid Highly Increases Mortality of Honeybees Previously Infected by Nosema Ceranae. *PloS One* **2011**, *6* (6), e21550.

(3) Cravedi, J. P.; Delous, G.; Zalko, D.; Viguié, C.; Debrauwer, L. Disposition of Fipronil in Rats. *Chemosphere* **2013**, *93* (10), 2276–2283.

(4) Shanshan, Y.; Bo, Z.; Yuanyuan, Z.; Tianrui, R. Fluorescent labeling of fish GABA receptor and Ro7-1986/1 and Fipronil interaction. *Chem. J. Chin. Univ.* **2015**, *36* (3), 456–462.

(5) Yang, W.; Wu, H.-X.; Xu, H.-H.; Hu, A.-L.; Lu, M.-L. Synthesis of Glucose–Fipronil Conjugate and Its Phloem Mobility. *J. Agric. Food Chem.* **2011**, *59* (23), 12534–12542.

(6) Onizuka, K.; Shibata, A.; Taniguchi, Y.; Sasaki, S. Pin-Point Chemical Modification of RNA with Diverse Molecules through the Functionality Transfer Reaction and the Copper-Catalyzed Azide–alkyne Cycloaddition Reaction. *Chem. Commun.* **2011**, *47* (17), 5004–5006.

Experimental section

Fipronil-fluoresceinisothiocyanate (Fipro-FITC)

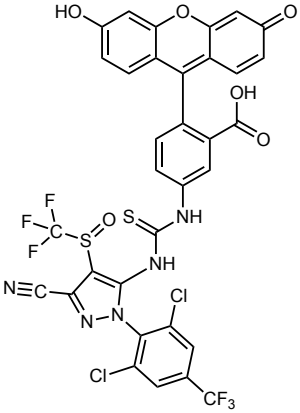

Fluorescein isothiocyanate (77.8 mg, 0.20 mmol), fipronil (174.8 mg, 0.40 mmol) and triethylamine (100 µL, 0.72 mmol) were dissolved in anhydrous DMF (3 mL) and stirred overnight at 40 °C. The crude product was purified by preparative HPLC to give compound **3** as an orange powder. ^{1}H NMR (MeOD, 400 MHz) δ: 8.18 (*s*, 1H, Ar-*H*), 8.12 (*s*, 2H, Ar-*H*), 8.05 (*s*, 1H, *Ar*-H), 7.81(*d*, J = 8.5, 1H, Ar-*H*), 7.22 (*d*, J = 8.5 Hz, 1H, Ar-*H*), 7.32 (*br s*, 4H, Ar-*H*), 6.69 (*br d*, 2H, Ar-*H*). ESI mass spectrometry (*m/z* = 827.8 $[M+H]^+$).

Fipronil-fluorescein

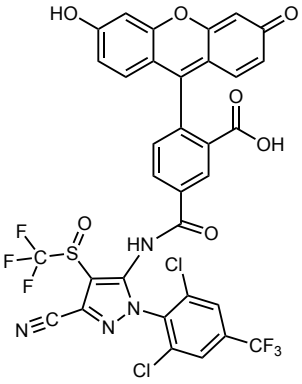

5(6)-Carboxyfluorescein (8.6 mg, 0.023 mmol) was dissolved in anhydrous DMF (2 mL) and cooled down to 0 °C. N-Hydroxysuccinimide (2.9 mg, 0.025 mmol) and DIC (3.95 µL, 0.025 mmol) were added and the solution was stirred at rt for 2 h. A solution of fipronil (10 mg, 0.023 mmol) in anhydrous DMF (1 mL) and triethylamine (3.20 µL, 0.023 mmol) was added. The reaction was stirred in the dark at room temperature for one night. Due to the low yield, only a little amount of compound **5** was isolated by preparative HPLC and characterized by mass spectrometry. ESI: (*m/z* = 794.8 $[M+H]^+$).

Propargyl-fipronil

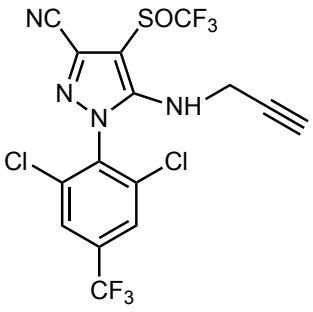

Fipronil (55 mg, 0.125 mmol) and potassium hydroxide (16 mg, 0.225 mmol) were solubilized in dry acetone (5 mL) and cooled down to 0 °C. A solution of propargyl bromide (11.2 µL, 0.125 mmol) in acetone (3 mL) was added dropwise (during 15 min). The mixture was stirred overnight at rt and the acetone was removed under vacuum. The crude product was solubilized in ethyl acetate (30 mL) and washed with saturated aqueous solution ($NaHCO_3$ and NH_4Cl. The organic layer was dried, filtered and concentrated under vacuum. Column chromatography (eluant: ethyl acetate/cyclohexane, 1:4) was performed to give compound **7** (29.7 mg, 0.063 mmol, 50 %). Compound **7** was characterized by mass spectrometry (*m/z* = 474.15 $[M+H]^+$) and ^{1}H NMR ($CDCl_3$, 400 MHz) δ: 7.80 (*s*, 2H, Ar-*H*), 5.92 (*br t,* J = 6.5 Hz, 1H, N-*H*), 3.72 (*td*, J = 6.5 and 2.9 Hz, 2H, CH_2), 2.25 (*t*, J = 2.9 Hz, 1H, C*H*).

Fluorescein-azide

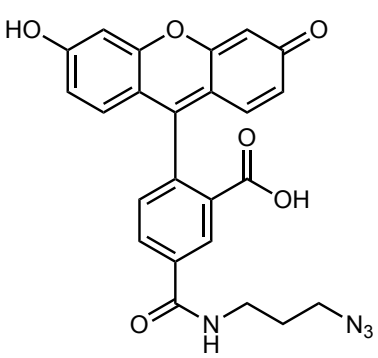

5-Carboxyfluorescein (100 mg, 0.26 mmol), TBTU (171 mg, 0.53 mmol) and DIEA (175 µL, 1.01 mmol) were solubilized in dry DMF (5 mL) and stirred 5 min at rt. 3-Azidopropylamine (45 mg, 0.40 mmol) in DMF (3 mL) was added and the mixture was stirred at rt for 24 h. DMF was partially removed under vacuum and ethyl acetate (100 mL) was added. Organic phase was washed with acidic water (pH = 2), dried, filtered and concentrated under vacuum. The crude product was solubilized in DMF (3 mL) and purified by preparative HPLC to give compound **11** (18.3 mg, 0.040 mmol, 15 %). The fluorescein azide derivative was characterized by mass spectrometry (*m/z* = 459.0 $[M+H]^+$) and by ^{1}H NMR (MeOD, 400 MHz) δ: 8.48 (*s*, 1H, Ar-*H*), 8.20 (*d*, J = 8.5 Hz, 1H, Ar-*H*), 7.34 (*d*, J = 8.5 Hz, 1H, Ar-*H*), 6.81 (*s*, 2H, Ar-*H*), 6.75 (*d*, J = 10.2 Hz, 2H, Ar-*H*), 6.65 (*d*, J = 10.2 Hz, 2H, Ar-*H*), 3.51 (*t*, J = 7.0 Hz, 2H, CH_2), 3.44 (*t*, J = 7.0 Hz, 2H, CH_2), 1.92 (*t*, J = 7.0 Hz, 2H, CH_2).

Fipronil-fluorescein (Fipronil-fluorescein)

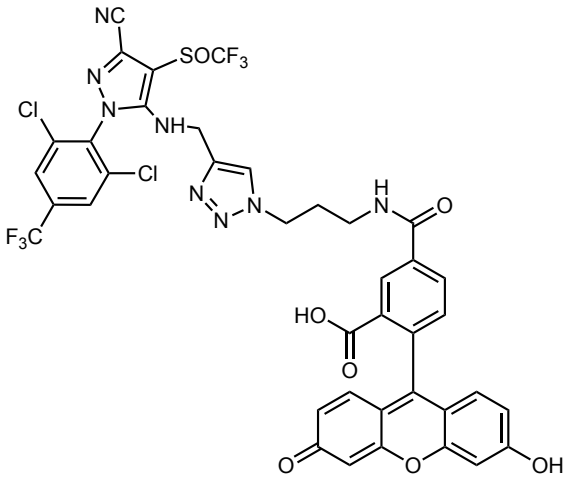

Propargyl-fipronil **7** (19.3 mg, 0.04 mmol) and fluorescein-azide **11** (18 mg, 0.04 mmol) were solubilized in 1:1 THF/H_2O (2 mL). Copper sulfate pentahydrate (4 mg, 0.016 mmol) and ascorbic acid (6.5 mg, 0.032 mmol) were added and the mixture was stirred at rt overnight. THF was removed under vacuum and compound was extracted with ethyl acetate and washed with saturated aqueous solution ($NaHCO_3$ and NH_4Cl). The organic layer was dried, filtered and concentrated under vacuum. Column chromatography (eluant: ethyl acetate) was performed to give fipronil-fluorescein conjugate **12** (31.7 mg, 0.034 mmol, 85 %). The compound was characterized by mass spectrometry (*m/z* = 933.0 $[M+H]^+$) and by NMR: ^{1}H NMR (MeOD, 500 MHz) δ: 8.40 (*s*, 1H, Ar-*H*), 8.18 (*d*, J = 8.4 Hz, 2H, Ar-*H*), 8.06 (*s*, 2H, Ar-*H*), 7.31 (*d*, J = 8.4 Hz, 2H, Ar-*H*), 6.69 (*d*, J = 2.2 Hz, 2H, Ar-*H*), 6.59 (*d*, J = 8.4 Hz, 2H, Ar-*H*), 6.54 (*d*, J = 2.2 Hz, 1H, Ar-*H*), 6.52 (*d*, J = 2.2 Hz, 1H, Ar-*H*), 4.62 (*d*, J = 16.0 Hz, 2H, CH_2), 4.51 (*t*, J = 6.5 Hz, 2H, CH_2), 3.45 (*t*, J = 6.5 Hz, 2H, CH_2), 2.24 (*t*, J = 6.5 Hz, 2H, CH_2); ^{13}C NMR (MeOD, 125 MHz) δ: 178.03, 167.15, 152.34, 149.92, 143.27, 137.43, 136.53, 135.21, 134.88, 134.64, 134.03, 132.56, 128.74, 128.51, 127.49, 126.61, 124.39, 123.68, 123.56, 123.35, 112.29, 110.80, 109.44, 102.25, 96.23, 95.3, 65.49, 39.71, 36.74, 29.74, 29.32.

Communications

Poster

Adriano ALOISI, Niels. J. Christensen, Kasper. K. Sørensen, Knud. J. Jensen, Alberto Bianco
Title : Adamantane derivatives to build foldamers
53rd International Conference on Medicinal Chemistry, RICT 2017, Drug Discovery & Selection, 5-7 Juillet 2017, Toulouse, France

Oral presentation

Adriano ALOISI, Niels. J. Christensen, Kasper. K. Sørensen, Knud. J. Jensen, Alberto Bianco
Title: Foldamers based on adamantane
Journée des Docotrants 2017, University of Strasbourg, 10 Novembre 2017, Strasbourg, France

Adriano ALOISI

Nanoparticules dendritiques à base d'adamantane: Conception, synthèse et étude de leur auto-assemblage

Résumé

L'adamantane est un hydrocarbure polycyclique, rigide et assez encombrant. En médecine, plusieurs dérivés à base d'adamantane ont été développés notamment comme agent antiviraux. Facilement fonctionnalisés, sa conformation 3D permet d'amoindrir les encombrements stériques entre les différents groupements fonctionnels. Nous avons décidé d'utiliser ses propriétés pour concevoir des structures plus complexes, à savoir, des dendrons et des foldamers. Les dendrons sont des polymères synthétiques possédant des propriétés intéressantes. De par leurs tailles, ils sont considérés comme des nanoparticules et possèdent un ciblage passif des cellules cancéreuses. De plus, facilement fonctionnalisés ils peuvent être utilisés comme molécule cargo dans la vectorisation de principes actifs. Outre la vectorisation, les dendrons permettent d'améliorer les propriétés physico-chimiques d'un médicament (absorption, distribution, métabolisme, élimination et toxicité). Nous avons alors choisi de concevoir des dendrons à base d'adamantane. Ces derniers ont la particularité de ne pas posséder d'espaceur entre les molécules d'adamantane se qui les rend hautement rigides. L'analyse par microscopie électronique à transmission de différents dendrons a permis d'étudier leurs morphologies selon leurs fonctionnalisations ainsi que l'effet du solvant, de la concentration et du support sur leurs auto-assemblages. Dans un second temps, nous avons conçu un acide aminé basé sur l'adamantane. Cet acide γ-aminé a ensuite été incorporé dans des séquences peptidiques et les effets de l'adamantane sur la structure secondaire des peptides ont été étudiés par dichroïsme circulaire.

Mots clés : Adamantane, Dendrons, Foldamers, Applications thérapeutiques

Résumé en anglais

Adamantane is a polycyclic hydrocarbon, rigid and quite bulky. In medicine, several adamantane-based derivatives have been developed especially as antiviral agents. Easily functionalized, its 3D well-defined structure considerably decrease the sterical hindrance between its different functional groups. In this context, we decided to use adamantane to build more complex structures such as dendrons and foldamers. Dendrons are synthetic polymers with interesting properties. Because of their size, they are considered as nanoparticles and possess a passive cancer cell targeting. In addition, they are easily functionalized and can be use as vector of drugs. Indeed, the dendrons improve the physochemical properties of a drug (absorption, distribution, metabolism, elimination and toxicity). We decided to combine adamantane and dendrons to build adamantane-based dendrons. However, these dendrons have the particularity of not having spacer between the adamantane moieties, thus, they are highly rigid. Transmission electron microscopy analysis of the different functionalized dendrons allowed to study their self-assembly capacity and their morphology according to their functional groups, the solvent, the concentration and the support. In a second step, we designed an amino acid based on adamantane. This γ-amino acid has been introduced in a peptide backbone using solid phase peptide synthesis. Then, the effects of adamantane onto peptide secondary structures have been studied by circular dichroism.

Keywords: Adamantane, Dendrons, Foldamers, Therapeutic application